THE SYNTHESIS, CHARACTERISATION AND ELECTRO-OPTICAL PROPERTIES OF POLYPENTENYLENE-BLOCK-CO-ACETYLENE

TREVOR RICHARD FARREN

A thesis submitted for the degree of

DOCTOR OF PHILOSOPHY

THE UNIVERSITY OF ASTON IN BIRMINGHAM

JULY 1989

THE UNIVERSITY OF ASTON IN BIRMINGHAM

THE SYNTHESIS CHARACTERISATION AND ELECTRO-OPTICAL PROPERTIES OF POLYPENTENYLENE-BLOCK-CO-ACETYLENE

A thesis submitted for the degree of Doctor of philosophy by

TREVOR RICHARD FARREN **JULY 1989**

SUMMARY

Acetylene was polymerised using the metathesis catalysts $WCl_6/LiBu$, $WCl_6/AlEtCl_2$ and $WCl_6/AlEt_3$. The polyacetylene was characterised by infra-red spectroscopy, elemental analysis and scanning electron microscopy.

Block copolymers containing polyacetylene and polypentenylene segments were synthesised by sequential addition of cyclopentene and acetylene to an active metathesis catalyst system. When $WCl_6/AlEtCl_2$ was used as catalyst, the copolymer was a black elastomeric material that was soluble in a range of organic solvents and dissolved to give intensely coloured solutions even at low concentration. Soluble copolymers were characterised by uv/visible spectroscopy, infra-red spectroscopy and gel permeation chromatography.

The results of these studies indicated that the catalytic species that polymerises cyclopentene is not identical to the one that is responsible for the polymerisation of acetylene. It seemed likely that the polymerisation of acetylene using metathesis catalysts proceeded by a Ziegler/Natta co-ordinated anionic type mechanism.

An improved synthetic route to polypentenylene-block-co-acetylene employed a reaction scheme that involved an active site transformation reaction. The synthetic conditions were manipulated to effect control over block length of the polyene blocks. The length of the blocks of polypentenylene were reduced by the incorporation of a linear alkene during the ring opening metathesis polymerisation step of the synthesis.

A simple electro-optical technique was developed for the simultaneous measurement of electrically induced birefringence and electrically induced dichroism. This technique was used to determine the electric birefringence and dichroism of solutions of polypentenylene-block-co-acetylene in cyclohexane. The results indicated that the copolymer exists as a polydisperse distribution of optically anisotropic aggregates in solution. The most plausible model of the electro-optical behaviour is one in which the polyacetylene segments of the copolymer form a rod-like core that is surrounded by a shell comprising chains of polypentenylene.

KEY WORDS: POLYACETYLENE, METATHESIS, BLOCK-COPOLYMER, ELECTRO-OPTICAL PROPERTIES, RING OPENING POLYMERISATION.

To my mother

ACKNOWLEDGEMENTS

I wish to express my sincere thanks and gratitude to my supervisor, Dr. Allan J. Amass and to my co-supervisor, Dr. Martin S. Beevers for their constant support, patience and encouragement throughout the course of this project.

My thanks are also extended to the academic and technical staff of the department, in particular to Mr. A. Stuart (glassblowing workshop) and Mr. R. Wheeler (engineering workshop) for their experties in the construction of certain pieces of apparatus used in this study.

Thanks are also due to my colleagues, in particular to Mr. I. Surry, Mr. T. West and Miss A. Smith for their advice and encouragement.

Special thanks are due to my mother for her invaluble support.

Finally I am indebted to the University of Aston for the provision of funding during the period 1985-1988.

LIST OF CONTENTS

CHAPTER 1 INTRODUCTION

CHAPTER 2 EXPERIMENTAL

CHAPTER 3 THE POLYMERISATION OF ACETYLENE USING OLEFIN METATHESIS CATALYSTS

CHAPTER 4 SYNTHESIS OF BLOCK COPOLYMERS OF ACETYLENE AND CYCLOPENTENE USING METATHESIS CATALYSTS

CHAPTER 6 THEORY ASSOCIATED WITH THE MEASUREMENT OF ELECTRO-OPTICAL ANISOTROPY

CHAPTER 7 MEASUREMENT OF THE ELECTRO-OPTICAL PROPERTIES OF POLYACETYLENE COPOLYMERS

CHAPTER 8 ELECTRO-OPTICAL AND DIELECTRIC RESULTS

CHAPTER 9 DISCUSSION AND CONCLUSIONS

APPENDIX 1 DESIGN AND CONSTRUCTION OF THE REVERSED VOLTAGE PULSE GENERATOR

APPENDIX 3 DATA OBTAINED FROM PLOTS OF TRANSIENT ELECTRIC DICHROISM

LIST OF FIGURES

LIST OF TABLES

LIST OF PLATES

CHAPTER 1

INTRODUCTION

1.1 INTRODUCTION

The development of polymers as electronic materials has attracted increasing professional interest in recent years owing to the maturation of both the electronics and the synthetic polymer industries.(1) Traditionally the electronics industry has utilised the conducting properties of metals and the insulating nature of non-metals in the construction of circuits. The discovery of inorganic semiconductors stimulated a change in the 1960's from the use of vacuum technology (valves) to the production of solid state devices (transistors). The rapid development of integrated circuits in the 1980's resulted from the ability to produce patterns of thin films of metals, dielectrics and semiconductors of increasing complexity on the surface of a substrate such as silicon. Improvements in both the fabrication process and the intrinsic properties of the materials employed are now required if a further decrease in size and an increase in efficiency is to be realised.(2,3)

The ability to fabricate cheap, light weight, chemically inert polymeric materials is now commonplace and commercial interest is beginning to focus on the production of high-value materials for specialist applications. The production of "tailor-made" polymers with specified properties demands the ability to accurately control the synthesis and processing of these materials.

In this chapter, the role of polymers as electronic materials will be discussed briefly, with particular emphasis on the properties of polyacetylene. The chapter concludes with a discussion of how the control of the synthesis of copolymers has been used in an attempt to retain the desired electrical properties of polyacetylene while circumventing some of the intrinsic problems associated with this material.

1.2 POLYMERS AS ELECTRONIC MATERIALS

The electrically insulating nature of many naturally occurring and most synthetic polymers has for many years been exploited in the production of cheap, easy to process insulating materials for protecting electric currents in wiring, electrical components and consumer goods. The very low levels of electronic conduction in these materials also allows a diverse and subtle range of electrical effects to be observed.(4,5) Certain polymer films cause electricity to flow when they are deformed (piezoelectricity) or when heated (pyroelectricity). Others may build up and retain static charges for long periods of time, which is a useful property in the production of capacitor dielectrics, but may be an undesirable attribute in other circumstances since it can lead to electric discharges and the attraction of dust.

To reduce these unwanted effects a certain degree of intrinsic conductivity in the polymer would be useful and this has been achieved to some extent by compounding existing polymers with a conducting material such as carbon black or by depositing a conducting (metallic) layer on the surface of a polymeric substrate. However, there is still considerable interest in the production of cheap polymers that are easy to process and which show a wide range of conductivity.(6) The lightweight, flexible, chemically inert properties of a suitable polymer could be combined advantageously with high intrinsic conductivity for power/signal transmission or with intermediate conductivity for heating elements and graded cable insulation. It is anticipated that polymers of this type may show a range of interesting properties not known hitherto, thus making them fundamentally unique and potentially useful for new applications in the electronics industry.(7-16)

Two main classes of polymer have been found to exhibit abnormally high electrical conductivities. The first type involves the introduction along the polymer backbone of pendant groups that may participate in charge transfer reactions with added species. Generally the donor (D) moieties, which donate negative charge, are attached to the polymer and the acceptor (A) molecules are interspaced between them as shown in figure 1.1.

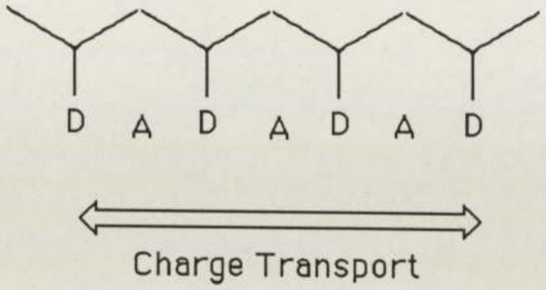

Figure 1.1 Conduction along a polymer chain by charge transfer

1.2.1 Conjugated chains

The structure of most synthetic polymers consists of monomer units connected to one another to give saturated structures in which all of the available electrons are localised in strong covalent bonds. If each carbon atom along the polymer chain has only one substituent attached to it, then an unsaturated structure, represented by alternate single and double bonds is the result. The π-electrons of the double bonds are not held tightly and may be delocalised over the carbon atoms thereby forming a conjugated structure. In principle, electronic transport is then possible along the entire polymer backbone.

The simplest conjugated polymer, polyacetylene, exhibits a bulk conductivity that is considerably higher than that of polyethylene. Several conjugated polymers based on aromatic and unsaturated heterocyclic compounds also show anomalously high conductivities. Some examples are shown in figure 1.2.(17)

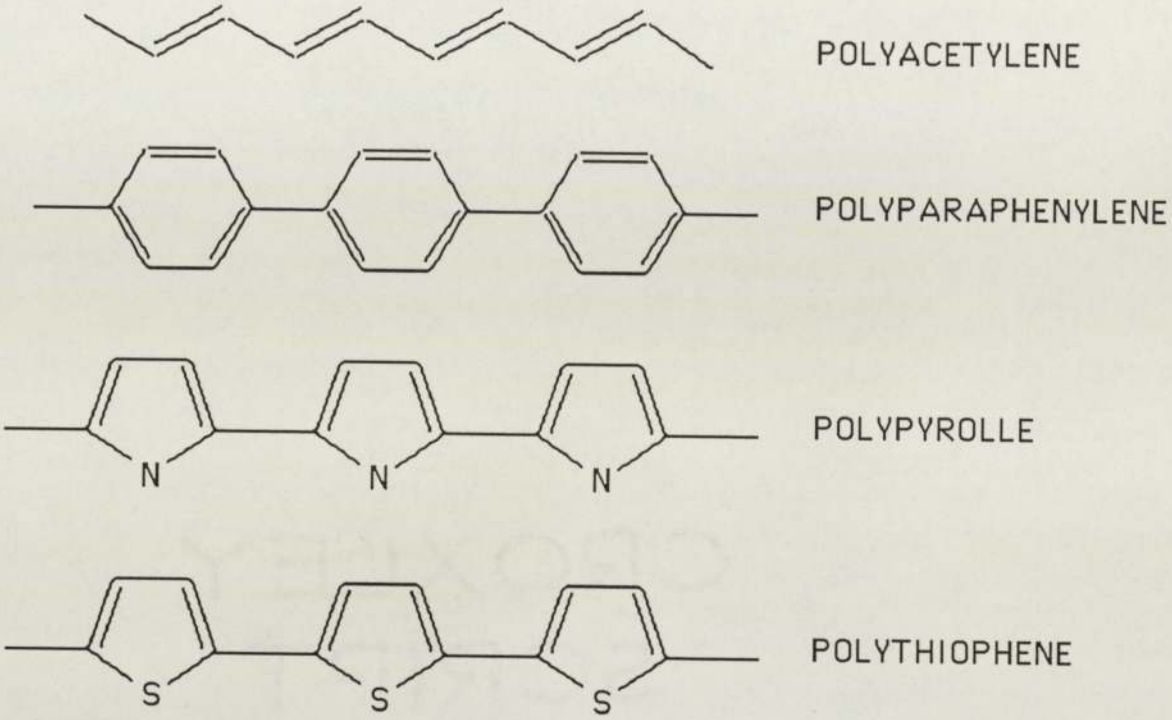

Figure 1.2 Examples of polyconjugated polymers

The major portion of this thesis will be concerned with the production of polyacetylene and of copolymers that contain segments of polyacetylene using metathesis polymerisation.

1.3 GENERAL ASPECTS OF METATHESIS POLYMERISATION(18-24)

1.3.1 General Description

A wide variety of double and triple bonded systems have been shown to participate in a catalytic reaction which may be sumarised as

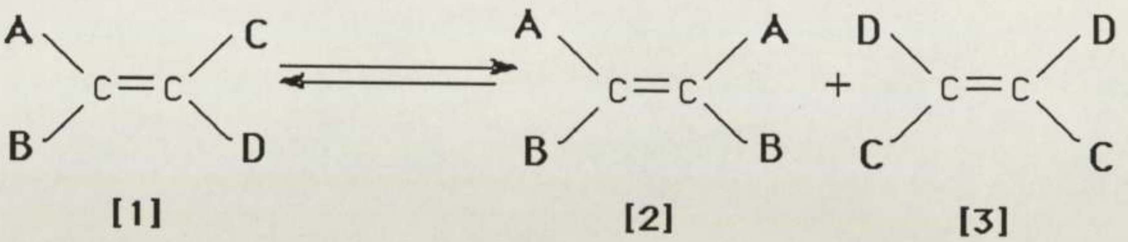

Figure 1.3 The olefin metathesis reaction

The substituents A,B,C and D may be either linear or branched chain alkyl groups but not usually structures that possess or which may generate conjugated double bonds, because such systems normally deactivate the catalyst. The reaction is an equilibrium for which the enthalpy is zero, or very close to zero for linear substituents. Accordingly the position of equilibrium is determined entropically and at equilibrium, the molar ratio [1] : [2] : [3] is 2 : 1 : 1 and both stereostructural forms (cis and trans) of all three molecules may be present. The cis/trans molar ratios of [1], [2] and [3] are often determined by the nature of the catalyst used.

When the alkene is cyclic, a ring opening polymerisation occurs and an unsaturated polymer is formed. Using the monomer cyclopentene as an example, this process may be described as shown in figure 1.4.

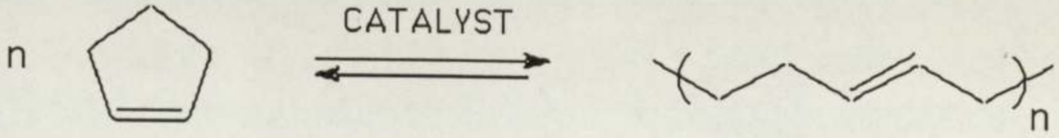

Figure 1.4 The ring opening polymerisation of cyclopentene

Ring opening polymerisations of this type were reported long before Banks and Bailey(25) observed the metathesis of linear alkenes. However the similarity between the two was recognised by Calderon and coworkers(26) who suggested that both reactions proceeded via the exchange of alkylidene groups. Natta(27) had originally proposed that ring opening polymerisation occurred by cleavage of the carbon-carbon bond α to the C-C double bond as this was assumed to be the weakest bond in the ring. This corresponded in the metathesis of linear alkenes to an exchange of alkyl groups. Calderon(28) considered the metathesis of a mixture of but-2-ene and its perdeuterated analog using the catalyst $WCl_6/AlEtCl_2/EtOH$. The only product found was 1,1,1,2-tetradeuterobut-2-ene which is consistent with the cleavage of double bonds and the exchange of alkylidene groups. Exchange by transalkylation would have resulted in two new alkene products. Further evidence that indicated cleavage of the double bond, was obtained from the copolymerisation of cyclooctene and cyclopentene, the cyclopentene being ^{14}C labelled at the double bond.(29)

1.3.2 Monomers for metathesis polymerisation

In common with the polymerisation of 1-alkenes by Ziegler/Natta catalysts, the ring opening metathesis polymerisation (ROMP) of cycloalkenes is catalysed by the product of a reaction between a transition metal compound and a metal alkyl or Lewis acid. Consequently the substrates that may be considered as monomers for metathesis polymerisation are severely limited in structure since monomers that possess functional groups that react with transition metal carbenes or form strong complexes with transition metal atoms must be excluded. Monomers that contain amino, hydroxyl, carbonyl, carboxyl, ester, ether, amide or thiol groups are not normally suitable for metathesis polymerisation.

The principal monomers that have been used in ROMP are monocyclic alkenes. The first cyclo-olefin found to undergo this reaction was cyclopentene.(30) Subsequently, 4, 7, 8, 9 and 10 membered rings were also found to be active, the driving factors for the reaction appearing to be :

(i) The release of ring strain energy (ΔH is often strongly negative)

(ii) The polymerisation is generally accompanied by an increase in entropy as the vibration and rotation of bonds is easier in chains than in rings.

Such arguments explain why cyclohexene and its derivatives will not polymerise under ambient conditions, since there is virtually no ring strain ($\Delta H = 0$) and only a small change in entropy. However cyclohexene has been shown to polymerise slowly at low temperature(31).

A range of substituted cyclic alkenes have also been polymerised using metathesis catalysts, but generally monomers that contain substituents at the site of the double bond are inactive. This correlates with the decreasing order of activity towards metathesis in the series of alkenes $R^1CH{=}CHR^2 > R^1R^2C{=}CHR^3 > R^1R^2C{=}CR^3R^4$.

Monomers containing more than one double bond, such as 1,5-cyclo-octadiene may be polymerised provided that the unsaturated groups are not conjugated. However, recent developments in the production of well characterised metal carbene catalysts which are highly active in metathesis polymerisations have resulted in systems which are able to polymerise conjugated structures. An interesting example is the conversion of cyclo-octatetrene to polyacetylene.

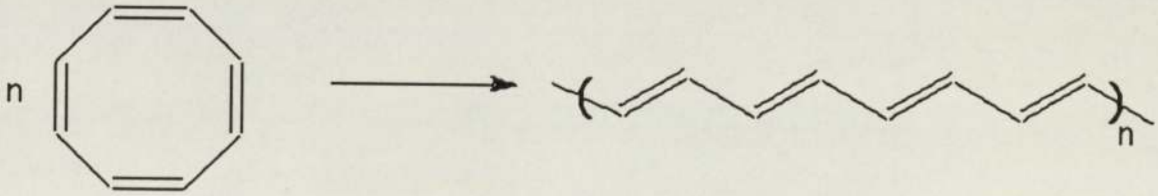

Figure 1.5 ROMP of cyclooctatetrene

Although Korshak(31) demonstrated the feasibility of this reaction using a conventional metathesis catalyst ($WCl_6/AlEt_2Cl$), Grubbs(32) has recently reported that, when a carbene catalyst is used, high quality films of polyacetylene may be prepared by this route .

Bicyclic and polycyclic monomers such as bicyclo-(2,2,1)-heptene (norbornene) often polymerise rapidly, the equilibrium lying very much in the direction of the polymer.

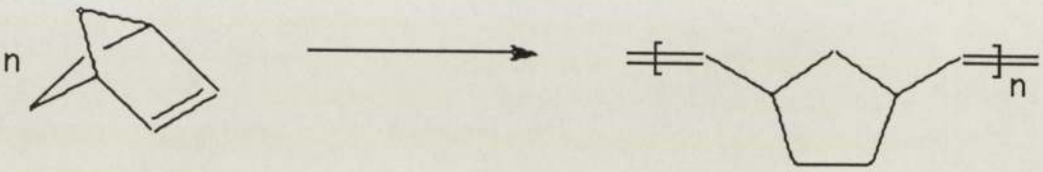

Figure 1.6 ROMP of norbornene

In these systems, the carbon-carbon double bond in the polymer does not participate in secondary metathesis reactions such as intramolecular and intermolecular back-biting reactions.(34)

The reactions of alkynes with metathesis catalysts fall into three catagories, metathesis, cyclotrimerisation, and polymerisation. The relative extent to which each process contributes is determined by the nature of the catalyst and the structure of the reactant.

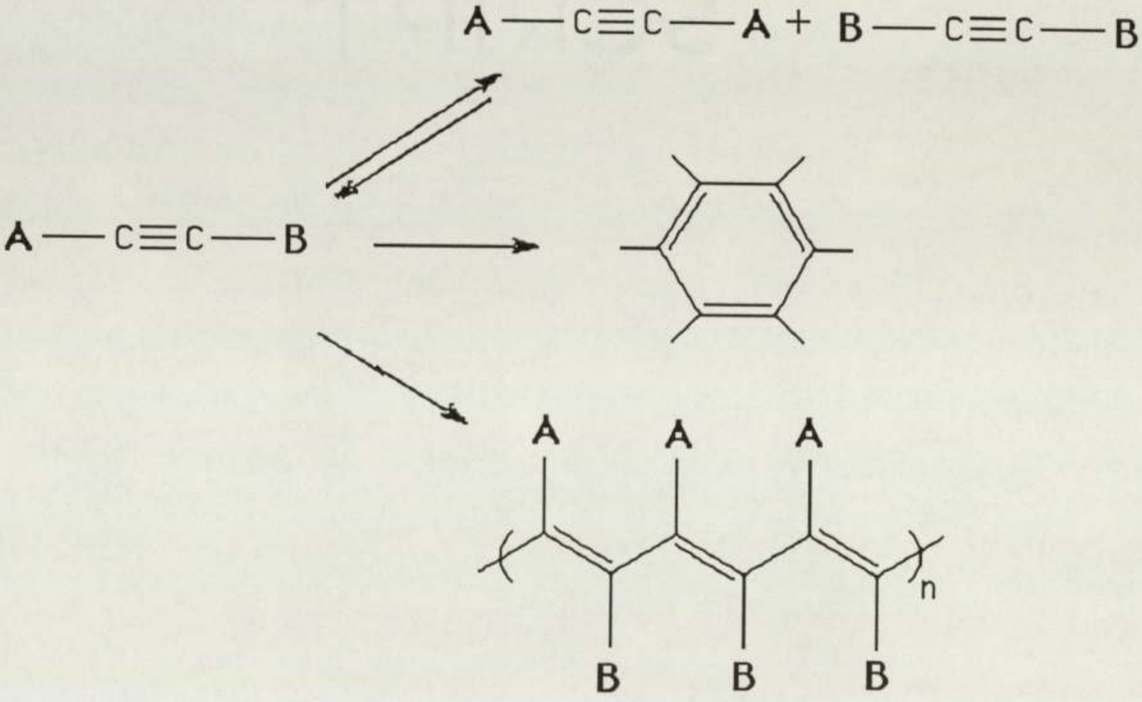

Figure 1.7 Metathesis reactions of acetylenes

1.3.3 Catalyst systems for metathesis polymerisation

A wide variety of metallic derivatives and combinations with other species have been found to initiate metathesis and/or ring opening polymerisation. The catalysts may act homogeneously or heterogeneously and a wide variety of activities have been reported. Catalysts that are stereospecific in terms of the cis and trans arrangement of the groups around the carbon/carbon double bond are generally less reactive than those in which no particular form of stereoregularity is achieved. In the majority of cases a transition metal compound, usually a halide or carbonyl is used as the catalyst. The transition metal is normally tungsten or molybdnum but rhenium, tantalum, ruthenium, niobium and rhodium have also been used. The catalyst is combined with a metal alkyl (e.g. triethyl, dichloroethyl, or tri-isobutyl aluminium; tetraphenyltin or tetramethyltin; dimethylzinc, butyl lithium or Grignard reagents).

Heterogeneous catalysts are usually formed by depositing the transition metal oxide, carbonyl or sulphide onto a large surface area support such as alumina or silica and activated by heating the catalyst to high temperatures (400^oC) in an inert atmosphere.

Apart from one or two notable examples (WCl_6 and cyclopentene, $AlEtCl_2$ and norbornene) most of the homogeneous catalyst systems are multicomponent. Four main factors affect the reactivity and the nature of the products formed:

(i) the combination of the catalyst components,

(ii) the molar ratios of the components,

(iii) the order of mixing and the mixing times and

(iv) the temperature and pressure of the reaction medium.

1.3.4 Mechanism of the metathesis reaction(35)

Several schemes have proposed to explain the main features of the metathesis reaction and of ring opening metathesis polymerisation. The most plausible mechanism postulated to date involves metallocarbene intermediates and is shown in figure 1.8 By some mechanism (which still remains unclear) a tungstanocarbene with a vacant co-ordination site is produced, **[A]**, by reaction between the catalyst components and the monomer.

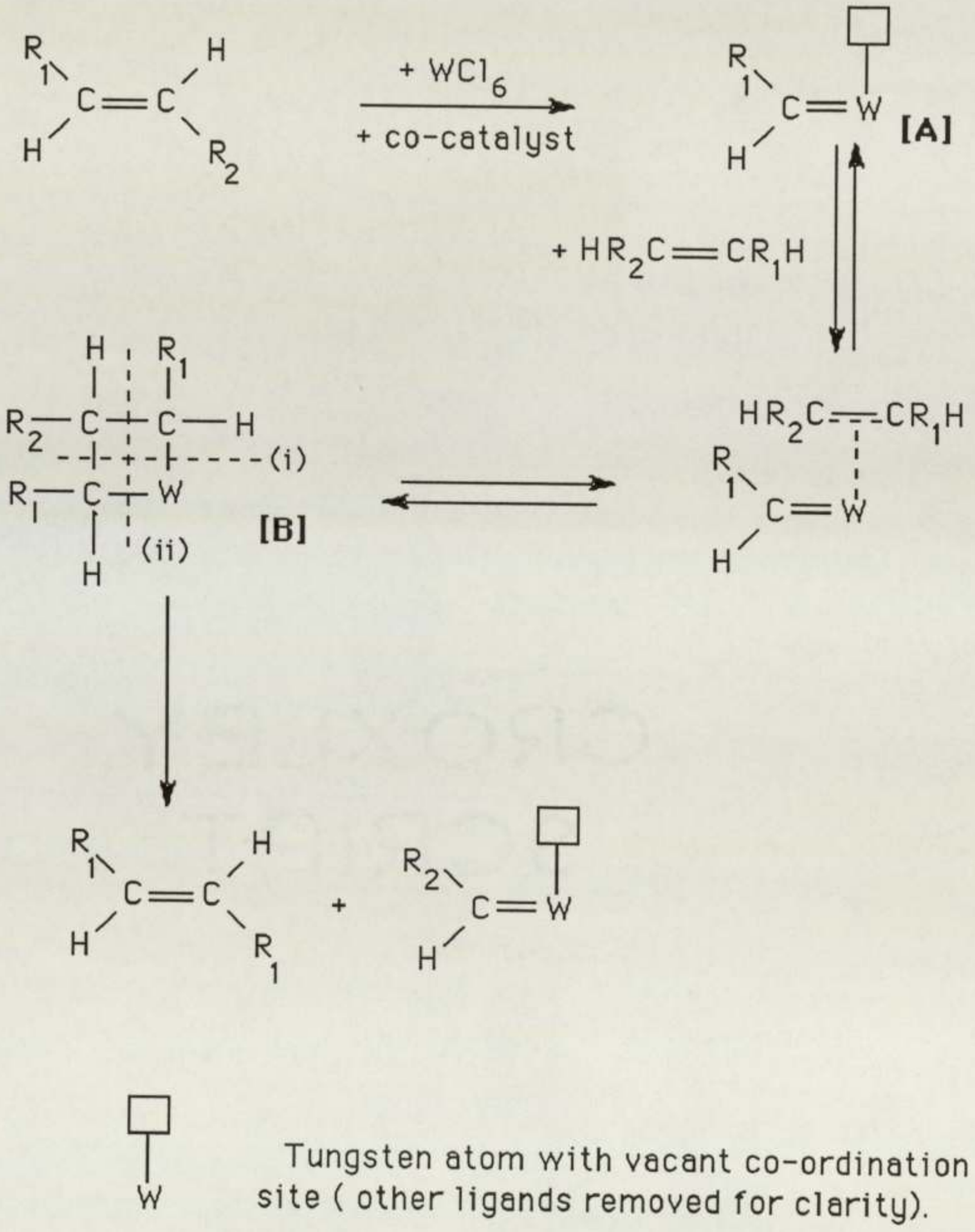

Tungsten atom with vacant co-ordination site (other ligands removed for clarity).

Figure 1.8 Mechanism of the olefin metathesis reaction

This carbene then reacts with a molecule of olefin via the π-complex to yield a four-membered metallocyclobutane intermediate, **[B]**. This may break down along axis (i) or (ii). If cleavage occurs along axis (i) then the reactants are reformed (this process is known as degenerate metathesis). However, if the intermediate breaks along axis (ii) then productive metathesis occurs yielding a new olefin and a new metal carbene. A similar mechanism has been proposed for ROMP and is shown in figure 1.9.

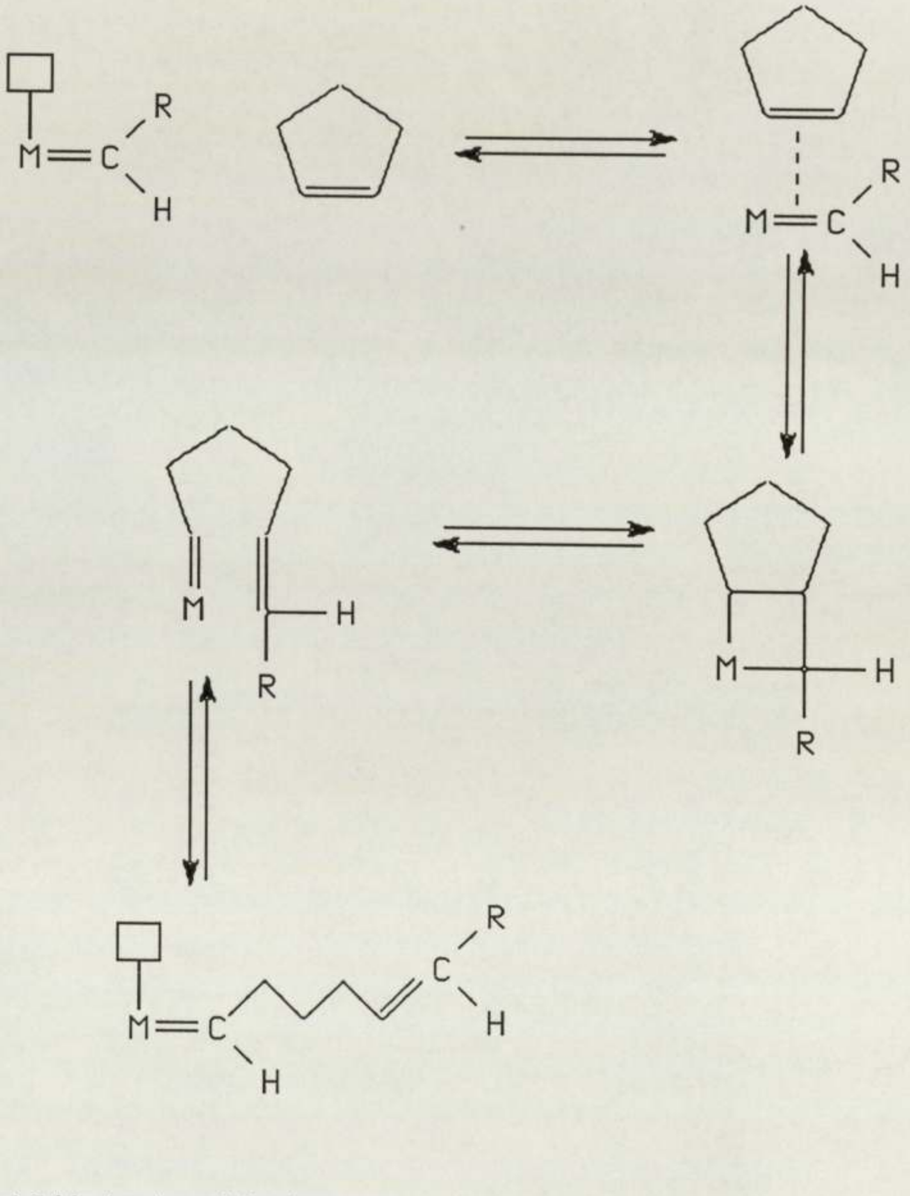

Figure 1.9 Mechanism of the ring opening metathesis polymerisation of cyclopentene

The intermediate may decompose to reform cyclopentene or may undergo ring opening, with release of ring strain, to yield a new tungsten species which has a pentenylene ligand and a vacant co-ordination site. Sequential additions of cyclopentene lead to high molecular weight polymer chains containing unsaturated units.

Much evidence has been reported supporting the existence of carbene type intermediates and for their participation in mechanisms of the type shown in figures 1.8 and 1.9, not least of which was the synthesis of isolatable carbene complexes, such as those shown in figure 1.10, which initiate metathesis directly.

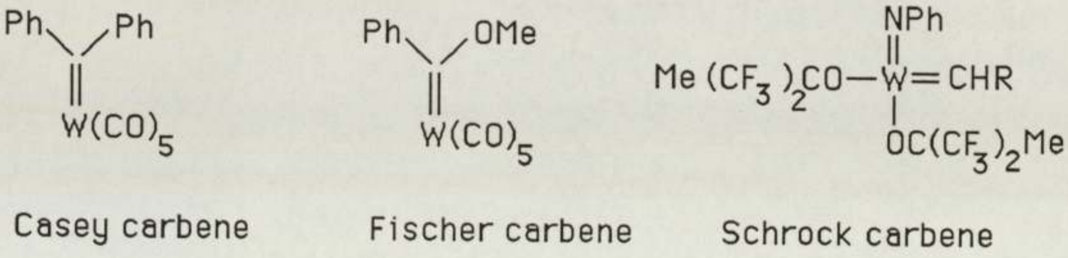

Casey carbene

Fischer carbene

Schrock carbene

Figure 1.10 Carbene complex initiators for metathesis

1.4 POLYACETYLENE

1.4.1 Direct synthesis

The literature contains a variety of reports concerning the polymerisation of acetylene initiated by radiation, ionic or radical initiatiors and by a selection of transition metal and rare earth catalysts.(36-41) A diverse array of side reactions also occurs during the polymerisation which, depending on the mechanism of initiation, lead to varying degrees of oligomerisation (in particular cyclotrimerisation to benzene), chain branching and crosslinking in the product. Generally, transition metal catalysts are by far the most efficient at producing linear, high molecular weight, crystalline polyacetylene. The catalyst system, $Ti(OBu)_4$ / $AlEt_3$ is perhaps the most efficient of these and was first used as a catalyst for acetylene polymerisations by Natta(42). At low catalyst concentrations, a gray powder was formed which decomposed before melting and was insoluble in common organic solvents. Less than 1% of benzene was isolated in polymerisations of this type and crystallographic data was reported to show that this catalyst produced high yields of linear polyacetylene.

Shirakawa and Ikeda(43) showed that when acetylene was blown across the surface of a concentrated (> 3mmol/l) 1:4 $Ti(OBu)_4/AlEt_3$ catalyst solution, a film of polyacetylene formed, which floated on the surface and became thicker as the gas flow was maintained. At low temperatures (< 255K) the film was red and developed a copper coloured lustre and was shown to be comprised almost exclusively of cis-polyacetylene (Figure 1.11). Polymerisations of acetylene performed at room temperature yielded blue/black films with a silver coloured lustre and were shown to possess a high content of trans-polyacetylene (figure 1.3). Films containing exclusively trans-polyacetylene were prepared at temperatures above 373K. This technique allowed the synthesis of free standing films of polyacetylene the thicknesses of which could be varied between 1μm and several millimeters. A variation of this technique involved blowing acetylene gas onto a surface which had previously been wetted with a concentrated solution of catalyst. This method is especially useful for coating substrates with a thin layer of polyacetylene. At intermediate catalyst concentrations, a dark red gel was produced which, like both powder and film showed no melting point.

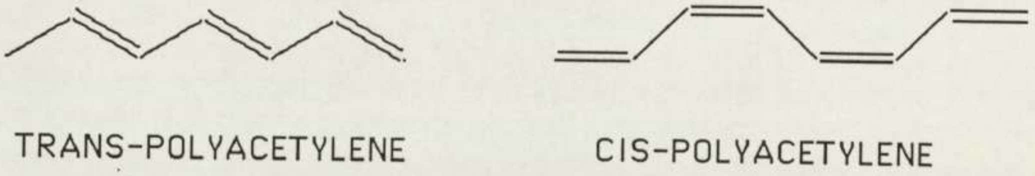

Figure 1.11 Structure of cis and trans polyacetylene

1.4.2 Electrical properties(44-46)

In its pristine form, cis-polyacetylene is an insulating material with a conductivity of 10^{-7}-10^{-9} Sm^{-1}. Trans-polyacetylene may be described as a semiconductor, the conductivity of which has been determined to be approximately 10^{-1} Sm^{-1}. In view of the extensive electron delocalisation possible in both forms of the polymer it is, at first sight, surprising that these materials do not exhibit conductivities as high as those shown by metals. Metals exhibit isotropic three dimensional conduction, but the electrons in polyacetylene are only mobile along the polymer backbone and therefore the level of bulk conductivity in this material depends on the efficiency of the interchain hopping of electrons.(47)

This effect is also present at the macroscopic level where the polyacetylene chains often pack in randomly oriented fibrils approximately 20nm in diameter forming web like structures.(45,48,49) The non-uniform arrangement of the fibrils generates inter-fibrillar contacts yielding various conduction pathways and barriers. Orientation of the fibrils has been shown to produce materials which show enhanced bulk conductivities accompanied by marked anisotropic behaviour. Films of 'aligned' polyacetylene have been prepared by several techniques, the most simple being mechanical stretching of the film.(50,51) In another case, liquid crystalline compounds have been used as solvents for the polymerisation of acetylene.(52) The polymerisation of acetylene was performed by dissolving the components of the catalyst in the solvent and allowing the solution to flow down a vertical wall of the reactor. The solvent molecules were aligned by the flow gradient and converted to their nematic state. When acetylene was admitted, the orientation of the growing chains of polyacetylene was dictated by the highly ordered arrangement of the solvent molecules in their liquid crystalline state. When external magnetic fields were used to preserve the ordered structure of the mesophase, free-standing films of aligned polyacetylene formed on the surface of the catalyst solution.(53)

Although morphological factors provide the main explanation for the bulk conductivity of polyacetylene being lower than expected, another important factor to be considered is bond alternation. It is well known that the carbon-carbon bonds in conjugated structures are of uniform length, intermediate between that of a single and a double bond. As the number of carbon atoms in the conjugated structure increases, the stability of this arrangement, compared with that in which alternate single and double bonds are present, decreases. This effect, known as Pierls instability, suggests that conjugation and therefore electronic transport are severely limited in chains of pristine polyacetylene.

Dramatic improvements in the bulk electrical conductivity of polyconjugated polymers may be achieved by the addition of certain oxidising and reducing agents. This behaviour is analogous to the doping of inorganic materials to produce semiconductors. MacDiarmid and Heeger(54) first reported this effect for polyacetylene doped with iodine. A vast array of p-type electron attracting dopants (e.g. I_2, Br_2, AsF_5, ClO_4^-) and n-type electron donating dopants (e.g. Li, K, Na) are now known that are thought to form charge transfer complexes at sites of conjugational defect along the polyacetylene backbone. This results in improvements in both intra- and inter-chain electron transport.(55-59)

Recently Naarman(60-61) has produced films of polyacetylene of high structural purity. Acetylene was polymerised by the Shirakawa method using a silicone oil as the solvent. It is believed that the greater than normal viscosity of the medium resulted in a decreased rate of bimolecular reactions of the active polymerisation centres and therefore reactions which lead to chain branching, crosslinking or termination were surpressed. Indeed the absence of sp^3 defect sites in Naarmans samples offers strong evidence for the absence of crosslinking and possibly an increase in polyene chain length in these materials. The conductivity reported for stretched aligned films of doped Naarman polyacetylene is 8.0×10^6 Sm^{-1} which is presently the highest conductivity recorded at room temperature for an organic material.(62-64)

1.5 MODIFICATION OF POLYACETYLENE

1.5.1 Introduction

Despite the remarkable electrical properties of doped polyacetylene, the material has found few commercial applications. The principal reasons for which include:

(i) polyacetylene is an inconvenient material for fabrication; its intractibility and infusibility exclude its use in standard melt processing techniques.

(ii) polyacetylene is insoluble in all common solvents which renders characterisation of the material difficult. Little information is available concerning the effect of the polymerisation conditions on average molecular weights, polymer structures and morphologies. The nature of the doping reaction is also not fully understood and the non-uniformity of the doping throughout the polymer sample raises several, as yet unanswered, questions concerning the mode of conduction in these materials. Its general insolubility also hinders the removal of impurities such as catalyst residues which may be present in the polymer.

(iii) polyacetylene is unstable to atmospheric oxidation and doping often enhances this effect. The conductivity has been shown to decrease rapidly and in an unpredictable manner on oxidation.(65,66)

Research into methods of circumventing these problems has received considerable interest. The approaches include, the use of blends or composite materials, synthetic routes involving precursor polymers and the use of copolymerisation techniques.

1.5.2 Composite materials

A suitable carrier polymer, such as polyethylene, is prefabricated in the form required for the conductive component and this polymer impregnated with a solution of Ziegler/Natta catalyst which, when contacted with acetylene, forms polyacetylene within the carrier matrix.(67) Several composite fibres have been produced in this manner. Polyacetylene has been coated onto glass and Kevlar fibres(68) and acetylene has been polymerised within a polyethylene fibre.(69) Although these materials exhibit enhanced oxidative stabilities, the bulk conductivity is limited by the amount of insulating material used as the matrix.

1.5.3 Synthesis involving precursor polymers.

The synthesis of a soluble polymer which may be purified and fabricated into the desired form before conversion to polyacetylene is a procedure by which highly pure polyacetylene may be prepared. Feast et al(70-72) have described a route, shown in figure 1.12, in which a substituted tricyclo[4,2,2,0]-3,7,9-decatriene is polymerised by a metathesis ring opening process to produce a "precursor" polymer which is soluble in common organic solvents and may be cast from solution into the desired final form of the polyacetylene component. A substituted benzene is then thermally eliminated from the precursor to yield polyacetylene.

The temperature at which the retro-Diels/Alder elimination (step (ii)) occurs is governed by the nature of the groups R_1, R_2, R_3, and R_4 and it is this factor which determines the convenience of the route. A similar route which involves a photochemical elimination step has also been used.(73)

This procedure, which has become known as the Durham route, has advantages over other synthetic routes to polyacetylene in that it is possible to synthesise products which are free from catalyst residues and other impurities, thus enabling reproducible morphologies to be obtained.

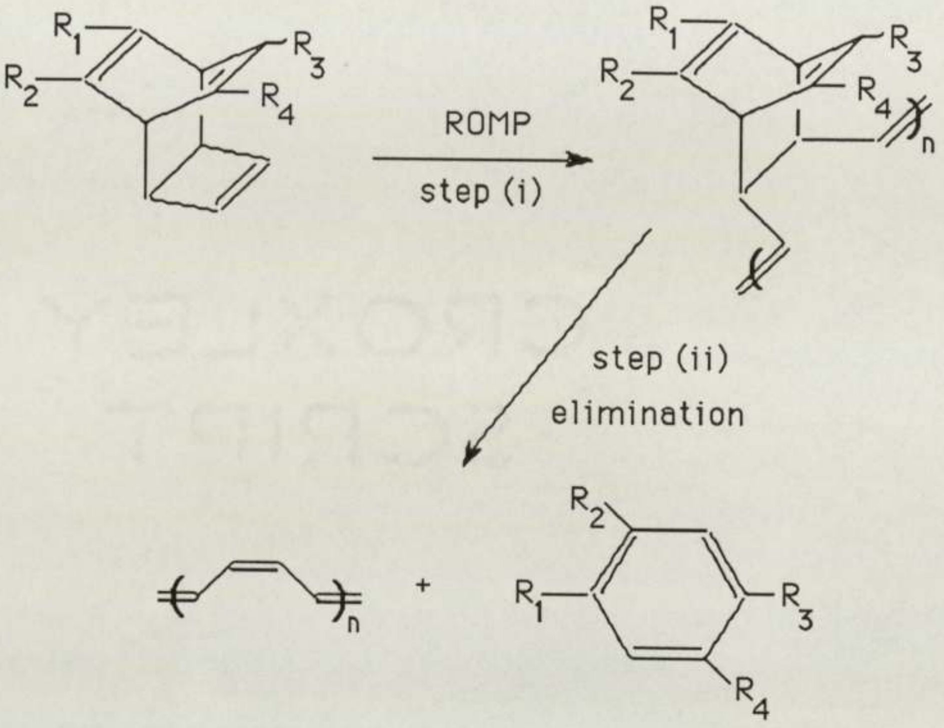

Figure 1.12 The Durham route to polyacetylene

A variation on this technique has recently been reported by Grubbs$^{(74)}$ and has a significant advantage over the Durham route in that no molecules are eliminated in the conversion of precursor to polyacetylene. The method (figure 1.13) involves the ROMP of benzvalene (a) followed by a transition metal catalysed isomerisation of the bicyclobutane rings of the precursor to 1,3-diene units.

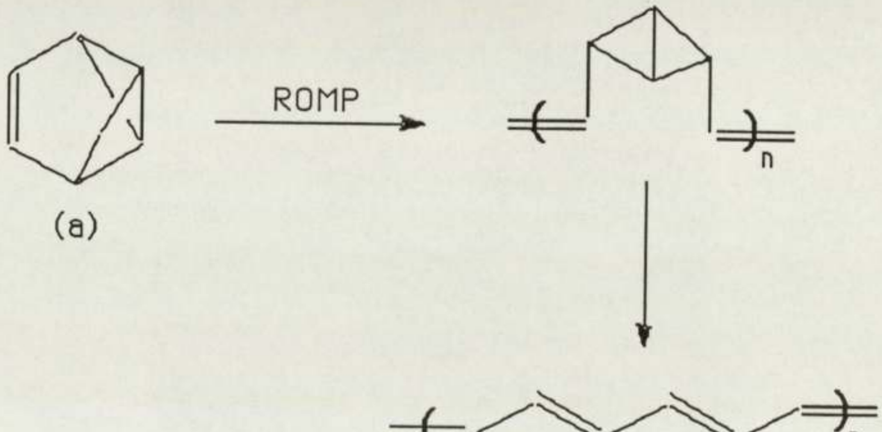

Figure1.13 The Grubbs route to polyacetylene

1.6 MODIFICATION OF POLYACETYLENE BY COPOLYMERISATION

Polymeric materials show a wide variety of physical and chemical properties that are dependent on the properties of their constituent monomers. Although it may be postulated that simple combination of two homopolymers would produce a material which combined the desirable properties of both, this is rarely the case and commonly the inferior characteristics of one homopolymer become exaggerated in the blend. Sometimes, these undesirable properties can be tolerated under economic considerations but significant improvements are often available through the production of copolymers.

Copolymers comprise polymer chains which consist of two or more different types of monomer unit, covalently bonded together. The distribution of comonomer units within a chain governs the type of copolymer formed. Schematic structures of the four basic types of copolymer which may be formed from two types of comonomer, A and B, are shown in figure 1.14.

Random ABBABBBABAAABBABAAABABAB

Alternating ABABABABABABABABABABABAB

Block AAAAAAAAAAABBBBBBBBBBB

Graft

AAAAAAAAAAAAAAA
B B
B B
B B
B B
B B

Figure 1.14 Schematic structures of block copolymers

The properties of a copolymer are generally more easily predicted and controlled than those of the analogous blended materials. Random copolymers often show properties intermediate between those of the two parent homopolymers, which change steadily as the relative proportions of the comonomers in the polymerising mixture are varied. Conversely, block and graft copolymers usually exhibit the characteristics of both their constituent homopolymers and often show properties such as novel phase separation effects which are not observed in the analogous polymer blends.

The presence of extensive unsaturation along the backbone of polyconjugated polymers, such as polyacetylene, explains why the properties of these materials are so unlike those of typical vinyl polymers. Although some of these properties may be advantageously exploited, in particular the high electrical conductivities which are achieved through doping with appropriate reagents, the intractable, insoluble and oxidatively unstable nature of these polymers impedes proper characterisation and makes the materials difficult to process. The hypothesis that copolymerisation of acetylene with another monomer may produce materials which retain desirable electrical properties but which show improved solubility and stability, characteristic of the comonomer chains has been explored by a number of workers and a variety of random, block and graft copolymers have been produced. In this section the main synthetic approaches will be reviewed and the properties of the materials highlighted.

1.6.1 Random copolymers

A number of random copolymers comprising acetylene and a substituted alkyne have been prepared using the catalyst $Ti(OBu)_4/AlEt_3$.(75,77) The substituted alkynes that have been used as comonomers are 1-propyne, 1-pentyne, 1-hexyne, 1-heptyne, phenyl acetylene and propargyl alcohol, most of which only form cyclic oligomers or low molecular weight homopolymers under the experimental conditions used for the polymerisation of acetylene. Acetylene and the the comonomer were mixed in the required proportions and introduced into a solution of the catalyst. With 1-hexyne, the amount of soluble copolymer was found to increase as the fraction of comonomer in the feed increased. The copolymer was examined by uv/visible spectroscopy and a shift to shorter wavelengths of the maximum absorbance recorded in the visible region was observed as the proportion of 1-hexyne in the feed increased. This suggested that the incorporation of this comonomer decreased the effective conjugation length in the polymeric chains.(75) These results are detailed in table 1.1.

Table 1.1 Dependence of the amount of soluble copolymer, composition and absorption of the insoluble copolymer films on composition of the feed solution

Conc. of 1-hexyne in solution (% mol)	Conc. of 1-hexyne in insoluble film	λ_{max} (nm)	Soluble fraction (mol %)
0	0	700	2.5
19	5.5	610	41
32	6.5	600	53
39	7.4	580	64
57	8.3	570	76
66	9.3	550	89
76	17.7	550	98
87	-	-	100
95	-	-	100

The copolymerisation of acetylene with methyl acetylene has been studied in detail by Chien.(78) This comonomer was chosen for three reasons:

(i) It was thought that the methyl substituent would cause minimal disruption to the planarity of the copolymer backbone,(79) an essential requirement for conjugated π-orbital formation and consequently high electrical conductivity.

(ii) Homo-poly(methylacetylene) is soluble in a range of organic solvents, implying that certain monomer/comonomer ratios should produce soluble copolymers.

(iii) Both methylacetylene and acetylene are gaseous at room temperature which enabled standard film synthesis techniques to be employed.(36)

Copolymer films were produced of increasing methylacetylene content, up to a maximum of three times that of acetylene. Soluble materials were not produced and the electrical conductivity of the iodine doped films decreased with increasing methylacetylene content. The stabilities of the copolymer films, with respect to thermal and oxidative degradation(80), were also inferior to that of polyacetylene and deteriorated as the methylacetylene content increased. Such effects are common to all the random copolymers of acetylene.

Copolymers containing phenylacetylene were prepared by Diets and Cukor(76) using a catalyst which was formed by the action of water on WCl_6, the molar ratio of these components being 0.5 to 1. Toluene was used as polymerisation solvent. By varying the relative proportions of the comonomers used in the copolymerisation, a range of soluble and insoluble materials was produced, the electrical and stability characteristics of which were similar to those of the methylacetylene copolymers. Data representative of this behaviour is shown in table 1.2.

Table 1.2 Properties of acetylene/ phenylacetylene copolymers

Conc. of phenylacetylene in feed (mmol/25ml)	phenylacetylene in copolymer (mol %)	solubility of copolymer in CH_2Cl_2	Conductivity of I_2 doped copolymer ($\Omega^{-1}cm^{-1}$)
0	0	Insol	3×10^1
0.3	22	insol	5.0×10^{-1}
1.0	10	insol	2.9×10^{-2}
3.0	16	insol	1.5×10^{-3}
5.0	33	part. sol.	2×10^{-3}
7.0	38	part. sol	2.7×10^{-4}
10	53	soluble	1.4×10^{-4}
15	63	soluble	1.0×10^{-5}
20	83	soluble	3.0×10^{-5}
25	97	soluble	6.8×10^{-6}
25	100	soluble	5.0×10^{-6}

Attempts to improve the stability to autoxidation were made by encapsulating samples of the copolymer in a range of materials such as silicone rubber, glass polyethylene and epoxy resin. Although the conductivity decreased less rapidly than in the absence of the encapsulent, the long term instability of the materials remained.

1.6.2 Block copolymers

Although random copolymerisation of acetylene with other monomers can be controlled in order to produce soluble materials, the polyene backbone becomes severely disrupted leading to a drastic reduction in the average conjugation length. Diblock copolymers of acetylene are of considerable interest because the integrity of the polyacetylene chain is maintained throughout the course of the copolymerisation.

Living polymerisation techniques, which involve sequential addition of the comonomers to an active catalyst, are commonly employed to synthesise block copolymers. Although acetylene may be polymerised efficiently using several co-ordination catalysts, these species have been deemed unsuitable for use in block copolymerisation by alternating the monomer in the feed, owing to the presence of chain transfer reactions which produce dead polymer and may also deactivate the catalyst. Block copolymers in which the comonomers cannot be polymerised by a similar mechanism may often be produced by a route which involves a transformation reaction. This indirect approach involves the polymerisation of a monomer A with an initiator which produces a polymer containing an active centre. The latter may then be converted, by chemical reaction, into a species which will initiate the polymerisation of monomer B.

1.6.2.1 Anionic to Ziegler/Natta Transformations

Diblock copolymers of styrene and acetylene have been prepared by Wnek et al(81-84,91,92) who employed an anionic to Ziegler/Natta transformation reaction (figure 1.15). The synthesis involved the anionic polymerisation of styrene with n-butyl lithium in THF to produce living polystyryl lithium. In early experiments this was used to alkylate $AlCl_3$, the product was then used as a polymeric cocatalyst for the polymerisation of acetylene using $Ti(OBu)_4$.

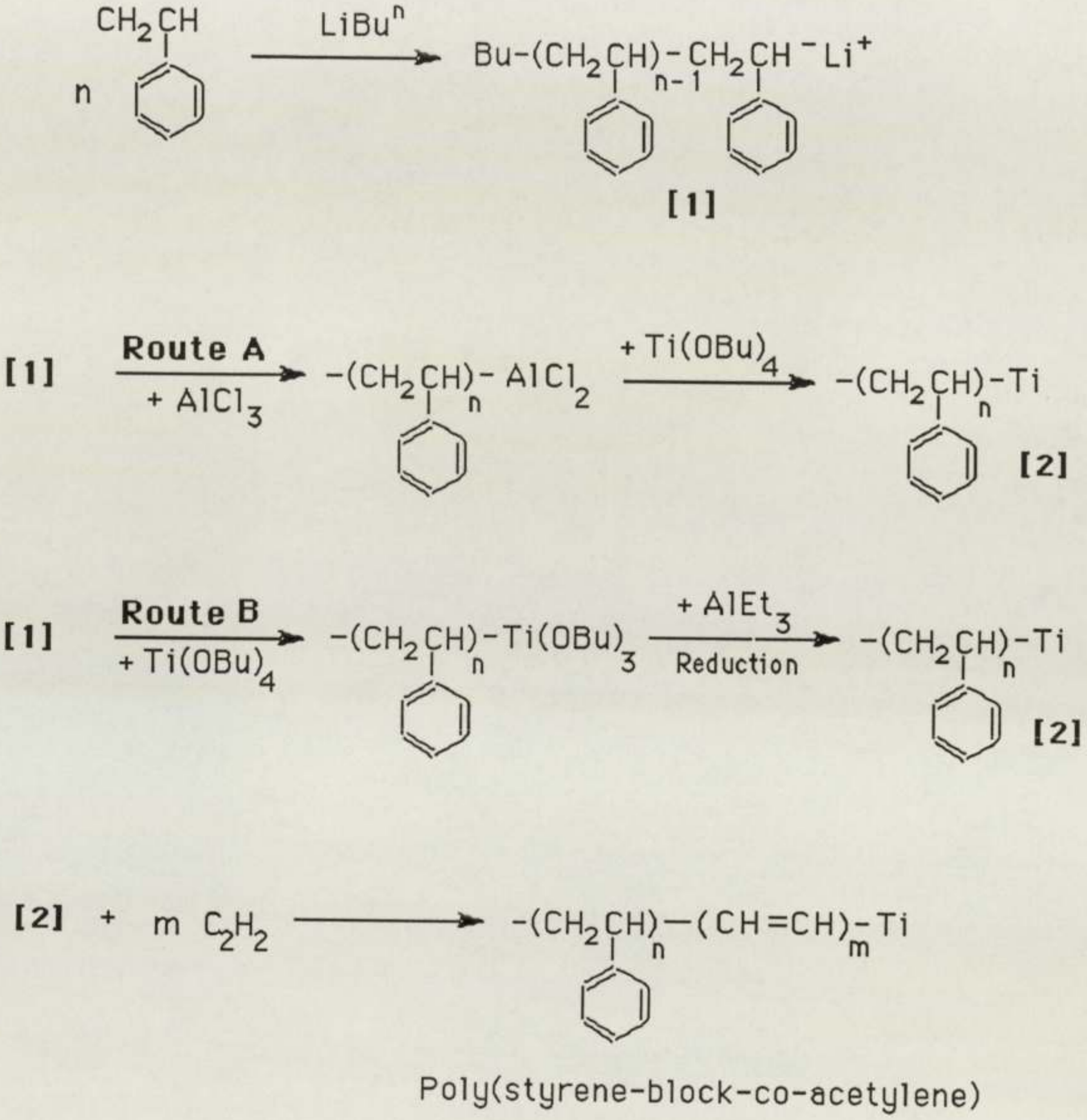

Figure 1.15 Anionic to Ziegler/Natta transformation reaction

Following reports that $Ti(OBu)_4$/LiBu was itself an active catalyst for the polymerisation of acetylene, polystyryl lithium was used to alkylate $Ti(OBu)_4$ directly, displacing a butoxide ligand and after reduction with $AlEt_3$, formed a species that was active towards acetylene polymerisation. The use of anionic polymerisation in this scheme offers several attractive features. The molecular weight distribution of the polystyrene component is characteristically narrow and the average chain length can easily be varied. THF was chosen as solvent since it was an excellent solvent for polystyrene and promoted the formation of ion pair type intermediates which enhance the efficiency of anionic polymerisations and generate narrower molecular weight distribution polymers. It was also thought that THF would co-ordinate at vacant sites on the active titanium atom and in conjunction with the electron donating effect of the butoxide ligands prevent premature termination of the active acetylene polymerisation centers by ß-hydride elimination.

PSty--Ti ----------> Ti--H + PSty

As the acetylene polymerisation proceeded, blue/violet solutions were produced which eventually formed black precipitates after long reaction times. The time required before precipitation occurred varied with the length of the polystyrene block. For example, 36 minutes elapsed before the precipitation of a copolymer formed from a sample of polystyrene of $<M_n> = 42,000$. In most cases the precipitates could be redissolved in THF and precipitated in a 10% THF/90% acetone mixture. Whilst such observations may suggest that the precipitate was a copolymer, they are ambiguous because acetylene, when polymerised in a solution containing dissolved polystyrene, forms a purple solution from which homopolyacetylene can be obtained by precipitation in acetone. Simple adhesion of polystyrene onto the polyacetylene particle may provide an equally plausible explanation of these phenomena.

Gel permeation chromatographic data indicated an increase in $<M_n>$ on addition of acetylene. However owing to the anomalous adsorption effects shown by polyene chains in solution, the copolymers were first brominated which may in turn have caused side reactions such as crosslinking and thereby invalidated the results.

Radio-labelling experiments(81) were claimed to offer conclusive proof of block copolymer formation. ^{14}C labelled n-butyl lithium was used as an anionic initiator and tritiated methanol used to terminate the acetylene polymerisation. The products of an unlabelled copolymerisation performed in the presence of ^{14}C and ^{3}H containing polystyrene sample showed only low ^{14}C and ^{3}H contents, whereas labelling experiments showed significant ^{14}C and ^{3}H counts. This result suggests that polystyrene is effectively removed by washing and so it is likely that chemical combination of the two blocks has taken place during the copolymer synthesis By isolating the unreacted polystyrene the yields of copolymer were estimated to be between 2 and 5 percent. Such low yields may arise because of the competition between THF and acetylene for the active polymerising centre, but such low yields are not uncommon among soluble Ziegler/Natta systems.

Aldissi(85-90) has studied the formation of block copolymers of acetylene using the anionic to Ziegler/Natta transformation route with the comonomers, isoprene, ethylene and styrene. The fibrillar morphology, which is characteristic of polyacetylene chains, became less apparent as the quantity of the comonomer in the sample was increased.

GPC analysis showed that the narrow distributions characteristic of the block prepared by anionic polymerisation were maintained in the samples of copolymer, the polydispersity typically being 1.15-1.2. The molecular weight distribution curve for the copolymer sample was displaced with respect to that of the non-acetylenic homopolymer and by comparison of the two curves, an estimate of the polyacetylene chain length could be made. This value was found to vary with carrier block length, long carrier chains were associated with short polyene units. For example polyacetylene chains of molecular weight 7000-10000 were observed with carrier blocks of molecular weight 1500 to 1900. This effect was also observed when considering the activities of the polymeric catalyst. The rate of acetylene uptake was found to be lower for the polymeric catalyst formed by alkylation of $Ti(OBu)_4$ by the living polymer than for $Ti(OBu)_4$ alone and the activity was found to differ in each of the three carrier chain types and chain lengths.

The uv/visible absorption spectrum of the copolymer film exhibits a broad absorption similar to that observed for films of polyacetylene. When the two bands are compared the wavelength at which the maximum absorbance occurs is reduced and the band width greater in the copolymer film. These observations indicate that the copolymers contain on average shorter conjugated sequences than polyacetylene and that the distribution of conjugation lengths has increased as a result of copolymerisation. The disruption of the conjugated structure of the polyacetylene chain by steric interaction with blocks of the comonomer has been used to explain this result.

At high polyacetylene content, the copolymers show electrical properties similar to those of polyacetylene itself. The materials can be doped and metallic conductivities can be attained. Figure 1.16 shows the variation in conductivity of an I_2 doped sample of polystyrene-block-co-acetylene as a function of the composition of the copolymer.

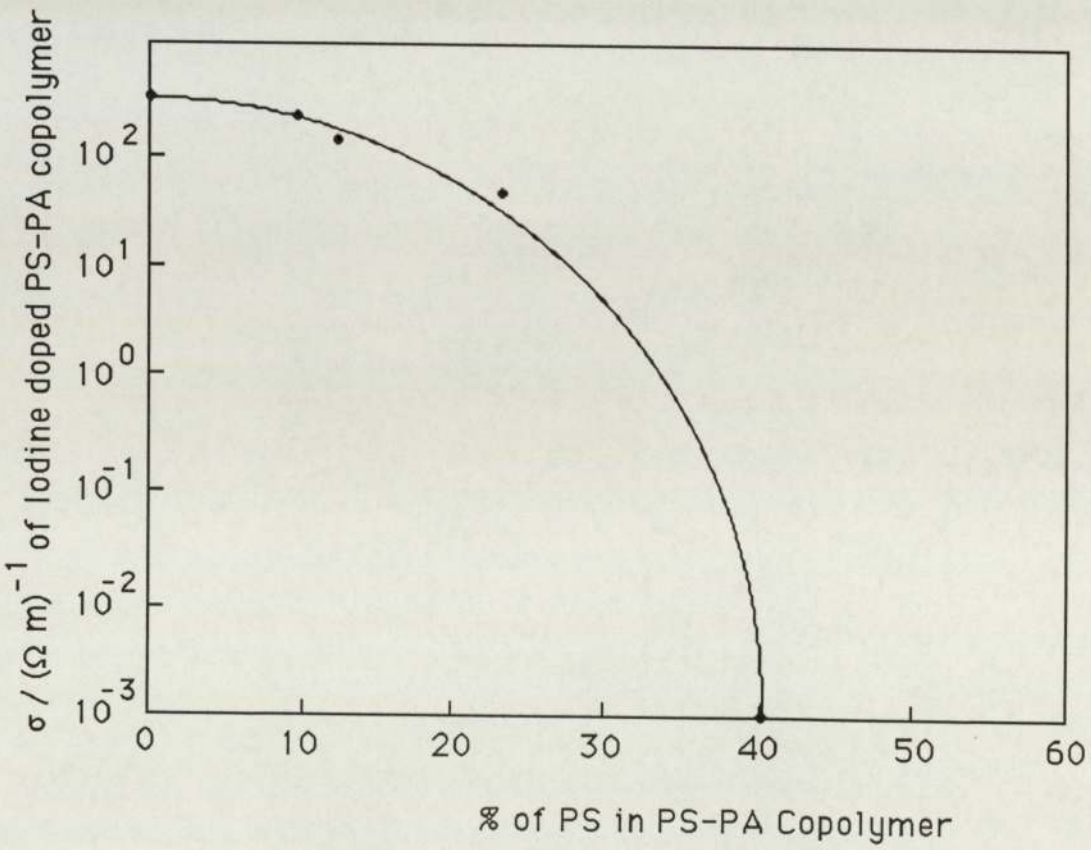

Figure 1.16 Electrical Conductivity of PS-PA copolymer films saturated with Iodine as a function of composition (vol. fraction PS)

The conductivity decreased as the amount of "insulating" material in the copolymer increased. However the observed tail-off became dramatic at about 16% volume fraction of polyacetylene. The observed conductivity in these samples has been attributed to the existence of small metallic domains of doped polyacetylene within the insulating matrix. In the "conducting state" the concentration of these domains is high enough to form a network of interdomain contacts throughout the material. As the concentration of the insulating chains of the copolymer is increased, a point is reached at which the network is broken and a barrier to interdomain conduction is created. If the concentration of insulating polymer is increased further past this point (which is known as the percolation threshold,(93) the conductivity of the material decreases dramatically as observed in figure 1.16. This conclusion is supported by the effects observed on compression of the sample. The conductivity of a sample containing 40% volume fraction polystyrene increased when the pressure was raised to 10 KBar. This increase may be interpreted in terms of a decrease in the inter-chain void volume and subsequent increase in the density of the polyacetylene domains.

The copolymers may be classified according to the chain lengths of the block prepared by anionic polymerisation. The materials then fall into one of the following categories:

(i) Soluble short chain anionic blocks that produce insoluble copolymer films that become conducting after doping.

(ii) Soluble medium length anionic blocks ($<M_w>$ = 8000-10000 when polyisoprene is used) that yield soluble copolymers that become conducting after doping.

(iii) Soluble long chain anionic blocks that produce soluble copolymers the electrical properties of which are unaffected by doping and remain insulating.

The range of chain lengths of the soluble block accommodated within each of the three categories is determined by the nature of the comonomer. Shorter chains of polyisoprene are required to confer solubility on a conducting polyisoprene-block-co-acetylene compared with the length of polystyrene segments required to produce soluble and conducting polystyrene-block-co-acetylene. It should also be noted that in samples of polyethylene-block-co-acetylene prepared using an anionic to Zieger/Natta transformation reaction, the length of the chains of polyethylene prepared by anionic polymerisation is limited to 18 monomer units because of the insolubility of chains of length exceeding this.

The electro-chemical properties of these copolymers have been investigated and electrochemical cells analogous to those fabricated from two polyacetylene electrodes and a lithium perchlorate electrolyte(94) have been constructed. It was observed that the copolymer electrodes could be charged and discharged at a faster rate than those of the polyacetylene counterpart. This observation suggests that the polyacetylene chains are more accessible to electrolyte when in the copolymer form which presumably results from the swelling effects of the anionic chain in the electrolyte solution.

Polyacetylene is an environmentally unstable polymer and its degradation, which proceeds by an autoxidation mechanism, can be followed by monitoring the decay in conductivity of the material as a function of the time of its exposure to air. The conductivity of a copolymer was found to decay more rapidly than that of polyacetylene itself when the materials were examined under similar conditions which suggests that the inter-chain interactions between the polyacetylene blocks are reduced in the copolymer rendering the doped chains more susceptible to oxidative attack.

1.6.2.2 Anionic-to-Luttinger transformation reactions

Soluble block copolymers of acetylene and isoprene have been synthesised by a transformation route which exploits the activity of certain cobalt species towards acetylene polymerisation.(95) The route involves the synthesis of polyisoprenyl lithium by anionic polymerisation, followed by alkylation of a suitable cobalt species with the living polymer. The cobalt species generally used in acetylene polymerisations is $Co(NO_3)_2 \cdot 6H_2O$(96). This compound is clearly unsuitable for use in the transformation scheme since the water would destroy the living polymeric carbanion before carbon-cobalt bond formation could occur. The species chosen for this study was therefore anhydrous $CoCl_2$ in dry THF.

Acetylene polymerisations using Luttinger catalysts are normally performed at low temperatures (about -80°C) to avoid catalyst decomposition. It is interesting to note that the catalyst with the polymeric component can be used at ambient temperature and is less sensitive to oxygen and moisture than the corresponding titanium one.

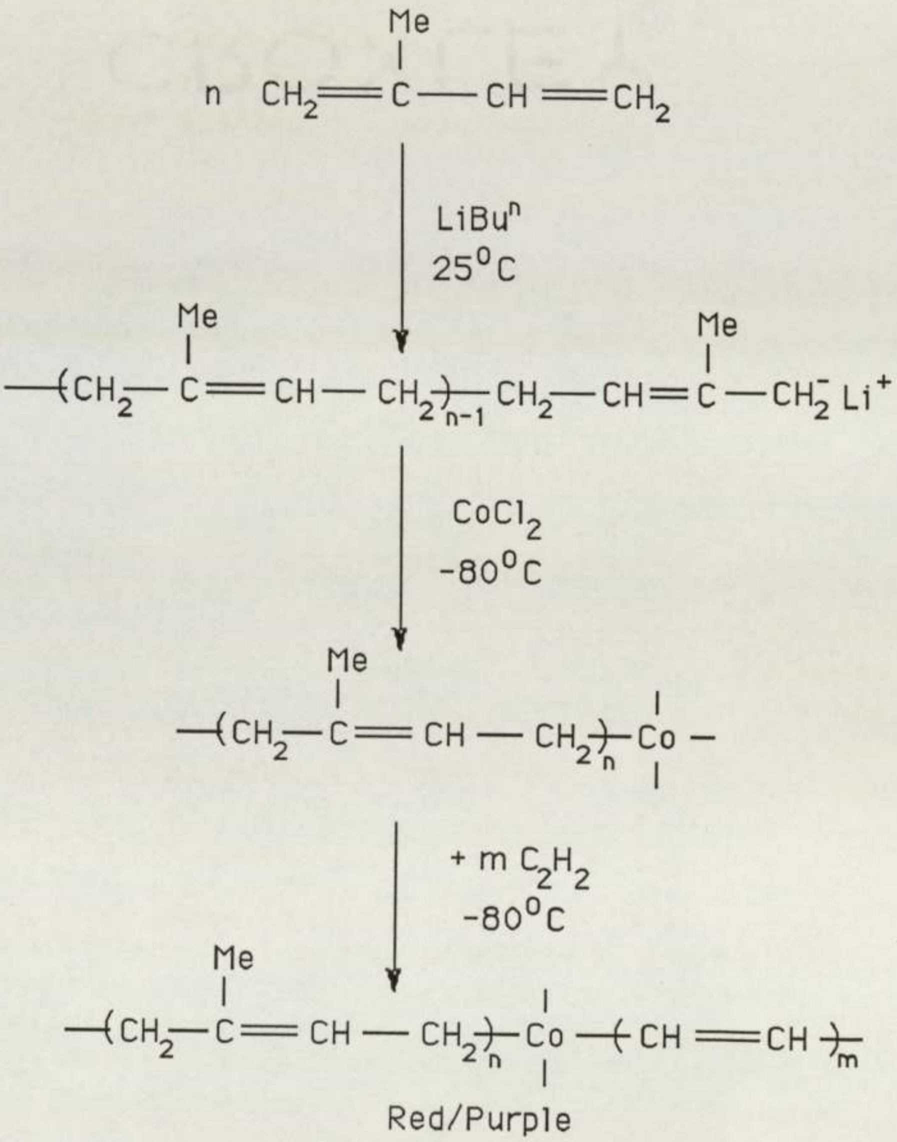

Figure 1.17 Anionic to Luttinger transformation reaction

1.6.2.3 Block copolymers by modification of a suitable soluble homopolymer

Block copolymers which contain polyacetylene segments have been prepared by the modification of a suitable homopolymer. Two mechanisms by which the conversion can be achieved involve (a) the base catalysed elimination of HCl from polyvinylchloride (PVC) and (b) the base catalysed rearrangement of polybutadiene.

Although Marvel(105) noticed that polyenes were generated from the reaction of potassium hydroxide and PVC in organic solvents, the reaction products were not fully characterised. Aqueous solutions of sodium, potassium and calcium hydroxides have been reported as effective dehydrochlorination reagents for PVC, but the products contained considerable quantities of aromatic compounds and oxidation products. Several non-aqueous, basic systems e.g. sodium amide in liquid ammonia have also been investigated and these required elevated temperatures before satisfactory reaction rates were achieved. The most convenient and controlled elimination of this type appears to be that described by Kise(106). PVC as a powder, film or in solution was reacted with aqueous sodium hydroxide at 60-80°C in the presence of a phase transfer catalyst. The catalysts used were long chain alkyl quarternary ammonium or phosphonium compounds. Solutions of PVC, when treated with the base and phase transfer catalyst, immediately turned red/brown and within a few minutes a black precipitate formed. The infra-red spectrum of this precipitate resembled that of trans-polyacetylene and showed a reduction in the absorption strength of the bands, characteristic of PVC, relative to the starting material. The degree of elimination of the dehydrochlorinated PVC was estimated by the reduction in weight which occurred during the reaction.

When low concentrations of base and catalyst were used, the progress of the reaction could be monitored by uv/visible spectroscopy. Solution samples displayed fine structure which resembled the characteristic spectrum of a mixture of polyenes with an average conjugation length of ten. Films of the dehydrochlorinated PVC exhibited a broad absorption, centred at 420nm, that increased in intensity as the reaction proceeded.

The nature of the phase transfer catalyst appeared crucial in determining the efficiency of the elimination process. Optimum efficiency was achieved by balancing the lipophilic and hydrophilic properties of the catalytically active compound.

The observation that the percentage conversion increased with increasing PVC molecular weight was used as evidence for the elimination proceeding by a `zipping` type mechanism. The carbon atoms α to the double bond were activated and hence their associated hydrogen atoms more susceptible to attack by the base. Large numbers of chain ends, present in the low molecular weight samples, would then be thought to produce lower conversions.

Although the electrical conductivities of these copolymers were not reported, materials produced by the base catalysed elimination of poly(vinylidene halides) in the presence of phase transfer catalysts(107,108) could be doped with iodine to produce a conductivity of $6.0 \times 10^{-5}\ \Omega^{-1}\mathrm{cm}^{-1}$. It is interesting to note that these copolymers contain polyconjugated sequences which are substituted analogues of polyacetylene.

Poly(1,3-butadiene), an alternating copolymer of acetylene and ethylene and poly(ethylene-block-co-acetylene) are isomers. Thermodynamic calculations show that the equilibrium for this pair of isomers should lie in favour of the block copolymer.

$$-(CH_2\text{-}CH_2\text{-}CH{=}CH)_n\text{-} \quad \text{<------->} \quad \text{-}[\text{-}(CH_2\text{-}CH_2)_x\text{-}(CH{=}CH)_Y\text{-}]_n\text{-}$$

If a kinetically feasible route could be found then the double bonds present in the repeat units of 1,3 butadiene should undergo a rearrangement to yield a block copolymer containing polyene segments. Dias and McCarthy(97,98) have reported the base catalysed isomerisation of polybutadiene using potassium t-butoxide in THF and dimethyl sulphoxide. The proposed mechanism is shown in figure 1.18.

The colour changes that occur during the isomerisation reaction were monitored by uv/visible spectroscopy and indicated the appearance of conjugated sequences along the polybutadiene backbone. The solution of polybutadiene in THF changed from colourless to blue/black when the base catalyst was added. This change was most probably due to the presence of the polyanion, as the blue colour could be instantly discharged by the addition of oxygen to yield an orange/red solution and a precipitate of crosslinked polymer. When the reaction mixture was quenched with methanol, the colour became violet. Following isomerisation for 72 hours, the uv/visible spectrum of a methanol quenched sample exhibited a maximum absorbance at 230nm indicating that most of the induced conjugation was in the form of dienes and trienes. A broad peak centred at 512nm indicated that the polymer contained a range of conjugation lengths, the average length corresponding to ten conjugated double bonds. The polymer was isolated as a violet, air sensitive solid.

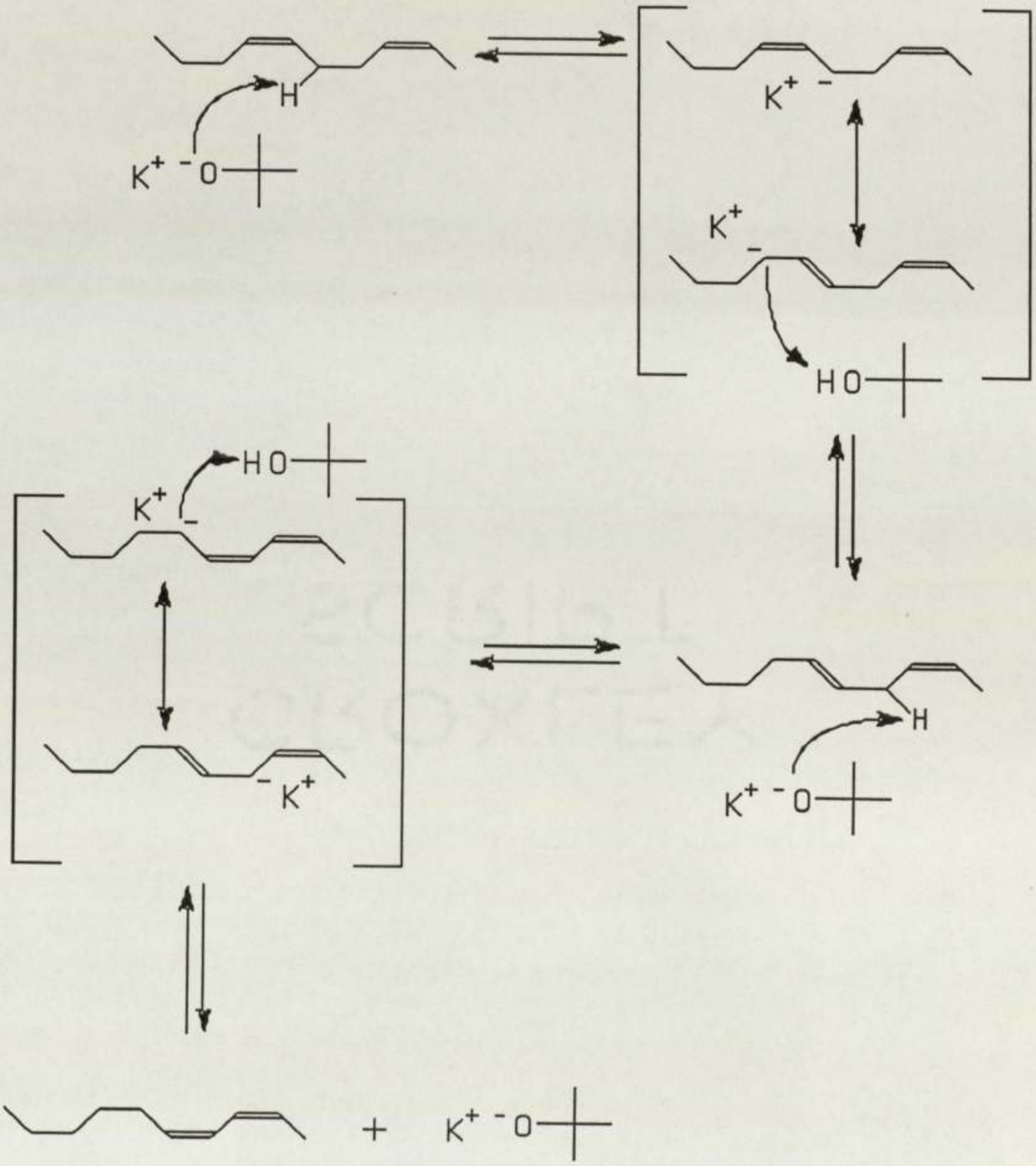

Figure 1.18 Poly(acetylene-co-ethylene) via isomerisation of poly (1,3-butadiene)

The isomerisation was also followed by ^{1}H NMR spectroscopy. The resonance at δ = 1.87, attributable to the allylic protons, four of which are lost each time the conjugated sequence is extended by one acetylene unit, is seen to decrease with respect to an internal standard. The infra-red spectrum also shows the development of a broad asymmetric shoulder on the long wavelength side of the carbon-carbon double bond absorbance at 1630cm^{-1}, characteristic of conjugated double bonds.

Although the rate of isomeration was temperature dependent, the average conjugation length of the copolymer was unchanged with temperature. This indicates that the degree of isomerisation is controlled by kinetic rather than thermodynamic factors. From figure 1.18, it can be seen that the feasibility of the isomerisation process will be determined by the relative ease with which the base abstracts the allylic hydrogen of the growing polymer chain and the ability of the polyanion to regain the proton from the protonated base.

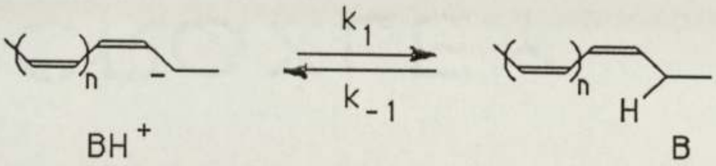

The average conjugation length should therefore be a function of base strength, low basicity being associated with long conjugation lengths. Dias and McCarthy used potassium acetonitrilide, potassium tertiarybutoxide and potassium cyclopentadienide as base catalysts in three separate isomerisation reactions. All three isomerised samples showed a broad polyene absorption in the uv/visible spectrum. The maximum absorbance of this band in the spectra occurred at 526nm, 512nm and <412nm for potassium cyclopentadienide (weakest base), potassium t-butoxide and potassium acetonitrilide (strongest base), respectively.

Doping experiments showed that iodine could interact with the isomerised polymer film and the conductivities of the resulting materials were approximately 5 x 10^{-5} Ω^{-1}cm^{-1}.

1.6.3 Graft copolymers

1.6.3.1 1:1 Graft copolymers

Copolymers in which a single chain of polyacetylene was grafted onto a polystyrene or polyisoprene carrier have been prepared by Baker and Bates.(99-102) The polymerisation, depicted in figure 1.19, was effected by adding $AlEt_3$ in toluene to a solution of $Ti(OBu)_4$, acetylene and the carrier polymer. In order for the grafting reaction to occur, the carrier polymer was first modified to incorporate electrophilic sites which attack the growing polyacetylene chains at the nucleophilic sites of the titanium/carbon terminus.

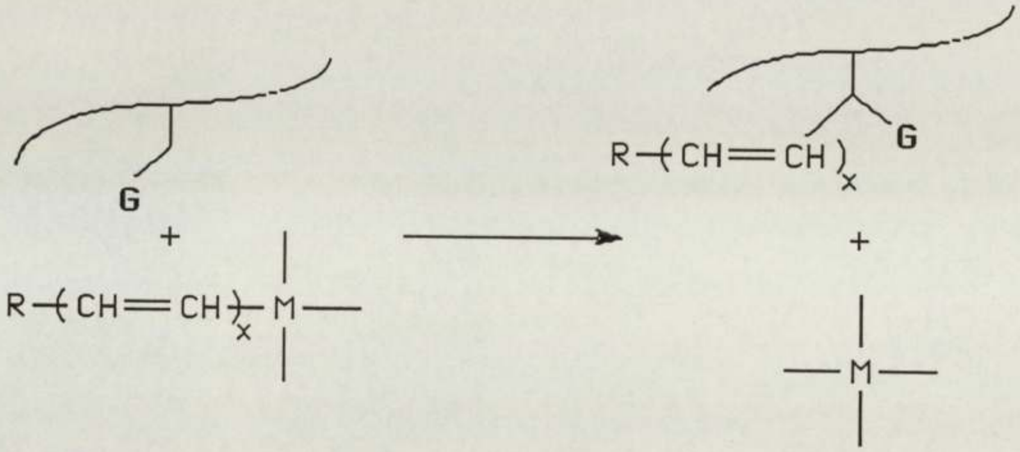

M = titanium atom on growing polyacetylene chain

G = electrophilic graft site (e.g. epoxide) on carrier polymer

Figure 1.19 Schematic representation of the graft copolymerisation of acetylene and isoprene.

Carrier polymers with narrow molecular weight distributions ($\langle M_n \rangle = 2 \times 10^5$) were prepared by anionic polymerisation and the graft sites in the form of carbonyl or epoxide groups were introduced by reacting the polymer with molecular oxygen or 3-chloroperoxybenzoic acid. Although polyisoprene was amenable to such chemistry, polystyrene had to be used as a random copolymer containing a small amount of butadiene. The grafting reaction was enhanced, by the introduction of 15-20 graft sites per carrier chain. The grafting reaction was then carried out using a large excess of carrier to ensure that only one polyacetylene block was grafted onto each carrier macromolecule. The reaction was complete within several minutes and the resulting maroon/blue solution of copolymer could be stored under an inert atmosphere for several months before it degraded. Oxidation of the solutions occurred on exposure to air and within a few days the colour changed to red then yellow.

Proof that grafting had occurred during these reactions was obtained from the results of a control experiment in which unmodified polyisoprene was used in place of the activated carrier polymer and methylethylketone added to stimulate termination by electrophilic attack. Macroscopic black particles were rapidly evolved which were shown to contain only traces of polyisoprene.

The catalyst residues were removed from the copolymer by digestion with acetic acid in methanol. Although this step prevented catalytic gelation, by the reaction of unsaturated groups in the carrier chain with catalyst residues, its effect on the nature of the copolymer was uncertain. Under conditions employing excess carrier, the product of the grafting reaction consists of copolymer and large amounts (>95%) of unreacted homopolymer. Attempts to separate these mixtures by ultracentrifugation failed and no alternative method of separation was found. Consequently, standard techniques such as elemental analysis and molecular spectroscopy could not be used to determine directly the composition of the copolymer. Furthermore the solubilised polyacetylene was found to adsorb strongly onto a wide variety of surfaces, particularly metals, which made molecular weight determination by normal chromatographic analyses impossible.

Infra-red and uv/visible spectroscopy were used to estimate the overall composition of the samples of copolymer and the trans content of the polyacetylene block. The carrier polymer was assumed to act as an inert diluent and the resulting spectrum was interpreted merely as a linear combination of the spectra of the two parent homopolymers. The method relied on the measurement of extinction coefficients for the two homopolymers, however the actual values of these parameters and the method used for their determination was not quoted in the literature. The composition of each copolymer sample was then calculated by comparing the intensity of the infra-red absorption at 1013cm^{-1} (characteristic of polyacetylene) with a peak characteristic of the carrier polymer. Absorptions in the uv/visible region of the spectrum were used to calculate the compositions of samples of copolymer in solution.

The chain length of the polyacetylene segment in the copolymer was controlled by a termination reaction that exploited the nucleophilic properties of the propagating polyacetylene. When acetone was substituted for the carrier polymer in the grafting reaction, a mixture of low molecular weight acetylene oligomers (polyenes) was produced the average chain length of which was controlled by adjusting the concentration of acetone relative to that of acetylene. In a similar manner, the length of the polyacetylene segments in the copolymer was controlled by varying the number of electrophilic graft sites relative to the concentration of acetylene. The uv/visible absorption spectrum of the graft copolymer showed a broad feature in the visible region similar to that exhibited by solutions of the block copolymers prepared using anionic to Ziegler/Natta transformation reactions. A shift in the position of the maximum absorbance of this peak to longer wavelengths was observed as the concentration of acetylene was increased. This was interpreted as indicating that an increase in the length of the polyene segment of the copolymer had occurred. When the size of the polyacetylene block became sufficiently long, the copolymer precipitated from solution. The term "solubilised polyacetylene " was used to denote solutions of graft copolymer that would pass through filters with a pore size of 2000 Å.

Initial investigations concerning the structure of the copolymers in solution were made by ^{13}C NMR spectroscopy. The NMR spectrum of a sample of copolymer exhibited a doublet at 128.2ppm which was claimed to arise from the solubilised polyacetylene chains. A more rigorous investigation revealed that the original assignment of these peaks was in error(101) and that they were most likely produced by traces of toluene which were present as an impurity. The total absence of resonances attributable to polyacetylene was interpreted in terms of the reduced mobility of these segments in solution which broadens the resonance to such a degree that it is indistinguishable from the baseline. Similar reasoning has been invoked to explain why the polystyrene blocks of a styrene butadiene block copolymer dissolved in hexane escape detection by ^{13}C NMR. This result is not surprising in view of the results obtained from light scattering experiments (which will be discussed in a later section) and is also inferred by the detection of resonances from solid state copolymer samples. When dried samples of the copolymer were examined in the solid state using `magic angle spinning`, a resonance at 138ppm relative to Me_4Si was observed. This value is in agreement with the reported chemical shift of trans-polyacetylene.(104)

As the conditions employed during the synthesis of the graft copolymers favoured the introduction of only one polyacetylene segment per carrier chain, a graft site at the terminus of the carrier would produce a block copolymer identical to those described in section 1.5.4.2. While such species are undoubtedly present in the samples of graft copolymer, the method by which the carrier polymer was modified does not allow selective synthesis of these species.

Diblock copolymers(101) have been synthesised by the grafting technique using polystyrene chains of molecular weight 1×10^5 terminated by methylketone groups. The carbonyl group was presumably introduced by termination of the anionic polymerisation of styrene using acetyl chloride or a similar reagent. Based on the results of infra-red spectroscopy and a knowledge of the molecular weight of the polystyrene, the molecular weight of the polyacetylene segments was estimated to be $\langle M_n \rangle = 6 \times 10^4$. Selective staining of the polyacetylene segments with osmium tetroxide allowed the microstructure of the polystyrene-graft-co-acetylene to be investigated using transmission electron microscopy. When the molecular weight of the polystyrene was 2×10^5 and the polyacetylene content was 15-20%, microdomains of amorphous polyacetylene, 10 to 15nm in diameter, were observed in a matrix of polystyrene. With the diblock copolymers, where the polystyrene molecular weight was 1×10^5 and the polyacetylene content was 35-40%, polyacetylene inclusions, 0.1 to 1 micron in diameter, were observed and when examined by electron diffraction these were found to be single crystals of polyacetylene. The difference in size and crystallinity of the polyacetylene aggregates may be explained by considering the effect of the carrier chain on the polymerisation of acetylene. Large carrier blocks cause disruption of the emerging polyacetylene chains which prevents them from crystallising. Smaller carrier blocks do not produce as great a steric hindrance towards polyacetylene crystallisation. Dynamic light scattering measurements(103) performed on dilute solutions of copolymer indicated the existence of species with a radius of gyration of 1050 ± 200 Å. The presence of such large particles provides yet more evidence for the association of polyacetylene chains in solution.

1.6.3.2 Multigraft copolymers- Lithiation routes

Bolognesi and coworkers(109-116) have prepared graft copolymers containing polyene units where the number of grafted chains per carrier molecule is greater than unity. As the molecular assembly consists of a carrier backbone, which supports numerous pendant chains, the term "comb-like" was used to identify these materials, thereby highlighting the structural difference between these materials and the graft copolymers described in the previous section.

Two principal routes have been devised to synthesise these comb-like graft copolymers, both of which involve reaction of a polydiene with a lithium alkyl.

The $Ti(OBu)_4$ /$AlEt_3$ catalyst system has been shown to be an effective catalyst for the homopolymerisation of acetylene and ethylene. Propagation is thought to occur by a cis insertion reaction of the monomer into a titanium carbon bond. The insertion reaction of pendant vinyl groups on a polybutadiene chain was used to bond titanium atoms to the polymeric matrix. These sites subsequently formed the centres of acetylene polymerisation (Figure 1.20).

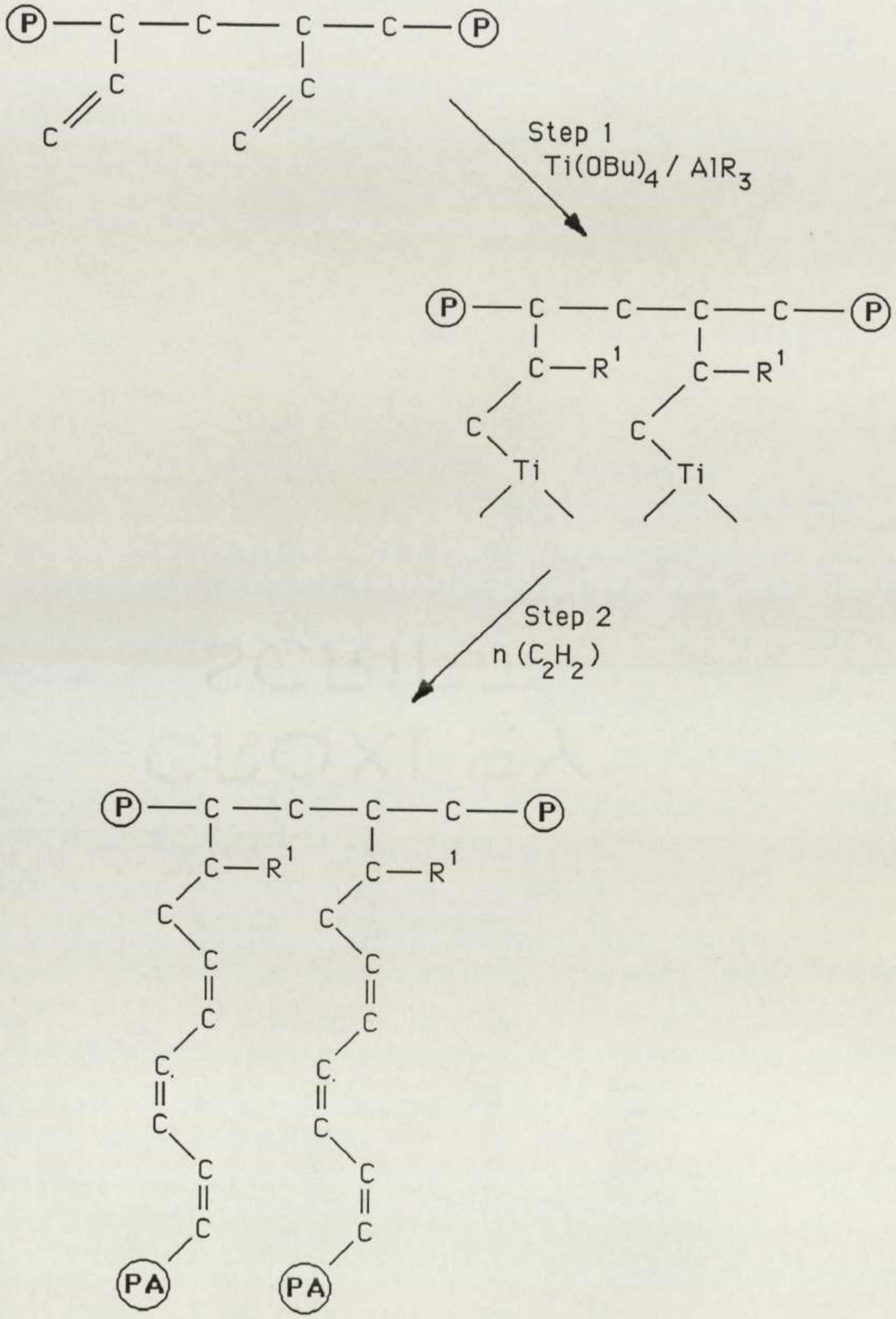

Figure 1.20 Synthesis of a comblike graft coplymer of polyacetylene

The number of polyacetylene chains per polybutadiene molecule was estimated by NMR spectroscopic analysis of the number of unreacted 1,2-vinyl groups remaining after grafting. Control of the number of polyacetylene chains incorporated per polybutadiene backbone was achieved by varying the concentration of catalyst. The percentage of polyacetylene in the copolymer increased as the molar ratio of $Ti(OBu)_4$ to pendant vinyl groups (1,2-units) of the polybutadiene carrier increased. At compositions exceeding 51% by weight of polyacetylene, the number of polyene chains per carrier presumably becomes so large that the polybutadiene backbone can no longer support these units in solution and precipitation of the copolymer results. The nature of the carrier chain, its molecular weight and the percentage of 1,2-units also affect the solubility of the copolymer. Polyisoprene of $<M_v>$ = 700,000 and 1% 1,2 content produces an insoluble powder when used as a carrier ; polybutadiene of $<M_v>$ = 210,000 and 4% 1,2 content yields soluble copolymer under similar conditions. The polyacetylene content was also controlled by varying the flow rate of acetylene and adjusting the reaction time.

Infra-red and uv/visible spectroscopic investigations revealed the presence of absorptions due to both polyacetylene and the carrier polymer in the spectrum of the copolymer. A peak at $1015cm^{-1}$ was assigned to the out-of-plane bending mode of trans polyacetylene. The cis-polyacetylene absorption, which is usually observed at $740cm^{-1}$ could not be used to estimate the cis/trans ratio due to overlapping of this peak with polybutadiene absorptions. In the uv/visible spectrum of the solution, a broad peak was observed centred at 580nm, similar to that observed for suspensions of crystalline polyacetylene. The shift of this absorption to shorter wavelengths, compared to that of polyacetylene, has been explained in terms of a decrease in the average conjugation length and a reduction of polyacetylene interchain interactions. Indeed the results of Raman spectroscopy suggest that the average length of the polyacetylene segments is relatively short (20-25 acetylenic units).

In an alternative preparation of graft copolymers, carbanions were introduced at the allylic positions of a polydiolefinic backbone by reaction of polybutadiene with s-butyllithium in the presence of tetramethylethylenediamine. The carbanions were capable of alkylating $Ti(OBu)_4$ to produce carbon titanium bonds thus forming catalytic sites at which acetylene could polymerise to produce a graft copolymer. The optimum Li:Ti molar ratio for the production of copolymers with high polyacetylene content was found to be 2:1. This result is in agreement with that obtained for the graft copolymerisation of ethylene with polybutadienyllithium/$TiCl_4$ using a similar route which also suggested that the maximum number of graft sites occurs at Li:Ti = 2:1.(117) When the Li:Ti ratio was 1:1, the copolymer precipitated as a gel, presumably due to cross linking.

Thin films of the copolymer were cast from solution, stained with osmium tetroxide and examined by transmission electron microscopy. An inhomogeneous morphology was observed in which spherical polyacetylene microdomains less than 50Å in diameter were embedded in an amorphous matrix. Some "worm like" aggregates 1000-4000Å in length and 100-500Å in diameter were also apparent. Wide angle X-ray analysis and electron diffraction studies showed that these structures consisted of randomly oriented spherical polyacetylene microdomains less than 100Å in diameter. Dilute solutions of the copolymer were examined by light scattering. Because the wavelength of light used fell within the broad polyene absorption band of the copolymer, resonance enhanced scattering resulted in the scattered intensity being three orders of magnitude greater than that observed for polybutadiene. For this reason, analysis of the results was performed making the assumption that the scattering was predominantly due to the polyacetylene segments. For polybutadiene solutions the average radius of gyration (R_G) of the polymer molecules in solution was estimated to be 6-7nm. R_G for the copolymer in toluene was calculated to be 20-65nm depending on the polyacetylene content, indicating significant aggregation of the polyacetylene segments in solution. Large ρ_V (the depolarisation ratio for vertically polarised light) values were also observed which indicate that the polymer particles exhibit considerable optical anisotropy, which may have been due to the intrinsic anisotropy of the polyacetylene chains and/or the anisometry of the particle. If R_G is calculated from the dimensions of a typical worm-like aggregate observed in thin films of the copolymer, then assuming an elipsoidal shape, the value obtained is 22-90nm. This value correlates well with the values obtained from solution measurements and suggests that the structure of the aggregates in solution may also be worm like.

The reaction of the graft copolymer with iodine and bromine was investigated by infra-red spectroscopy. Whilst iodine gave no reaction, bromine added to the unsaturated units of both polacetylene and polybutadiene producing carbon-bromine bonds which were observed in the infra-red spectrum. Infra-red investigations on stretched samples of copolymer showed large dichroic ratios for certain polyacetylene bands, behaviour attributed to the alignment of the polyacetylene chains along the stretching direction. Upon reaction with iodine, the conductivity of the copolymer films increased up to a maximum of 1.4×10^{-3} Sm^{-1}, but the value was found to depend markedly on polyacetylene content.

1.6.3.3 Multigraft copolymers from p-doped polyacetylene

The work outlined in section 1.6.3.2 was based on the production of a graft copolymer by the growth of polyacetylene chains on the backbone of a soluble, carrier polymer. An alternative synthesis of graft copolymers involves the growth of soluble polymer chains at selected sites along a polyacetylene backbone. Although the structure of this type of graft copolymer is fundamentally different from that of the graft copolymers described earlier, the ability of the soluble polymer grafts to solubilise the polyacetylene backbone is retained. Kminek and Trekoval(118,119) have prepared graft copolymers in which polymethylmethacrylate (PMMA) or polybutylmethacrylate (PBMA) chains have been grown onto a sodium doped polyacetylene backbone. Polyacetylene was first prepared as a powder using the Ziegler/Natta catalyst $Ti(OBu)_4/AlEt_3$ in toluene. Sodium napthalide was then reacted with a suspension of the powder in THF to produce the charge transfer complex $[Na_{(0.057)}(CH)_x]$. Anionic polymerisation of methylmethacrylate at the carbanion sites of the polymeric complex resulted in the grafting of the polymethylmethacrylate chains onto the polyacetylene matrix. During the grafting reaction, the suspended polyacetylene dissolved yielding a purple/blue solution which showed the characteristic broad polyene absorbance in the uv/visible spectrum. The λ_{max} of this peak occurred at 500nm which was similar to the wavelength quoted by Baker and Bates (Section 1.6.3.1) The authors concluded that the 100nm difference in the position of the two peak maxima was primarily due to the differences in the molecular weight of polyacetylene in the two systems. However it should be noted that the difference could be due in part to differences in the structures of the two types of copolymer.

The solubility of the copolymer was seen to depend markedly on composition. Experiments showed that, for 100% solubility to be achieved, the mole ratio of methylmethacrylate to unsaturated acetylenic repeat units had to exceed 1.5. At lower ratios, quantities of precipitate remained suspended in a brown solution. The production of soluble material may have arisen by one or two mechanisms. (a) The PMMA chains, grafted onto the polyacetylene matrix, were long enough to confer solubility on the copolymer. (b) Electron transfer from the polymeric complex to methylmethacrylate had occurred which yielded a mixture of homopolymers. In the latter case the effect on the molecular weight and morphology of the polyacetylene may have been altered drastically perhaps resulting in chain cleavage and producing "soluble homopolyacetylene". Although mechanism (b) may have been occurring during the reaction, the marked dependence of the solubility on the concentration of methylmethacrylate was interpreted as indicating that mechanism (a) predominated.

The molecular weight distribution of the samples of copolymer was examined by gel permeation chromatography (GPC). Most of the material was present in a purple coloured fraction $<M_n> = 1.5 \times 10^4$ and polydispersity = 3.1. This broad distribution was attributed to the effect of chain transfer and autotermination reactions which are known to occur in methylmethacrylate polymerisations initiated by organo-sodium compounds.(120) The fact that the polyacetylene molecular weight before reaction had been estimated as 10^3 yet after reaction, the fraction of molecular weight 10^3 was colourless was claimed to offer strong evidence for the grafting of polymethylmethacrylate onto the polyacetylene matrix. It must however be stressed that the molecular weights were determined by two different techniques and that such comparisons may be invalid.

Films of the copolymer were found to be stable in an inert atmosphere but dilute solutions in THF decolourised within a few days. NMR spectroscopy of a dilute solution of copolymer in $CDCl_3$ detected only resonances that were attributable to polymethylmethacrylate.

Dandreaux, Galvin and Wnek(83) noted that a variety of monomers could be polymerised using alkali metal graphitides and modified this method to form graft copolymers from sodium doped polyacetylene. The mechanism proposed for the copolymerisation was similar to that described for the grafting of polyalkylmethacrylates involving attack of the polymeric carbanion on for example ethylene oxide to cause ring opening and oxyanion formation, followed by further ethylene oxide propagations (figure 1.21). The fact that half the product was soluble in methylene chloride was interpreted as resulting from chain transfer and termination reactions which produced low molecular weight polyethylene oxide.

Although no information was reported concerning the number or the length of the polyethylene oxide chains which had become attached to the polyacetylene backbone, the materials could be doped with iodine to give conductivities of 1 $\Omega^{-1}cm^{-1}$. The observed decrease in conductivity, relative to that of doped polyacetylene, was thought to be due to the formation of an insulating surface layer of polyethylene oxide. Alternatively, it should be noted that each grafted unit produced a saturated carbon at the polyacetylene chain which would disrupt the conjugation of the double bonds of the polyene and may have resulted in reduced conductivities when the number of grafts per polyacetylene was high.

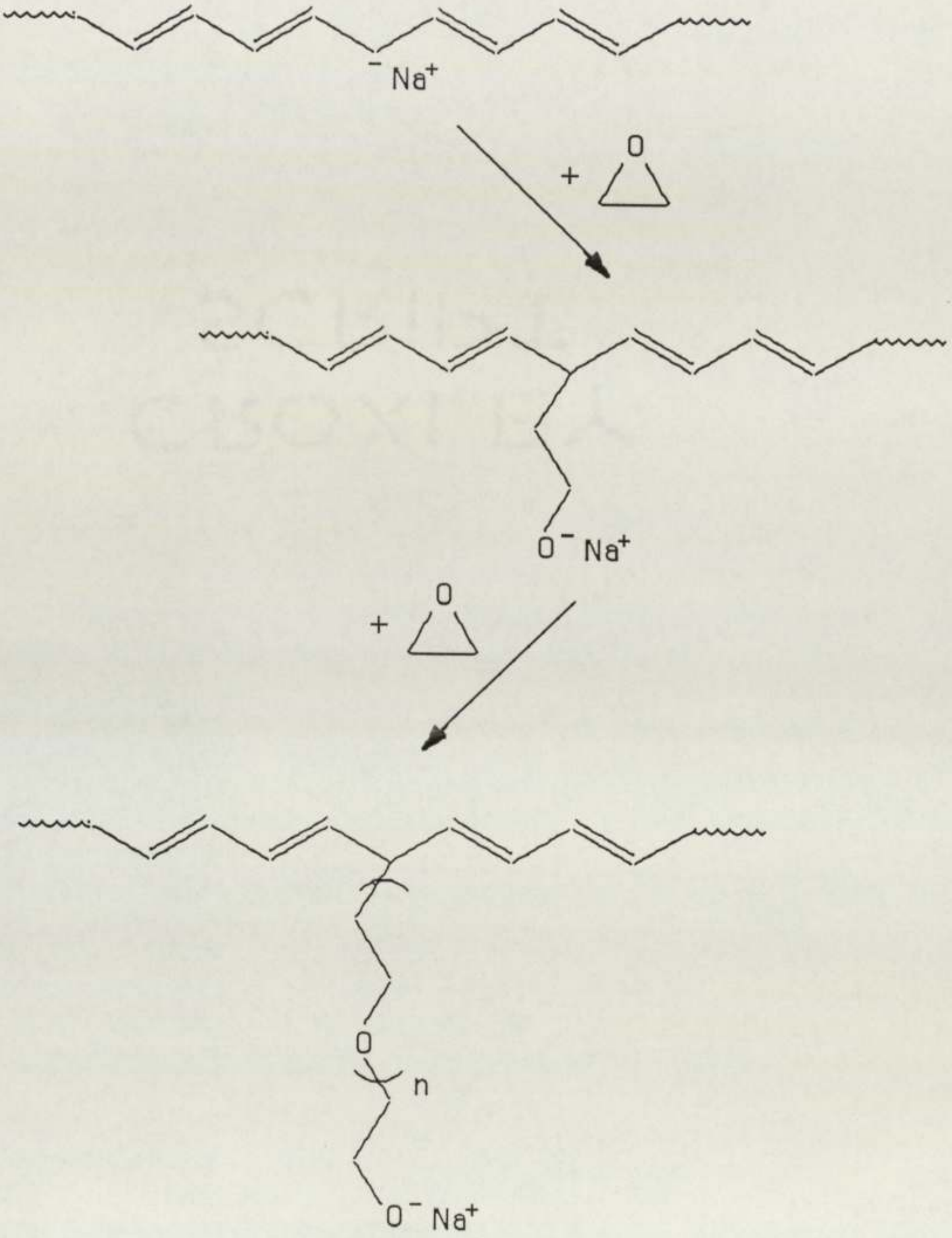

Figure 1.21 Multigraft copolymers from p-doped polyacetylene

1.6.4 Metathesis routes to acetylene copolymers

There is an extensive literature recording the ability of metathesis type catalysts to polymerise substituted acetylenes.(18) Copolymerisations of acetylene with substituted acetylenes, similar to those described in section 1.6.1, have also been reported and in one case, patented as a method of producing a soluble polyacetylene.(121) Copolymer formation between an alkyne and a cyclic olefin has been investigated by Katz.(122) It was claimed that the results of these experiments offered strong evidence for both the metathesis reaction and the acetylene polymerisation proceeding by similar mechanisms with a common intermediate, namely the metal carbene.

Recently, two metathesis routes to copolymers containing polyacetylene have been reported, both involving the synthesis of precursor polymer segments which may be converted to polyacetylene by thermal elimination.

Chein(123) has investigated the copolymerisation of cyclopentene with 7,8 - bis(trifluoromethyl)-tricyclo-[4,2,2,$0^{2,5}$]-deca-3,7,9-triene. The resulting polymer was cast from solution into films which thermally eliminated hexafluoroxylene yielding a copolymer which contained pentenylene and polyene units. The copolymerisation was performed by adding a mixture of the comonomers to a premixed solution of tungsten hexachloride and tetramethyltin in chlorobenzene. The reaction was allowed to proceed to 50% conversion to minimise homopolymer formation. The effect of varying the comonomer ratio of the feed on the composition of the copolymer was examined by elemental analysis and TGA. Even when the copolymer contained 75% polyacetylene, ESR measurements showed that the average conjugation length was only about four double bonds. The materials could be doped with iodine and a maximum conductivity of 5.9×10^{-4} Scm^{-1} was achieved for the sample containing 75% polyacetylene.

The design of isolatable, well characterised alkylidene complexes which show high activity in both metathesis reactions and ring opening polymerisations together with some tolerance towards functional groups in the monomer, provide the basis for a route to soluble block copolymers which contain polyene segments. Grubbs, Schrock(124-126) and Kress(127) have shown that norbornene may be efficiently polymerised by ring opening using catalysts with the general formula

$M(CHR)(NAr)(OCMe_3)_2$ where R = alkyl, M = Mo or W and Ar = $2,6\text{-}C_6H_3\text{-}iPr_2$. NMR studies indicate that the alkylidene group of the catalyst is retained at the terminus of the polymer chain and addition of a second monomer such as endo-5,6 dicarbomethoxynorbornene yields a block copolymer with a polydispersity approaching unity. Behaviour of this nature is similar to that observed in polymers prepared by ionic living polymerisation techniques, where termination reactions are essentially absent. One characteristic of ring opening metathesis polymerisations is that the polymer chain contains an unsaturated unit which may participate in metathesis reactions at the locus of polymerisation, thus causing the molecular weight distribution to broaden. It may be concluded that in the case of norbornene polymerisation steric hindrance inhibits both bimolecular termination and cross metathesis reactions thus allowing living polymerisation to occur.

Schrock(128) has copolymerised norbornene with 7,8-bis(trifluoromethyl)tricyclo[4.2.2.$0^{2.5}$]deca-3,7,9-triene by sequential addition using an alkylidene catalyst, the reaction being terminated by the addition of benzaldehyde (figure 1.22). Orange/red toluene soluble di- and triblock copolymers containing polyene segments were then prepared by thermal elimination of o-$C_6H_4(CF_3)_2$ from the precursor. GPC studies indicated that when B in figure 1.22 equalled five, the polymerisation was well behaved yielding materials of narrow molecular weight distribution. When B = 10 a high molecular weight peak was observed and was attributed to aggregation or cross linking of the polyene segments of the macromolecule. It was also claimed that cross linking/aggregation occurred when the length of the polyene segment exceeded 15 double bonds, the role of the polynorbornene chains being to solubilise the aggregate and to regulate the number of macromolecules present in each particle. The uv/visible spectrum of the diblock copolymer showed a broad absorption in the visible region, but λ_{max} for a sample supposedly containing a polyene segment of 41 double bonds, actually occurred at 475nm, equivalent to a conjugation length of only 11 units.

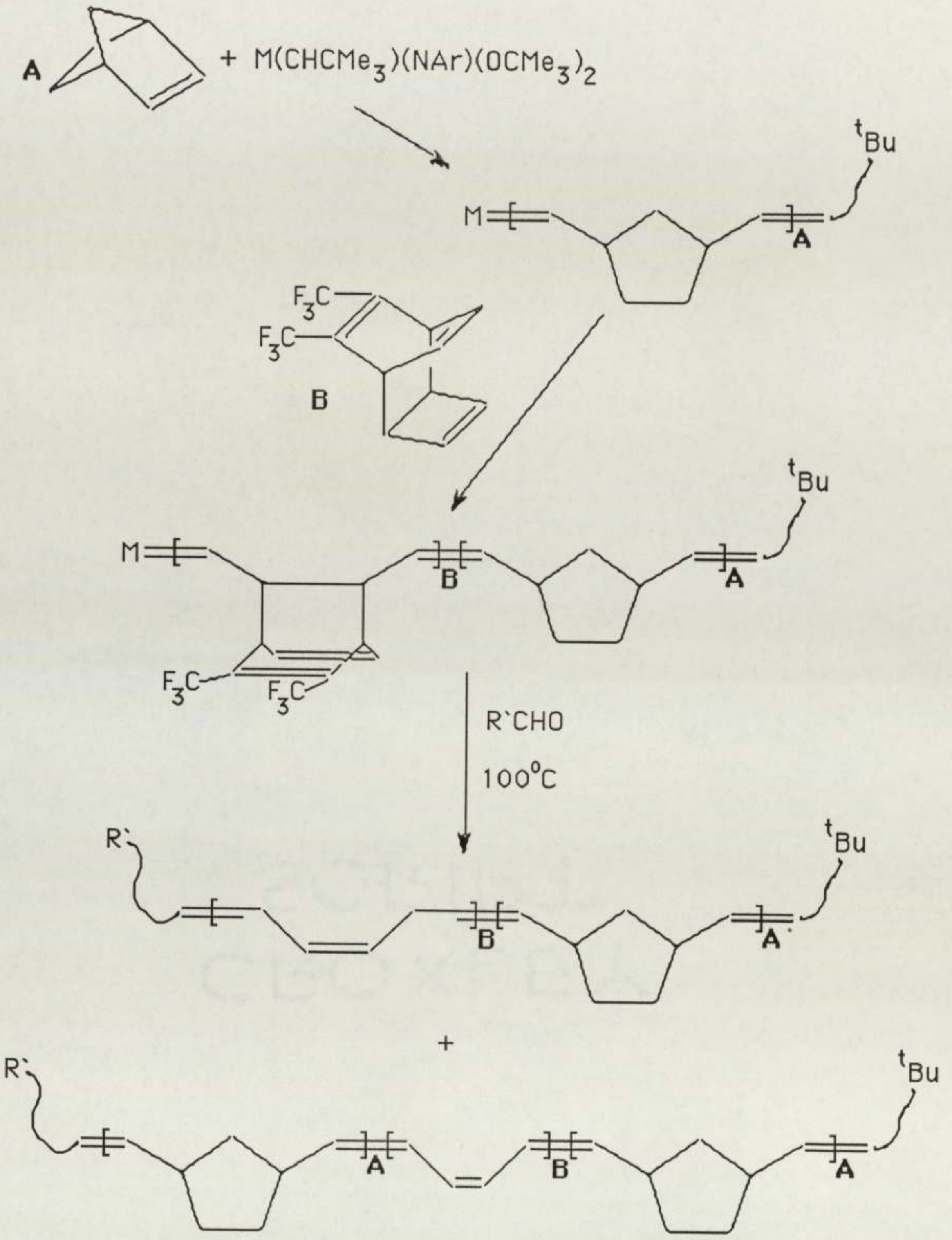

Figure 1.22 Copolymers containing polyene segments by living metathesis polymerisation

Triblock copolymers showed additional fine structure peaks reminiscent of those exhibited by low molecular weight polyenes. These observations suggest that the motion of the polynorbornene chain disrupts the planarity of the polyene sequence, effectively reducing the conjugation length, with the effect being most marked in the case of the triblock copolymer.

1.7 SCOPE OF THIS WORK

The aims of this project were:

(i) To investigate the activity of metathesis catalysts towards the polymerisation of acetylene.

(ii) To devise a route which involved using metathesis catalysts for the production of soluble block-co-polymers containing polyacetylene segments.

(iii) To characterise the materials using a variety of techniques.

(iv) To investigate the use of electro-optical methods for the determination of the electrical, optical and structural properties of solutions of copolymers that are partly comprised of polyacetylene segments.

CHAPTER 2

EXPERIMENTAL

2.1 VACUUM TECHNIQUES

Carbene intermediates of the type thought to be involved in metathesis polymerisations are known to be very reactive and are particularly sensitive towards oxygen and moisture. The same is true of the catalyst precursors, tungsten hexachloride and aluminium alkyls. For this reason, high vacuum handling techniques were required both during polymerisation and catalyst preparation.

2.1.1 The High-Vacuum Line

The high-vacuum line (figure 2.1) was constructed from glass and consisted of a manifold (a) which could be sealed or connected via a greased tap (b) to two vacuum pumps in series, an Edwards rotary pump (c) that could produce 10^{-3} torr and a mercury diffusion pump (d) which enabled pressures approaching 10^{-5} torr to be attained. The pressure inside the system was estimated be means of a mercury-filled vacustat gauge (e). To prevent the escape of vapours into the laboratory during evacuation and to prevent fouling of the pump oil, two liquid-nitrogen "cold" traps were used, (f) and (g). The mercury diffusion pump was positioned in the high-vacuum system between these two traps so that mercury vapour could neither contaminate the contents of the manifold nor be carried over into the pump oil. Apparatus could be attached to the vacuum line via four ground glass joints each of which could be isolated from the manifold by a P.T.F.E. tap (h). A bulb (i) enabled the volume of the manifold to be increased and was used for this purpose during degassing procedures.

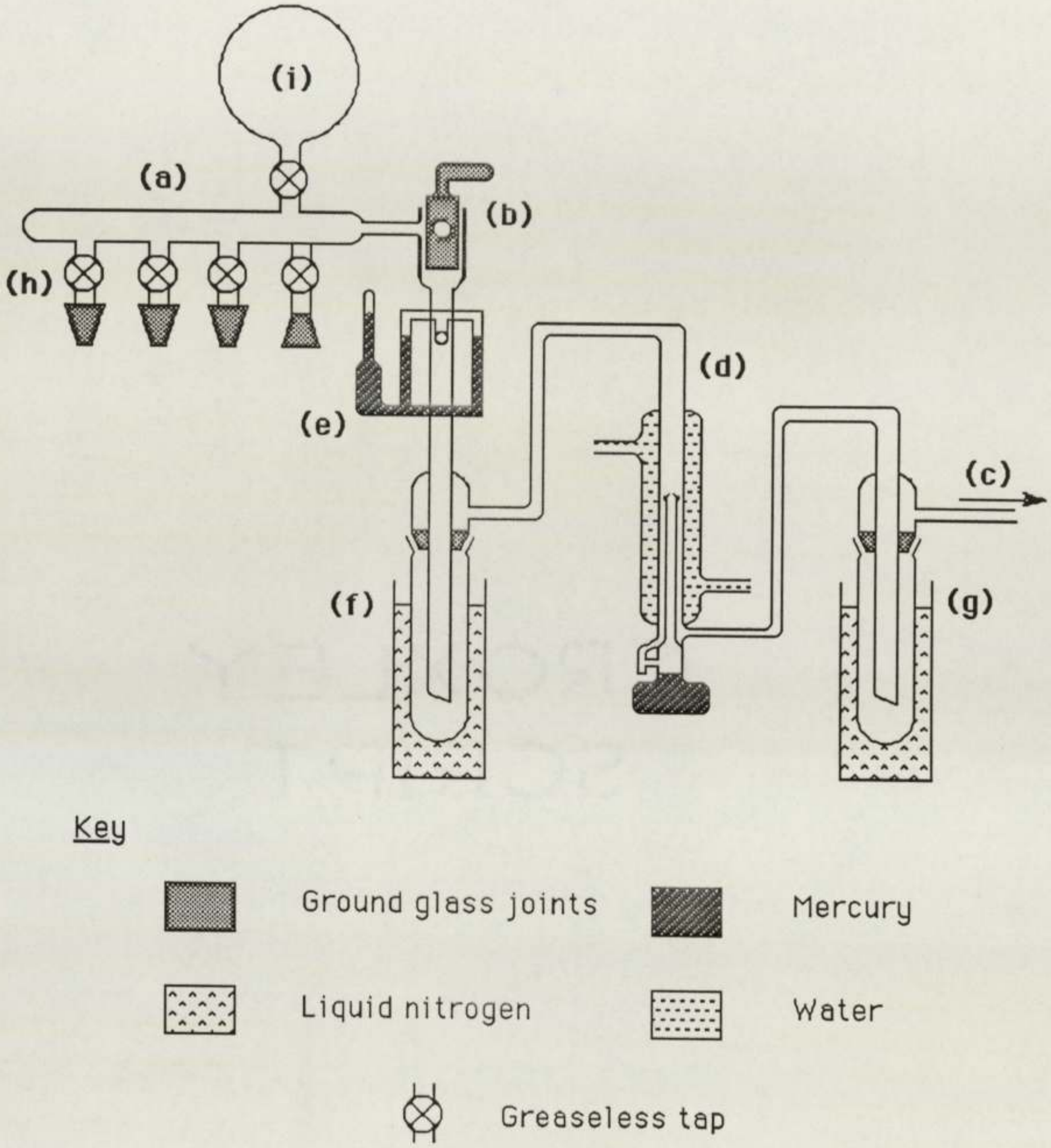

Figure 2.1 The High Vacuum Line

2.1.2 Evacuation

Flasks with the appropriate ground glass joints were attached to the manifold with tap (b) open and evacuated by opening the appropriate P.T.F.E. tap (h).

2.1.3 Freeze/Thaw Degassing

To carry out high-vacuum distillation of liquids, it was first necessary to remove all dissolved gases. A flask containing the liquid to be distilled was attached to the vacuum line and its contents were frozen in liquid nitrogen. The vessel was evacuated, tap (b) was closed and the liquid then allowed to warm up slowly. The gases dissolved in the liquid re-established equilibrium with the gas phase by boiling out of solution. The contents of the flask were then frozen by immersing in liquid nitrogen and the gases remained in the manifold and flask. When tap (b) was opened, the gases were evacuated from the system. On closing tap (b), the freezing and thawing process could be repeated until gaseous evolution on thawing the liquid ceased, indicating adequate removal of the dissolved gases. When the degassing procedure was complete, high-vacuum distillation could be carried out directly or the vessel could be sealed and removed from the vacuum line for storage.

2.1.4 High-Vacuum Distillation

A flask containing the degassed liquid was attached to the manifold and the manifold was evacuated with the tap to this flask closed. A receiving vessel was also attached to the manifold at another ground glass joint evacuated and then cooled with liquid nitrogen. When evacuation of the system was complete, tap (b) was closed and distillation was initiated by opening the P.T.F.E. tap on the first flask.

2.1.5 Apparatus

Glassware was cleaned and dried prior to use and was heated under vacuum in order to remove any moisture adhered to the walls. Glass syringes were cleaned, dried in an oven at 120^{o}C and stored in a dessicator until required.

The use of the high-vacuum system required specially designed glass vessels both for storage and polymerisation purposes. Solvents and liquid monomers were manipulated and dried under nitrogen or vacuum using flasks of the type shown in figure

2.2(a). Final distillates of the monomers and solvents were collected in flasks (figure 2.2(b)) for storage under high vacuum, which could be attached subsequently to the polymerisation apparatus.

Catalyst solutions were prepared and stored under vacuum in flasks of the type shown in figure 2.2(c). The stock solution was stored in bulb **A** and transferred in small portions to the evacuated bulb B as required (tap **D** closed). The flask could then be inverted and a dry nitrogen supply line attached at **C.** The key of tap **D** was removed and the required quantity of solution could be withdrawn from the vessel using a syringe.

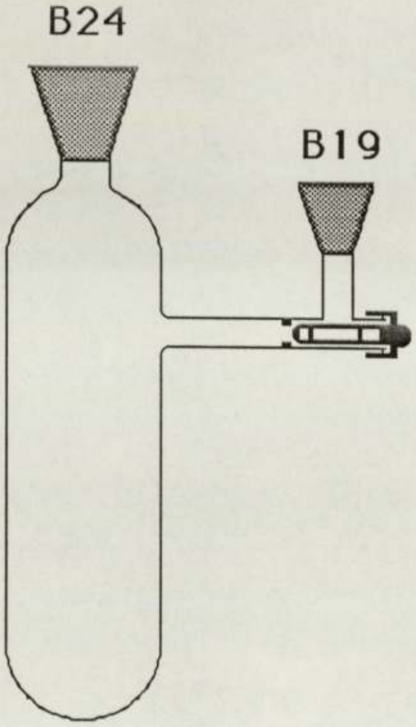

Figure 2.2(a) Solvent drying flask

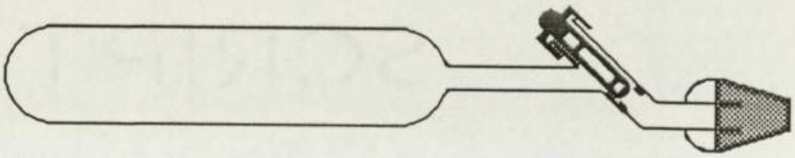

Figure 2.2(b) solvent storage flask

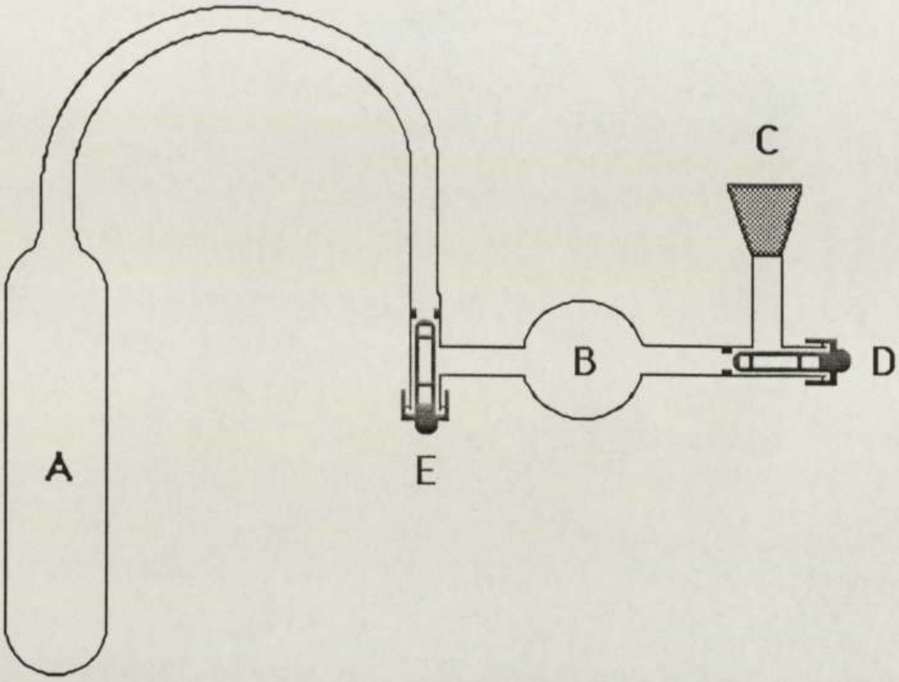

Figure 2.2(c) Catalyst storage flask

2.2 PREPARATION AND PURIFICATION OF STARTING MATERIALS

2.2.1 Acetylene

Acetylene was supplied by BOC Ltd. stored under pressure in solution in acetone. Acetone and water, being the main impurities, were removed by passing the gas through the purification system shown in figure 2.3. Concentrated sulphuric acid, which removed acetone vapour, was renewed when it became discoloured. The sodium hydroxide pellets ensured that no acidic vapours were carried over as impurities. After passage through the sulphuric acid container, any remaining water vapour was removed by passage along two calcium chloride drying columns. A $2dm^3$ evacuated glass bulb was attached to the purification chain by a ball and socket joint and was filled with purified acetylene by opening tap (a). When the bubbling in the sulphuric acid container had ceased, tap (a) was closed and the bulb removed.

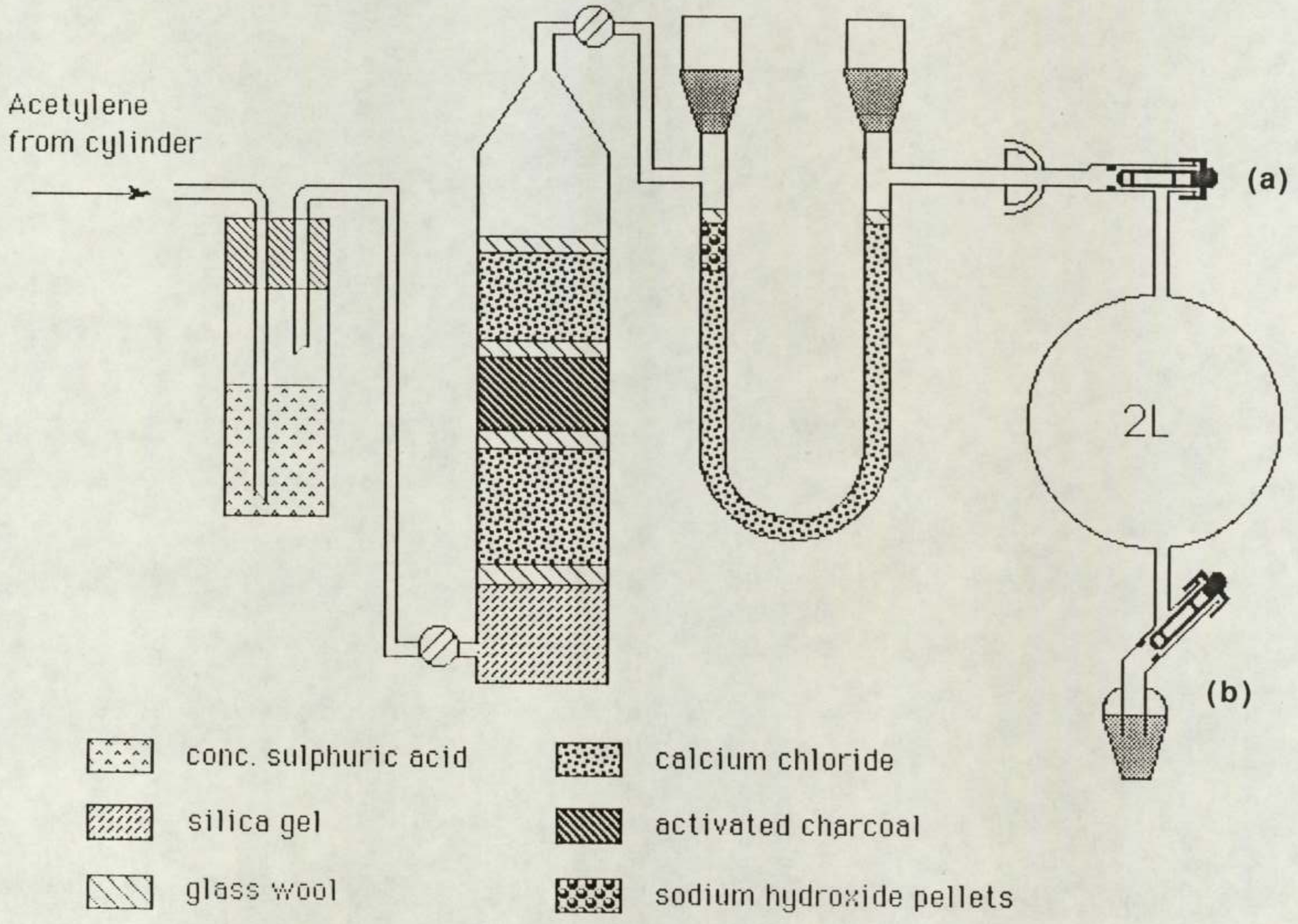

Figure 2.3 Acetylene Purification System

2.2.2 Cyclohexane

Cyclohexane (Fisons) was stored over calcium hydride in a flask stoppered with a calcium chloride drying tube. Portions of cyclohexane were transferred, as required, to a vessel and degassed on the vacuum line. The solvent was then transferred by high-vacuum distillation to a flask that contained freshly cut slices of sodium and a small amount of benzophenone. Following distillation, the solvent was repeatedly degassed until the characteristic colour (blue) of the sodium/benzophenone radical anion complex was observed.

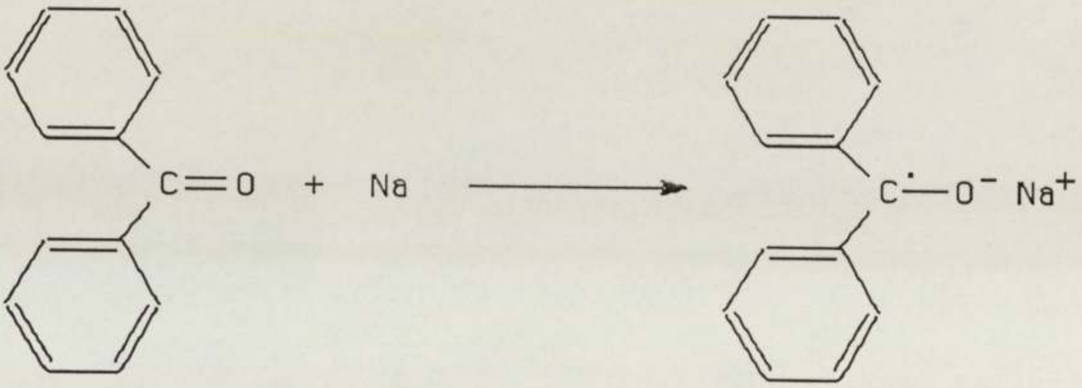

This complex is very sensitive to oxygen and moisture and so could be used as an indicator of the efficiency of the drying/degassing procedure.

The purified, dry cyclohexane was finally distilled into a reservoir flask (figure 2.2(b)) for storage.

2.2.3 Cyclopentene

Cyclopentene (Aldrich) was purified by standing the monomer over freshly cut slices of sodium which removed the main impurities, cyclopentanol and cyclopentadiene. The purified, dry cyclopentene was then distilled into a vessel which contained slices of sodium and a small amount of benzophenone. The liquid was repeatedly degassed until the characteristic blue of the sodium/benzophenone radical anion complex was observed. Finally, the degassed monomer was distilled into a reservoir flask (figure 2.2(b)) for storage.

2.2.4 1-Octene

The molecular weight modifier, 1-Octene, was dried over slices of sodium and subsequently distilled into a flask containing both sodium and benzophenone. The purified liquid was finally distilled into a reservoir flask for storage.

Solutions of 1-octene in cyclohexane were prepared by successively distilling octene and cyclohexane from the dried stock solutions into a reservoir flask. The weight of the reservoir flask was measured before and after each distillation and the concentration of 1-octene in cyclohexane determined by weight difference.

2.2.5 Tungsten Hexachloride

Aldrich Gold label tungsten hexachloride was obtained as a purple solid with quoted purity of 99.98% and was stored under vacuum. Solutions of WCl_6 were prepared by transferring a small portion of the solid to a pre-weighed, evacuated flask in a dry-box filled with high purity argon. The flask was then sealed, weighed and re-evacuated. The mass of WCl_6 contained within the flask was estimated by weight difference. The required quantity of dried, degassed cyclohexane was then distilled into the flask under reduced pressure. The volume of cyclohexane added was determined from the increase in the weight of the flask. The solubility limit of WCl_6 in cyclohexane was estimated to be 5×10^{-2} moles l^{-1}. In a typical preparation, 1.35g of WCl_6 was dissolved in 130cm^3 cyclohexane to produce a deep red, 2.6×10^{-2}M solution.

2.2.6 Aluminium Alkyls

Aluminium triethyl and aluminium dichloroethyl were supplied under nitrogen in specially constructed steel containers (Figure 2.4) as they react explosively on contact with air and moisture. Solutions of aluminium triethyl and aluminium dichloroethyl in cyclohexane were prepared by the following method.

The required quantity of dried/degassed cyclohexane was distilled into bulb (**A**) of a catalyst flask (figure 2.2(b)). The flask was then inverted and clamped in position with a nitrogen line attached at (**C**) and the key of tap (**E**) removed. A second nitrogen line was attached to the vessel that contained the aluminium alkyl and the threaded cap removed (figure 2.4). The required quantity of aluminium alkyl was then withdrawn by syringe and injected into the cyclohexane through the barrel of tap (**E**).

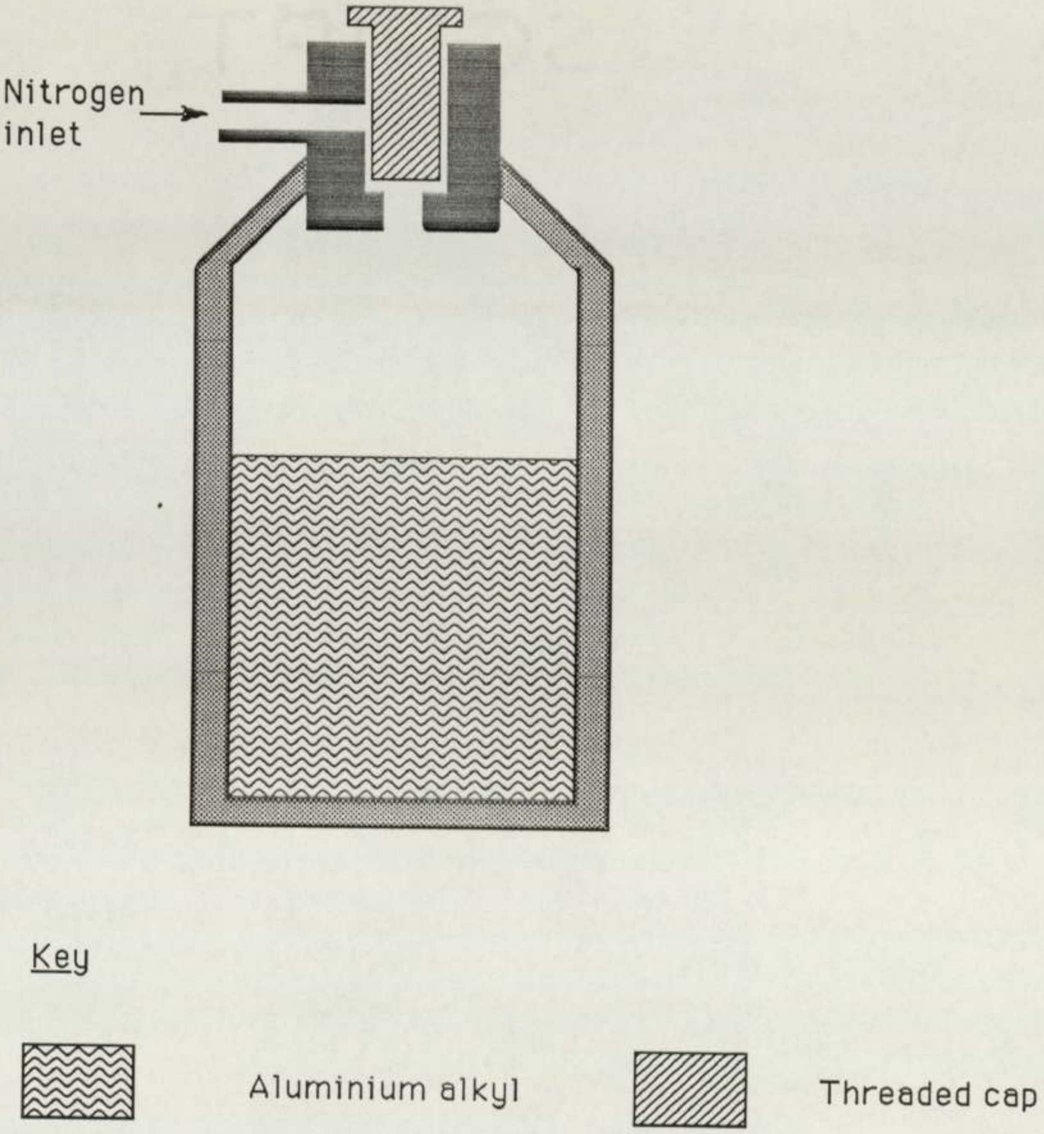

Figure 2.4 Aluminium alkyl storage vessel

2.2.7 n-Butyl Lithium

n-Butyl lithium was obtained as a 1.6M solution in hexane and stored under nitrogen in a bottle with a septum cap. When required, aliquots were withdrawn by syringe while maintaining the contents under a positive pressure of nitrogen. Solutions of n-butyl lithium in cyclohexane were prepared using a similar method to that described for the aluminium alkyls.

2.3 POLYMERISATION TECHNIQUES

2.3.1 Homopolymerisation

The polymerisation of acetylene was carried out in the vessel shown in figure 2.5. The flask was connected to the vacuum line manifold by one B19 ground glass joint and the bulb, filled with acetylene, was attached at another. The large (B34 male) cone facilitated removal of the polymer and allowed the attachment of a cyclohexane reservoir. The system was first evacuated and cyclohexane allowed to flow into the reaction chamber through tap (**a**). The volume of solvent was estimated from the weight of cyclohexane delivered.

Acetylene was admitted to the vigorously stirred liquid and after five minutes the required quantity of tungsten hexachloride solution was injected into the vessel through the rubber septum. After a pre-determined time, the required volume of the solution of cocatalyst was injected and tap (**b**) closed. The polymerisation was allowed to proceed at 20^{o}C for 20hrs. The rubber septum was renewed prior to each experiment.

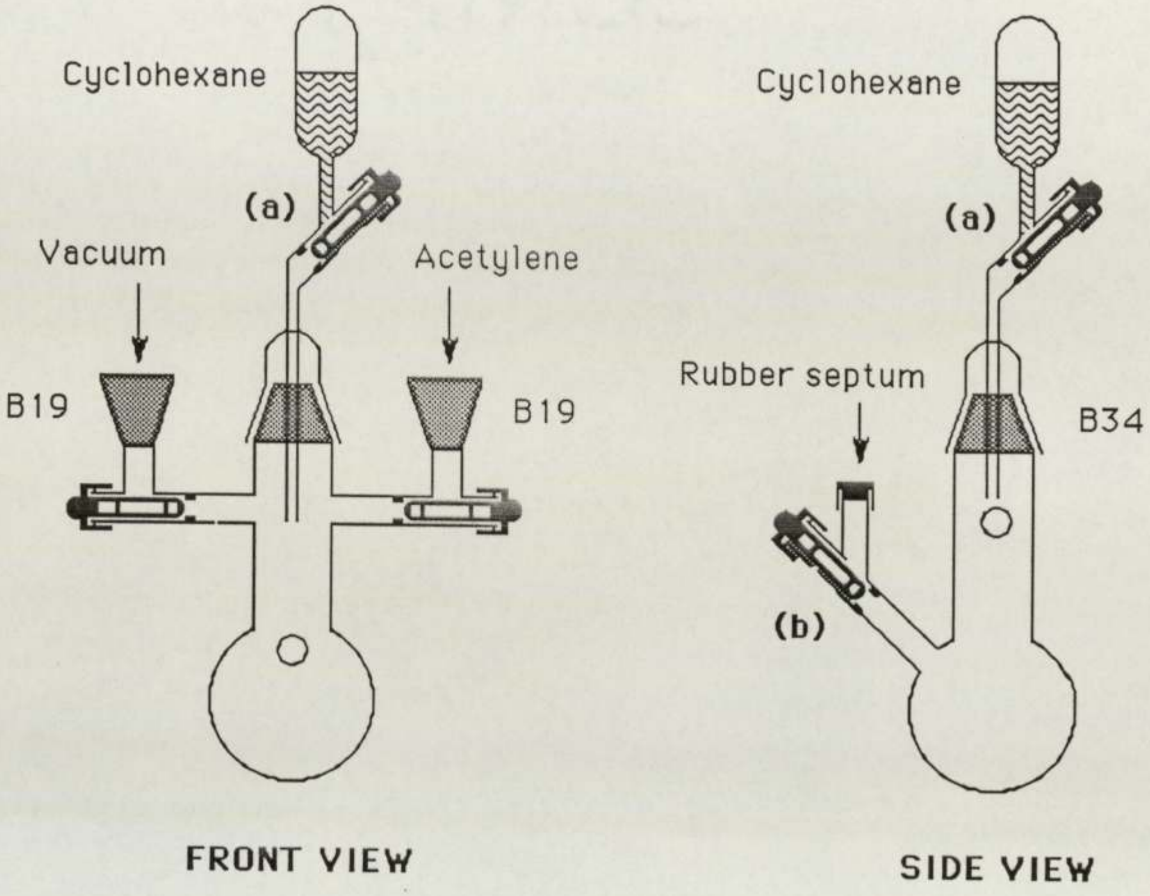

Figure 2.5 Vessel used for the polymerisation of acetylene

2.3.2 Copolymerisations

The copolymerisation apparatus (Figure 2.6 **[A]**) was similar to that used for homopolymerisation, but modified to include an internal tube and greaseless tap which enabled samples to be taken of the contents of the reaction chamber at any time during the reaction. The tube was connected via a greaseless joint to a 100cm^3 bulb (**h**) and the whole assembly evacuated at the start of each experiment. When a sample was required taps (**d**) and (**e**) were opened and the vapour pressure above the solution forced some of the liquid into the bulb.

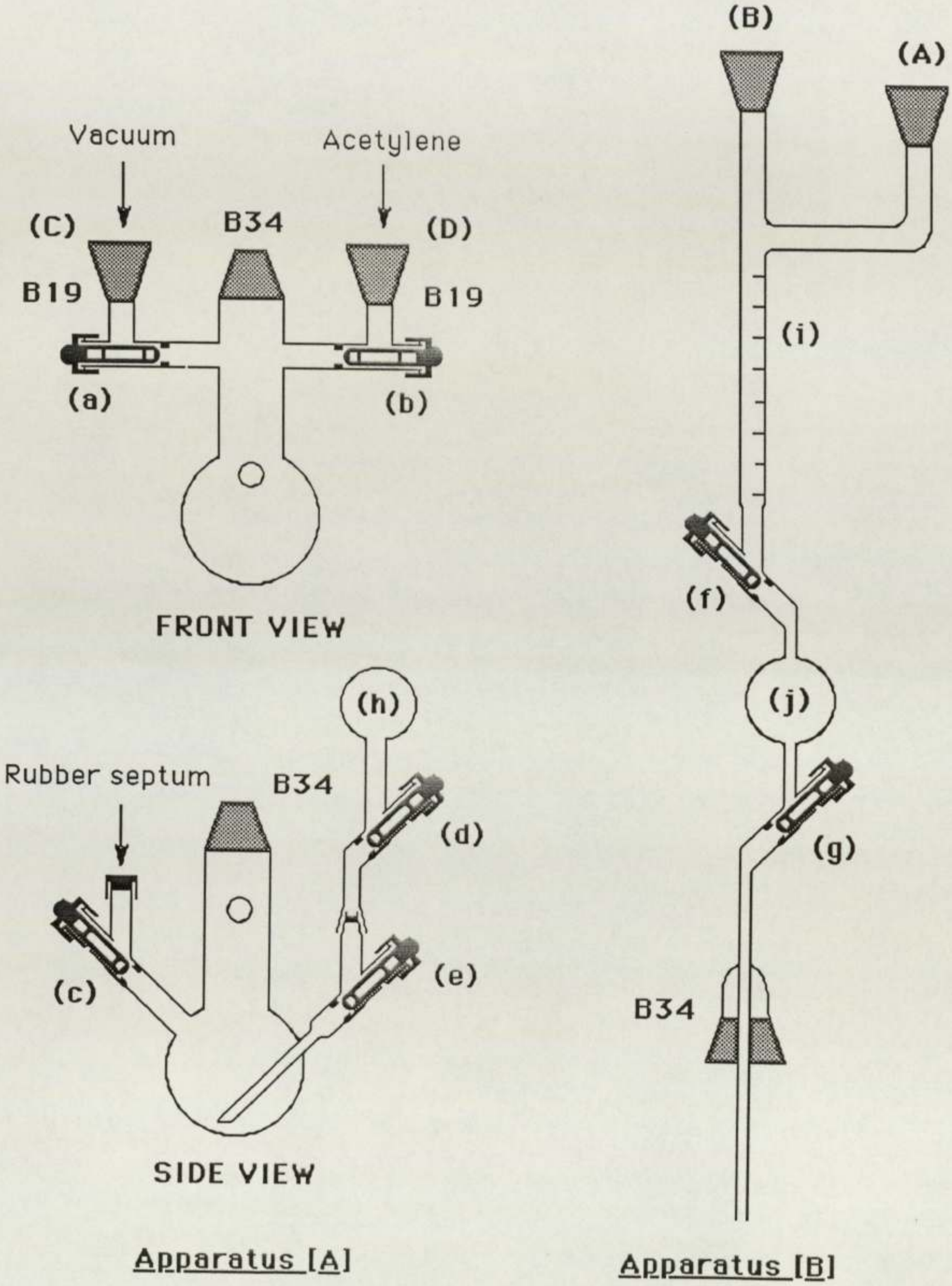

Apparatus [A]

Apparatus [B]

Figure 2.6 Apparatus for the copolymerisation of cyclopentene and acetylene

The apparatus [**B**] was designed to provide an estimate of the volumes of cyclohexane, cyclopentene and 1-octene used in each of the copolymerisation experiments. The graduated section (**i**) could be used to measure volumes of liquid up to 26.0 ± 0.5cm^3 under conditions of reduced pressure. When calibrated, the volume of the portion between the graduated section of the tube and the tap was found to be 1.0cm^3, so all measured volumes had to be corrected by this amount. The bulb (**j**) had a capacity of 71cm^3.

The ground glass joint (**A**) was first attached to the vacuum line and the appropriate liquid monomer or solvent reservoir connected at (**B**). The system was then evacuated, with tap (**g**) closed and (**f**) open, and warmed under vacuum to remove any water adhering to the walls. The tap to the vacuum line and tap (**f**) were then closed. Liquid from the reservoir was allowed into the graduated tube until the required volume was obtained. The greaseless tap on the reservoir flask was then closed and tap (**f**) opened to transfer the liquid to the storage bulb (**j**). With tap (**f**) closed traces of liquid in the graduated portion could be removed by evacuating this part of the system. The reservoir could then be removed and another liquid reservoir flask substituted at (**B**). Thus, by repeating the above procedure, a mixture of known composition was prepared and stored under reduced pressure in the bulb. In order to facilitate transfer, the components were added in order of increasing volatility.

Apparatus [**B**] and its contents were then removed from the vacuum line and connected to the polymerisation vessel at the B34 joint. With the filled acetylene bulb attached at (**C**) and joint (**D**) connected to the vacuum line, the system was evacuated with taps (**a**),(**b**),(**c**),(**d**) and (**e**) open. The polymerisation chamber was then isolated from the line and charged with monomer solution via tap (**g**). The required quantities of catalyst solutions were then added through the rubber septum. After a predetermined time acetylene was admitted and further catalyst additions made through the rubber septum as required.

2.4 POLYMER RECOVERY

2.4.1 Insoluble Polymers

After the desired polymerisation time, the activity of the catalyst was destroyed by the injection of 2mls. ethanol through the rubber septum. The polymerisation vessel was then transferred to a dry box which was filled with argon and dried with phosphorous pentoxide. Particles of precipitate were separated from the solution either by standard filtration or by vacuum filtration using sintered glass filters. The precipitate was then washed with cyclohexane and transferred to a vacuum oven where it was dried at 30°C overnight. The samples were stored under argon in sealed vials. The latter were covered with black tape to exclude light.

Polymers that blocked the pores of the sintered filter were separated from the solution of catalyst using a centrifuge. The supernatant liquor was then decanted off.

2.4.2 Soluble Polymers

When soluble polymers were obtained, these were recovered by diluting the active polymerisate with cyclohexane followed by precipitation in excess 'wet' methanol. Upon coagulation of the polymer, the methanol was decanted off and the crude polymer redissolved in fresh cyclohexane and reprecipitated in methanol. The product was then dried overnight in a vacuum oven at 30°C before being transferred to a taped vial for storage under argon.

2.5 ANALYTICAL TECHNIQUES

2.5.1 Elemental Analysis

A Carlo-Erba CHN combustion analyser was used to determine the relative proportions of carbon and hydrogen in the polymer samples. 1-3mg of dried polymer was weighed accurately and transferred to a small aluminium boat. The sample was heated in a gas stream containing oxygen and the constituent combustion gases were separated and estimated by gas chromatography. When hydrocarbon polymers are combusted totally, the product gas contains only carbon dioxide and water. After calibration of the instrument, the relative proportions of carbon dioxide and water produced by the combustion of the polymer were calculated from the areas of the peaks detected by the chromatograph. A computer then evaluated the weight percentages of hydrogen and carbon in the sample from the amounts of carbon dioxide and water produced. The results were quoted as weight percentages of each element. As the weight ratio of C:H in polyacetylene is 12:1, it is often convenient to express the C/H ratio in these materials as %C /(%H x 12), effectively the mole-atom ratio of C:H in the sample.

2.5.2 UV/Visible spectroscopy

Uv/visible spectroscopy has often been used to detect the presence of conjugation in multiple bonded systems. The $\pi - \pi^*$ transition is often intense and occurs at around 180nm for an isolated double bond. As the degree of conjugation increases, the absorption shifts to progressively longer wavelengths. (e.g. butadiene, λ_{max}= 217nm; 1,3,5 hexatriene, λ_{max}= 258nm.)

The uv/visible spectra of the soluble polymer samples were recorded on a Beckman DU7 spectrometer using a solution of the polymer in a quartz cuvette cell with an optical path length of 10mm. Cyclohexane, "spectrosol" grade was used as solvent and reference.

2.5.3 Infra-red spectroscopy

Infra-red spectra were recorded on a Perkin-Elmer FTIR machine. Materials that were soluble in cyclohexane were cast from solution onto sodium chloride plates, dried and their spectra recorded. Insoluble materials were incorporated into KBr discs.

2.5.4 Gel Permeation Chromatography (GPC)

Gel permeation chromatography may be used to analyse the molecular weight distribution of a polymer sample provided that it is soluble in the solvent used for GPC. Fractionation of the polymer, according to hydrodynamic volume, is achieved by a sieving process that may be described as follows.

The stationary phase usually consists of crosslinked polystyrene beads packed into a column or series of columns. When solvent is introduced into the column, the beads swell and generate surfaces which possess pores. The synthesis of the beads is carefully controlled to yield a narrow distribution of pore sizes. When a polymer solution is eluted along the column at constant solvent flow rate, the smaller molecules are able to permeate a greater fraction of the available pores. Larger molecules are excluded from all but the largest pores and hence will travel down the column faster.

The GPC equipment used in this work employed tetrahydrofuran (BDH Hipersolve) as eluent. This solvent was delivered at 1ml per minute by a Perkin-Elmer series 10 liquid chromatography pump. Solutions (1-2 w/v%) of the polymer samples in THF were injected onto the columns by a 100µl valve and loop injector system. Five µ-PLgel columns (Polymer Laboratories) were connected in series, the first being a short pre-column to remove suspended material and the remainder having exclusion limits of 10^2, 10^3, 10^4 and 10^5Å respectively. The eluent from the columns was analysed by a Knauer differential refractometer and a Perkin-Elmer LC-85B variable wavelength spectrophotometer, connected in series. The output of each detector was recorded simultaneously on a dual-pen chart recorder. The differential refractometer compares continuously the refractive index of the eluent with that of pure solvent. The magnitude of the signal resulting from differences in refractive index is proportional to the amount of material passing through the sample cell and to the refractive index of the species present in solution. The uv/visible detector responds to chromophoric groups either attached to, or part of the polymer backbone. Its response is therefore proportional to the concentration of the solute present in the solution and the molar extinction coefficient of the solute at the set wavelength. A schematic diagram of the GPC apparatus is shown in figure 2.7.

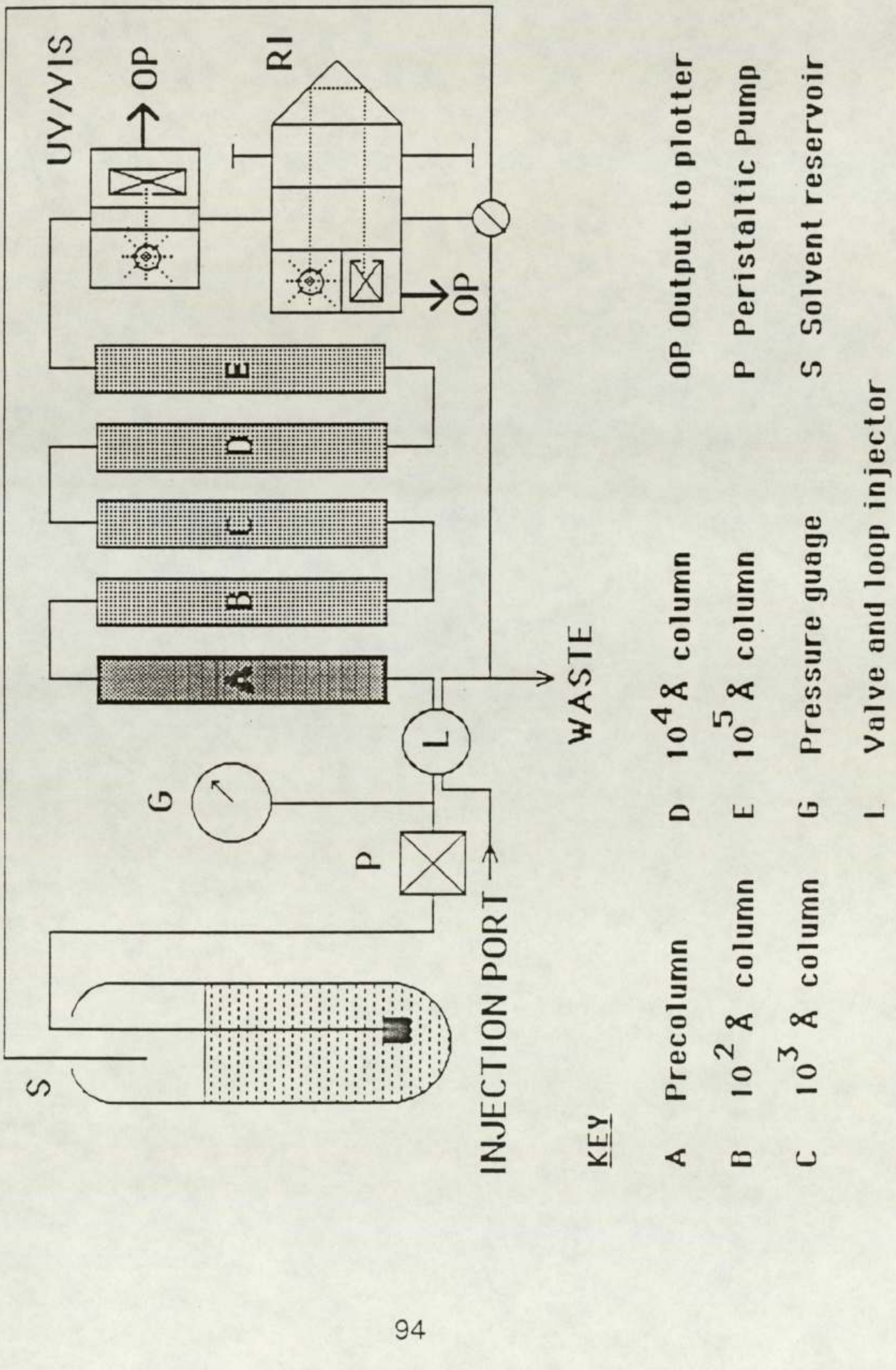

Figure 2.7 Scematic Diagram of the apparatus used for GPC

The chromatograms produced by this method have an important advantage over other methods of polymer molecular weight estimation in that the whole molecular weight distribution is recorded. However quantitative determination of molecular weight by GPC can only be achieved by comparison with chromatograms obtained for samples of known molecular weight. In these experiments the columns were calibrated using a series of narrow molecular weight distribution polystyrene standards. The calibration plot is shown in figure 2.8.

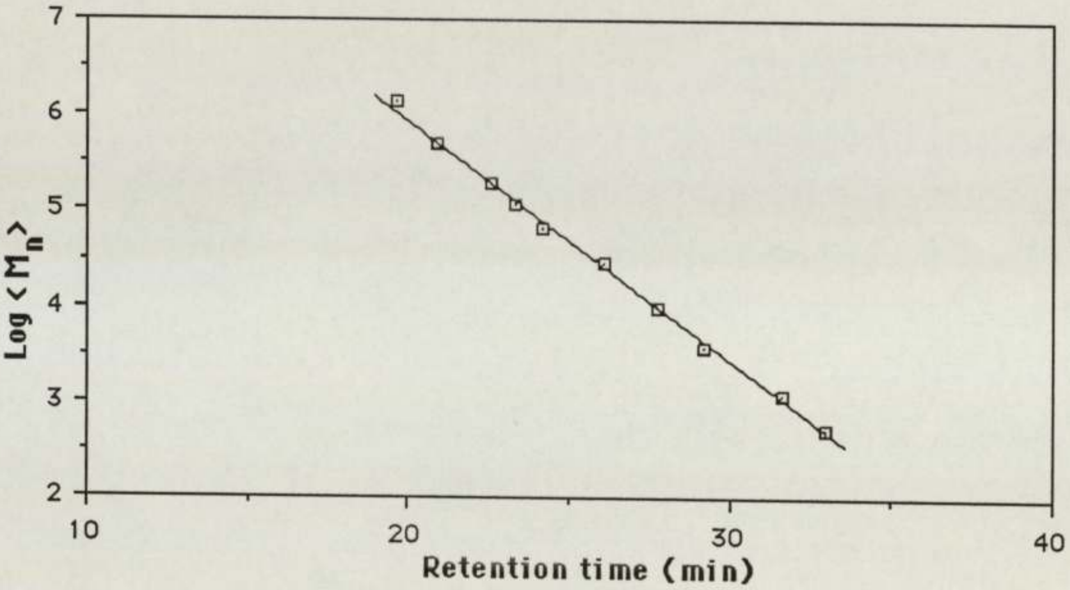

Figure 2.8 GPC calibration using polystyrene standards

2.5.5 Scanning Electron Microscopy (SEM)

Scanning electron micrographs of the product polymers were recorded on a Cambridge S150 instrument. Samples were prepared by dissecting the material under examination so that its dimensions were approximately 5mm x 5mm and did not exceed 5mm in thickness. The sample was then mounted on a 10mm diameter, copper stub with the aid of a double-sided adhesive patch. To prevent surface charging and the distortion of images, that often occurs when non-conductive surfaces are subjected to electron beams, a thin coating of gold was applied to the upper surface of the specimen. This was achieved by connecting the stub to one of two electrodes. A second electrode, made of gold, was positioned directly above the sample. When a high-tension voltage was applied across the electrodes under vacuum, a gold ion current flowed, slowly coating the sample with gold atoms.

The stub was then placed on the rotating platen of the electron microscope. Once the sample chamber had been evacuated, the specimen was probed by the electron beam.

2.5.6 Nuclear Magnetic Resonance Spectroscopy

High resolution nuclear magnetic resonance spectra were obtained using a Bruecker AC300 spectrometer. Solutions of the samples were made by dissolving the solids in deuterated chloroform ($CDCl_3$) and adding a small quantity of tetramethylsilane (TMS) as reference to each solution.

Samples that could not be rendered soluble were examined in the solid state by the magic angle spinning technique. A poly(methylene oxide) (Delrin) rotor which consisted of a 3mm diameter hollow section (10mm long) attached to a 2mm diameter stem, was tightly packed with powdered material (approx 0.4g) and loaded into the instrument. Spinning was effected by a stream of compressed air.

Elastomeric samples could not be powdered and considerable difficulty was encountered in efficiently packing the rotor with such materials. Two methods were found to be effective :

(i) A film of the elastomer was cast onto a laboratory white tile. A rectangular strip of the film, 10mm in width, was cut from this and rolled up so that it would fit tightly into the rotor.

(ii) A thin, polymer film was applied to a sample of 100 mesh glass beads which could then be packed into the rotor. The coating was applied by mixing the beads with a 0.2% solution of the elastomer in cyclohexane and slowly removing the solvent by rotary evaporation.

CHAPTER 3

THE POLYMERISATION OF ACETYLENE USING OLEFIN METATHESIS CATALYSTS

3.1 INTRODUCTION

Monosubstituted acetylenes do not undergo metathesis in the presence of olefin metathesis catalysts; instead they cyclise or polymerise depending on the structure of the acetylene and the nature of the catalyst employed. Although several workers have studied the polymerisation and copolymerisation of substituted acetylenes using tungsten compounds,(129-137) little is known concerning the activity of these catalysts towards acetylene itself. Voronkov(138) reported that a 0.1 molar solution of WCl_6 in 1,2-dichloroethylene catalysed the polymerisation of acetylene when the monomer was present at an initial pressure of 14atm, but the product contained a high concentration of carbonyl groups. The latter were thought to originate from autoxidation reactions of the polymer. Experiments reported by Diets(139) and by Schue(140-144) have shown that when a two-component catalyst is used, the polymerisation may proceed under less extreme conditions.

Diets(139) reported that, when acetylene was bubbled for 2.5 hours through a catalyst solution comprised of a 2:1 mixture of WCl_6 (4×10^{-3}M, 7^oC) and water in toluene, a black precipitate of polyacetylene was formed.

Schue`s catalyst was formed from a 1:1 mixture of WCl_6 and tetraphenyltin ($SnPh_4$) in toluene, which was aged for 15 minutes before use. Although this system has been used extensively in the polymerisation of phenylacetylene,(132) kinetic data showed that its activity, with respect to the polymerisation of acetylene, was significantly lower than that exhibited by the Shirakawa type of catalyst ($Ti(OBu)_4/AlEt_3$).

The ring opening metathesis polymerisation of cyclic olefins may be catalysed by several types of bimetallic system including $WCl_6/SnPh_4$. When WCl_6 is used as catalyst, the activity is seen to depend on the nature of the cocatalyst. In this chapter three bimetallic systems, known to catalyse metathesis reactions, were examined as possible catalysts for the polymerisation of acetylene. The effect of the cocatalyst on the activity of the system towards acetylene was considered by comparing the results of polymerisations using WCl_6 complexed with n-butyl-lithium (LiBu), dichloroethylaluminium ($AlEtCl_2$) and triethylaluminium ($AlEt_3$) respectively.

3.2 THE POLYMERISATION OF ACETYLENE USING WCl_6/LiBu AS CATALYST

3.2.1 Polymerisation

The polymerisation was carried out using the procedure described in section 2.3.1. In a typical experiment, 1.00 x 10^{-4} moles of tungsten hexachloride were added to a saturated solution of acetylene in cyclohexane at 20°C. After two minutes, 2.00 x 10^{-4} moles of n-butyl lithium were added. The initially red solution turned through golden yellow to green and a black precipitate formed within an hour. After allowing the polymerisation to continue for 20 hours, the polymer was recovered and dried by the method described in section 2.4.1. The yield of precipitated polymer was 0.03g.

3.2.2 Characterisation

The black precipitates were analysed by elemental analysis as described in section 2.5.1. Although the use of this technique alone would not normally be considered sufficient evidence for a particular structure, under these circumstances no other method of analysis was suitable owing to the low yields of precipitate and the intractable nature of the product. Table 3.1 shows the results of elemental analyses of the products of two typical polymerisations performed according to the method described in section 3.2.1.

Table 3.1 Elemental Analysis of Polyacetylene produced using the catalyst system WCl_6/LiBu

Reference	% C	% H	C:H mole-atom ratio
A1	37.2	3.8	0.82
	36.8	3.7	0.83
A2	26.8	2.0	1.12
	27.1	2.1	1.08

It is clear from these results that for the conditions cited above, this catalyst system is not very effective towards the polymerisation of acetylene; the conversion being only about 1% by weight. Although sample A2 shows fairly good agreement with the carbon/hydrogen mole-atom ratio expected for polyacetylene, the total combustible material in the sample is only 30-40%. This would seem to imply that significant quantities of catalyst residues were present in the materials even after washing. The possibility that the active polymerisation site of the catalyst may become occluded in the polymer particle thus terminating the polymerisation could explain both the low conversions and the high ash residues produced by this system.

Recently Schue(142) has reported the polymerisation of acetylene by a tungsten hexachloride/lithium butyl catalyst and has produced SEM evidence for the presence of microscopic inclusions in the product. It should be noted however that the concentrations of catalyst and monomer used in Schue`s experiments were respectively fifty times and four times greater than those used typically in the series of experiments reported in this thesis.

3.2 THE POLYMERISATION OF ACETYLENE USING $WCl_6/AlEtCl_2$ AS CATALYST

3.3.1 Sequential addition of the catalyst components to a solution of the monomer

3.3.1.1 Polymerisation

The polymerisation of acetylene was carried out by the method described in section 2.3.1. In a typical experiment, 0.50×10^{-4} moles of WCl_6 were added to a saturated solution of acetylene in cyclohexane followed, 2 minutes later, by the addition of 1.00×10^{-4} mol $AlEtCl_2$. The polymerisation mixture turned from red through golden yellow to green. The final colour change was accompanied by the precipitation of polyacetylene as a black powder. The temperature was maintained at 20°C and the polymerisation allowed to continue for 20 hours. The precipitate was recovered and dried as described in section 2.4.1. The yield of polymer was 0.09g.

Table 3.2 shows some typical results of a number of similar polymerisation experiments.

Table 3.2 The polymerisation of acetylene using tungsten hexachloride and aluminium dichloroethyl

Ref.	WCl_6 (mol $\times 10^4$)	$AlEtCl_2$ (mol $\times 10^4$)	W:Al	Yield (g)	C:H-mole/atom ratio
B1	4.25	2.50	1:0.6	0.03	0.88
B2	0.50	1.00	1:2	0.09	1.03
B3	1.00	2.00	1:2	0.08	1.65
B4	1.00	4.00	1:4	0.07	1.05

Volume of solution = $40 cm^3$ Polymerisation time = 20 hours

Volume of acetylene = $2 dm^3 \approx 0.1 mol$ Temp = 20°C

A comparison between the yields of polyacetylene obtained when $WCl_6/AlEtCl_2$ and WCl_6/LiBu catalysts were used (section 3.2.1) shows that yields obtained using the former catalyst system are generally the greater. This may suggest that $AlEtCl_2$ is a more effective activator of WCl_6 in the production of species which will catalyse the polymerisation of acetylene.

3.3.1.2 Effect of the order of addition of the catalyst components

When a cyclic alkene is polymerised by ring opening using a tungsten based, multicomponent metathesis catalyst, the accepted order of addition of the catalyst species to the solution of monomer is: tungsten component followed after a predetermined time by the cocatalyst(s). Indeed Amass and Tuck(145) have shown that the interval of time before the addition of the second component can be vitally important in determining the activity of the catalyst and the outcome of the polymerisation. Table 3.3 shows the results of three typical experiments in which the effect of omitting one of the catalyst components and of reversing the "normal" order of their addition were investigated.

Table 3.3 Effect of the omission and the order of addition of components of the catalyst.

Expt.	WCl_6 (mol x10^4)	$AlEtCl_2$ (mol x 10^4)	W:Al	Yield (g)	C:H mole-atom ratio
B5	1.00	-	-	none	-
B6	-	10.00	-	none	-
B7	1.00	10.00	1:10	none	-

Volume of solution = $40cm^3$ Polymerisation time = 48 hours

Volume of acetylene = $2dm^3 \approx 0.1mol$ Temp = 20^oC

Refering to experiments B5 and B6 in table 3.3, it can be seen that the individual catalyst components show little if any catalytic activity under these conditions. In experiment B5, where acetylene was added to a solution of tungsten hexachloride, no precipitate was obtained but the colour changed slowly from deep red to yellow/green over 16 hours. Voronkov et al(138) have reported the polymerisation of acetylene using tungsten hexachloride alone, but this necessitated the use of elevated pressures and high concentrations of catalyst.

In experiment B7, $AlEtCl_2$ was added to a saturated solution of acetylene in cyclohexane followed three days later, by WCl_6. No polyacetylene was formed which may suggest that the acetylene reacts with $AlEtCl_2$ to give a complex that will not subsequently promote polymerisation on addition of WCl_6. This indicates that for polymerisation to occur, the tungsten containing catalyst component must be added to the solution of acetylene prior to the cocatalyst. Therefore, the order of addition of the catalytic constituents for the polymerisation of acetylene would seem to be a critical factor. This behaviour has also been observed for the metathesis polymerisation of cyclic alkenes.

3.3.1.3 Characterisation

Comparison of the results of elemental analysis performed on samples of polyacetylene prepared by the technique described in section 3.3.1.1 with those prepared using the WCl_6/LiBu catalyst (table 3.1) showed that for the former, the percentage of combustible material in the samples had increased to 40-65%. A separate combustion experiment in which 0.0710g of polyacetylene product was pyrolysed in a furnace at 600°C for 48hrs in air gave 0.0162g of a pale yellow residue. The combined carbon and hydrogen content of this residue was less than 0.5%. From this data it can be concluded that significant amounts of high-melting components were present in the polymers, probably due to the attachment or physical inclusion of catalyst by the polymer. The possible encapsulation of the active site during the polymerisation may explain the low efficiency of the catalyst towards acetylene polymerisation under these conditions. When using the Shirakawa type catalysts ($Ti(OBu)_4/AlEt_3$), the effects of encapsulation may be crudely circumvented by simply increasing the concentration of catalyst. It is then observed that gels or films of polyacetylene may be produced in good yield. However, this approach could not be used with the metathesis type systems due to the limited solubility of WCl_6 in cyclohexane.

The carbon/hydrogen mole-atom ratios quoted in table 3.2 were calculated from the data derived from the CHN combustion analyser described in section 2.5.1. Although the C:H ratios for products B2 and B4 correlate well with the theoretical value of 1 expected for polyacetylene, samples B1 and B3 show significant deviations. Departures of C:H ratios from unity may possibly be due to contamination of the samples during transfer between vessels. It is well known that polyacetylene is susceptible to oxidation by atmospheric oxygen.(36)

3.3.2 Premixed catalyst studies

A procedure commonly employed during the polymerisation of acetylene using either Shirakawa or Luttinger catalysts is that of premixing: This procedure involves mixing the catalyst components and ageing the mixture for a predetermined period before it is allowed into contact with acetylene. A range of aging times and temperatures for the various catalyst systems have been reported in the literature; however 30 minutes at 20°C is often used. In this section the effect of premixing the components of the metathesis catalyst, WCl_6 and $AlEtCl_2$, on the polymerisation of acetylene will be described.

3.3.2.1 Polymerisation

In a typical experiment, 1.00×10^{-4} moles of WCl_6 were mixed with 2.00×10^{-4} moles of $AlEtCl_2$ in $40cm^3$ of cyclohexane. After 60 minutes at room temperature (20°C), a clear light-brown solution resulted. When acetylene was admitted, the solution changed to blue/green and a black precipitate formed almost immediately. The product (0.14g) was isolated by the method described in section 2.4.1. The results of similar polymerisations are summarised in table 3.4.

Table 3.4 The polymerisation of acetylene using premixed catalysts

Expt.	WCl_6 molx10^4	$AlEtCl_2$ molx10^4	Ageing time (min)	Yield (g)	W:Al ratio	C:H mole-atom ratio
C1	1.00	2	960	0.12	1:2	0.87
C2	1.00	2	60	0.14	1:2	0.75
C3	3.00	6	5	0.20	1:2	0.73
C4	1.30	2	5	0.11	1:1.6	1.17
C5	1.30	4	45	0.18	1:3.2	1.07

Solution volume = 40cm^3 Polymerisation time = 20hrs.

Volume of acetylene = 2dm^3 ≈ 0.1 mol Temp.= 20°C

The average yields of polyacetylene in this series of experiments were greater than those obtained with the same catalyst, but using the sequential addition technique (table 3.2). Therefore, it may be concluded that premixing the catalyst components, before admitting acetylene, substantially enhances the production of polyacetylene. This result is in contrast to the observations made concerning component premixing in metathesis catalysis. When WCl_6 and $AlEtCl_2$ are mixed the effectiveness of the mixture in promoting the metathesis polymerisation of cyclic alkenes is substantially reduced, compared with that of the catalyst system formed by sequential addition of WCl_6 and $AlEtCl_2$ to a solution of the monomer.(146) The differences in catalyst activity towards alkene and alkyne polymerisation may suggest that different types of active centre are responsible for the polymerisation of each of the two classes of monomer. It is well known that aluminium alkyls and certain transition metal compounds form the basis of a typical Ziegler/Natta co-ordinated anionic polymerisation system and it is possible that the polymerisation of acetylene occurs by a similar mechanism in this instance. When premixed catalysts are used for ring opening metathesis polymerisations, reduction of the transition metal occurs prior to the addition of the monomer and it is thought that this process may be responsible for their low activity. Although the nature of the active site responsible for the polymerisation of acetylene catalysed by $WCl_6/AlEtCl_2$ is not known at present, one may speculate that a lower oxidation state of the tungsten atom is required compared to that responsible for alkene metathesis.

The results of the various polymerisations of acetylene presented in table 3.3 do not appear to show any significant dependence of the yields on either the premixing time or the molar ratio of the catalyst components. However a meaningful appraisal of this data is difficult because true catalytic behaviour may not be observed, possibly because of occlusion of the active sites by newly formed polyacetylene.

3.3.2.2 Characterisation

The carbon/hydrogen mole-atom ratios of the products of the polymerisations, in which catalyst premixing was used, were determined by the technique described in section 2.5.1 and are included in table 3.4. The deviations of the values from the theoretical ratio of unity, expected for polyacetylene, were similar to those observed for products prepared using the sequential addition technique (section 3.3.1.3) and may also be attributed to sample contamination.

Scanning Electron Microscopy (SEM) was used to investigate the morphology of the polyacetylene produced using the $WCl_6/AlEtCl_2$ premixing technique and a typical micrograph is shown in plate 3.1. The matted, fibrillar morphology is characteristic of samples of polyacetylene prepared by catalytic polymerisation. The average diameter of a fibril was estimated to be 3μm. This may be compared with a fibril diameter of 12μm reported by Aldissi and Schue for polyacetylene prepared using $WCl_6/SnPh_4$(140) and 0.04μm quoted by Schue for the diameter of a fibril of polyacetylene obtained using the catalyst $WCl_6/LiBu$(142).

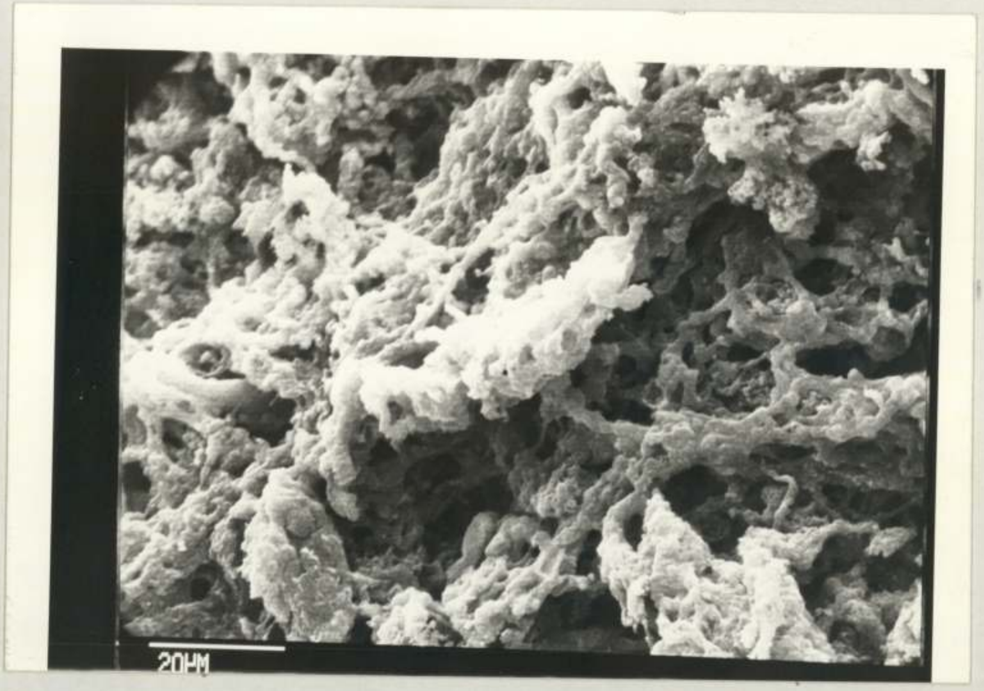

Plate 3.1 Scanning Electron Micrograph of polyacetylene prepared using a metathesis catalyst

3.4 THE POLYMERISATION OF ACETYLENE USING $WCl_6/AlEt_3$ AS CATALYST

3.4.1 Polymerisation

The polymerisation of acetylene was carried out using the method outlined in section 2.3.1. In a typical experiment, 1.00×10^{-4} moles of WCl_6 were premixed with 1.35×10^{-3} moles of $AlEt_3$ for 15 minutes. When acetylene was admitted, the dark brown solution turned from deep red, through maroon to purple and a black precipitate formed within a few minutes. The polymerisation was allowed to proceed for 20 hours at 20°C. The precipitate was isolated by the method described in section 2.4.1 and the yield was 0.21g. Generally, the yields of polymer obtained using this catalyst system were comparable with those obtained when the premixed $WCl_6/AlEtCl_2$ catalyst was used.

3.4.2 Characterisation

The infra-red (ir) spectra of samples of polyacetylene prepared using $WCl_6/AlEt_3$ were recorded by the method described in section 2.5.3. The ir spectrum of a typical sample is shown in figure 3.1. The strong band occurring at $1013cm^{-1}$ is characteristic of the C-H out of plane deformation of trans-polyacetylene units while the band at $740cm^{-1}$ may be assigned to the C-H out of plane bending mode of cis-polyacetylene segments. It is possible to estimate the relative proportions of cis and trans-polyacetylene segments in a sample from ir spectral data using the formula

$$\%cis = 100\,A_{cis} / (A_{cis} + 0.77\,A_{trans})$$

where A_{cis} is the absorbance (optical density) of the cis-polyacetylene band at $740cm^{-1}$ and A_{trans} is the absorbance of the trans-polyacetylene band at $1013cm^{-1}$.(147) The optical densities for these bands in the spectrum presented in figure 3.1 show that the sample was comprised of nearly equal amounts of cis (48%) and trans (52%) forms of polyacetylene.

Polyacetylene is known to be readily oxidised when exposed to the atmosphere by a mechanism(36) which may be summarised as

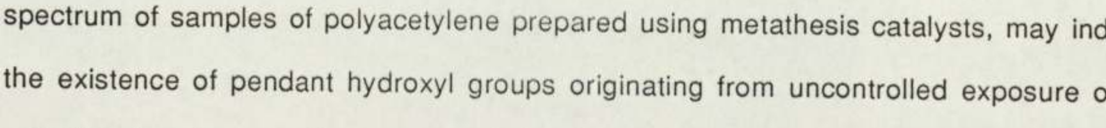

$$-CH{=}CH- + \tfrac{1}{2}O_2 \longrightarrow -CH{=}\underset{\displaystyle OH}{\underset{|}{C}}- \longrightarrow -CH_2-\underset{\displaystyle O}{\underset{\|}{C}}-$$

The presence of a broad absorbtion band centred at $3400cm^{-1}$, often observed in the ir spectrum of samples of polyacetylene prepared using metathesis catalysts, may indicate the existence of pendant hydroxyl groups originating from uncontrolled exposure of the samples to atmospheric oxygen. Indeed the infra-red absorption band centred at $1630cm^{-1}$ is not too different in frequency from the infra-red band observed for unsaturated ketones, which commonly occur at $1665cm^{-1}$.

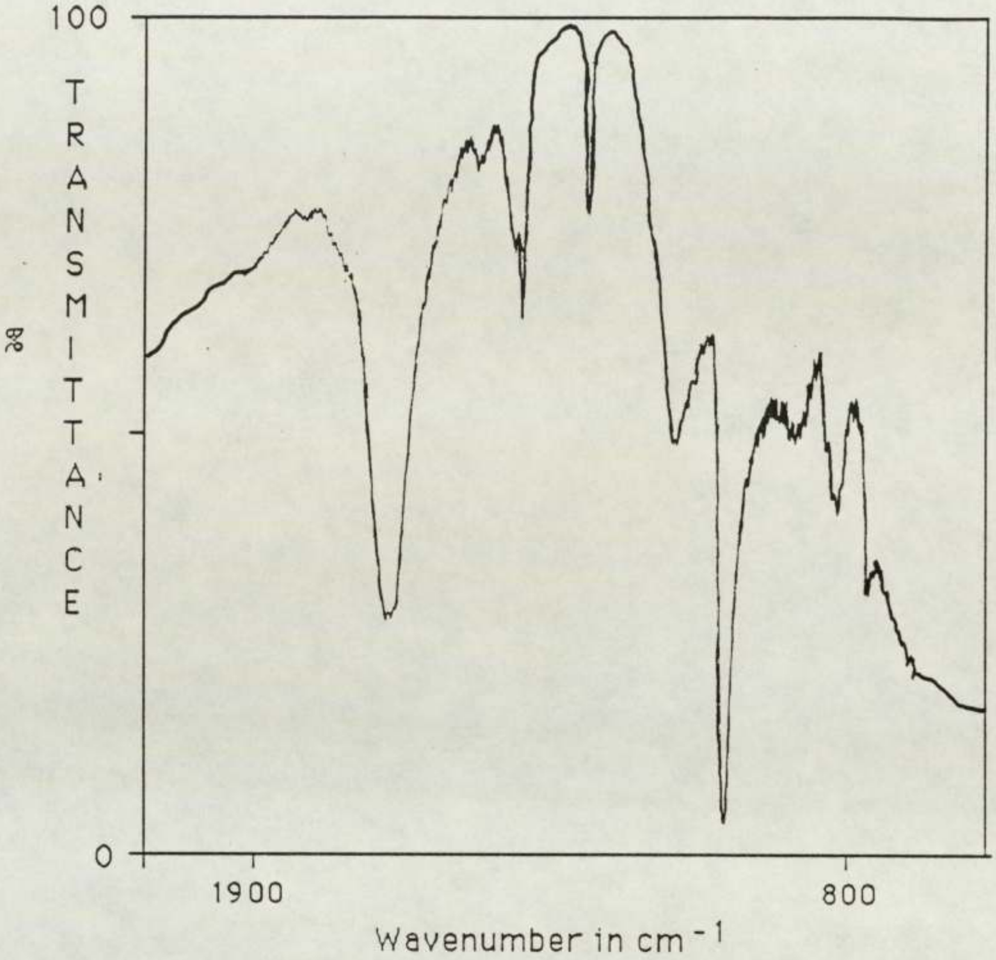

Figure 3.1 Infra-red spectrum of polyacetylene prepared using a metathesis catalyst

CHAPTER 4

SYNTHESIS OF BLOCK COPOLYMERS OF ACETYLENE AND CYCLOPENTENE USING METATHESIS CATALYSTS

4.1 INTRODUCTION

Certain polymerisations, particularly those in which propagation occurs at an anionic centre, are known to produce systems in which termination and chain transfer are absent.(148) Therefore, even when propagation has ceased, because the concentration of monomer has reached its equilibrium value, the propagating centre remains intact and is still active. Active polymer systems such as these have often been termed "living polymers" because of the extraordinarily long lifetimes of the active centres and because the active chains will continue to grow if more monomer is subsequently introduced to the system. If a different monomer is added to the living polymer, then a block copolymer may form. For example, a simple diblock copolymer may be prepared by adding a monomer (B) to a living polymer of monomer (A) provided that the living system is capable of initiating the polymerisation of the second monomer.

In principle, block copolymers that contain polyacetylene and polystyrene segments, could be synthesised by a living polymer route similar to that described above. Ziegler/Natta catalyst systems, which are the most effective catalysts for the polymerisation of acetylene, will also polymerise styrene. However, the lifetimes of the active centres in both systems are too short for them to be classed as "living polymers" because chain transfer and termination reactions occur which produce "dead" homopolymers and deactivate the catalyst. The most common route to block copolymers that contain polyacetylene segments involves the use of an anionic to Ziegler/Natta transformation reaction (see section 1.6.2.1).

The feasibility of an anionic-to-metathesis transformation reaction has been investigated by Amass and Gregory(149) who successfully prepared block copolymers that contained polypentenylene and polystyrene segments. The work presented in chapter 3 showed that acetylene could be polymerised using the metathesis catalyst WCl_6/LiBu and an anionic-to-metathesis transformation route to block copolymers which contain polyacetylene sequences was then developed (figure 4.1). This route has subsequently been employed to prepare block copolymers of acetylene and styrene.(150)

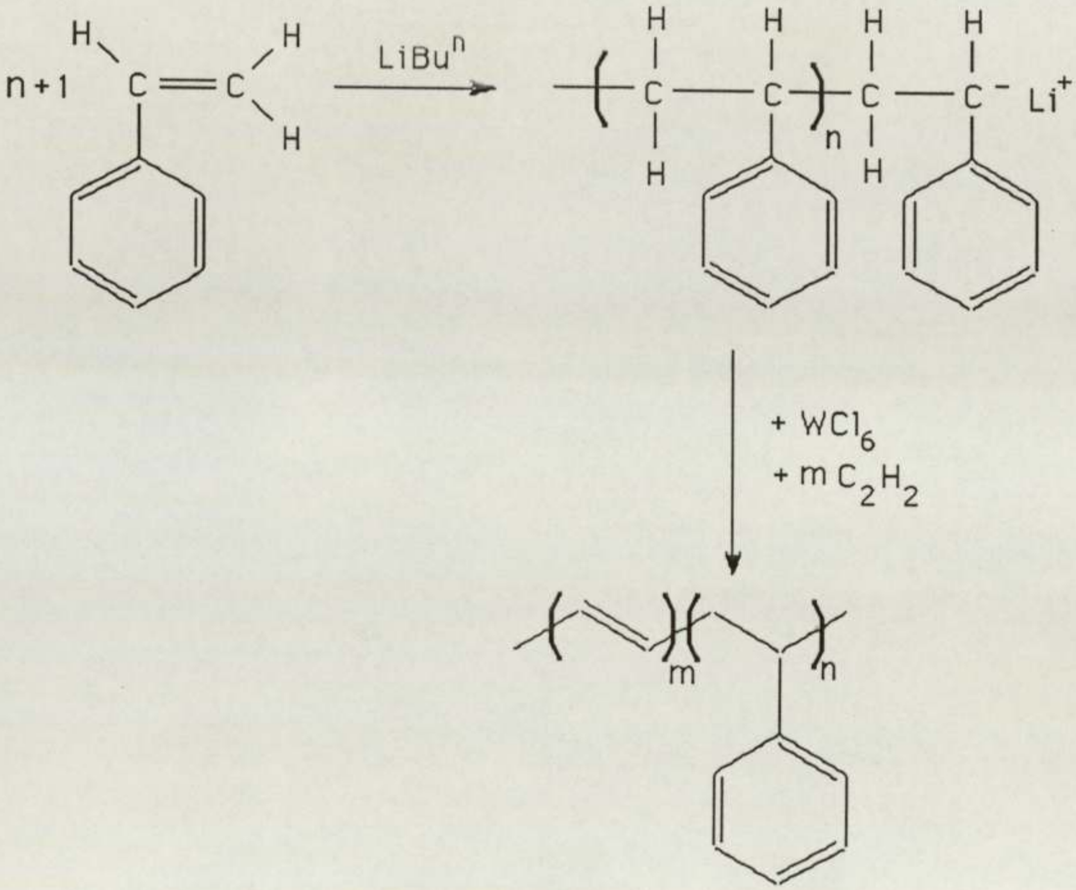

Polystyrene-block-co-acetylene

Figure 4.1 Anionic-to-metathesis transformation route to Poly (styrene-block-co-acetylene)

Although there is some evidence that termination reactions occur during metathesis polymerisations, these reactions are reported to be less significant than those which occur in Ziegler/Natta systems.(151) This suggests that the average lifetime of the propagating centres present during metathesis polymerisations may be longer than that of the active sites present in Ziegler/Natta systems. If it is the case that the ring opening metathesis polymerisation of a cyclic alkene produces a "quasi-living polymer" then it may be possible to prepare block copolymers by the introduction of a second monomer to this type of living system. Until recently, only one attempt to exploit quasi-living metathesis as a synthetic route to block copolymers has appeared in the literature.(152) This involved the polymerisation of a bicyclic monomer initiated using $WCl_6/AlEtCl_2$ at 50°C. After two hours cyclopentene was added followed, after a further two hours, by more bicyclic monomer. However, it is doubtful if the polymeric product had the claimed A-B-A structure since the concentration of cyclopentene used in the preparation of the polymer was far below its equilibrium value at this temperature.

Catalyst systems which are comprised of WCl_6 and an alkyl aluminium compound can initiate the polymerisation of acetylene (see chapter 3). These systems will also catalyse the ring opening metathesis polymerisation of cyclic alkenes. Therefore the preparation of a quasi-living polymer by ring opening metathesis polymerisation may be considered as the basis of a route for the production of block copolymers that contain polyacetylene segments (figure 4.2).

The aim of the experiments described in this chapter was to investigate the feasibility of the reaction scheme presented in figure 4.2 for the production of soluble copolymers that contain polyacetylene segments.

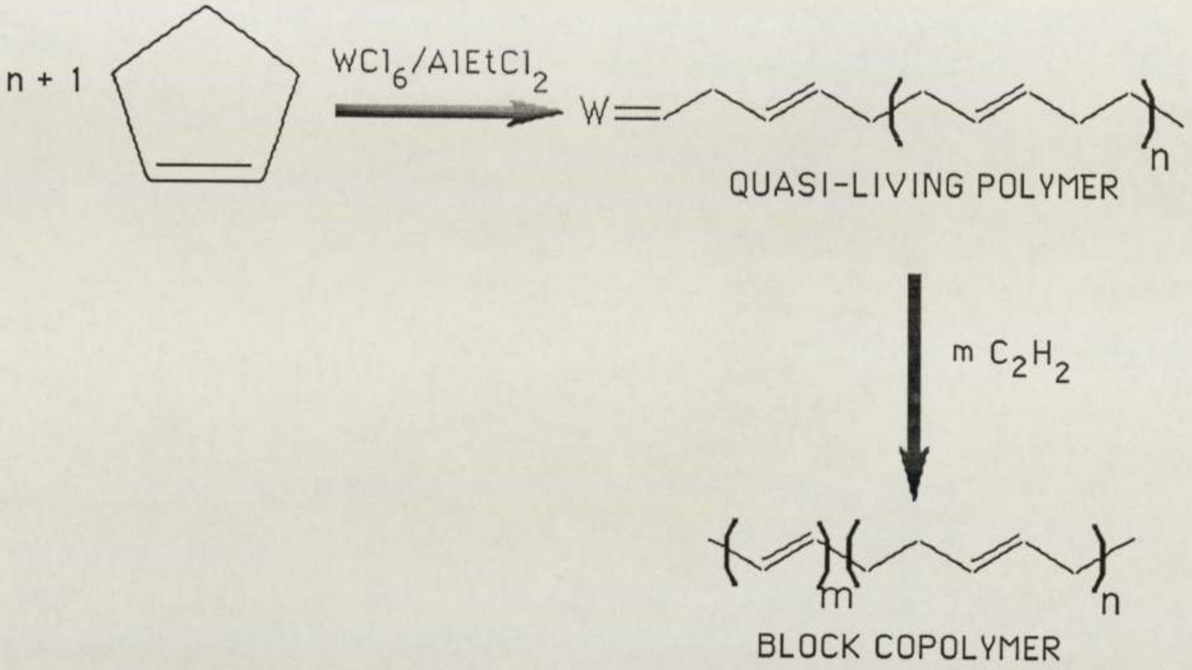

Figure 4.2 Synthesis of polypentenylene-block-co-acetylene by sequential addition of the two monomers to an active metathesis catalyst

4.2 THE COPOLYMERISATION OF ACETYLENE AND CYCLOPENTENE USING THE CATALYST $WCl_6/AlEtCl_2$

4.2.1 Polymerisation

The polymerisation was carried out by the method described in section 2.3.2. In a typical experiment, 3×10^{-4} mol WCl_6 was added to a solution of 0.22 mol cyclopentene in $50cm^3$ cyclohexane. After a delay of two minutes, 1.2×10^{-3} mol $AlEtCl_2$ was added. A viscous dark brown solution of polypentenylene was produced and after 1.5 hours acetylene was admitted. The mixture darkened and after a further five minutes appeared black . The reaction was allowed to proceed for a further 20 hours after which time the active polymerisate was poured into methanol and a black elastomeric product was isolated.

The product was found to be soluble in a range of organic solvents. A two percent by weight to volume solution in cyclohexane appeared black. However the solution was a clear deep red when viewed with the aid of a strong lamp. When the solution was passed through a Whatman number 1 filter, no solid material was isolated.

4.2.2 Effect of varying the time allowed for the ring opening polymerisation of cyclopentene during the copolymerisation of acetylene and cyclopentene.

A series of experiments was performed in which the time allowed for the ring opening polymerisation of cyclopentene was varied. The results of these experiments are shown in table 4.1.

Table 4.1 Copolymerisation of cyclopentene and acetylene: Effect of cyclopentene polymerisation time.

Reference	[cyclopentene] /mol.dm^{-3}	[WCl_6] /mol.dm^{-3}	cyclopentene polymerisation time /mins	state (yield /g)
D1	2.7	3.6	0	insoluble (0.2)
D2	2.8	3.1	5	soluble (0.9)
D3	2.8	3.5	13	soluble (1.4)
D4	2.8	3.6	90	soluble (3.5)

Molar ratio [WCl_6]/[$AlEtCl_2$] = 1 : 4 ; volume of solution = 45cm^3

acetylene polymerisation time = 20 hrs ; reaction temperature = 20^{o}C

Volume of acetylene = 2dm^3 ≈ 0.1 mol

Experiment D1 was performed by adding the solutions of catalyst and co-catalyst to a mixture of the monomers in cyclohexane. The time delay between the additions was two minutes. The golden yellow solution immediately turned purple and within two minutes a black precipitate formed. The product of this polymerisation can be considered to be either a random or block copolymer, or a homopolymer of either of the participating co-monomers. Cyclopentene, polypentenylene and low molecular weight polyenes are soluble in cyclohexane, accordingly the product of this reaction cannot be polypentenylene or a random copolymer of the two monomers because the product was insoluble in this solvent. The yield of polymer was greater than that obtained when acetylene alone was polymerised under similar conditions, therefore it is possible that both polypentenylene and polyacetylene units are present in the sample. This conclusion is supported by the elemental analysis of the material which shows that the carbon : hydrogen weight ratio in the black precipitate is 9.4 : 1. This value lies midway between the expected values of 12 : 1 for polyacetylene and 7.5 : 1 for polypentenylene. It is possible that the product was a mixture of homopolymers, the polypentenylene adhering to or occluded within polyacetylene particles. However the C:H ratios could also be explained by the formation of a copolymer that consisted of long chains of polyacetylene terminated with or connected by polypentenylene sequences. For a copolymer such as this to be formed, acetylene must be a far more reactive monomer than cyclopentene, for this particular catalyst system, because the concentration of cyclopentene (2.5M) far exceeds the concentration of acetylene (estimated to be below 0.01M) in the solution.

In experiment D2, the ring opening polymerisation of cyclopentene was allowed to proceed for five minutes and then acetylene was added to the reaction mixture. An ink blue solution remained after twenty hours together with a small quantity of precipitate. When this solution was exposed to air, a colour change to cherry red occurred and eventually a black precipitate and a colourless solution were formed.

The products of experiments D3 and D4 remained dissolved throughout the course of the polymerisation. They were isolated as black elastomeric materials by precipitation of the polymer solution in methanol and could be redissolved in a range of organic solvents to produce cherry red solutions.

The results outlined in table 4.1 show that the amount of soluble material increased as the time allowed for the polymerisation of cyclopentene was increased. This may suggest that the average length of the polypentenylene chains, relative to that of the polyacetylene sequences, increased with cyclopentene polymerisation time. However it is well documented that high molecular weight material is produced very rapidly in ring opening metathesis polymerisations and so this simple view may not fully describe the situation.

4.2.3 Effect of the concentration of cyclopentene on the copolymerisation of acetylene and cyclopentene

In section 1.3.1, it was shown that the ring opening metathesis polymerisation of cycloalkenes could be described in terms of an equilibrium between ring and chain species. The feasibility of the polymerisation process was shown, by consideration of the relative magnitudes of the thermodynamic parameters ΔS and ΔH for a given monomer/polymer system, to depend markedly on the concentration of monomer and the temperature of reaction. The existence, for some systems of a temperature called the ceiling temperature has also been predicted. Above this temperature, even pure monomer cannot polymerise. Below this temperature there exists a temperature dependent equilibrium concentration of monomer which must be exceeded if high molecular weight material is to be produced. Experimental verification of this behaviour for the ring opening polymerisation of cyclopentene using $WCl_6/AlEtCl_2$ as catalyst has been reported by Ofstead(153) and the results of these studies are depicted graphically in figure 4.3. It can be concluded from this data that the concentration of cyclopentene must exceed 1M if the polymerisation of cyclopentene is to proceed at 20^oC.

To investigate the effect of the concentration of cyclopentene on the copolymerisation of acetylene and cyclopentene, a series of experiments was performed in which the concentration of cyclopentene was varied. The results of these experiments are summarised in table 4.2.

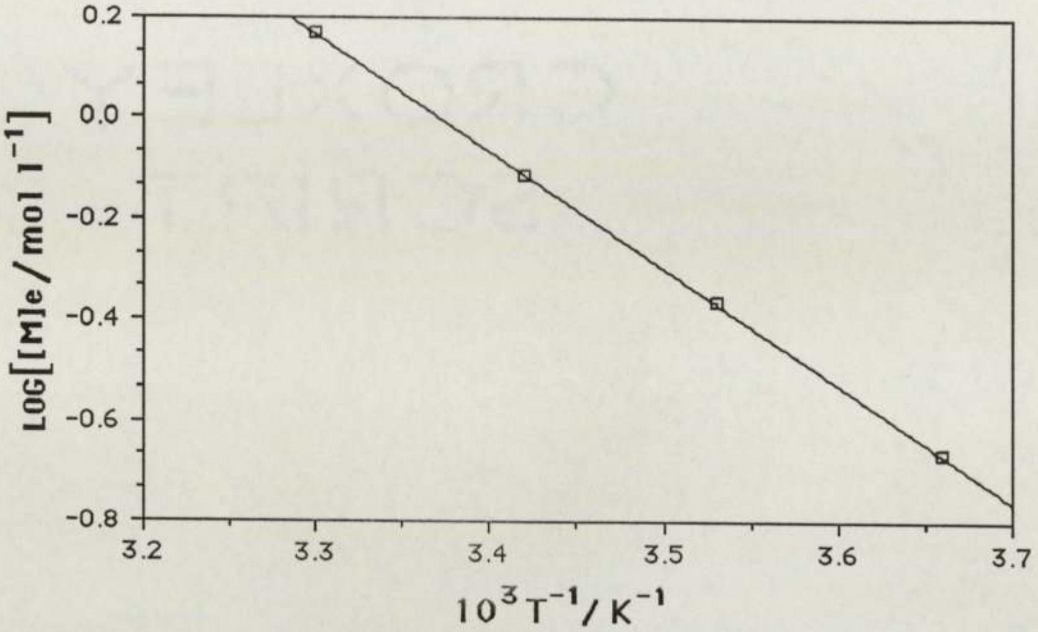

Figure 4.3 Equilibrium concentration of cyclopentene using $WCl_6/AlEtCl_2$ as catalyst.

Table 4.2 Effect of the concentration of cyclopentene (cp) on the copolymerisation of acetylene and cyclopentene

Reference	[cp] /mol dm^{-3}	[WCl_6] /mol dm^{-3}	t_{cp}* /min	state
E1	0.6	2.0 x10^{-3}	1200	insol. powder
E2	3.0	1.5 x10^{-3}	1200	sol. elastomer
E3	5.3	3.1 x10^{-3}	5	insol. gel
E4	6.3	3.8 x10^{-3}	3	insol. gel

Molar ratio $[WCl_6]/[AlEt_3] = 1 : 4$ Volume of acetylene = $2dm^3 \approx 0.1$ mol

Temperature of reaction = 20°C   Acetylene polymerisation time = 20 hrs

* Time allowed for the polymerisation of cyclopentene before acetylene was admitted.

In experiment E1 the concentration of cyclopentene was below its equilibrium concentration at 20°C. Hence, even after 20 hours, gpc analysis of a sample of the cyclopentene polymerisation mixture showed that it contained no high molecular weight polymer. A black fibrous precipitate, which had a golden lustre, formed when acetylene was added to the mixture of cyclopentene and catalyst. Samples of doped polyacetylene commonly exhibit metallic lustrous surfaces, indeed recent reports claim that polyacetylene may be doped with WCl_6 to produce golden lustrous materials.(144) This observation may suggest that the polymer sample produced in this experiment had been solution doped with WCl_6. However, to achieve this state, high concentrations of dopant are normally required which were not available in this case. If this effect indeed occurs, then it may suggest that cyclopentene, whilst not engaged in the production of high molecular weight polymer, can enhance the ability of WCl_6 to act as a dopant of conjugated polymers. It is quite possible that WCl_6 is not actually the doping material, but a product of the reaction of WCl_6 with an alkene is the active dopant. In this case the presence of cyclopentene would promote the production of the dopant.

At higher concentrations of cyclopentene, as employed in experiments E3 and E4, green/black elastomers were produced that swelled but did not dissolve in cyclohexane and other common organic solvents. When the material was extracted with toluene for five days at 60°C, the product did not dissolve and a sligthly yellow extract was produced. The lack of solubility of these polymers coupled with their ability to swell in organic solvents suggests that they may be di-block copolymers consisting of long chains of polyacetylene. In that case the polypentenylene chain would not be long enough to render these materials soluble. However, since polyacetylene chains are known to form aggregates in copolymeric materials the product would be expected to be particulate. An alternative explanation is that the polymer may be a tri or multi-block copolymer in which aggregated polyacetylene chains form cross-links, preventing the polypentenylene units from entering solution. The morphology which is expected for this type of system is shown in figure 4.4.

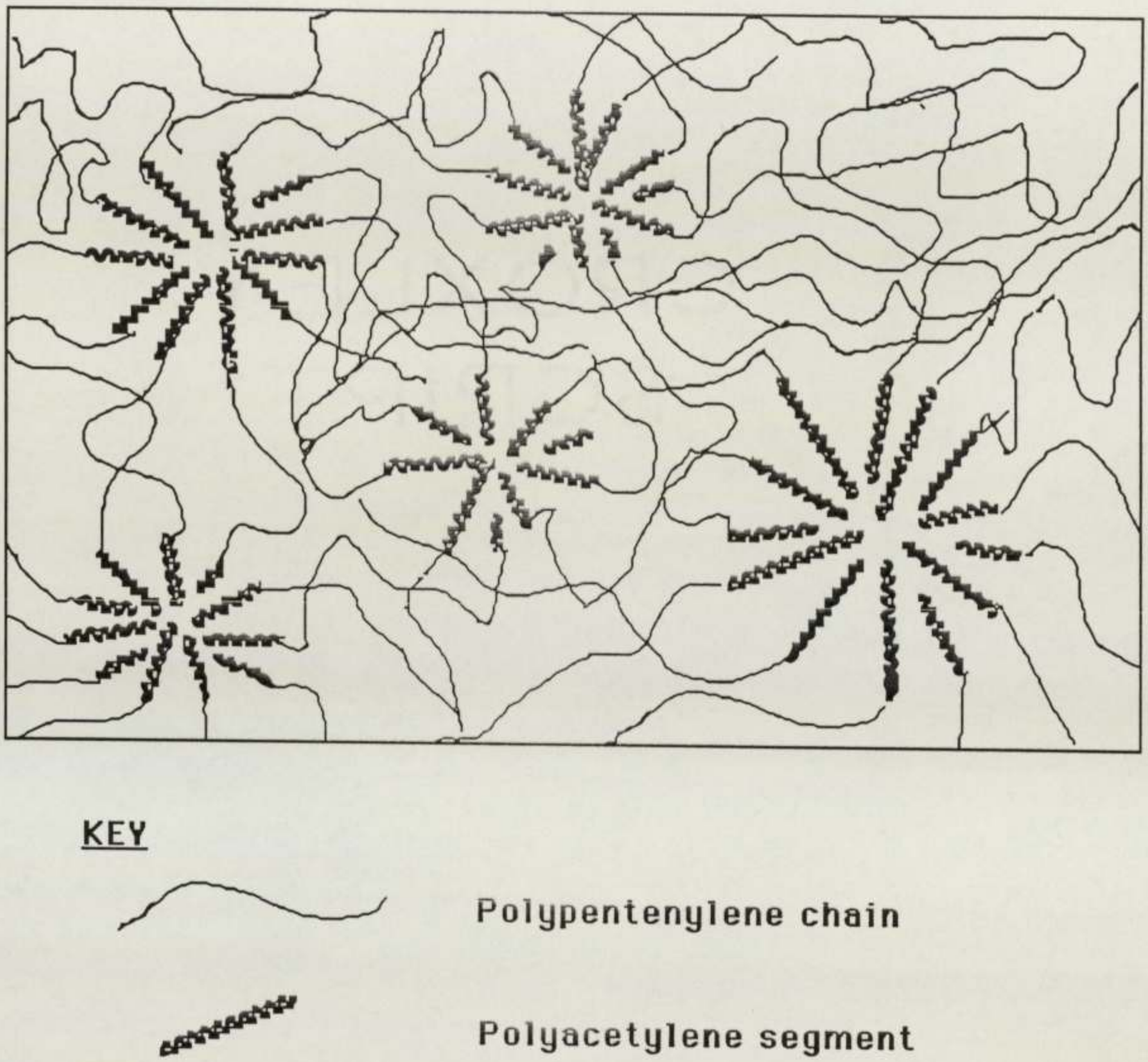

Figure 4.4 Suggested structure of a multiblock copolymer containing polypentenylene and polyacetylene segments.

Naarman(61) has shown that the rate of the bimolecular termination of acetylene polymerisation depends on the viscosity of the medium; similar properties are exhibited by the "gel effect" in free radical polymerisation which shows diffusion controlled termination reactions. When the polymerisation of acetylene is carried out in the highly viscous medium resulting from the prior polymerisation of cyclopentene, it might be expected that the rate of termination of the propagating polyacetylene sites would be reduced. In this case the propagating centre may be able to react occasionally with a molecule of cyclopentene to generate a typical olefin metathesis centre, which, once formed, may continue to add cyclopentene to form a short polypentenylene block before reforming the acetylene propagating centre by addition of acetylene. Sequences of reactions such as these have been described by Katz for the formation of multi-block copolymers of phenylacetylene and cyclopentene.(154) The mechanism for the termination of acetylene polymerisation is unknown but is thought to involve the aggregation of the polyacetylene segments.

4.3 THE COPOLYMERISATION OF ACETYLENE AND CYCLOPENTENE USING THE CATALYST $WCl_6/AlEt_3$

The work described in chapter 3 showed $AlEt_3$ to be a more effective activator than $AlEtCl_2$ in the polymerisation of acetylene using WCl_6 as the catalyst. Two experiments were carried out to investigate the effect of changing the cocatalyst in the reaction to form block copolymers of cyclopentene and acetylene.

The polymerisations were carried out using the method described in section 2.3.2. Addition of the catalyst components (WCl_6 and $AlEt_3$) to the cyclopentene solution produced a clear light brown mixture. Although the viscosity of the solution increased with time, the increase was not as marked as that observed when cyclopentene was polymerised using $WCl_6/AlEtCl_2$ as catalyst. The addition of acetylene produced an immediate colour change and a black precipitate in a pale yellow solution. The experimental conditions and results of these experiments are summarised in table 4.3.

Ivin(18) has studied the effect of varying the number of alkyl substituents on the aluminium alkyl cocatalyst used with WCl_6 for the ring opening polymerisation of cyclopentene. The activity of the catalyst, which results from mixing WCl_6 and the aluminium alkyl, in the polymerisation of cyclopentene decreases in the order $AlEtCl_2$ > $AlEt_2Cl$ > $AlEt_3$.

Table 4.3 The copolymerisation of acetylene and cyclopentene using $WCl_6/AlEt_3$ as catalyst

Sample	[cp] /mol dm^{-3}	[WCl_6] /mol dm^{-3}	cyclopentene polymn. time/ min	state (yield /mg)
F1	2.69	2.3×10^{-3}	18	insoluble (25)
F2	2.69	2.3×10^{-3}	2880	insoluble (30)

$WCl_6/AlEt_3$ ratio = 1 : 4 Acetylene polymerisation time = 20 hours

Volume of acetylene = $2dm^3 \approx 0.1$ mol Temp = 20^oC

It was suggested by Ivin that as the number of alkyl substituents increased, there was an increased possibility of forming olefins as by-products of the reaction. The molecular weights of the polymers produced using $AlEt_3$ would thus be limited by cross metathesis processes. This effect has also been studied by Hein(55), who found that WCl_6/Bu_4Sn gave low molecular weight polypentenylenes ($<M_n> = 5000$), whereas higher molecular weights were obtained when WCl_6/Ph_4Sn was used for the polymerisation of cyclopentene.

The materials produced in the copolymerisation experiments using $WCl_6/AlEt_3$ were insoluble and it must be concluded that the polypentenylene chains were insufficiently long to confer solubility on the copolymer. It would seem, in agreement with results presented earlier in this chapter, that the time allowed for the polymerisation of cyclopentene had no advantageous effects in this respect.

The conclusion that a copolymer was produced may be inferred from two important observations: Firstly, the yields were generally greater than those obtained when acetylene alone was polymerised under similar conditions (Section 3.4). Secondly, the carbon/hydrogen ratios were generally close to 10 : 1 i.e. about midway between the values calculated for polyacetylene (12 : 1) and polypentenamer (7.5 : 1).

4.4 CHARACTERISATION

4.4.1 Uv/visible spectroscopy

The uv/visible absorption spectrum of a sample of polypentenylene, prepared using the $WCl_6/AlEtCl_2$ catalyst system, was recorded by the method outlined in section 2.5.2 and is shown in figure 4.5. There is no observable absorption in the visible region. The peak at 214 nm may be attributed to a π to π^* transition of the isolated double bonds in the polymer repeat unit.

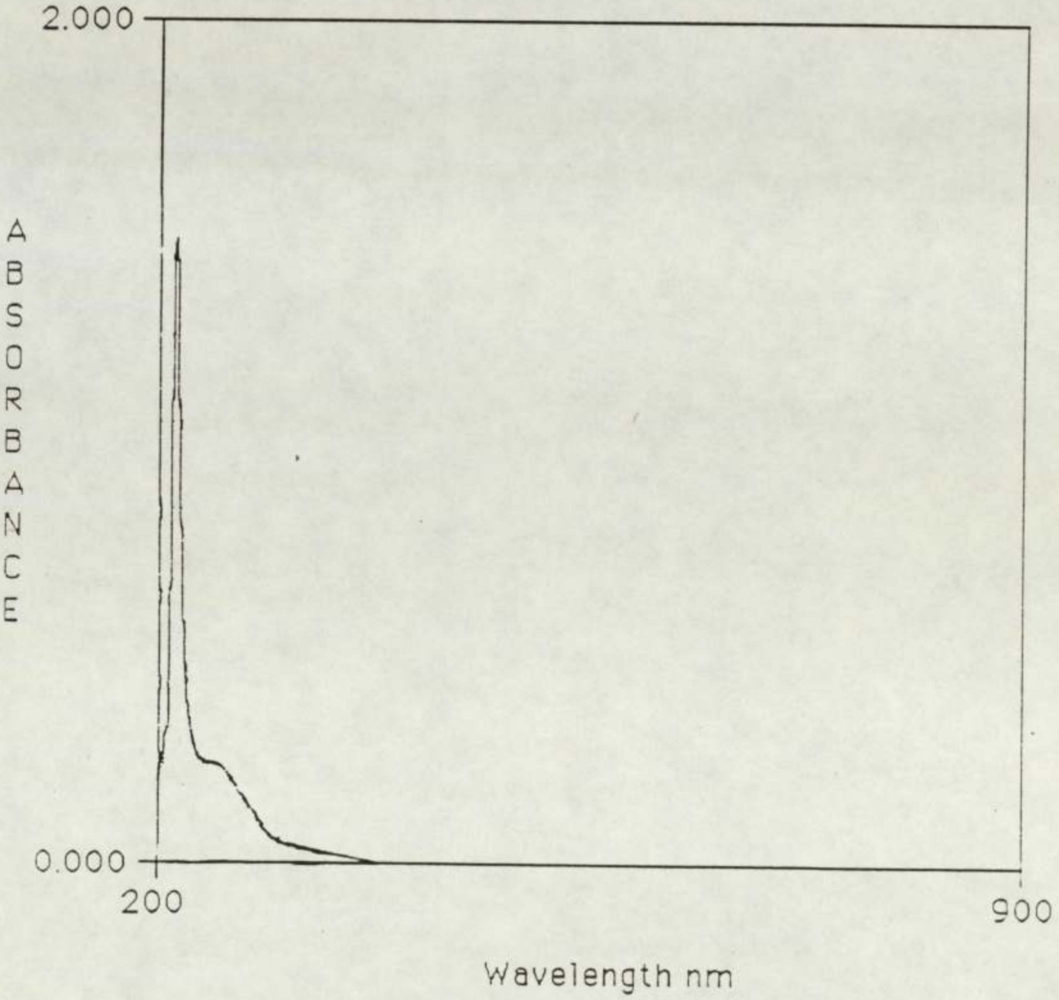

Figure 4.5 Uv/visible absorption spectrum of polypentenamer

Figure 4.6 shows a typical example of the uv/visible spectrum of a solution of copolymer prepared using $WCl_6/AlEtCl_2$. It can be seen that apart from the peak at 214 nm, which is due to polypentenamer, a broad absorption extends into the visible region and is centred at 400nm. This absorption has been assigned to the polyene segments of the copolymer and resembles that exhibited by films of polyacetylene.

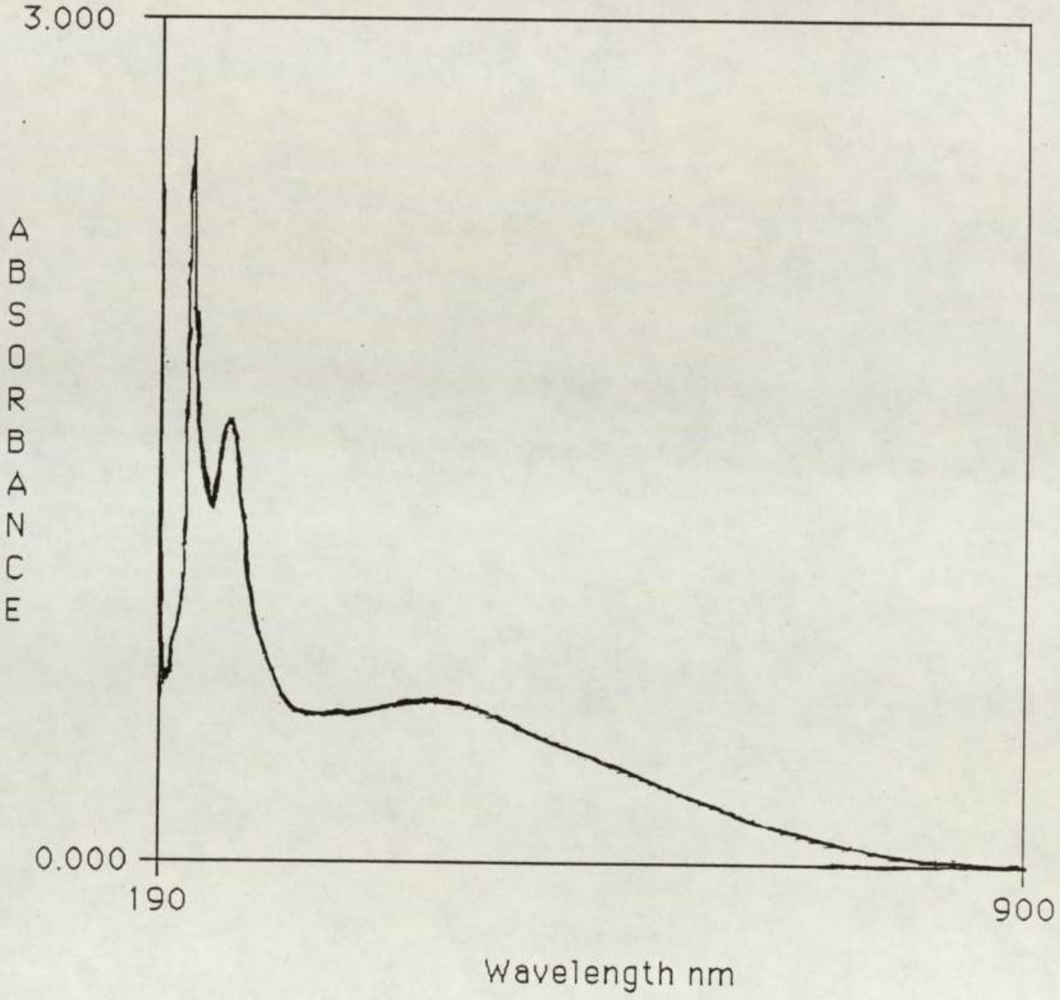

Figure 4.6 uv/visible absorption spectrum of soluble poly (pentenamer-co-acetylene)

A similar absorption has also been observed in the spectrum of graft copolymers of acetylene and butadiene. For the block copolymer, it is apparent that λ_{max} for this absorption ocurrs at shorter wavelengths than reported for both polyacetylene films and grafted copolymers where λ_{max} occurs at 500-600nm and 650-685nm, respectively.

The observed differences in the position of λ_{max} for the three types of material may be attributed to two factors: (i) The average conjugation length of the double bonds in the polyacetylene segment of the block copolymer may be shorter than that in polyacetylene films and graft copolymers; the average length of the sequences of polyacetylene may, or may not have decreased commensurately. It seems most likely that shorter chains of polyacetylene have been formed in the block copolymer as this would be expected to increase the solubility of the copolymer over that of a copolymer containing long polyacetylene chains. (ii) It has been shown that three dimesional interactions, of the type most likely to occur in films of polyacetylene, decrease the energy-gap and hence increase the maximum wavelength of the $\pi - \pi^*$ transition. Long range inter-chain interactions, such as those described above, would be drastically reduced when the copolymer dissolved and it would then be expected that the transition energy would be increased.

The uv/visible spectrum of a low molecular weight polyene, $Me(CH{=}CH)_nMe$, exhibits a characteristic series of absorptions which are often described as a "finger pattern".(156) As n increases, the absorptions move to progressively longer wavelengths. If the broad absorption, which is observed in the uv/visible spectrum of a sample of copolymer, is attributed to the presence of short polyene segments attached to chains of polypentenylene, then this absorbance may be compared with those of the isolated polyenes. The broad absorption of the copolymer then resembles that obtained from a mixture of low molecular weight polyenes where the average value of n is 10.

The spectrum of the copolymer also shows an absorption band centred around 250nm which is not seen for polypentenylene. The origin of this peak is uncertain but it can be linked to the presence of low molecular weight possibly oligomeric material (see section 4.4.2).

The soluble fractions obtained from copolymerisation experiments, in which the major products were insoluble solids, were also examined by uv/visible spectroscopy. These products were generally yellow and exhibited spectra characteristic of a mixture of low molecular weight polyenes. A typical spectrum of a material such as that described above is shown in figure 4.7.

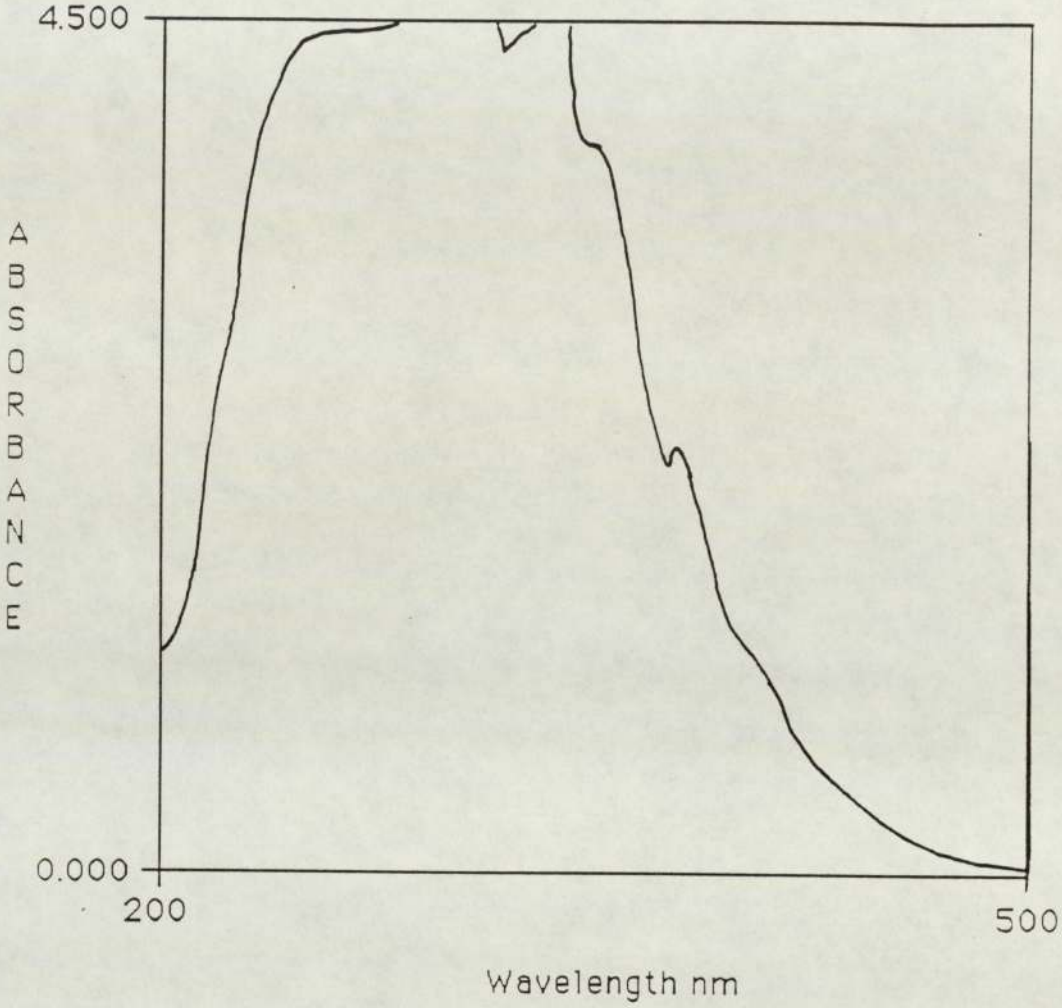

Figure 4.7 Uv/visible absorption spectrum of soluble extracts isolated from an insoluble sample of copolymer .

4.4.2 Gel Permeation Chromatography

Gel permeation chromatography (GPC) was performed on solutions of polypentenylene-block-co-acetylene, prepared in the experiments described in section 4.2. by the method described in section 2.5.4. A GPC trace typical of a sample of copolymer prepared using the $WCl_6/AlEtCl_6$ catalyst is shown in Figure 4.8. During this experiment, a sample of the polypentenylene was taken prior to the admission of acetylene. The chromatogram of this sample is shown in figure 4.9.

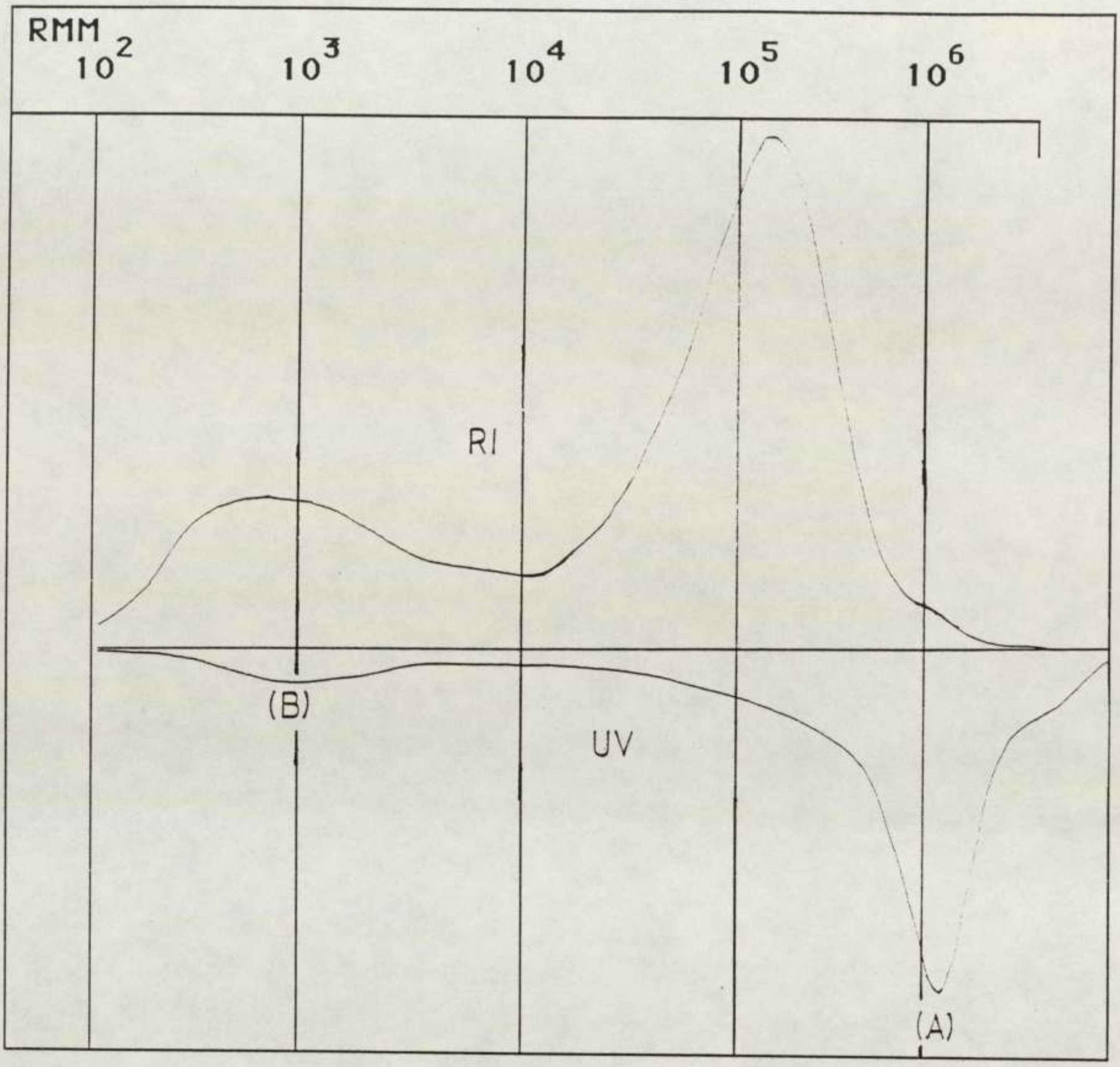

Figure 4.8 Gel Permeation Chromatogram of polypentenylene-block-co-acetylene 1% solution in THF.

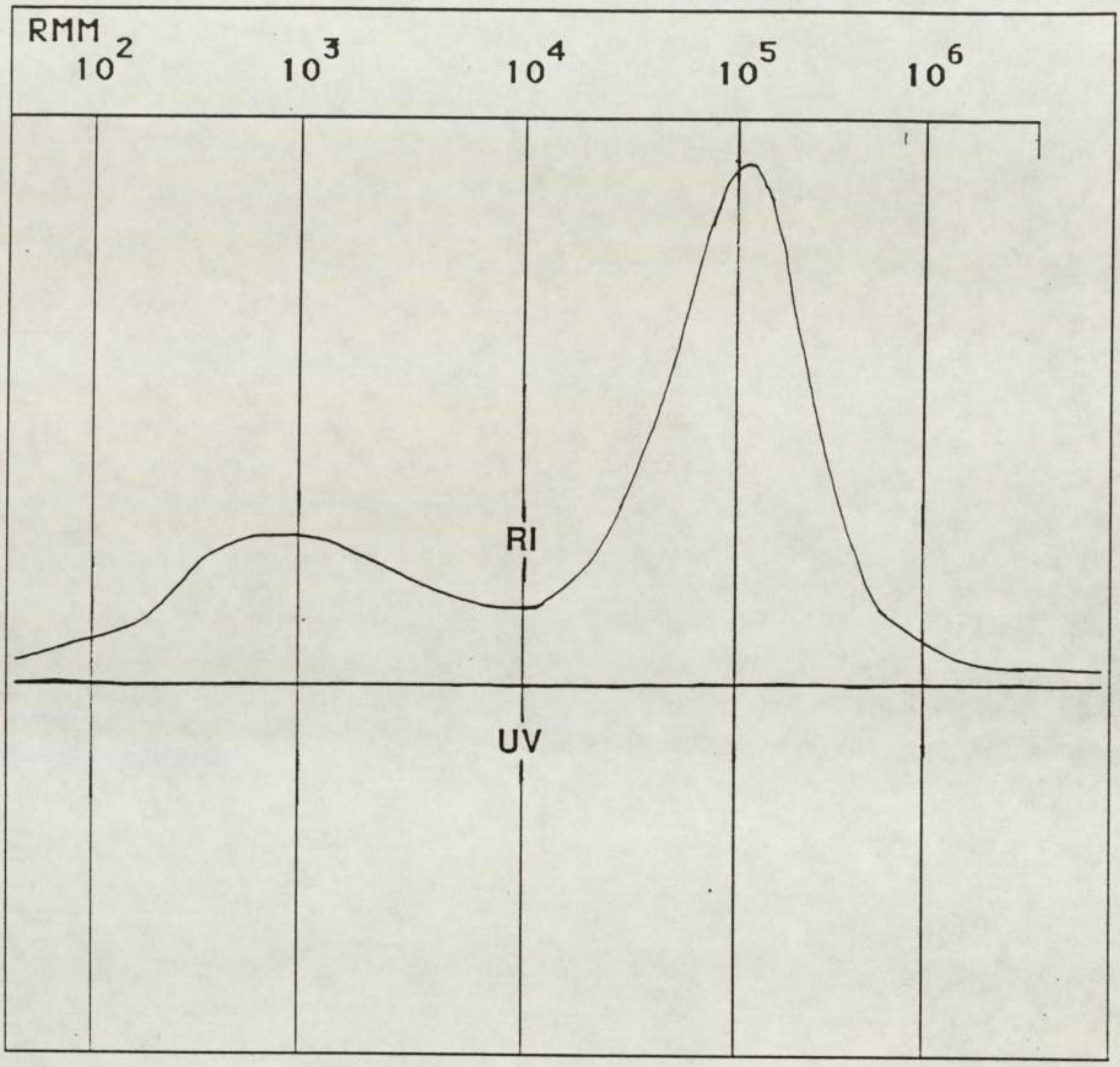

Figure 4.9 Gel Permeation Chromatogram of polypentenylene (1% solution in THF).

When comparing the two chromatograms, the most striking feature of the copolymer trace is the appearance of peaks in the absorption spectrometer trace (set at 400nm) which are not seen for polypentenylene. When comparing the differential refractometer traces, the copolymer shows the characteristic bimodal distribution which is commonly observed in samples of polypentenylene produced by metathesis polymerisation. A small sholder at high molecular weight ($<M_n> = 1.4 \times 10^6$ relative to standard samples of polystyrene) is also detected. This shoulder is connected with a large absorption (peak A) in the visible detector trace. Fine structure absorptions are also apparent which occur at even higher molecular weight and do not correlate with peaks in the refractometer output. It may be concluded that the material which is responsible for these peaks is absorbs strongly but is only present in low concentration. Indeed, it seems likely that the samples contain a large amount of unreacted polypentenylene homopolymer, which obscures the copolymer distribution in the refractometer trace, except for the small shoulder at high molecular weight .

The increase in the average molecular weight on copolymerisation cannot be explained in terms of the addition of small (8-10 acetylene units) polyene segments to polypentenylene chains of $<M_n> = 2 \times 10^5$. This would only yield an increase of $[(100 \times 26 \times 10)/(2 \times 10^5)] = 0.13\%$ in the molecular weight relative to that of the homopolymer. The observed difference in elution volume between the refractometer peak maximum for polypentenylene and the maximum in the absorption spectrometer trace for the copolymer may be estimated at 10%. This result suggests that the polyene chains of the copolymer aggregate to form large micellar-type structures. Aggregation would be expected to occur since the solubility parameters for the polyene chain in the solvent are so unfavourable. Polypentenylene chains in the copolymer may then be considered to form a solvent swolen layer which surrounds the polyacetylene aggregates.

Direct correlation between the broad polyene absorption, which occurs in the visible region of the uv/visible spectrum of the copolymer and the presence of high molecular weight material, which was observed in the GPC chromatograms, can be made by considering the change in the response of the GPC absorption spectrometer for fractions of the same sample of copolymer, as the wavelength of detection is varied. The chromatograms shown in figures 4.10 - 4.13 were obtained by GPC of four aliquots of a 1% solution of copolymer in THF. The detection wavelengths of the absorption spectrometer were 450, 400, 350, 300 nm respectively.

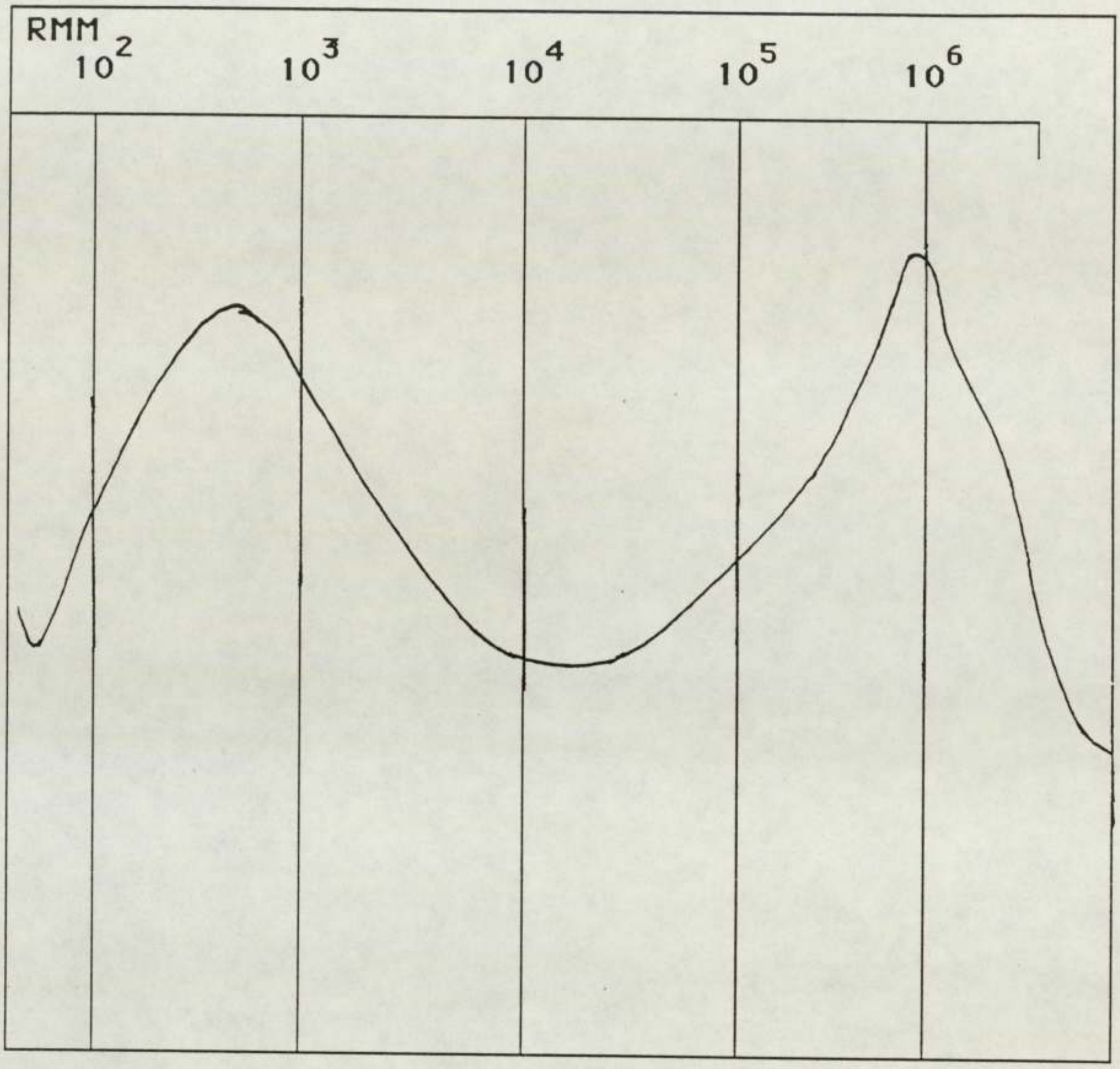

Figure 4.10 GPC chromatogram showing absorption detector response at 300nm

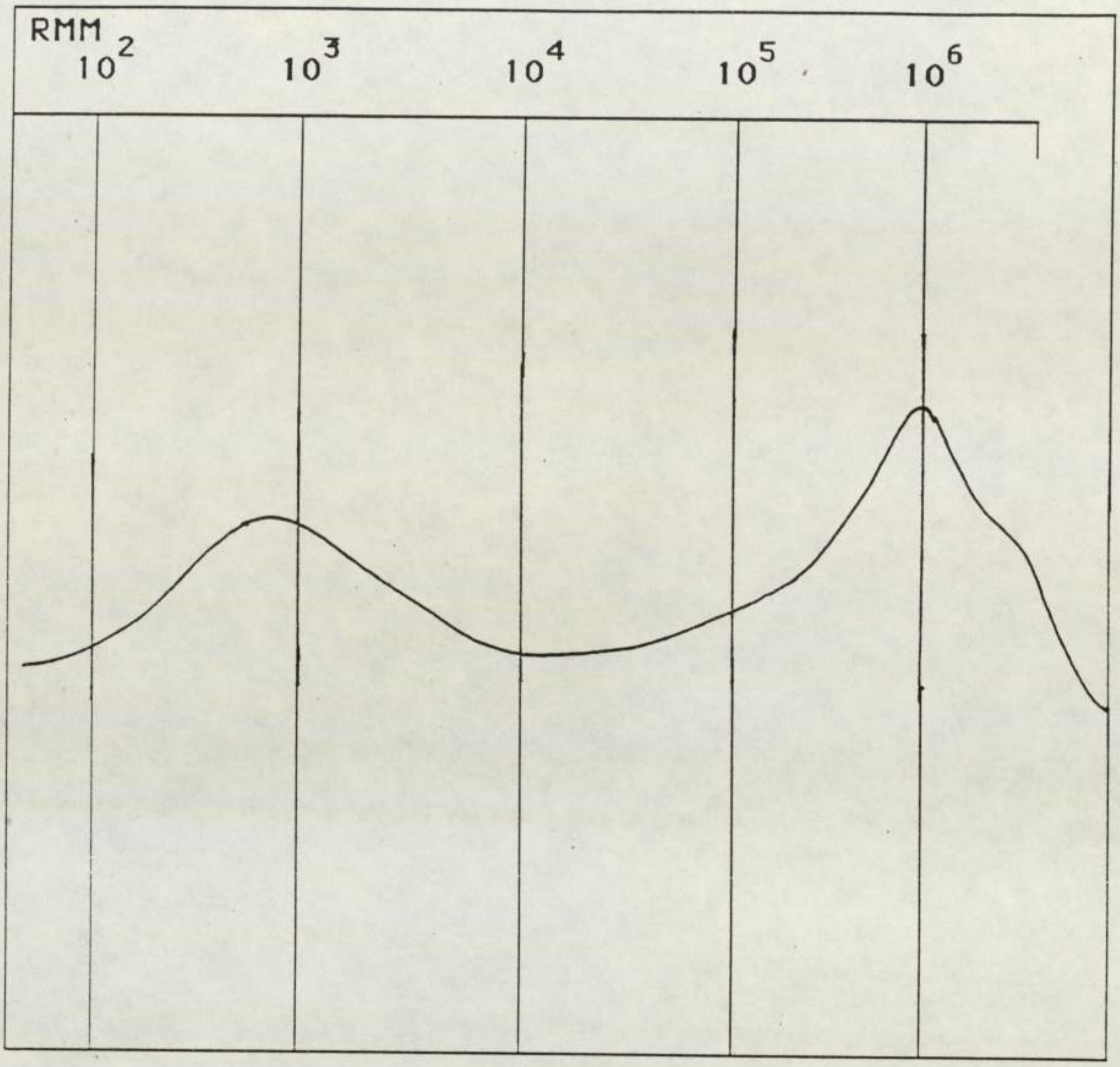

Figure 4.11 GPC chromatogram showing absorption detector response at 350nm

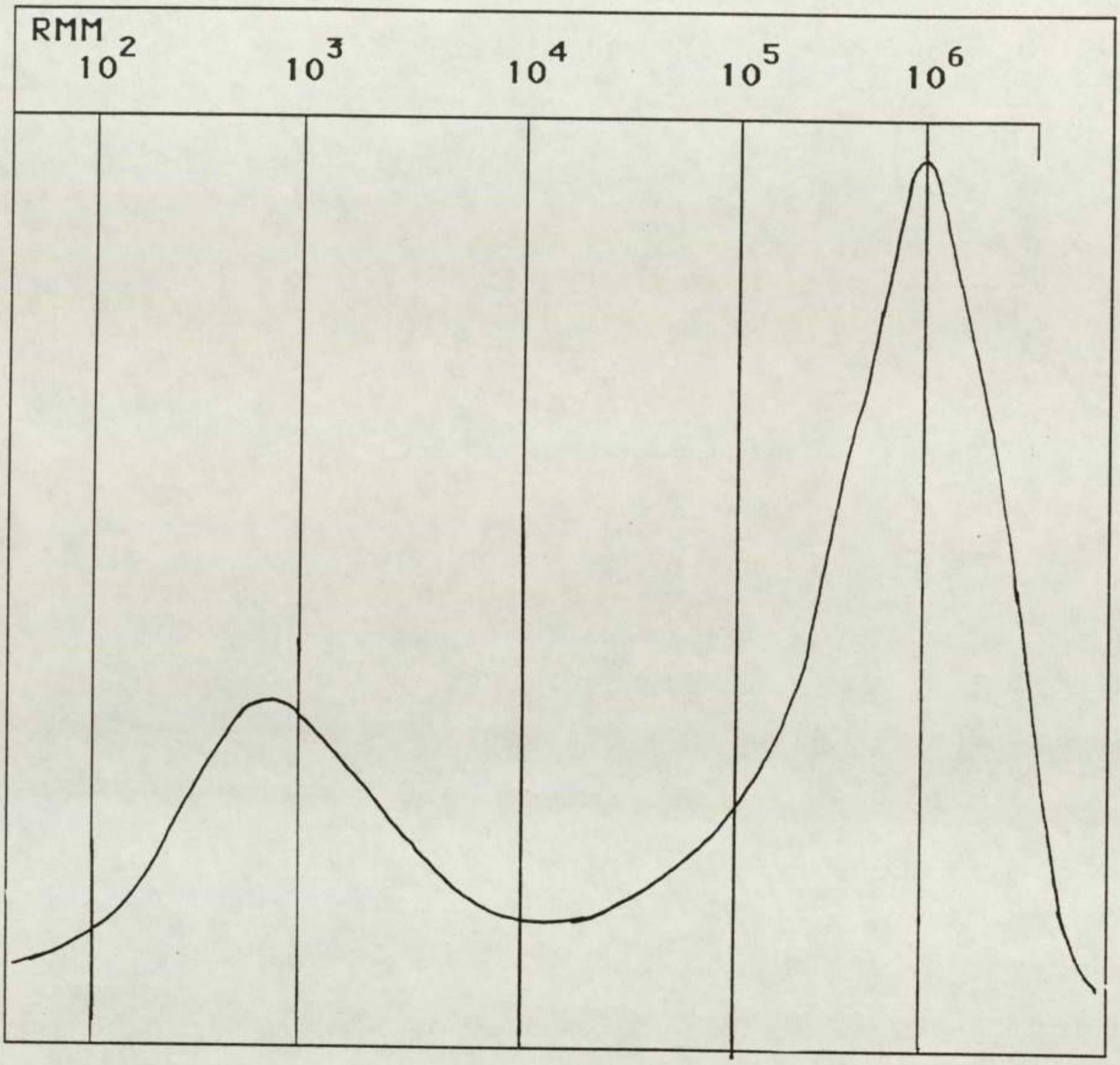

Figure 4.10 GPC chromatogram showing absorption detector response at 400nm

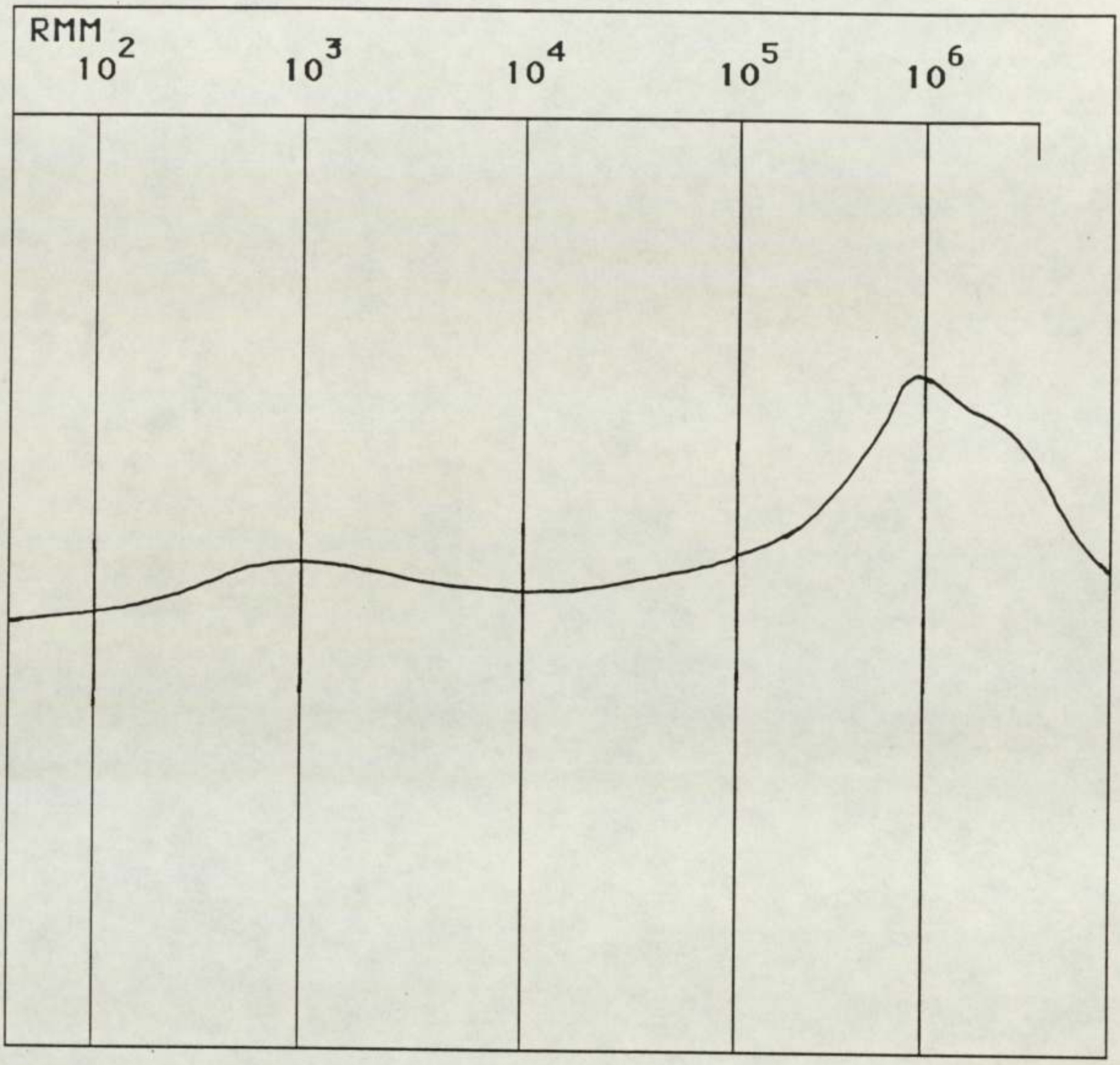

Figure 4.10 GPC chromatogram showing absorption detector response at 450nm

Table 4.4 details the relative heights of peaks A and B which were observed in the GPC absorption spectrometer traces of the chromatograms shown in figures 4.10 - 4.13. As the wavelength of detection was increased, the absorption due to higher molecular weight material increased relative to that of lower molecular weight species. It was also observed that, as the wavelength decreased, the peak (B) at lower molecular weight became more prominent.

Table 4.4 Variation of the absorption spectrometer response with wavelength

Detection wavelength /nm	Height of peak (A) / Height of peak (B)
450	4.1
400	2.9
350	1.9
300	1.2

The exact origin of this peak is not known, however it seems likely that it is linked to the absorption which is centred at 250nm in the uv/visible spectrum. (Section 4.3) As ring opening metathesis polymerisations often produce oligomers as by-products, it may be that oligomers which contain short polyene segments and which are insoluble in methanol are responsible for this peak.

4.4.3 Infra-red spectroscopy

The infra-red spectrum of a sample of soluble copolymer, recorded by the method described in section 2.5.3., was identical to that of a sample of polypentenylene except for a small, broad absorption in the 3100-3600 cm^{-1} region. This absorption, which is not observed in the spectrum of polypentenylene, is similar to, but less strong than the absorptions exhibited by samples of polyacetylene prepared using metathesis catalysts (section 3.4.2) and may be attributed to pendant hydroxyl groups which are distributed along the polymer backbone. The absence of any absorbances in this spectrum which are characteristic of polyacetylene, may be a consequence of the meagre ratio of copolymer to homopolymer in the sample. The absorptions due to polypentenylene units would then obscure those of the polyacetylene blocks in the copolymer.

The infra-red spectrum of the insoluble copolymer prepared in experiment D1 is shown in figure 4.14. The polyacetylene trans out of plane bending peak can be seen at 1014cm^{-1} and a small absorption at 966cm^{-1} indicates the presence of a small amount of polypentenylene.

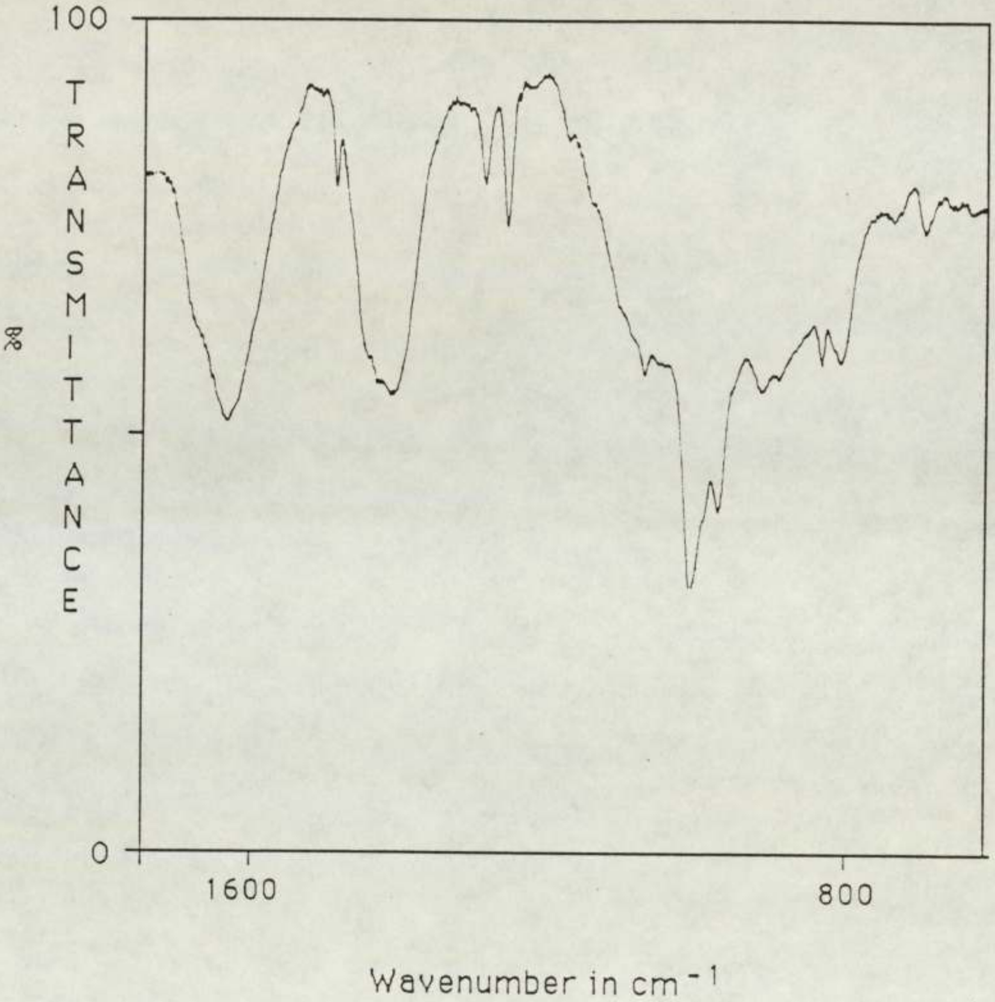

Figure 4.14 Infra-red spectrum of an insoluble copolymer.

CHAPTER 5

THE COPOLYMERISATION OF ACETYLENE AND CYCLOPENTENE USING AN ACTIVE SITE TRANSFORMATION REACTION

5.1 INTRODUCTION

The results presented in chapter 4 highlight some of the disadvantages of generating copolymers of pentenylene and acetylene units by a route employing only one type of catalyst. A soluble material was produced with $WCl_6/AlEtCl_2$ as catalyst, but in this case GPC and uv-visible spectroscopic evidence suggested that the copolymer content of the product was very low and that the length of the polyacetylene block was very short (eight to ten units long). The catalyst, $WCl_6/AlEtCl_2$, is a very efficient system for the polymerisation of cyclopentene. Varying the concentrations of the catalyst components or the molar ratio of $WCl_6/AlEtCl_2$ had no advantageous effects, either on the control of the length of the polyene segment or on the efficiency of acetylene polymerisation in the copolymerisation reaction. It was not possible to control the length of the polypentenylene unit of the copolymer either by varying the concentration of monomer or the molar ratio of the catalyst components. Previous work(157) had shown that this type of polymerisation produces high molecular weight polymer in the very early stages of the polymerisation, so that the time allowed for the ring opening polymerisation of cyclopentene could not be used to control the length of the polypentenylene block.

When the nature of the metal alkyl was altered, dramatic changes were observed in the relative ease with which the constituent monomers could be polymerised. For example, $WCl_6/AlEt_3$ is a relatively inefficient catalyst for the polymerisation of cyclopentene and the copolymers produced by these systems were invariably insoluble materials not amenable to unequivocal analysis. However, it did appear that the efficiency of the acetylene polymerisation was greater when $AlEt_3$ was used as cocatalyst and there appeared to be a greater prospect of controlling the length of the acetylenic block using the $WCl_6/AlEt_3$ system.

It was desirable however not only to control the length of the polyacetylene block, but to do this at the same time as controlling the block length of the polypentenylene. In other examples of block copolymer formation this may be achieved by adopting a reaction scheme which involves a transformation reaction (section 1.6.2.1). This approach requires polymerisation involving two different types of active centre. For example, Ziegler/Natta and anionic mechanisms. The results of experiments presented in chapters 3 and 4 have indicated that different types of active site are responsible for the homopolymerisation of acetylene and cyclopentene and hence it may be inferred that a catalyst transformation route such as that described in figure 5.1 may lead to a more satisfactory scheme for the production polypentenylene-block-co-acetylene on the following basis. Cyclopentene may be polymerised to high molecular weight polypentenylene using $WCl_6/AlEtCl_2$ as the catalyst. This particular catalyst combination is very active for the polymerisation of cyclopentene, but in the absence of cyclopentene shows low activity towards the polymerisation of acetylene. It might be concluded therefore that any sites able to polymerise acetylene are present only in low concentration during the rapid polymerisation of cyclopentene. The catalysts that are the most active for acetylene homopolymerisation, and are also more active catalysts for copolymerisation, are those that contain the more powerful reducing agent $AlEt_3$. It seemed reasonable to suggest that the site which was active for cyclopentene polymerisation (${}^{CP}W$) might be converted to a site that is active for acetylene polymerisation (${}^{AC}W$) by the addition of $AlEt_3$ to the quasi-living cyclopentene system. A study was therefore performed of the transformation of an active cyclopentene polymerisation into an active acetylene polymerisation by the addition of a second cocatalyst.

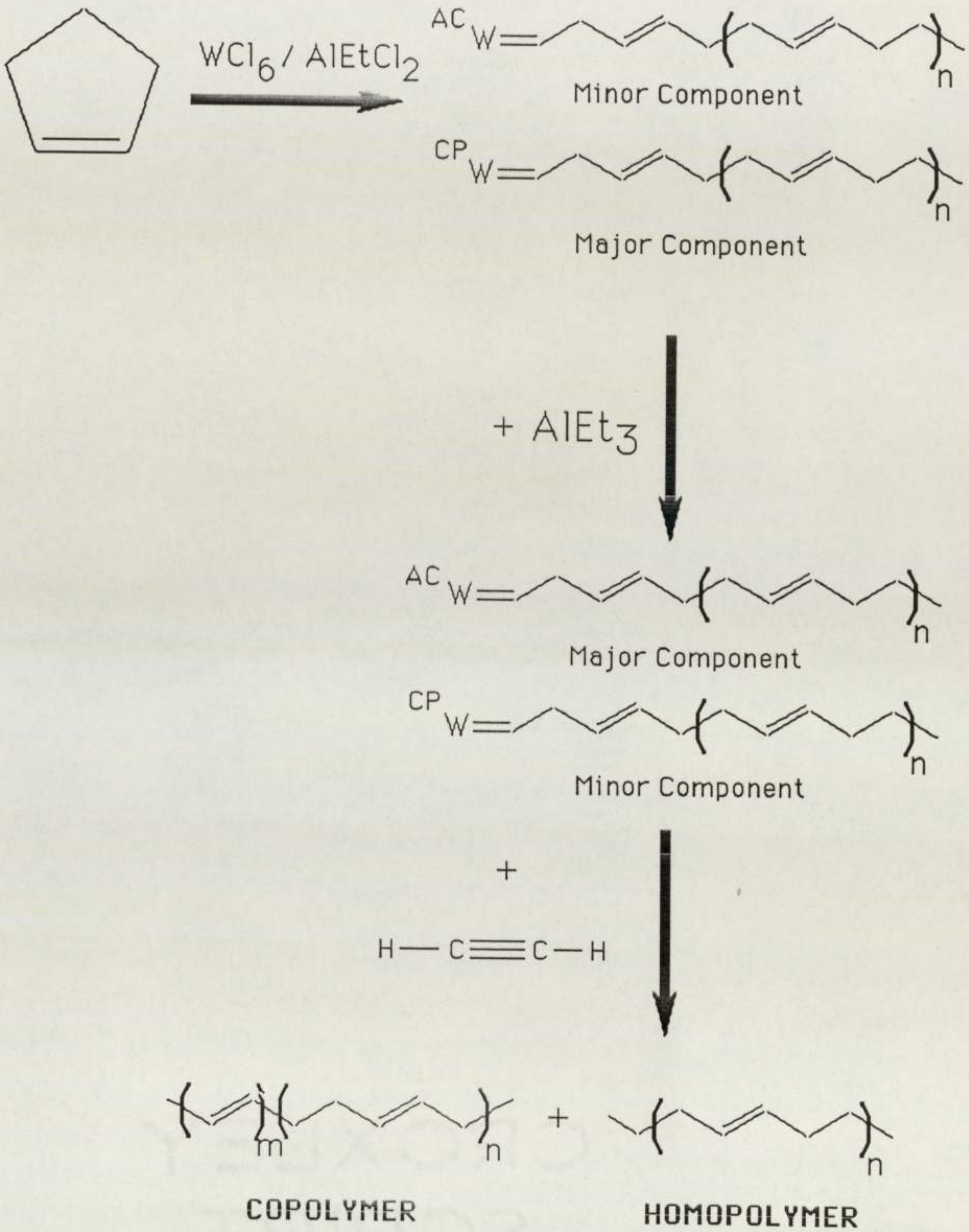

Figure 5.1 The copolymerisation of acetylene and cyclopentene using an active site transformation reaction

5.2 THE COPOLYMERISATION OF ACETYLENE AND CYCLOPENTENE USING $WCl_6/AlEtCl_2$ AND $AlEt_3$ AS CATALYST

5.2.1 Polymerisation

The polymerisation was carried out by the method described in section 2.3.2. In a typical experiment, 1.0×10^{-4} mol WCl_6 was added to a solution of cyclopentene ($11.0cm^3$, 0.12 mol) and cyclohexane ($26.0cm^3$). After two minutes, 4.0×10^{-4} mol $AlEtCl_2$ was added. The polymerisation of cyclopentene that ensued was allowed to proceed for 20hrs and produced a viscous, dark brown solution of polypentenylene. Upon addition of 4.0×10^{-4} mol $AlEt_3$ a gas was evolved and the solution changed to a clear light brown colour. After one hour, acetylene was admitted and the colour of the solution turned through red/maroon to a deep intense purple within ten minutes. The polymerisation of acetylene was allowed to proceed for 20hrs and the product was recovered and dried by the method described in section 2.4.2. The yield was 3.6g. The material isolated from this polymerisation was black, elastomeric and dissolved in a range of common organic solvents to form intense purple solutions even at low concentrations (<1%). The solutions decolourised slowly over several weeks leaving black precipitates. The results of a series of similar polymerisations are shown in table 5.1.

The reaction mixtures at the conclusion of experiments G2 and G3 were viscous, highly coloured and contained some precipitate. Attempts were made to filter the mixtures through several filters of different pore sizes, however, without exception the pores became blocked and separation of the fractions could not be achieved making it impossible to characterise the products of these polymerisations. The concentration of cyclopentene added in reaction G4 was much greater than that used in the other polymerisations. The product of this reaction was an intensely coloured, intractible material that swelled when mixed with organic solvents but did not dissolve. The product could not easily be removed from the reaction vessel as it adhered strongly to the glass walls. When a pin hole was made in the glass, the material gradually peeled away from the area surrounding the pin hole.

Table 5.1 The copolymerisation of acetylene and cyclopentene using $WCl_6/AlEtCl_2$ and $AlEt_3$ as catalyst.

Reference	[cyclopentene] /mol.dm^{-3}	[WCl_6] /mol.dm^{-3}	[$AlEt_3$] /mol.dm^{-3}	nature of product
G1	2.6	6.5	9.7	soluble
G2	2.7	2.2	10.0	partially soluble
G3	2.6	2.2	25.9	partially soluble
G4	5.0	2.9	24.6	insoluble

Molar ratio $[WCl_6]/[AlEtCl_2] = 1 : 4$ Acetylene polymerisation time, 20 hrs

Volume of acetylene = 2dm^3 ≈ 0.1 mol Reaction temperature = 20°C

It would seem plausible, in view of the adhesive effects exhibited by the polymer prepared in experiment G4, that certain components of the mixtures generated in reactions G2 and G3 adhered strongly to the matrix of the filters thus causing them to become blocked. Copolymers that contain polyacetylene and polyisoprene segments have also been reported to show unusually strong adhesion to glass and metal substrates(102).

5.2.2 Characterisation

5.2.2.1 Uv/visible absorption spectroscopy

The uv/visible absorption spectrum of a solution of the copolymer (G1) was measured by the technique described in section 2.5.2 and is shown in figure 5.2.

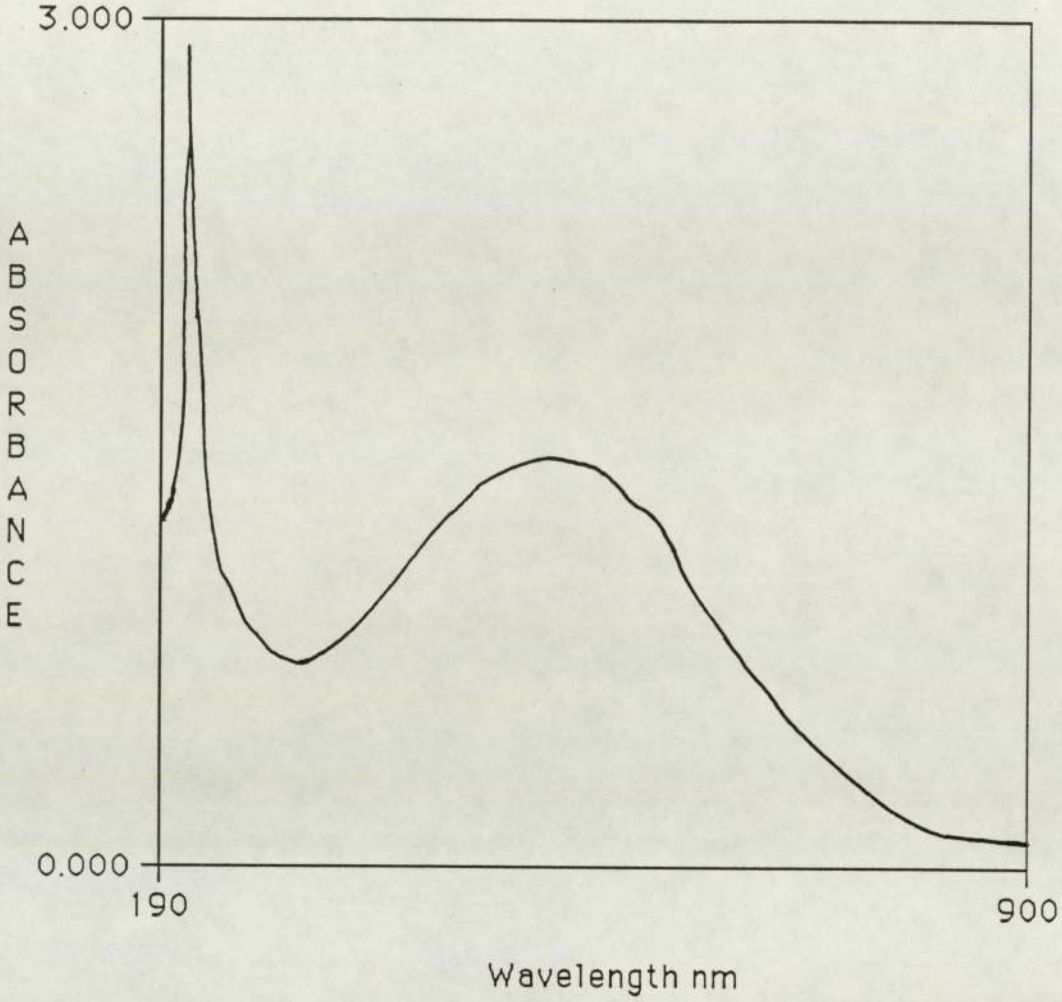

Figure 5.2 Uv/visible spectrum of polypentenylene-block-co-acetylene

A broad absorption which extended throughout the visible region was observed and may be assigned to the π-π^* transition of the polyene segments of the copolymer. A similar broad absorption was observed in the spectrum of a solution of polypentenylene-block-co-acetylene prepared using the $WCl_6/AlEtCl_2$ single catalyst system (figure 4.6) but in this case λ_{max} occurred at a shorter wavelength. This implies that the average conjugation length of the polyene segments, present in the copolymer prepared by the transformation technique, is longer than that of the polyene chains of the copolymer prepared with the single catalyst system, which in turn may suggest that the average length of the polyacetylene blocks in the former is greater than that of the latter.

The spectrum shown in figure 5.2 exhibits a peak at 214nm which was also observed in the spectrum of the copolymer prepared by the single catalyst method and is characteristic of the π-π^* transition of the isolated double bonds present in unreacted homopolypentenylene and in the polypentenylene blocks of the copolymer. If the area under the peaks of the absorptions due to polyene and polypentenylene sequences are measured from the spectra of the copolymers prepared by the transformation and single catalyst techniques, then it is apparent that the ratio of the area under the polyene peak to that of the polypentenylene is greater in samples prepared using the transformation method. The extinction coefficients of the polyene sequences are unknown, hence quantitative estimation is not possible but the ratios of the peak areas may be interpreted tentatively as indicating that the amount of copolymer relative to unreacted homopolypentnenylene is greater in the samples prepared using the transformation method

Figure 5.3 shows the uv/visible spectra of solutions of the copolymers prepared in experiments G1, G2 and G3. The positions of the peak maxima of the broad polyene absorptions were measured from figure 5.3 and are recorded in table 5.2. From table 5.2, it can be seen that λ_{max} for the polyene absorption of the copolymer moved to progressively longer wavelengths as the concentration of $AlEt_3$ incorporated during the synthesis was increased. This would indicate that the average conjugation lengths of the polyene sequences of the copolymers prepared using high concentrations of $AlEt_3$ were longer than that of the copolymer in which the standard 1:4 ratio of WCl_6 to $AlEt_3$ was used. As an increase in the average conjugation length may be explained by an increase in the average size of the blocks of polyacetylene in the copolymer, it would seem plausible that the length of the polyene sequences of the copolymer prepared by the transformation route is determined by the concentration of $AlEt_3$ used in the synthesis.

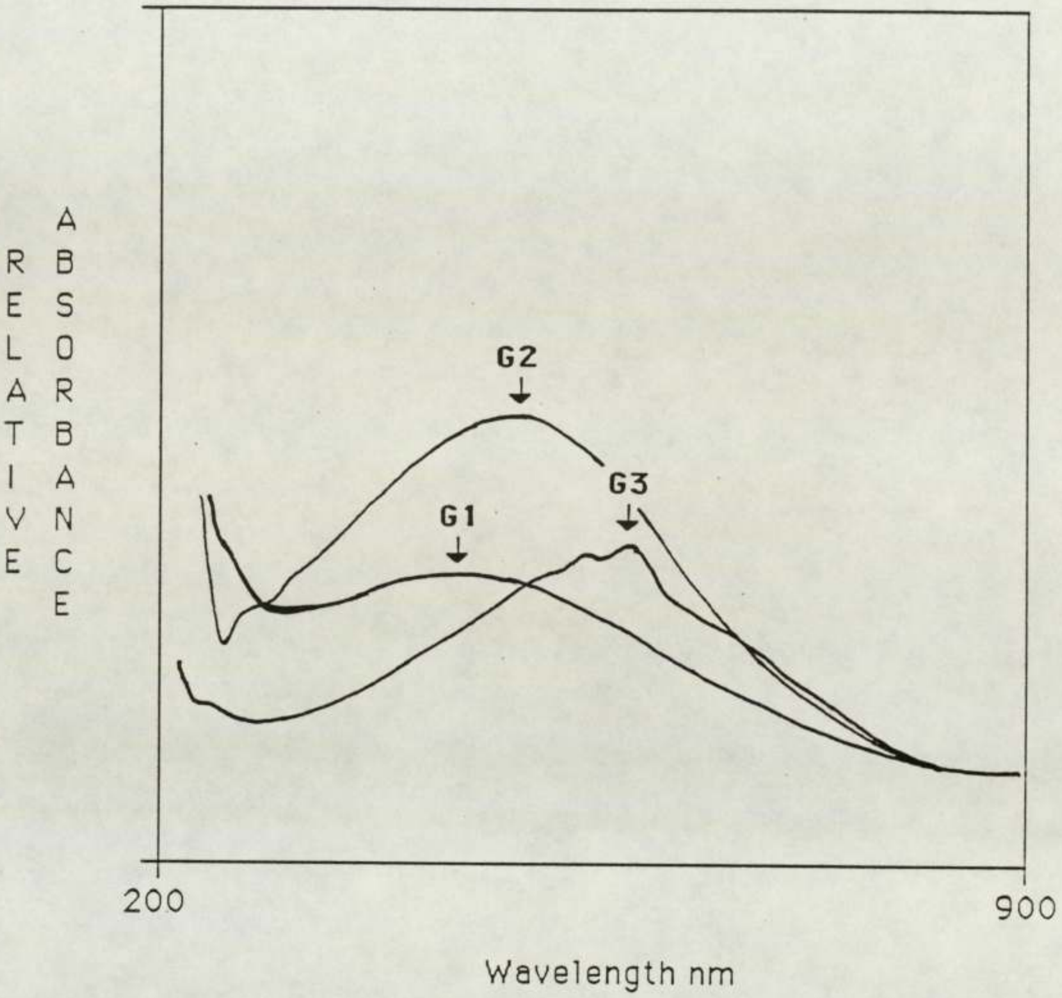

Figure 5.3 Effect of $[AlEt_3]$ on the uv/vis spectrum of polypentenylene-block-co-acetylene

Table 5.2 The Effect of $AlEt_3/WCl_6$ ratio on λ_{max} for copolymers prepared using the transformation technique.

sample	λ_{max} (nm)	$[AlEt_3]/[WCl_6]$
G1	452	1.5
G2	550	4.5
G3	593	12.0

5.2.2.2 Infra-red Spectroscopy

The infra-red spectrum of a thin film of the copolymer (G2), cast from cyclohexane onto a sodium chloride plate, was recorded by the method described in section 2.5.4. The spectrum is shown in figure 5.4. The bands which occur at 966cm^{-1} and 1404cm^{-1} may be assigned to the trans and cis bending modes, respectively, of the isolated double bonds present in polypentenylene homopolymer and in the polypentenylene blocks of the copolymer.(158) The spectrum also exhibits a broad absorption in the 3000-3300cm^{-1} region, which was observed in both samples of polyacetylene and polypentenylene-block-co-acetylene prepared using metathesis catalysts (sections 3.4.2 and 4.4.3). It seems likely that pendant hydroxyl groups formed by autoxidation of the conjugated polyene segments of the copolymer are responsible for this peak. Unlike the infra-red spectrum of the copolymer prepared using the single catalyst technique, which showed no peaks attributable to the polyene sequences of the copolymer, the spectrum of the copolymer prepared by the transformation route shows a small absorption at 1013cm^{-1}. This absorption band was also observed in the spectrum of polyacetylene (figure 3.1) and may be assigned to the trans out of plane bending mode of the polyacetylene blocks of the copolymer. The fact that an absorption due to the polyene sequences of the copolymer is detected in the samples prepared by the transformation route but not in those prepared using a single catalyst suggests that the concentration of copolymer in the samples prepared by the former technique is greater than that of the materials synthesised by the latter method. Alternatively, there may be a difference in the average length of the polyene segments of the copolymers prepared by the two methods.

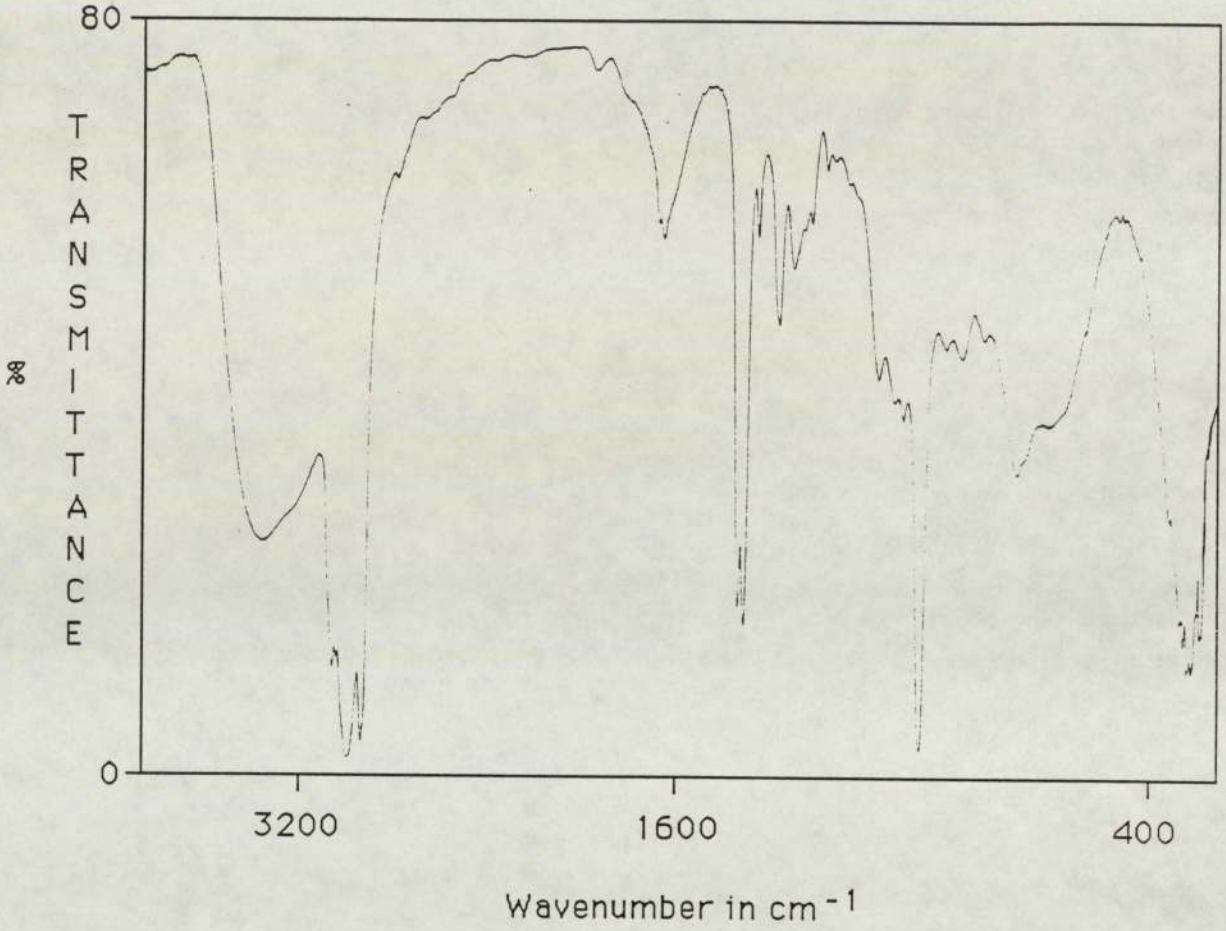

Figure 5.4 Infra-red spectrum of polypentenylene-block-co-acetylene prepared by the transformation technique.

5.2.2.3 Nuclear magnetic resonance spectroscopy (NMR)

Both ^{1}H and ^{13}C NMR were performed on samples of soluble polypentenylene-block-co-acetylene using the technique described in section 2.5.6. Samples of copolymer, prepared by the transformation and single catalyst techniques were examined both in solution in $CDCl_3$ and in the solid state using "magic angle spinning". In all the spectra, resonances attributable to polypentenylene were observed clearly, however no peaks were detected that could be assigned to the polyene sequences of the copolymer. Baker and Bates failed to observe NMR signals from the polyacetylene blocks of a solution of polyisoprene-block-co-acetylene and attributed this to the decreased mobility of the polyene segments in solution (see section 1.6.3.1). It would seem plausible therefore that in the NMR spectrum of polypentenylene-block-co-acetylene, the resonance of the polyene segments is broadened, as a consequence of their restricted mobility, to an extent that renders it indistinguishable from the baseline. Baker and Bates have claimed that dried samples of polyisoprene-block-co-acetylene show a resonance at 138ppm when subjected to solid state magic angle spinning. The position of this resonance coincides with that exhibited by polyacetylene suggesting that, in the case of the copolymer, the 138ppm signal arises from the polyacetylene blocks. The solid state NMR spectrum of polypentenylene-block-co-acetylene showed no resonant absorption in this region which may suggest that the concentration of polyene segments present in the copolymer sample was too low to be detected using this method. Indeed, Baker and Bates have revealed that 100% ^{13}C enrichment of the samples of polyisoprene-block-co-acetylene was necessary to obtain a satisfactory signal in the NMR spectra.

5.2.2.4 Gel Permeation Chromatography (GPC)

Gel permeation chromatography was performed on a solution of the polypentenylene-block-co-acetylene (G1) using the apparatus described in section 2.5.4. The response of the differential refractometer showed a bimodal distribution, typical of polypentenylene (figure 4.9) but, unlike the chromatogram of the copolymer prepared using the single catalyst technique (figure 4.8) no high molecular weight shoulder was observed. The uv/visible absorption spectrometer set at 400nm failed to show any response even when the amount of copolymer injected onto the columns was increased. When the columns were removed and the solution of copolymer was injected directly into the spectrometer flow cell, a large response was then observed. It may be concluded therefore that the copolymer was either adsorbed on the columns and not eluted within the timescale of the analysis, or formed particles that were too large to be transported even through the interstitial regions of the gel. Baker and Bates have reported that gel permeation chromatography could not be used for the analysis of their soluble copolymers which contained polyacetylene units due to adsorption effects.(102)

5.3 CONTROL OF THE AVERAGE LENGTH OF THE POLYPENTENYLENE SEQUENCES OF POLYPENTENYLENE-BLOCK-CO-ACETYLENE PREPARED USING THE TRANSFORMATION TECHNIQUE

5.3.1 Introduction

The co-metathesis of cyclic and acyclic alkenes has been observed using several catalyst systems. The outcome of these reactions depends on the molar ratio of the linear (A) to cyclic (B) alkene, the structure of the alkene and the nature of the catalyst used. When the molar ratio [A]/[B] is high, a series of low molecular weight telomers is produced. If the acyclic alkene is unsymmetrical, then three series of telomers may be produced as shown in figure 5.5. As the ratio [A]/[B] decreases, the average number of monomer units per chain (n) increases. Conversly, it may be inferred that the inclusion of a small amount of linear alkene in the solution of cyclic monomer prior to the polymerisation will result in a reduction in the molecular weight of the polymeric product.

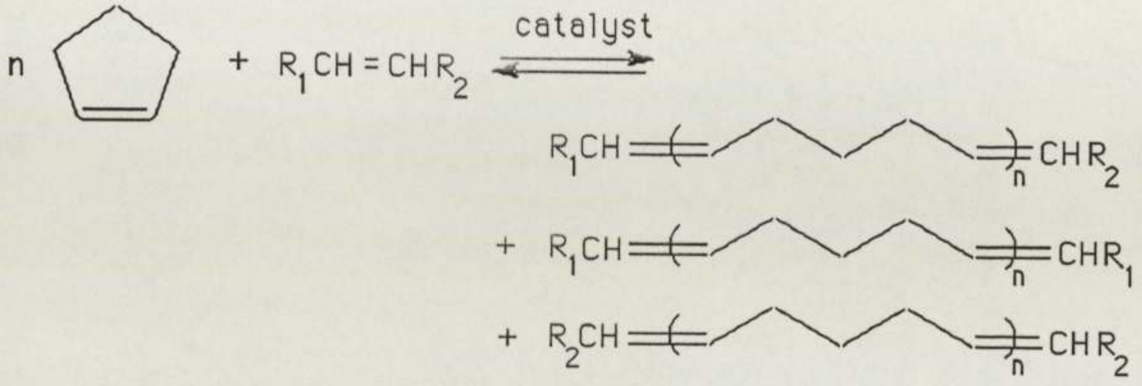

Figure 5.5 The production of telomers by co-metathesis of a linear and a cyclic alkene

The use of co-metathesis of linear and cyclic alkenes to reduce the molecular weight of polymers prepared by ring opening metathesis polymerisation has been examined in several studies.(159) In addition to a co-metathesis reaction between the linear alkene and the active chain propagating metal carbene, which results in premature termination of the polymer chain, intermolecular cross metathesis between the linear alkene and the double bonds present in the polymer backbone may also contribute to the molecular weight reducing process and predominates in the case of low [A]/[B]. The latter effect may be summarised as

$$P_nCH{=}CHP_m \quad + \quad M{=}CHR \quad \longleftrightarrow \quad M{=}CHP_n \quad + \quad RCH{=}CHP_m$$

where $M{=}CHR_2$ represents a metal carbene formed by the reaction of the catalyst with the acyclic olefin. P_m and P_n represent two halves of a polypentenylene chain initially linked by a double bond. The effect of the addition of various alkenes to a solution of cyclopentene, prior to ring opening metathesis polymerisation, on the molecular weight of the polymer produced is shown in figure 5.6.

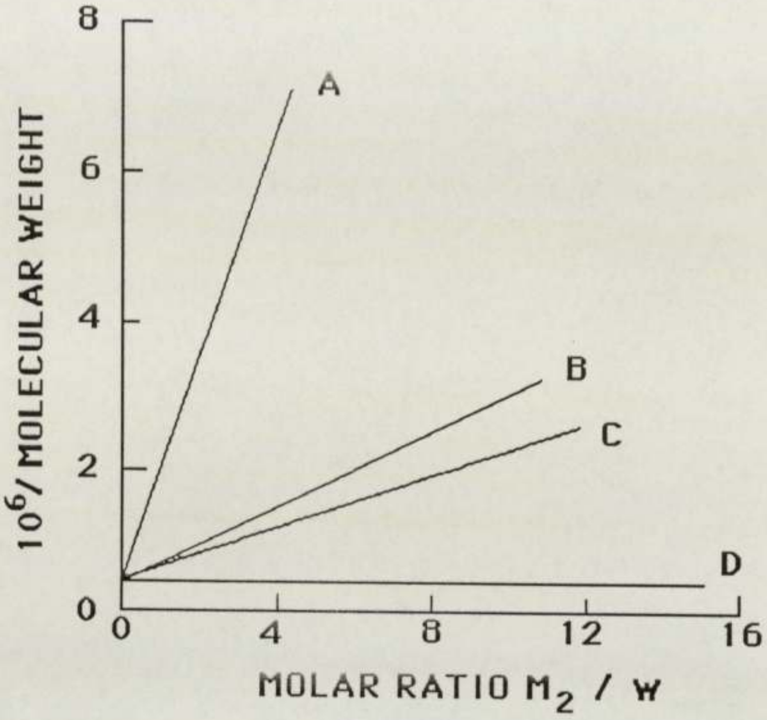

Figure 5.6 Molecular weight of polypentenylene formed by polymerisation of cyclopentene (M_1) as a function of concentration of acyclic olefin (M_2) relative to the tungsten catalyst concentration.

A = 1-butene, **B** = cis-2-butene, **C** = trans-2-butene, **D** = isobutene. Catalyst : $WCl_5(OCH_2CH_2Cl)/Al(Bu^i{}_3)$ in toluene. $[M_1]/[W] = 3700$.

The efficiency of molecular weight reduction decreases in the series $RCH_2=CH_2$ > RCH=CHR (cis) > RCH=CHR (trans) > $R_2C=CH_2$. Thus it may be concluded that by judicious choice of a linear alkene and [B]/[A] concentration ratio, effective control over the polymer molecular weight can be achieved.

In section 5.1 it was pointed out that the transformation route to polypentenylene-block-co-acetylene might allow the lengths of the constituent blocks to be controlled independently of one another. The results presented in section 5.2 have indicated that if the concentration of $AlEt_3$ used during the synthesis is increased, then the average length of the polyacetylene block in the copolymer also increases. The transformation route therefore allows some control over the lengths of the polyene segments in these materials. In chapter 4 it was observed that the molecular weight of the polypentenylene block of polypentenylene-block-co-acetylene could not be easily controlled by varying the time allowed for the ring opening polymerisation step of the synthesis. A study was therefore initiated in which a linear alkene (1-octene) was added to the solution of cyclopentene as a molecular weight limiting agent prior to the ring opening polymerisation step of the copolymerisation reaction (figure 5.1). The results of these experiments are presented in the folowing sections.

5.3.2. Polymerisation

Polymerisations were performed using the transformation technique described in section 5.2. 1-Octene was incorporated into the solution of monomer at the expense of the equivalent volume of cyclohexane in order to maintain a constant concentration of cyclopentene throughout the series of experiments. Any changes in the products of these experiments were therefore most likely brought about by changes in the [octene]/[cyclopentene] ratio rather than simply by changes in the initial concentration of monomer.

In a typical experiment, the reaction chamber was charged with a mixture containing 0.11 moles cyclopentene, 1.8×10^{-3} moles 1-octene and 11mls cyclohexane. Tungsten hexachloride (1×10^{-4} moles) was added to the solution of monomer followed, two minutes later, by the addition of 4×10^{-4} mol $AlEtCl_2$. After sixteen hours, the mixture appeared dark brown and the increase in viscosity was markedly less than that observed when cyclopentene was polymerised by metathesis ring opening in the absence of 1-octene. Aluminium triethyl (4×10^{-4} moles) was then added, whereupon a gas was evolved and the colour of the mixture changed rapidly to a clear light brown. After a further 40 minutes, acetylene was admitted and the colour of the mixture slowly changed to purple. A precipitate was detected four minutes after the addition of acetylene and when the reaction was terminated 16 hours later, a black precipitate remained in a pale yellow solution. The experiment was repeated for a series of 1-octene/cyclopentene molar ratios and the results are shown in table 5.3.

A precipitate formed in all the polymerisations even when the 1-octene/cyclopentene molar ratio was very low (1.5×10^{-3}). For the latter case, a fine precipitate was formed in a purple solution, but attempts to separate the mixture failed. A range of filters with different pore sizes was used but each became blocked. This effect was also observed in samples of polypentenylene-block-co-acetylene prepared by the transformation route (section 5.2) in which no 1-octene was present and has been attributed to the adsorption of the polymeric particles onto the surface of the filter.

Table 5.3 The effect of 1-octene on the copolymerisation of acetylene and cyclopentene using the transformation method.

Reference	[octene]/ [cyclopentene]	nature of product	t^*
H1	1.5×10^{-3}	partially soluble	960
H2	8.3×10^{-3}	insoluble	180
H3	0.016	insoluble	4
H4	0.16	insoluble	6
H5	0.5	insoluble	1

Molar ratio $[WCl_6] : [AlEtCl_2] : [AlEt_3] = 1 : 4 : 4$ $[WCl_6] = 2.3 \times 10^{-3}$ mol l^{-1}

[cyclopentene] = 3 mol l^{-1} Volume of acetylene = $2dm^3 \approx 0.1$ mol

acetylene polymerisation time = 20 hrs ; reaction temperature = 20°C

t^* is the time interval (minutes) between the addition of acetylene to the solution of polypentenylene and the detection of insoluble material during the ensuing polymerisation.

Quantitative estimation of the yields of the products of this series of polymerisations was not possible because the polymers showed anomalously high adhesion to the glass reactor vessel and to the surfaces of filters. It was observed however that the materials exhibited a change from purple/black elastomers to black powders as the octene/cyclopentene molar ratio was increased and the yield of polymer decreased dramatically. The low yields observed in the presence of high concentrations of 1-octene may be explained if 1-octene is able to compete with acetylene for the active sites of the catalyst. This would result in complexes that are unable to polymerise acetylene. This effect is demonstrated schematically in figure 5.7.

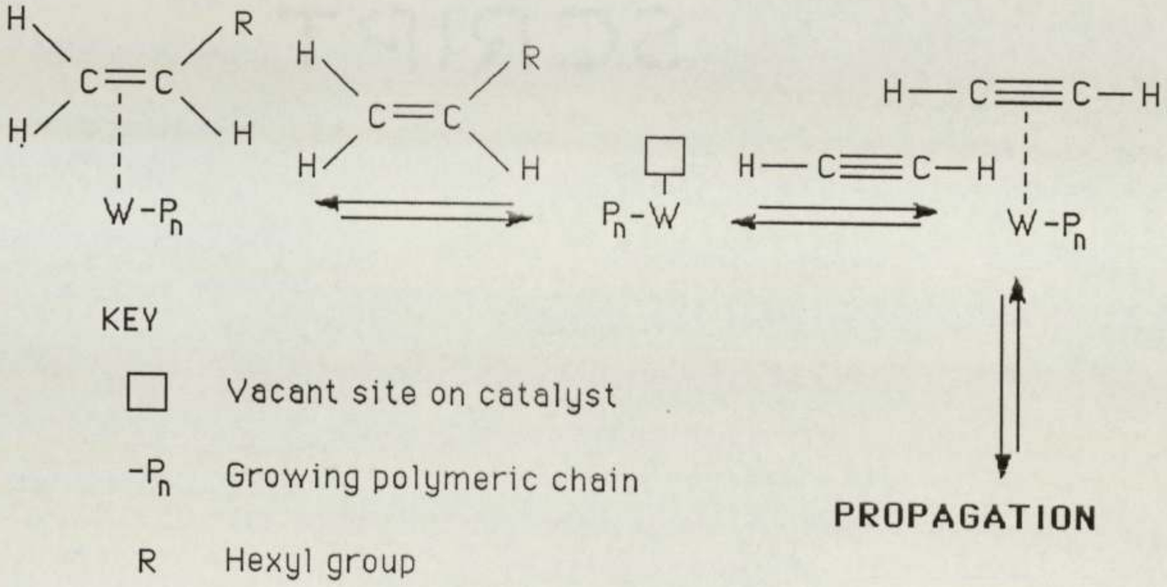

Figure 5.7 Schematic representation of the competition between acetylene and octene for catalytically active sites.

Values of t^*, the time interval between the addition of acetylene to the solution of polypentenylene and the detection of insoluble material during the resulting polymerisation, are included in table 5.2. As the octene/cyclopentene molar ratio increased, t^* decreased. This may suggest that as the length of the polypentenylene blocks of the copolymer decreased, coagulation of the particles into a precipitate became more facile. As the polypentenylene segments of the copolymer are thought to reduce the tendency towards aggregation of the polyacetylene chains, the decrease in molecular weight of the these segments would be expected to give rise to a reduction in the excluded volume and protecting effects of the polypentenylene chains.

5.3.3 Characterisation

5.3.3.1 Gel Permeation Chromatography (GPC)

Samples of the reaction mixtures produced by the ring opening metathesis polymerisation of cyclopentene in the presence of 1-octene were taken during the copolymerisation reactions described in section 5.2. The sample was withdrawn prior to the admission of acetylene using the method outlined in section 2.3.2 and poured into excess methanol. The polypentenylene was isolated and dried by the method presented in section 2.4.2. Solutions (1% w/v) of the purified polymer in THF (HPLC grade) were analysed by gel permeation chromatography using the apparatus described in section 2.5.4.

Figures 5.8-5.12 show the response of the differential refractometer during the GPC analyses of the samples of polypentenylene isolated during the copolymerisation reactions. A calibration curve of molecular weight against elution volume was obtained using samples of polystyrene of known molecular weight and narrow molecular weight distribution, (figure 2.8). A polystyrene equivalent value of the number average molecular weight $<M_n>$ of the samples of polypentenylene may be estimated from the elution volume at which the largest detector response is observed, assuming that the distributions are symmetrical. The dependence of the polystyrene equivalent molecular weight on the 1-octene/cyclopentene molar ratio is shown in table 5.4.

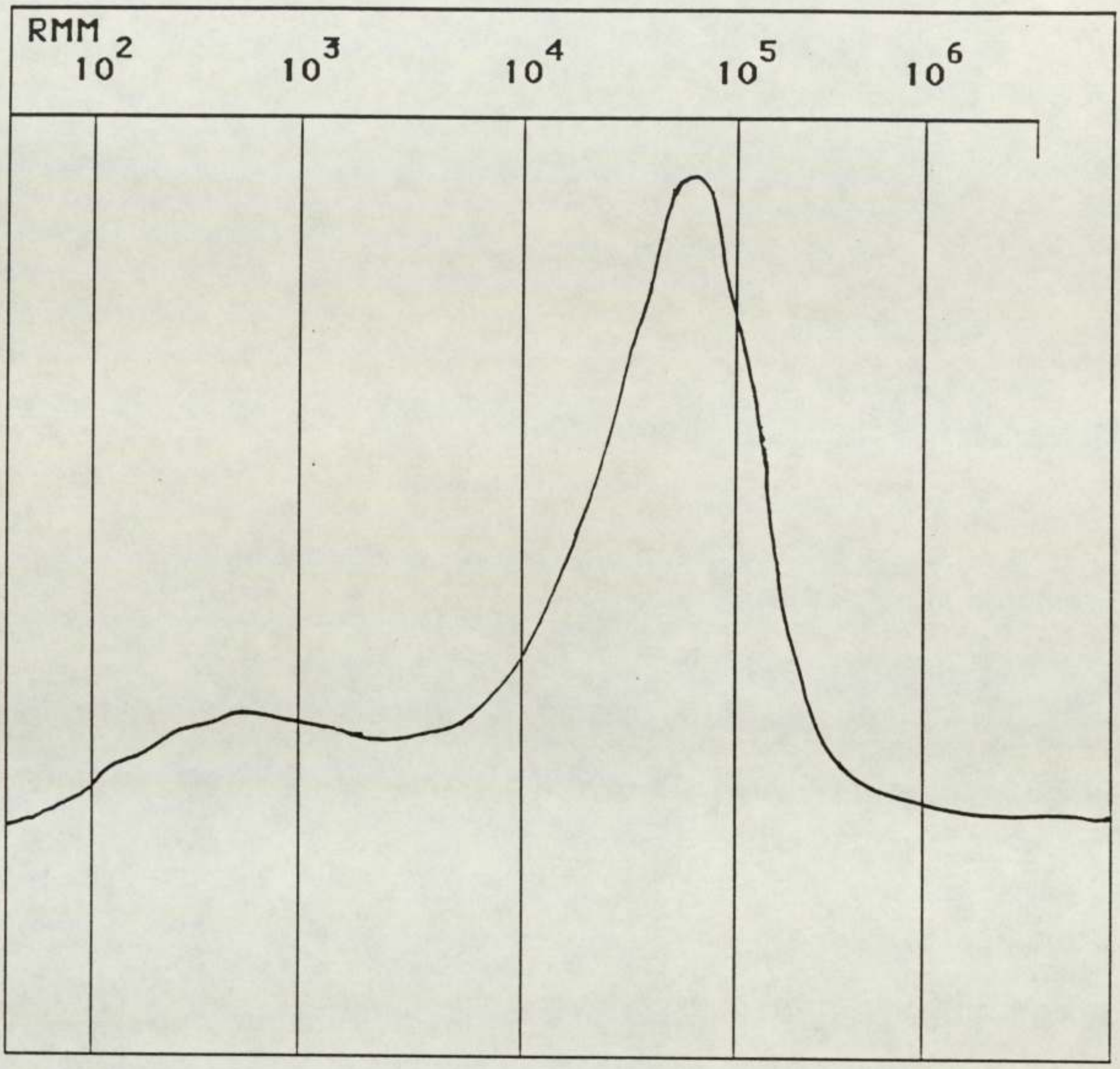

Figure 5.8 GPC analysis of polypentenylene sample isolated during experiment H1

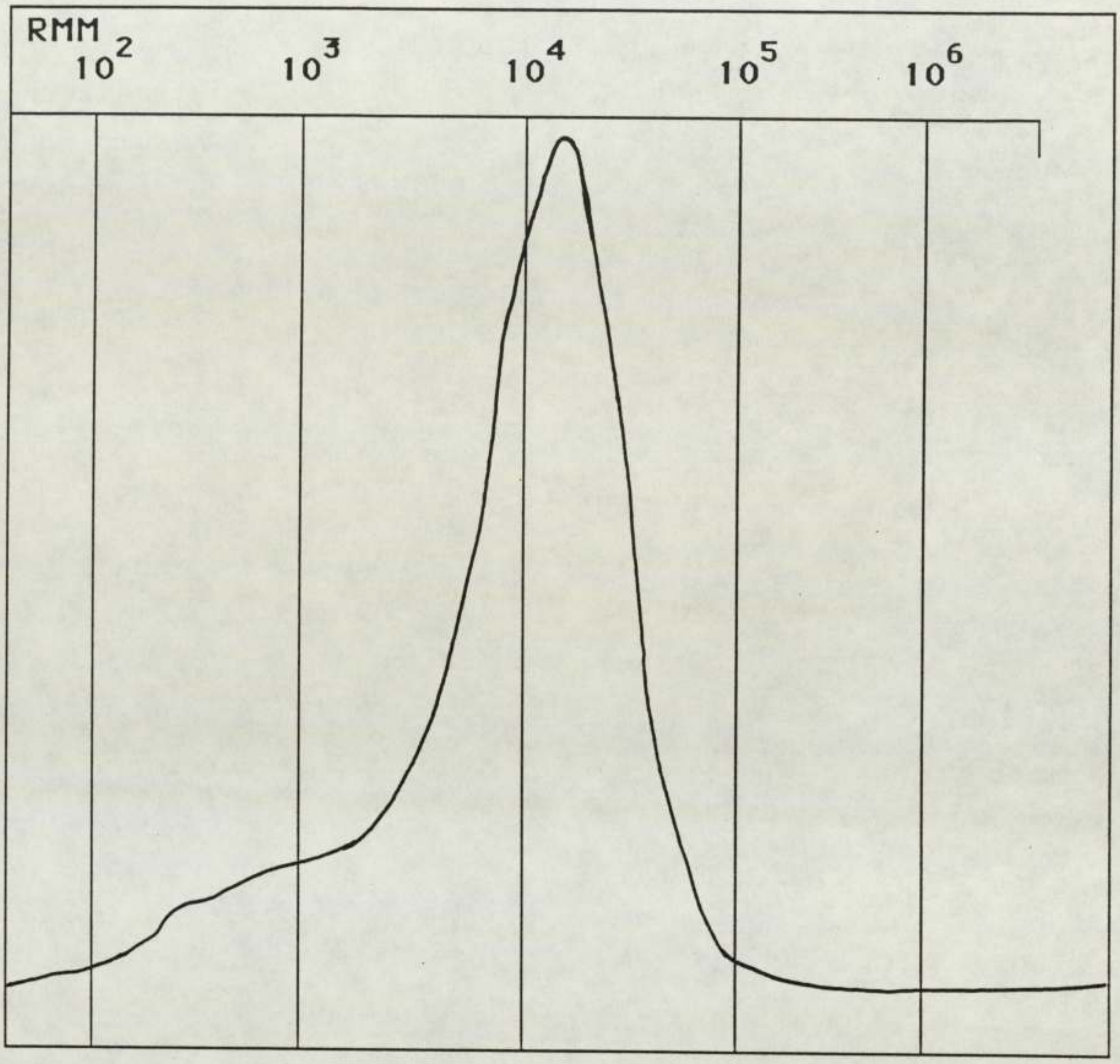

Figure 5.9 GPC analysis of polypentenylene sample isolated during experiment H2

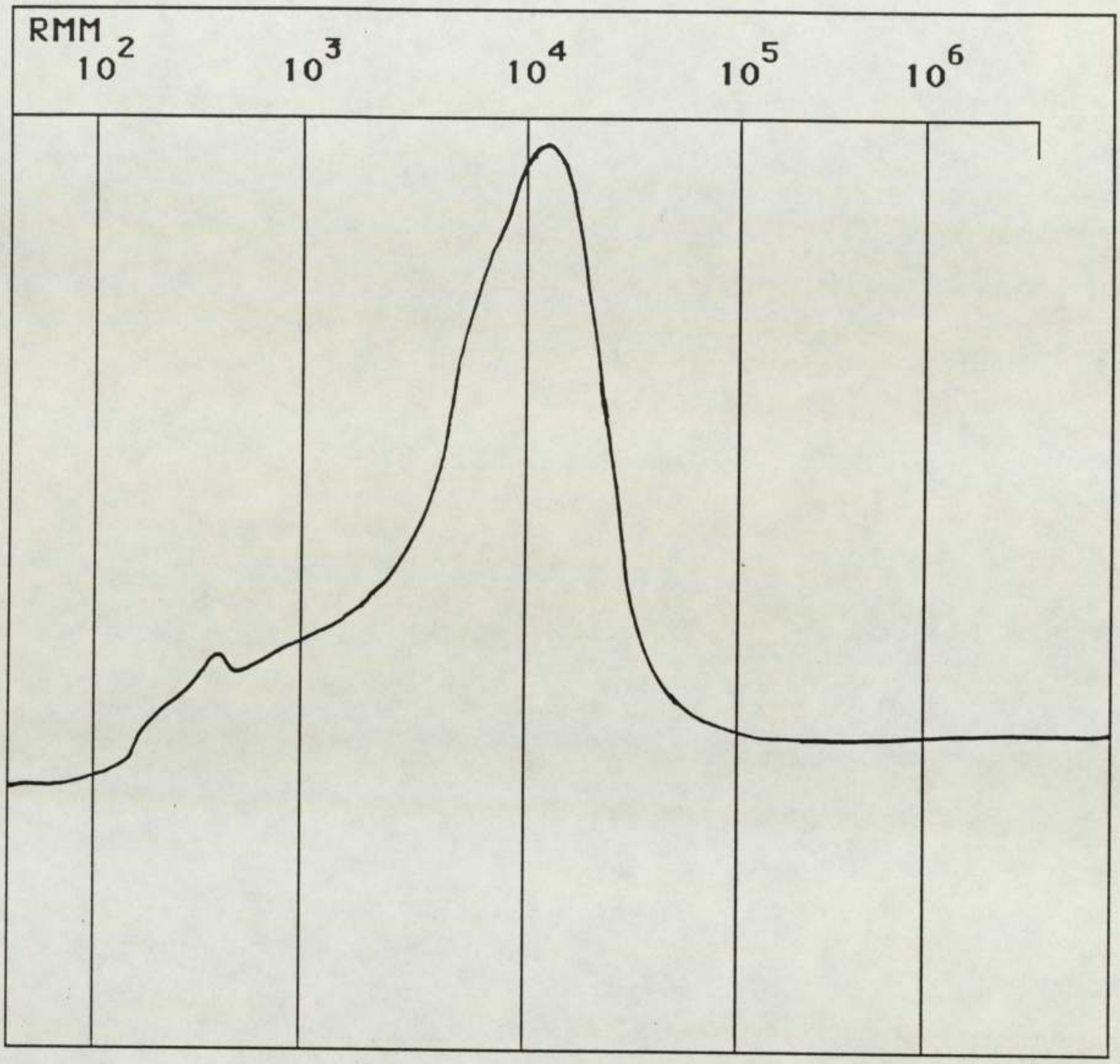

Figure 5.10 GPC analysis of polypentenylene sample isolated during experiment H3

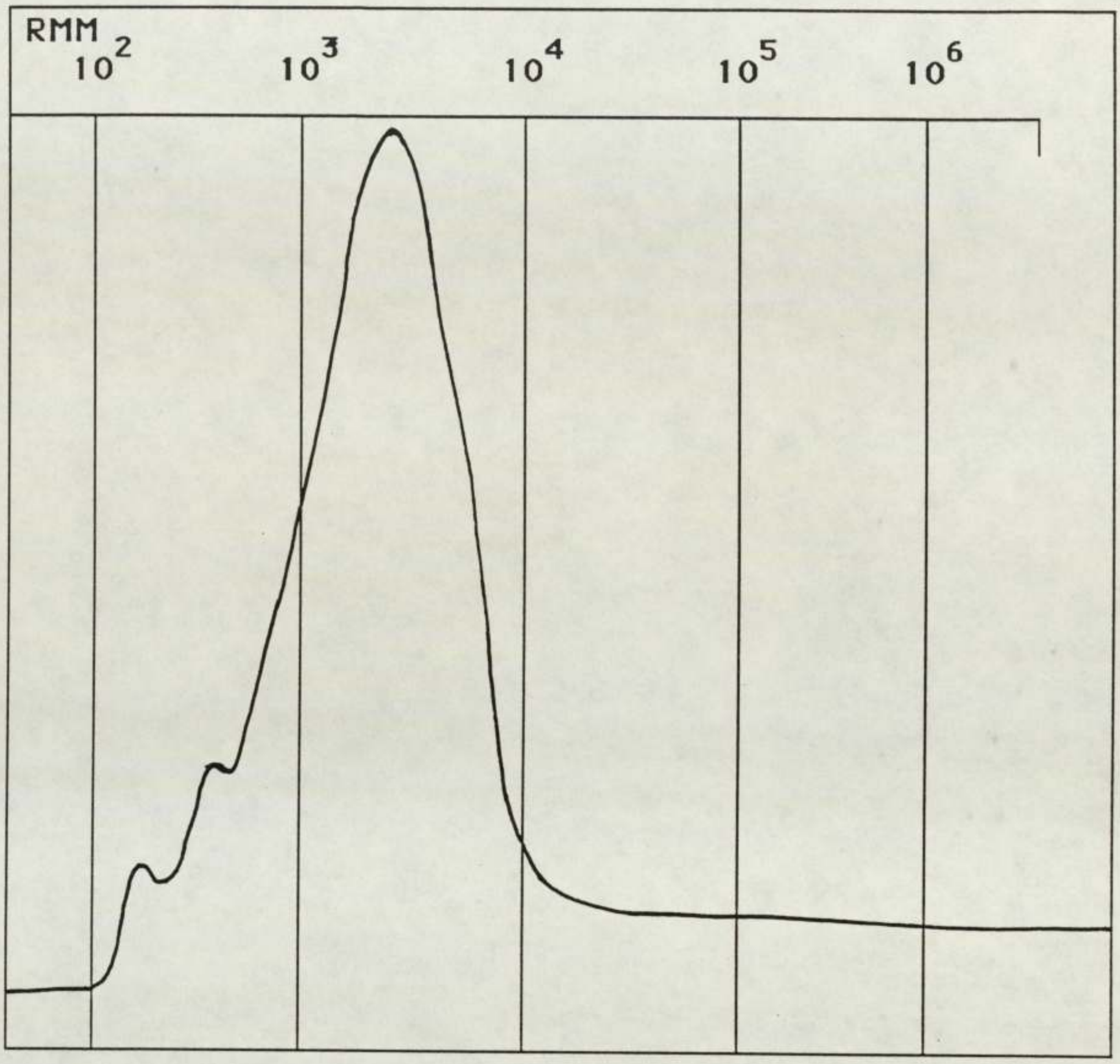

Figure 5.11 GPC analysis of polypentenylene sample isolated during experiment H4

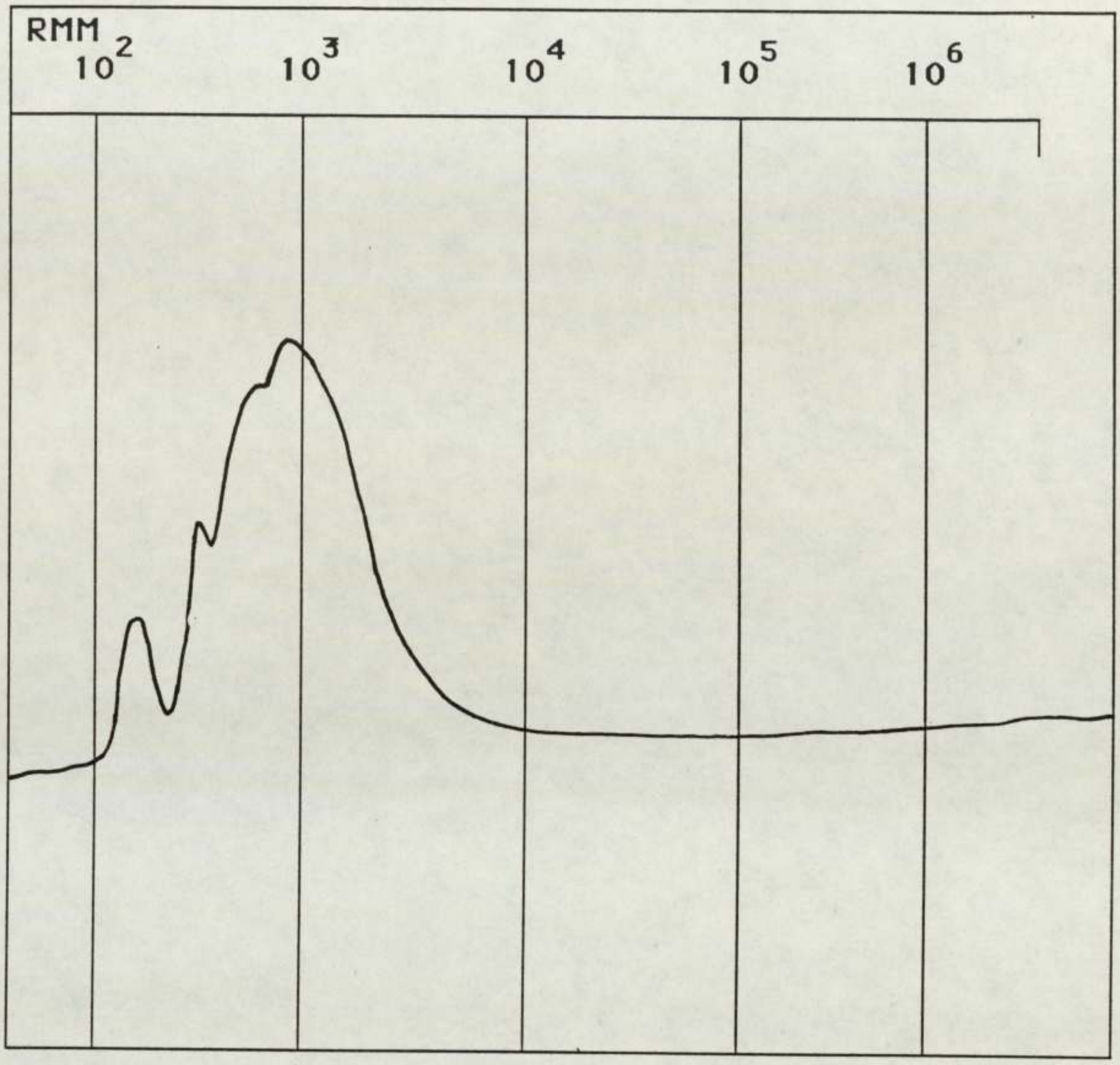

Figure 5.12 GPC analysis of polypentenylene sample isolated during experiment H5

It is clear that as the octene/cyclopentene molar ratio increases, the molecular weight of the polypentenamer decreases as expected and it may also be observed that as $<M_n>$ decreases, the molecular weight distribution narrows and becomes multi-nodal in appearance. The latter characteristic of the molecular weight distribution presumably arises from the presence of low molecular weight species formed either by oligomerisation of cyclopentene, from the homometathesis of 1-octene, or by the cometathesis of 1-octene and cyclopentene.

Table 5.4 Effect of the concentration of 1-octene on <M_n> of the polypentenylene block of polypentenylene-block-co-acetylene

Reference	10^2 [Octene]/ [Cyclopentene]	Mean Elution Volume (mls)	10^{-3}<M_n>*
PP1*	0	22.7	170
H1	0.15	24.7	55
H2	0.83	27.3	13
H3	1.60	27.5	12
H4	16.00	30.7	2
H5	50.00	33.1	1

[WCl_6] = 2.3 x 10^{-3} M [cyclopentene] = 3 M [WCl_6] : [$AlEtCl_2$] : [$AlEt_3$] :: 1 : 4 : 4

* <M_n> is the number average molecular weight of the polypentenylene relative to standard samples of polystyrene. PP1 corresponds to a sample of polypentenylene that was taken during a copolymerisation reaction in which no 1-octene was present.

5.3.3.2 Infra-red spectroscopy

Samples of the copolymers prepared in experiments H2, H3 and H5 (see section 5.3.2) were incorporated in KBr discs and were subjected to infra-red analysis using the instrument described in section 2.5.3. The spectra are shown in figures 5.13-5.15. In all samples the trans-polyacetylene out-of-plane bending mode absorption at 1013cm^{-1} (peak [B]) and the trans-polypentenylene out-of-plane bending peak at 966cm^{-1} (peak [A]) can be clearly seen.

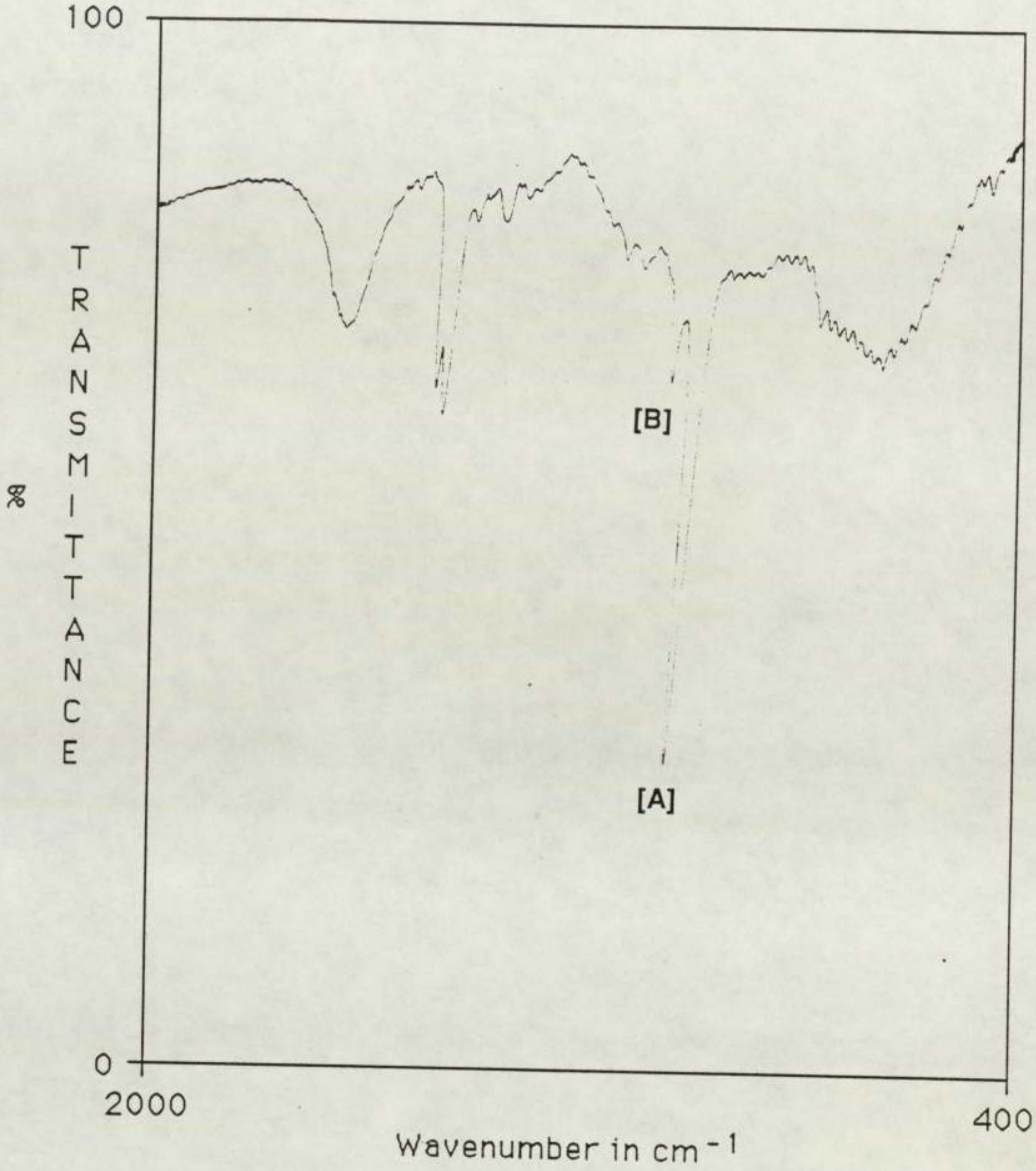

Figure 5.13 Infra-red spectrum of copolymer H2

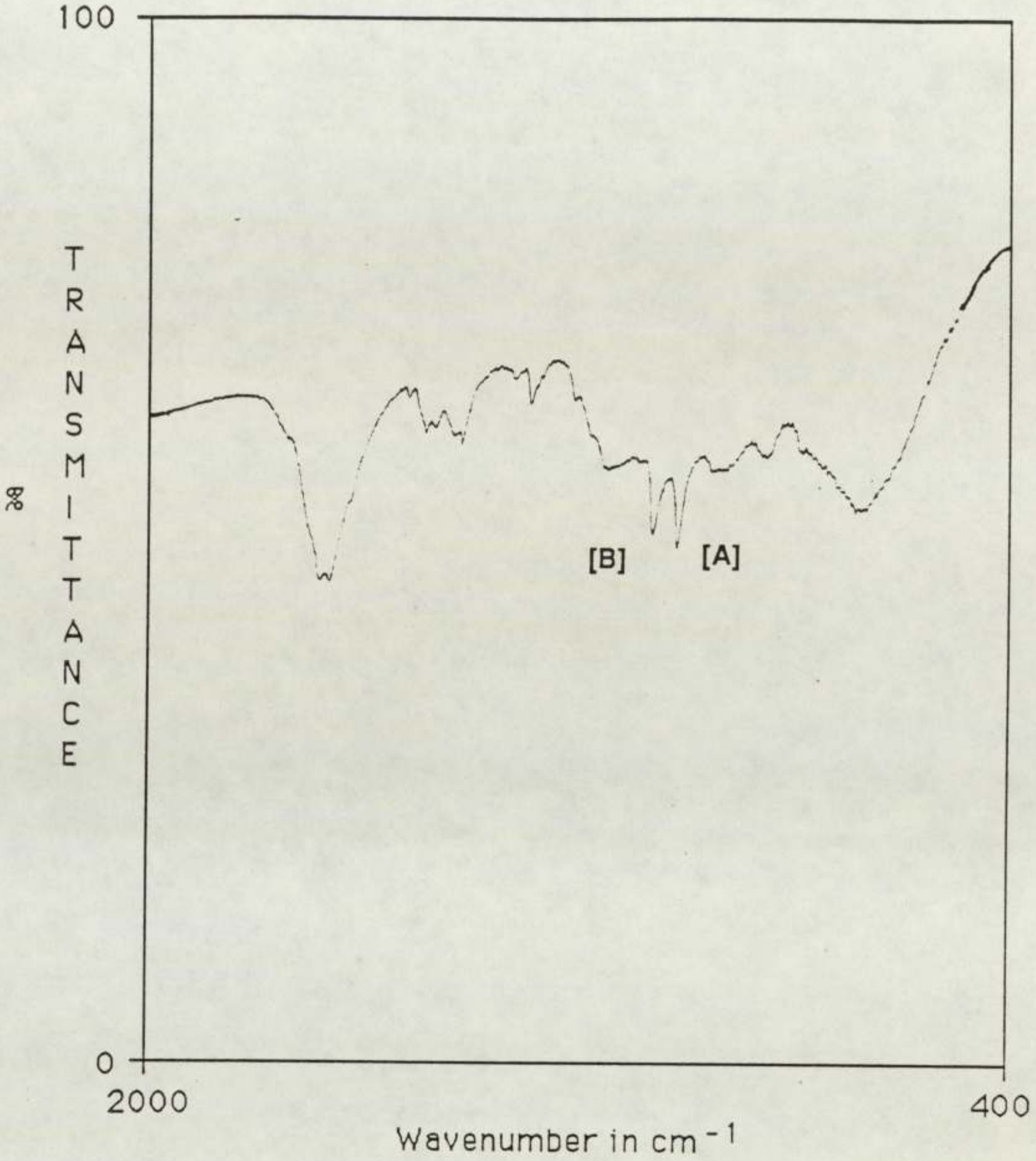

Figure 5.14 Infra-red spectrum of copolymer H3

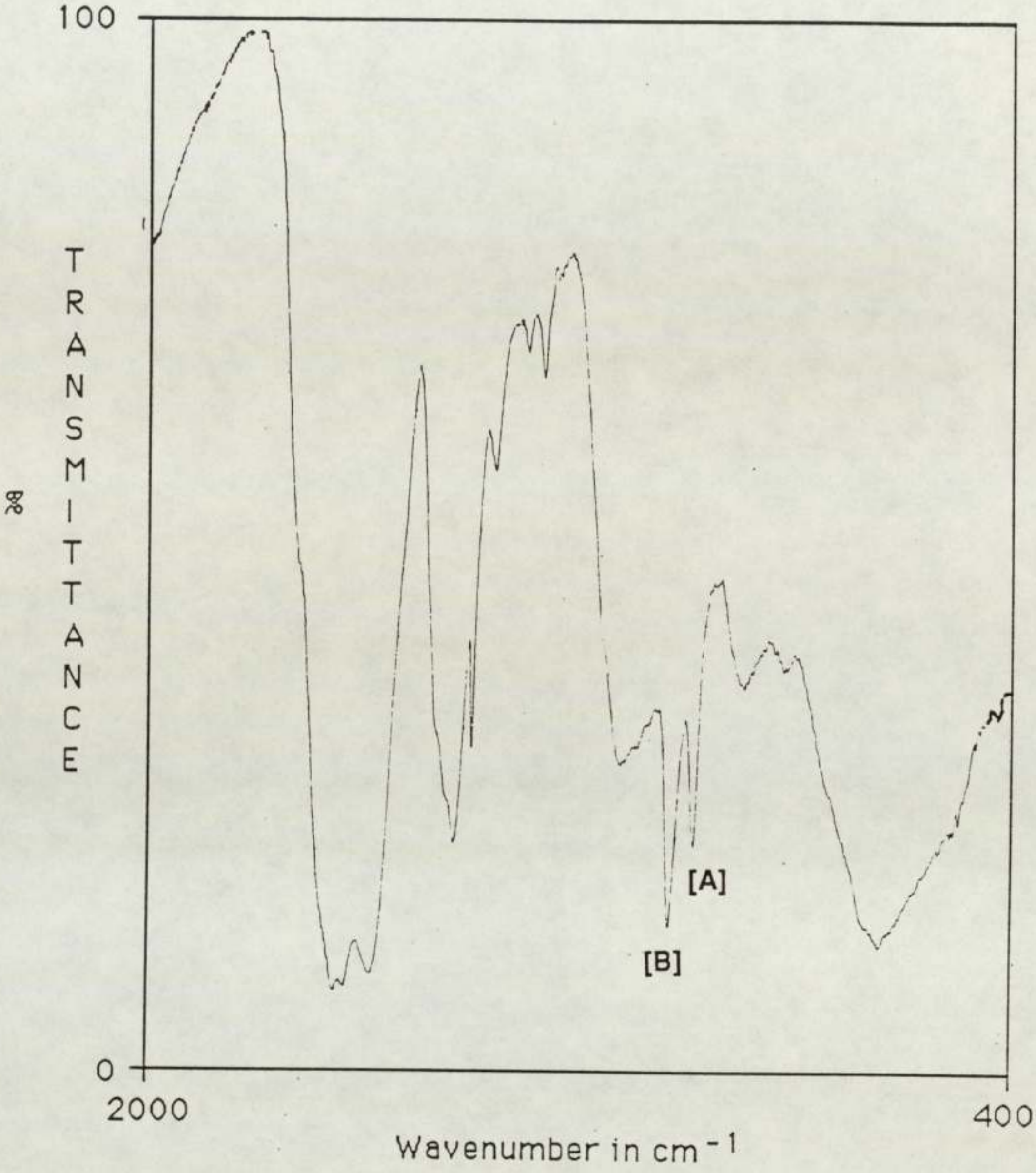

Figure 5.15 Infra-red spectrum of copolymer H5

By comparing the relative peak heights of these two absorptions, the relative composition of the copolymer samples can be estimated. These values are shown in table 5.4. The ratio [B]/[A] of the heights of the two peaks is seen to decrease as the 1-octene/cyclopentene molar ratio increases, indicating that the copolymeric materials synthesised using high levels of 1-octene contain a lower proportion of polypentenylene than those prepared using lower levels of this additive. This result, coupled with the observed decrease in the yield of copolymer as the 1-octene/cyclopentene molar ratio increases suggests that the degree of conversion of cyclopentene to polypentenylene is reduced when high levels of 1-octene are present.

Table 5.5 Relative composition of copolymeric materials determined by infra-red spectroscopy.

Reference	[octene]/ [cyclopentene]	height of peak [B] / height of peak [A]
H2	8.3×10^{-3}	2.2
H3	0.016	1.0
H5	0.5	0.9

5.3.3.3 Uv-visible spectroscopy

The soluble fractions that remained after the termination of the experiments described in section 5.3.2 were analysed by uv-visible spectroscopy using the method described in section 2.5.2. The spectrum of a typical fraction is shown in figure 5.16. The spectrum fails to exhibit the broad "soluble polyacetylene" absorption observed in the spectrum of polypentenylene-block-co-acetylene. Instead, it exhibits a series of peaks in the 300-400nm region similar to those obtained from the soluble products of copolymerisations associated with the formation of insoluble polypentenylene-block-co-acetylene (see section 4.4.1). These peaks resemble the "finger pattern" spectra exhibited by a mixture of low molecular weight (n = 3 to 10) linear polyenes, $(CH_2{=}CH_2)_n$ but the exact nature of the species present in the solutions and its origin remain uncertain. The samples decolourised rapidly on exposure to air and light.

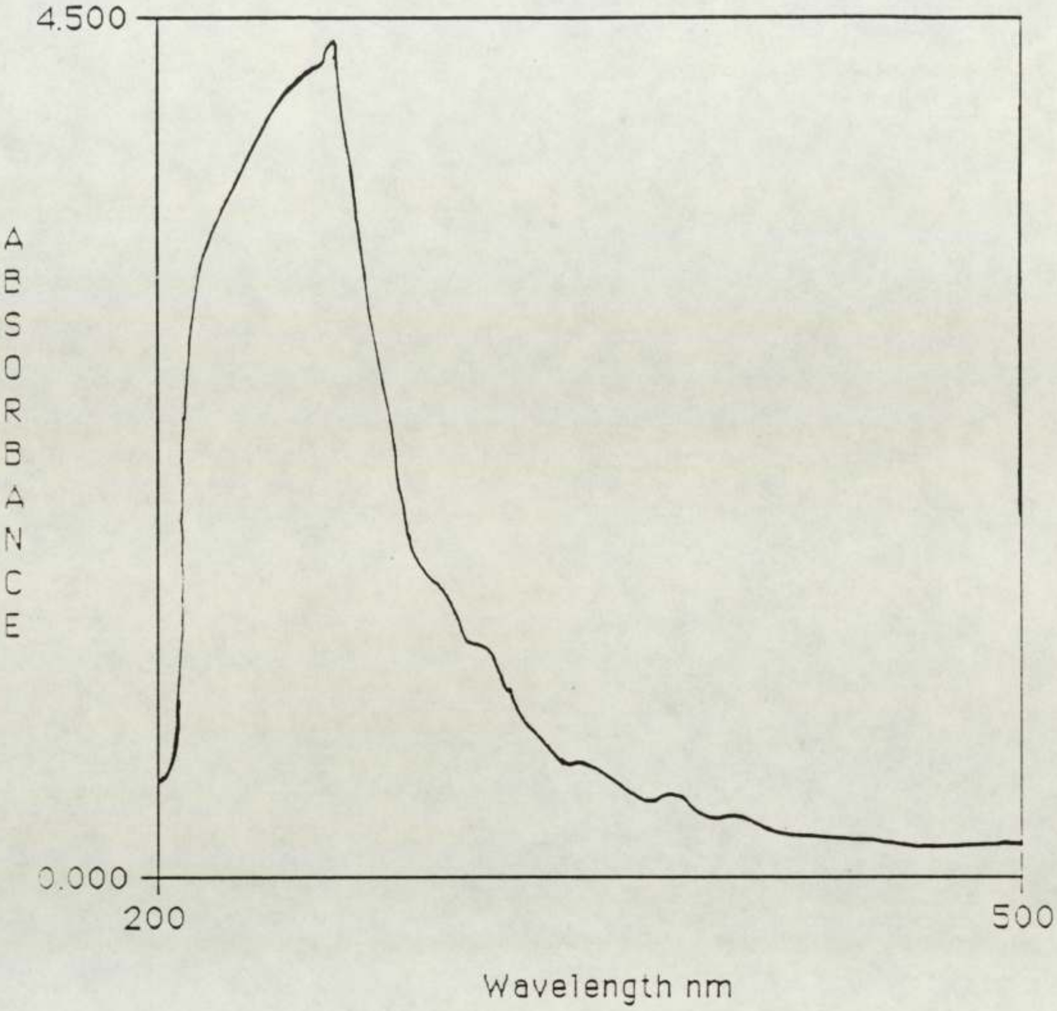

Figure 5.16 Uv/visible spectrum of a soluble fraction obtained from a copolymerisation experiment incorporating 1-octene

CHAPTER 6

THEORY ASSOCIATED WITH THE MEASUREMENT OF ELECTRO-OPTICAL ANISOTROPY

6.1 INTRODUCTION

Many crystalline substances transform an incident beam of light into two mutually perpendicular polarised beams that are propagated at different velocities in the medium(160). This property is called double refraction or birefringence. For individual molecules, the following behaviour may be considered. If two orthogonal axes are chosen, one of which is parallel to a plane or axis of symmetry of an optically anisotropic molecule, then the refractive indices for light propagating along each of the two axes will be different. If these molecules are packed into a crystal lattice, then generally there will be a macroscopic difference in the refractive index for light propagating parallel ($n_{||}$) and perpendicular ($n_{\perp}$) to the main crystal axis. The difference in refractive index

$$\Delta n = n_{||} - n_{\perp} \qquad 6.1$$

is defined as the birefringence of the crystal and is related to the phase difference (δ) incurred between the two perpendicular polarised beams after passage through the crystal by

$$\delta = 2\,\pi\,\mathbf{l}\,\Delta n / \lambda \qquad 6.2$$

where λ is the wavelength of the incident beam of light and **l** is the optical pathlength. Equations 6.1 and 6.2 may be applied to any doubly refracting medium.

When two orthogonal vibrations of light transmitted by the sample are differently absorbed, the substance is said to exhibit dichroism. The magnitude of the dichroism, ΔA, is defined as the difference in absorbance of the two beams.

$$\Delta A = A_{||} - A_{\perp} \qquad 6.3$$

Birefringence and dichroism are both examples of optical anisotropy and are often termed linear birefringence and linear dichroism to distinguish them from circular birefringence and circular dichroism, phenomena associated with optical activity. Like refraction and absorption, birefringence may be observed at any wavelength while dichroism will necessarily appear in absorption bands only.

In solution, molecules adopt random orientations and their intrinsic anisotropy does not result in a macroscopic birefringence or dichroism of the solution. However, optical anisotropy may be induced in an isotropic solution by the action of external forces such as hydrodynamic forces (flow birefringence) or by the application of electric and magnetic fields. These applied stresses tend to result in a small net alignment of the molecules which opposes the randomising factors of Brownian motion and molecular diffusion. When aligned in this manner, the solution then behaves as a birefringent material with its major optical axis relating to the direction of flow or to the direction of the applied electric or magnetic field. Under these conditions, a macroscopic optical anisotropy may be observed.

6.2 ORIENTATION OF MOLECULES IN AN ELECTRIC FIELD

An essential requirement for the observation of optical anisotropy induced by an electric field is that the species under examination must possess dipolar groups and/or must be polarisable. Permanent or induced dipole moments couple with the applied electeric field causing a reorientation which tends to result in a partial alignment of the molecules in the direction of the field. The measured optical anisotropy at a given field strength is determined by the degree of alignment of the molecules which may be characterised mathematically by an orientation parameter (Φ) that depends on the energy of interaction of the solute molecules with the electric field. The orientation parameter is a complex function of terms that depend on the permanent and induced electric dipoles. Figure 6.1 indicates the general form of the dependence of Φ on the square of the strength of the applied field.

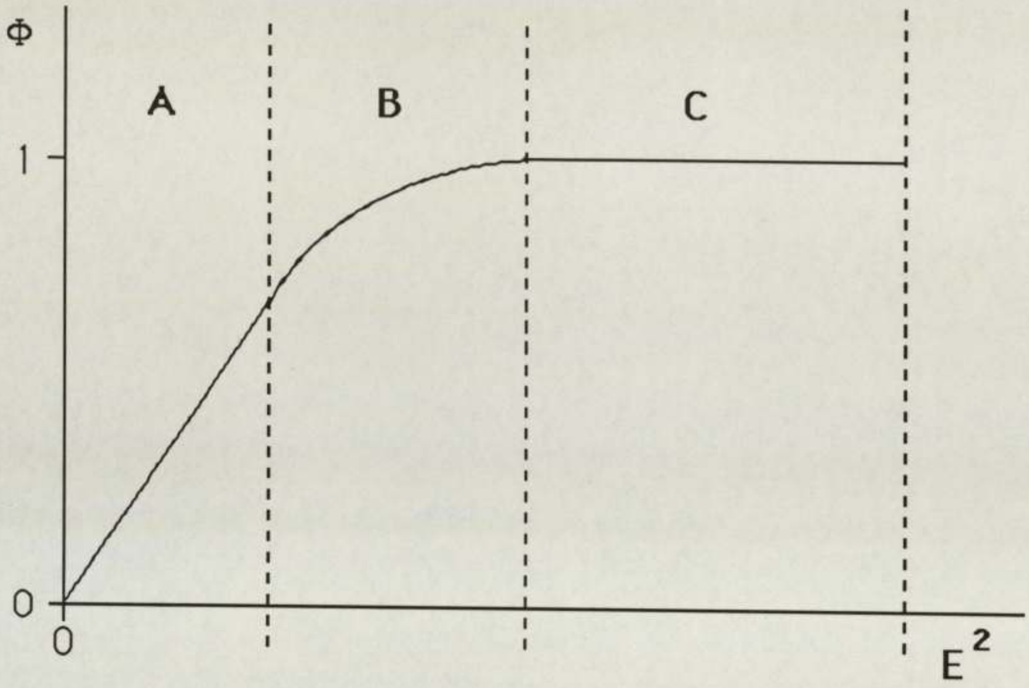

Figure 6.1 Dependence of the orientation parameter (Φ) on the square of the strength of the applied field

In the absence of the electric field $\Phi = 0$. When coupling between the molecules and the applied field is low (region A) a linear dependence is observed. This situation is known as Kerr law behaviour (section 6.3) and while it has been observed experimentally in many studies of birefringence, it should be noted that it is equally applicable to the study of electric dichroism. At moderate to high levels of coupling (region B), Φ becomes increasingly independent of the strength of the applied field until a condition is reached (region C) where orientational saturation occurs. Under these conditions, Φ tends to unity and the maximum attainable value of the induced optical anisotropy is observed.

If a molecule makes an angle, θ with respect to the direction of the applied electric field, then it is apparent that the molecule is free to adopt any orientation with respect to the other two Cartesian axes which are orthagonal to the direction of the field. Therefore, the optical properties measured along any axis orthogonal to the direction of the applied field remain constant and the optical medium is then described as uniaxial.

6.3 ELECTRIC BIREFRINGENCE

The phenomenon of electrical double refraction was first observed by John Kerr(161) in 1875. He found that when a block of glass was placed between crossed Nicol polarisers and the leads of a Rumkorff machine were attached to the block in such a way that the applied electric field was perpendicular to the plane of polarised light passing through the glass, he could see light through the analyser which could not be extinguished by rotating the Nicol. The glass had become birefringent and the emergent light elliptically polarised. Kerr established that a linear relationship existed between the birefringence (Δn) and the square of the strength (E) of the applied field. The equation which describes this dependence and bears his name is

$$\Delta n = B E^2 \lambda \qquad 6.4$$

where B (constant for a given optical medium) is known as the Kerr constant. The validity of this equation was proved experimentally on a range of pure non-viscous liquids some of which were positively birefringent ($\Delta n_{||} > \Delta n_{\perp}$) e.g. toluene and others negatively birefringent ($\Delta n_{\perp} > \Delta n_{||}$) e.g. benzyl alcohol. The Kerr effect has also been observed in gaseous samples of organic and inorganic compounds and methods have been developed for the evaluation of solids in dilute solution.(162) Absolute Kerr constants are difficult to measure as the dimensions of the Kerr cell and the applied voltage must be accurately known. For this reason the cell is often calibrated with a standard material of known Kerr constant thereby allowing a relative value to be calculated for the sample being studied (section 8.3).

When plane polarised light is incident on a molecule, the oscillating electric field of the light-wave interacts with the electron cloud of the molecule retarding the propagation of the beam. It is this process which is responsible for refraction and is characterised by the refractive index (n). Refraction is associated with the polarisibility of the electron cloud and as the distortion of the electron density is spatially restricted by orbital considerations, the refractive index will generally vary according to the orientation of the molecule with respect to the electric vector of the incident beam of light. If three Cartesian axes are drawn through a molecule, one of which is coincident with the major molecular axis, then the effective polarisibility along each axis (P_1, P_2, P_3) may be used to construct an ellipsoid of polarisibility which defines the potential optical anisotropy of the molecule. By invoking the theories developed by Langevin, Born and Gans, it is possible to calculate the values of P_1, P_2 and P_3 for a solute using the measured Kerr constants. The experimental values may then be compared with theroretical values calculated using bond polarisibility data. Using this approach much information can often be deduced concerning molecular conformation and structure.(163)

6.4 ELECTRIC DICHROISM

If the frequency of light incident on a molecule is close to the natural frequency of the oscillating electrons then absorption may occur. In an anisotropic medium the polarisibility differs in each direction of propagation of the light-wave (section 6.3) and hence the degree of absorption will also vary according to direction. If optical anisotropy is induced in a sample by the action of an external electric field, then this phenomenon will appear at the same time as birefringence.

The absorption of light by a molecule causes a change in the distribution of electron density around the nuclei. The magnitude and direction of this change may be characterised by a transition moment. Although the exact assignment of transition moments is rather complicated a simplified approach may be used which considers the shape of the molecular orbitals which describe the ground and excited states. Figure 6.2 (a) shows the shapes of the orbitals which are involved in the π - π^* transition of an alkene.

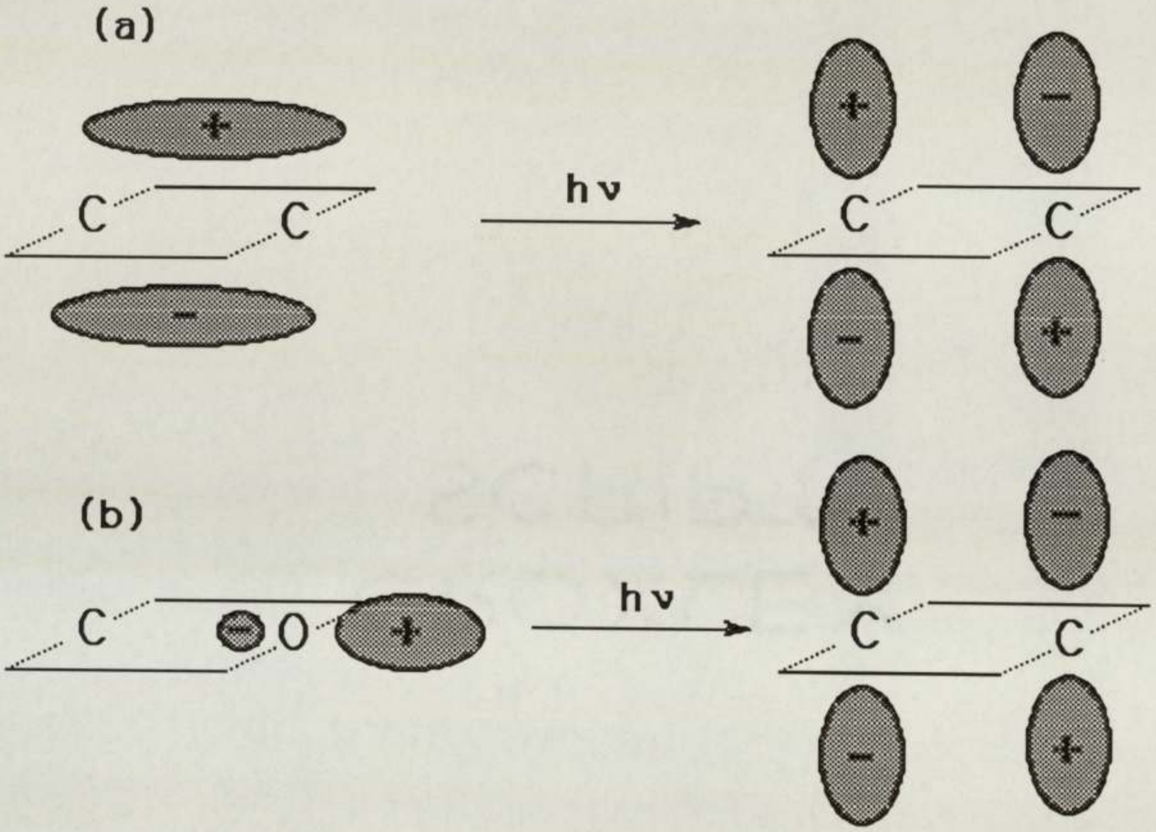

Figure 6.2 Molecular orbital representation of
(a) π - π^* and (b) n - π^* transitions.

The π-bonding orbital consists of two lobes which lie parallel to the C-C bond above and below the molecular plane. The π^*-antibonding orbitals comprise two lobes similarly situated above and below the molecular plane but much more localised to the atoms. During the π - π^* transition a shift in electron density occurs parallel to the molecular plane and hence the transition moment must also lie in this direction.

Figure 6.2(b) shows the shapes of the orbitals which are involved in the n - π^* transition of a carbonyl group. The sp^2 hybrid orbital of the oxygen atom is oriented in the molecular plane whereas the π^* orbital consists of two lobes situated above and below the plane. It is evident that during the $n - \pi^*$ transition a net displacement of charge occurs perpendicular to the molecular plane and hence the transition moment is orthogonal to and much greater than that of the $\pi - \pi^*$ transition.

Since the value of the reduced dichroism at saturation can be related to the average orientation of the transition moments of the optically anisotropic particles (see below) structural information can often be deduced provided the nature of the group giving rise to the dichroic absorption is known.

If the transition moment μ of a chromophore makes an angle θ with respect to the direction of the applied electric field, then the absorbance, $A_{||}$, for plane polarised light propagating parallel to the direction of the field may be derived from theory(164) as

$$A_{||} = A_{\mu} \cos^2\theta \qquad 6.5$$

where A_{μ} is the maximum possible absorbance of the transition (ie. when the transition moment lies parallel to the electric vector of the light). Similarly, the absorbance, $A_{\perp}$, for plane polarised light propagating perpendicular to the direction of the electric field is given by

$$A_{\perp} = (A_{\mu} \sin^2 \theta) / 2 \qquad 6.6$$

The mean absorbance in the absence of the applied electric field is

$$A = A_{\mu} / 3 \qquad 6.7$$

By adding 6.5 and 6.6 and comparing with 6.7 we obtain

$$A = (A_{||} + 2A_{\perp}) / 3 \qquad 6.8$$

Consequently, the parallel and perpendicular dichroism will be related to one another by

$$A_{||} - A = 2 (A - A_{\perp}) \qquad 6.9$$

Solving this expression for $A_{||}$ and $A_{\perp}$ gives,

$$A_{\perp} = (3A - A_{||}) / 2 \qquad 6.10$$

$$A_{||} = 3A - 2A_{\perp} \qquad 6.11$$

The dichroism ($\Delta A = A_{||} - A_{\perp}$) can therefore be obtained directly from the measured parallel or perpendicular absorbance,

$$\Delta A = 3 (A - A_{\perp}) \qquad 6.12$$

$$\Delta A = (A_{||} -3A) / 2 \qquad 6.13$$

If, for a solution of molecules, the directions of the transition moments adopt an average angle α relative to the direction of the electric field, then the reduced dichroism at saturation will be

$$(\Delta A/A)_{max} = 1.5 (3 \cos^2 \alpha -1) \qquad 6.14$$

Solving this equation for $\alpha = 0^o$ (transition moment parallel to the direction of the applied electric field) or $\alpha = 90^o$ (transition moment perpendicular to the direction of the applied electric field) shows that the reduced dichroism at saturation takes a value between +3 and -1.5. For a random arrangement of the transition moments, when $<3\cos^2 \alpha -1> = 0$, or for the special case of $\alpha = 54^o 54'$, the linear dichroism vanishes. The determination of the reduced dichroism at saturation, by extrapolation to infinite field strength, gives access to the average angle α of the transition moment with respect to the principal axis of polarisibility of the molecules.

6.5 ANALYSIS OF OPTICAL TRANSIENTS

When an electric field is applied to a solution of optically anisotropic species the birefringence and dichroism (if absorbing) increase until they reach a value that is related to the "steady state" orientation of the particles. When the electric field is suddenly removed, the aligned particles return to their random orientation state and the birefringence and dichroism fall asymptotically to zero. Figure 6.3 shows a curve typical of the variation of birefringence (or dichroism) resulting from the application of a rectangular shaped electrical pulse.

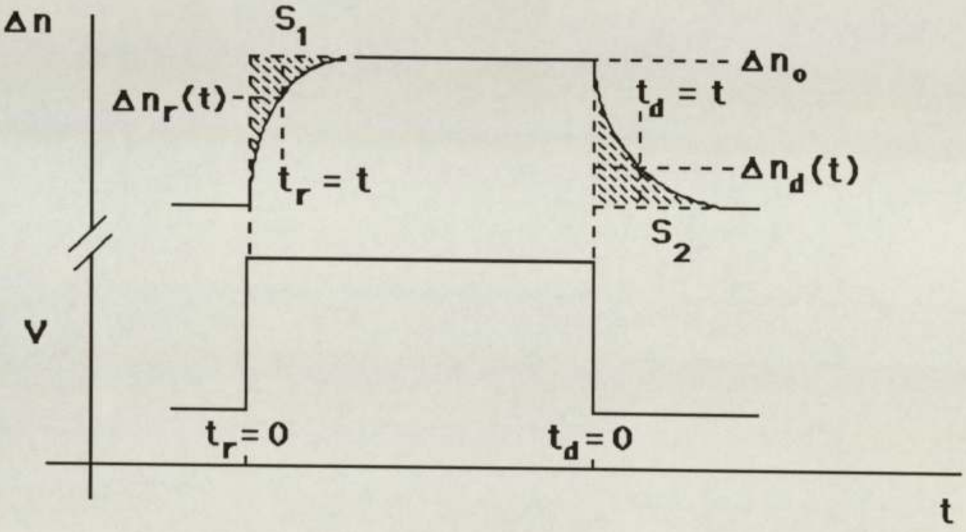

Figure 6.3 The variation of birefringence with time for a material subjected to a pulse of voltage .

Three distinct regions of optical response are observed, a "rise region" in which the birefringence is increasing and has a value $\Delta n_r(t)$ at time t following the application of the electric field, a "steady-state region" in which the birefringence remains constant ($\Delta n = \Delta n_o$) and a "decay period" during which the birefringence decreases to zero and has a value $\Delta n_d(t)$ at time t after the electric field has been removed. The rise and decay of the electro-optical parameters are characteristic of the particles and are usually refered to as relaxation curves or transient curves.

6.5.1 Relationship between optical relaxation decay curves and rotational diffusion

If a system of optically anisotropic particles are considered to be ellipsoids that are able to rotate about their three principal axes, then their rotation may be characterised by three rotational diffusion coefficients. The combined coefficient of rotational diffusion, D_r, may be regarded as a measure of the rate at which an ordered system of particles becomes random and is related to the dimensions of the particles, for a monodisperse system, by the following relationships(165): For ellipsoids of revolution,

$$D_r = 3\,k\,T/16\,\pi\,\eta\,\mathbf{a}^3\ \{2\ \ln(2\,\mathbf{a}/\mathbf{b})\ -1\} \qquad 6.15$$

where η is the viscosity of the solvent and the long and short semi-axes of the elipsoid are **a** and **b** respectively. For cylindrical rods of length 2**a** and diameter 2**b**,

$$D_r = 3\,k\,T/\,8\,\pi\,\eta\,\mathbf{a}^3\ \{\ln(2\mathbf{a}/\mathbf{b})\ -0.8\} \qquad 6.16$$

Provided that an estimate of the axial ratio **a/b** of the particles can be made, the measurement of D_r allows the length, **a**, of the particles to be calculated. The value of D_r can be deduced by analysing the decay curve of the birefringence or dichroism. For the transient period following the removal of the applied field, the variation in birefringence (or dichroism) with time, for a monodisperse distribution of particles, takes the form of an exponential decay:

$$\Delta n_d(t) = \Delta n_o\ \exp\ (-t/\tau) \qquad 6.17$$

where $\Delta n_d(t)$ is the birefringence at time t after the field has been removed, Δn_o the birefringence value for the steady state region and τ the relaxation time characteristic of the particles. Generally, τ is not affected by the strength of the applied field or by the mechanism of orientation of the particles and is related to the rotational diffusion coefficient by the simple relationship

$$\tau = 1 / 6 D_r \qquad 6.18$$

It should be noted that equation 6.17 is equally applicable to the transient decay of electric dichroism. However, birefringence measurements are generally preferred for performing this type of analysis because of their higher sensitivity.

6.5.2 Relationship between optical relaxation rise curves and rotational diffusion

The equation describing the curve for the rise of birefringence takes a more complicated form than that used to describe the decay. This is because the rise curve of the transient birefringence depends on the relative contributions of permanent and induced dipoles. When the strength of the applied field is low, the exact relationship may be simplified by including only the quadratic terms, E^2. The time-dependent birefringence for the rise portion of the optical signal is then given by$^{(164)}$

$$\Delta n_r(t) / \Delta n_o = 1-[3r/2(r+1)] \exp(-2 D_r t) + [(r-2)/2(r+1)] \exp(-6D_r t) \qquad 6.19$$

where r = P/Q. The quantity P is proportional to the square of the magnitude of the permenant dipole moment, μ_p and Q is a function of the polarisibility of the optically anistropic particles. When there is no permanent dipolar contribution (r=0) and the equation for the rise transient reduces to

$$\Delta n_r(t) / \Delta n_o = [1 - \exp(-6 D_r t)] \qquad 6.20$$

which may be re-written as

$$\Delta n_r(t) = \Delta n_o \; [\; 1 - \exp\,(-t/\tau_r)] \qquad 6.21$$

If equation 6.21 is compared with equation 6.17 then it is apparent that the rise curve is symmetrical to that of the decay in the case of orientation resulting from a purely induced dipolar mechanism.

As the value of r increases, the time between the application of the field and the point at which the steady-state birefringence is established increases. Hence, for a molecule which possesses a permanent dipole the relaxation time, τ_r, measured for the rise curve of birefringence is predicted to be greater than τ_d obtained for the decay curve of birefringence.

6.5.3 Determination of the mechanism of orientation using transient field reversal.

The ratio (r) of the induced to the permanent dipolar contribution to the mechanism of orientation of a system of particles can be evaluated by comparing the areas under the rise (S_1) and decay (S_2) curves (figure 6.3). The ratio (S_1/S_2) is unity for the case in which orientation is due solely to an induced dipolar mechanism. This ratio attains a maximum value of 4 when the permanent dipolar orientation dominates ie. $r \to \infty$. Unfortunately this method of analysis does not always give reliable results particularly when orientation of molecular segments (intramolecular relaxation) occurs or when the strength of the applied field is sufficiently high to cause saturation effects. For these reasons, a second technique has been employed to measure r. This technique, which involves the use of "reversed" pulses of voltage, seems to offer the best method for obtaining unambiguous values of r.

If, during the steady-state birefringence region, the polarity of the applied field is rapidly reversed then, for induced moment polarisation, the birefringence remains unchanged. When oriented dipolar groups are present, the reversal of the field causes the polarisation vector to rotate through 180° in order to maintain a minimum free energy with respect to orientation. During this rotational process, the birefringence will decrease below its equilibrium value. Thus, for contributions arising from permanent dipoles, the reversal of the electric field results in a birefringence curve that exhibits a minimum (figure 6.4). The depth of this minimum, Δn_{min}, is dependent on the relative contribution of induced to permanent dipolar orientation mechanisms, characterised by the ratio r. Measurement of Δn_{min} allows r to be calculated using the expression(166),

$$r = 1 - (\Delta n_{min} / \Delta n_o) / (0.1547 + \Delta n_{min} / \Delta n_o) \qquad 6.22$$

This equation has been found to be valid over a wide range of electric field strengths(167).

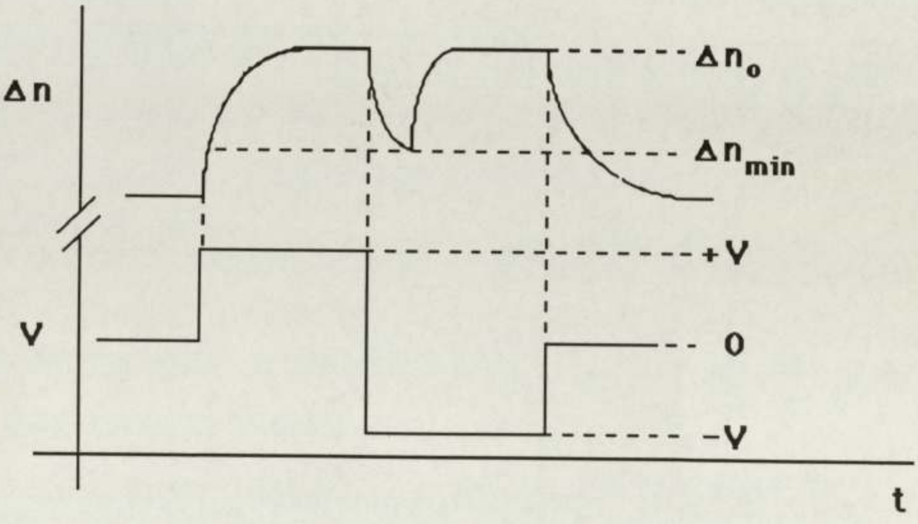

Figure 6.4 Variation of birefringence with time in response to a reversed pulse of voltage

6.6 THE MEASUREMENT OF ELECTRO-OPTICAL ANISOTROPY FOR OPTICALLY ABSORBING SYSTEMS USING PULSED ELECTRIC FIELDS

6.6.1 Introduction

The application of an electric field to the electro-optical cell in the form of a short pulse of voltage offers several advantages over the use of steady state D.C. electric fields and sinusoidally varying A.C. electric fields used in early studies of the Kerr effect(168). Measurements made using A.C. or D.C. electric fields are often hindered by conductivity, electrophoresis, electrode polarisation and heating effects, all of which may be minimised when pulsed electric fields are employed. In addition, the use of pulsed electric fields permits relaxation phenomena to be more readily observed and measured (section 6.5). If the polarity of the electric pulse is reversed during its application, then the contribution of conductive effects can be further minimised, thereby allowing electro-optical measurements to be reliably made even on the most sensitive materials.(166,169)

6.6.2 Measurement of electrically induced birefringence for optically transparent systems.

A convenient optical arrangement for the measurement of electric birefringence in materials that are optically transparent is depicted in figure 7.6. Polariser P_1 is set so that the plane of polarisation of a beam of light incident on the Kerr cell is at 45^o to the direction of the applied electric field. In the absence of the electric field, with the quarter-wave plate removed and analyser P_2 crossed relative to P_1, no light impinges on the detection system. When the contents of the cell become birefringent during the application of an electric field, the beam of light emerging from the Kerr cell is generally elliptically polarised. If the intensity of light transmitted by the analyser is measured for two orientations of polariser P_2 then the optical retardation (δ) may be evaluated.(164,170) However, the sign of the birefringence cannot be determined using this method. This deficiency can be overcome by introducing a quarter-wave retarder between the Kerr cell and the analyser, which not only enables a distinction to be made between positive and negative birefringences but also improves sensitivity. The preferred orientation of the quarter-wave plate is that in which its slow axis is at 45^o to the direction of the electric field. Other orientations of the quarter-wave plate result in high levels of transmitted light, even in the absence of the electric field and for these cases the sensitivity of the detection system is usually drastically reduced. This observation highlights one of the major disadvantages inherent in the evaluation of electro-optical parameters using techniques that depend on the comparison of measured intensities of light. For this reason, methods that rely on using optical techniques to achieve a minimum in the intensity of light due to birefringence have been the most successful. One such method is the nulled-pulse technique.(171) The analyser (P_2) is rotated gradually until a pulse of voltage produces no change in the intensity of light detected by the photomultiplier. When this "null" condition is achieved, the displacement angle, (α) of the analyser from its original crossed position (E=0) is then related to the phase retardation δ by(172)

$$\alpha = \delta / 4 \qquad 6.23$$

Another type of null can be achieved when the analyser is rotated to obtain an extinction of the light during the application of the electric pulse. For this condition it can be shown that(172)

$$\alpha = \delta / 2 \qquad 6.24$$

6.6.3 The measurement of birefringence in the presence of an absorption band

If the birefringence of an optically absorbing material is measured by techniques which involve the measurement of the intensity of light (section 8.6.2.1) then the light transmitted by the analyser will include a component due to dichroism.

Thus, for the measurement of electric birefringence in these systems it is necessary to correct for the effects of electric dichroism. The technique generally employed is to measure separately the dichroism of the sample, using a single polariser method.(169) The optical system is then re-configured to include both birefringence and dichroism and the composite light-intensities are recorded. By deriving an appropriate relationship between the dichroic terms and measured intensities of light, it is possible to compute a value for the electrically induced phase retardation, δ.

Using the optical arrangement shown in figure 7.6 with the quarter-wave plate oriented such that its slow axis lies parallel to the direction of the applied field, then the change in the normalised intensity of light, $\Delta I/I$, due to birefringence and dichroism is given by, (see appendix 4),.

$$\Delta I/I = -1 + 0.5[\ 10^{(A-A_{||})} + 10^{(A-A_{\perp})} -2 \times 10^{(A - A_{||} - A_{\perp})/2} \sin \delta] \qquad 6.25$$

6.6.4 Simultaneous determination of birefringence and dichroism using the nulled pulse technique

An "improved" method for the determination of the birefringence and dichroism of a sample has been reported by Ravey,(173) using an optical arrangement similar to that shown in figure 7.6. The quarter-wave plate is oriented with its slow axis at 45° to the direction of the applied field and the polarisers are crossed. If the analyser (P_2) is then rotated from the crossed position by an angle α, the change in the intensity of transmitted light is given by

$$\Delta I/I_{\alpha} = -1 + [\exp(-\gamma \quad /3)\{\cosh\gamma - \cos(\delta \quad + 2\alpha \quad)\}]/(1 - \cos 2\alpha) \qquad 6.26$$

where $\gamma = 2.3\,\Delta A/2$. For small values of δ and α this may be approximated to

$$(\Delta I/I_{\alpha}) \sin^2 \alpha = (\gamma / 2)^2 + (\delta / 2)^2 + (\delta / 2) \sin 2\alpha \qquad 6.27$$

The slope of a plot of $(\Delta I/I_{\alpha}) \sin^2 \alpha$ versus $\sin 2\alpha$ gives the sign and magnitude of the birefringence. The dichroism, ΔA can be calculated from the intercept on the ordinate axis. Conversely, if the polariser P_1 is rotated by an angle α' (with the analyser returned to its original position, $\alpha = 0$) then for small values of α', γ and δ the following approximation may be obtained,

$$(\Delta I/I_{\alpha'}) \sin^2 \alpha' = (\gamma / 2)^2 + (\delta / 2)^2 - (\gamma / 2) \sin 2\alpha' \quad 6.28$$

The slope of a plot of $(\Delta I/I_{\alpha'}) \sin^2 \alpha'$ against $\sin 2\alpha'$ gives the dichroism (including its sign) and the intercept allows estimation of the magnitude of the birefringence.

Therefore, a number of measurements of intensities of light are required to characterise the electro-optical anisotropy of the material (ie. observations at respective rotations α' and α of the polariser and analyser and at $\alpha = \alpha' = 0^{\circ}$). To calculate the reduced dichroism, the absorbance of the material is also required and must be measured in a separate experiment.

Although this technique has advantages over the methods described in section 6.6.3, numerous disadvantages are apparent:

(i) the measurement of the intensity of light assumes a linear response of the detector system and a correction for stray light must be applied.

(ii) the approximations introduced during the derivation of equations 6.27 and 6.28 indicate that the technique cannot be used for substances which exhibit large dichroisms and/or large birefringences.

(iii) considerable mathematical manipulation of the experimental data is required to obtain values of the electro-optical parameters.

The determination of birefringence using methods that involve the "nulling" of an optical response do not suffer from these limitations and it will be shown that they also provide a rapid technique for the simultaneous determination of birefringence and dichroism (Section 8.3). The arrangement of the optical components used for this analysis is identical to that described in section 6.6.2 (Figure 7.6).

The optical properties of the Kerr cell, when filled with a sample which exhibits both birefringence and dichroism, may be considered equivalent to two separate cells in series; one cell exhibiting dichroism, [D], the other cell exhibiting birefringence only, [B] (figure 6.5).

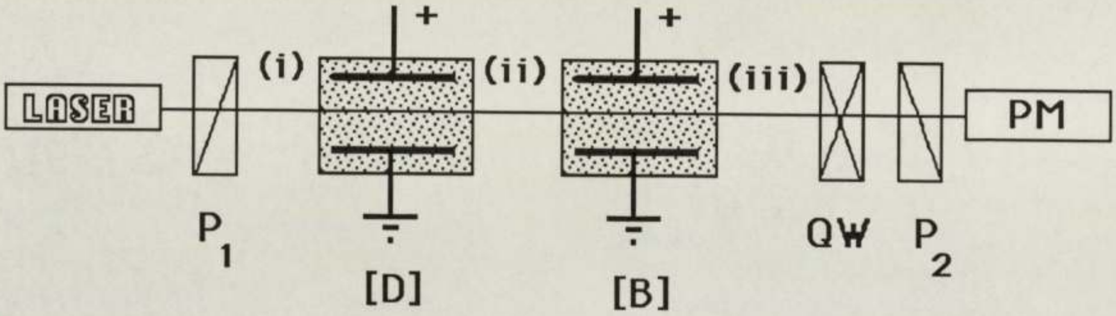

Figure 6.5 Dual cell representation of a system which exhibits both birefringence and dichroism. [D] = dichroic cell [B] = birefringent cell

If the plane of polarisation of the beam of light propagating at (i) lies at 45° with respect to the direction of the applied electric field, then the beam may be resolved into two orthogonal components of equal magnitude that propagate with their electric vectors parallel and perpendicular to the direction of the applied electric field. In the absence of the applied field, both components are absorbed by the same amount during passage through "cell [D]" and the amplitude of the resultant waveform at (ii) is reduced compared to that at position (i). The components are unaffected by passage through "cell [B]" and the waveform of the light which propagates at (iii) is identical to that at (ii). If a voltage is applied to cell [B] then material within the cell becomes birefringent and for a typical positive birefringence this results in the parallel component being retarded relative to the component propagating in the perpendicular direction (figure 6.6(a)).

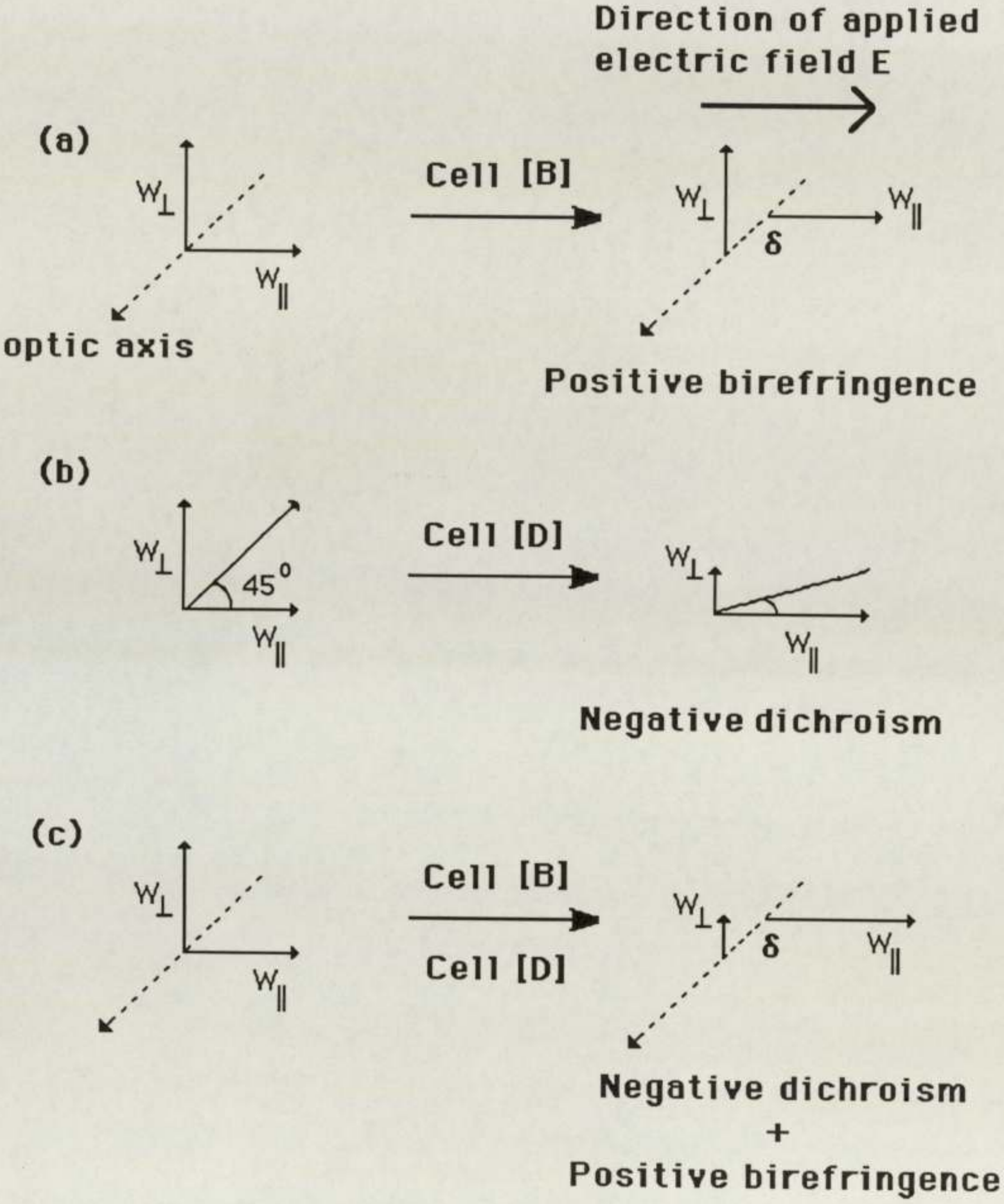

Figure 6.6 Effect of electro-optical anisotropy on the components of an incident beam of plane polarised light

If the field is applied to "cell [D]" then the contents of the cell may exhibit negative dichroism and the intensity of the perpendicular component of the incident beam of light will be reduced and the intensity in the parallel direction increased (figure 6.6(b)). When the electric field is applied simultaneously to both cells, the parallel and perpendicular components of the beam of light at position (iii) will differ in both phase and intensity (figure 6.6 (c)).

If the angular position of the plane of polarisation of the beam of light at position (i) is adjusted by rotating polariser P_1 away from the 45^o orientation, then the intensities of the components resolved in directions parallel and perpendicular to that of the field will no longer be identical. At a certain orientation of polariser P_1 (β^o with respect to the initial crossed position) the effect of the dichroic "cell [D]" on the magnitudes of the components of the incident beam will be exactly balanced by the effect of polariser P_1. Thus, the parallel and perpendicular components of the light emerging from "cell [D]" will have the same intensity (see figure 6.7). The dichroism is then given by the expression $\Delta A = -2 \log_{10} [\tan (45^o - \beta)]$ (see section 8.3).

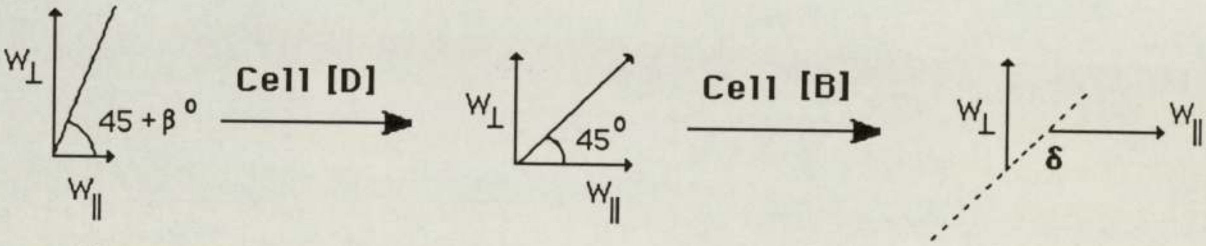

Figure 6.7 Compensation technique for simultaneous determination of dichroism and birefringence

Since both components have equal amplitude the plane of polarisation of the composite beam leaving cell [D] will lie at 45^o to the direction of the field. If this beam is allowed to propagate through "cell [B]" then the situation is clearly identical to that shown in figure 6.6 (a) and the intensity of the light transmitted by the analyser will be due to birefringence alone. The optical retardation (birefringence) can then be estimated by rotating polariser P_2 to a position, α which corresponds to a minimum in the intensity of transmitted light detected by the photomultiplier. The retardation (δ) is then given by $\delta = 2\alpha$ (see section 6.6.2).

6.7 DIELECTRIC RELAXATION

Dielectric relaxation is a powerful technique for directly probing the rate of re-orientation of permanent molecular dipoles. Unlike electro-optical measurements, which are often hindered by absorption phenomenon, the dielectric method is able to operate over a far greater range of concentration.

When a constant electrical potential is applied to a system, dipolar groups couple with the field leading to a re-orientation of the molecules (section 6.2). As this process is opposed by thermal agitation, there will exist an equilibrium state that is determined by the static dielectric permittivity (dielectric constant) of the medium (ε_s). The instantaneous dielectric constant (ε_∞) which is measured immediately an electric field is applied is lower than ε_s and is due to distortion (electronic and atomic) polarisation alone. After the application of a D.C. electric field, the dielectric constant will increase with time as the molecular re-orientation process occurs, until it reaches an equilibrium value, ε_s. If an electric field of alternating polarity is applied, then a dispersion of the measured dielectric constant between ε_s and ε_∞ will occur as the frequency is scanned from very low (~D.C.) to very high (~10^{15} Hz) values, respectively. Here, ε_∞ corresponds to the condition where the frequency is so great that no net molecular motion is induced and ε_s corresponds to the region in which complete dipolar reorientation may occur exactly in step with the changing strength and polarity of the electric field.

If an alternating field E, of amplitude E_o and frequency ω is applied to a dielectric material then

$$E = E_o \cos \omega t \qquad 6.29$$

This will result in a polarisation which alternates in direction with time and if the frequency is sufficiently great, the orientation of permenant dipoles will lag behind the field. The electric displacement (D) due to the dipoles will then be retarded by a phase lag (δ) (which should not be confused with the optical phase retardation described earlier) where

$$D = D_o \cos(\omega t - \delta) \qquad 6.30$$

This may be rewritten as

$$D = D_1 \cos \omega t + D_2 \sin \omega t \qquad 6.31$$

$$\text{where} \quad D_1 = D_o \cos \delta \quad \text{and} \quad D_2 = D_o \sin \delta$$

This allows the identification of two dielectric constants, defined by

$$\varepsilon' = D_1 / \varepsilon_o E_o \quad \text{and} \quad \varepsilon'' = D_2 / \varepsilon_o E_o$$

where ε_o (= 8.856×10^{-12} Fm^{-1}) is the permitivity of free space. The constants ε' (the static dielectric permitivity, "dielectric constant") and ε'' (dielectric loss factor) are linked by the simple relationship

$$\varepsilon'' / \varepsilon' = \tan \delta \quad (\equiv \text{energy dissipated per cycle / energy stored per cycle}) \qquad 6.32$$

Both $\tan \delta$ and ε' (proportional to the parallel capacitance) are measurable quantities which allow calculation of ε''. Equations which relate ε'' and ε' to molecular properties have been derived from the theory of dielectrics pioneered by Debye. It may be shown that, for many polar liquids for which a single relaxation process is dominant, ε'' and ε' depend on the frequency of the applied field in the following manner,

$$\varepsilon'(\omega) = \varepsilon_\infty + (\varepsilon_S - \varepsilon_\infty) / (1 + \omega^2\tau^2) \qquad 6.33$$

$$\varepsilon''(\omega) = \omega\tau[(\varepsilon_S - \varepsilon_\infty) / (1 + \omega^2\tau^2)] \qquad 6.34$$

where τ is the relaxation time which characterises not only the dielectric decay, but also serves as a direct measure of the rate of orientation of the dipolar unit.

The dependence of ε'' and ε' on frequency for a single relaxation process is shown in figure 6.8. The dielectric loss curve (ε'') shows a maximum at a critical frequency, ω_{max}. The latter is related to the dielectric relaxation time, τ, by the simple relationship, $\omega_{max} = 1/\tau$ The difference in the dielectric constant measured at high and low frequencies is called the strength of the relaxation and is directly proportional to the area under the loss curve.

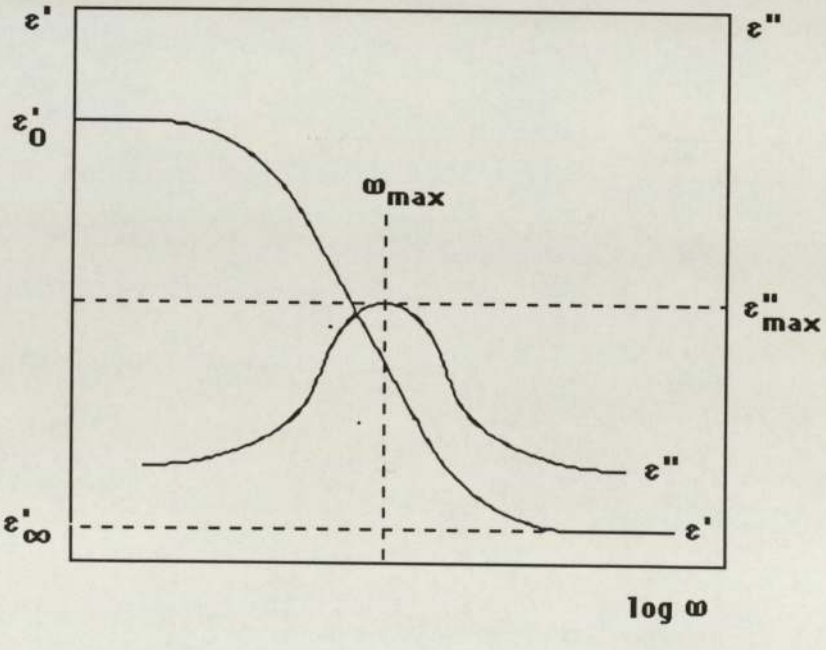

Figure 6.8 Frequency dependence of ε'' and ε' for a permenant molecular dipole undergoing a single relaxation process.

CHAPTER 7

MEASUREMENT OF THE ELECTRO-OPTICAL PROPERTIES OF POLYACETYLENE COPOLYMERS

7.1 PREPARATION OF SOLUTIONS FOR ELECTRO-OPTICAL MEASUREMENTS

A sample of soluble polypentenylene-block-co-acetylene was prepared by the transformation method outlined in section 5.2. This was stored in a sealed container under argon and kept in the dark. Solutions were prepared by weighing out accurately about 0.1g of copolymer and adding, from a pipette, 5.0 ml of Aldrich Gold Label (Spectrosol) cyclohexane. To effect solution, a mechanical agitator was used for approximately 30 minutes. The solutions were filtered through a Whatman filter (No.1) to remove dust and insoluble material. A Beckman DU7 instrument was used to record the uv/visible absorption spectrum of the solutions in a quartz cuvette (10mm path length) using cyclohexane as a reference material. The instrument was also used to measure accurate absorbances at 632.8nm (the wavelength of the laser light used in the electro-optical experiments). An average value was calculated from forty independent measurements of the absorbance and this figure was multiplied by five to account for the longer path length of the Kerr cell (50mm).

A calibration plot was constructed by plotting the absorbance (at 632.8nm) of solutions of the copolymer in cyclohexane against the concentration of copolymer (figure 7.1). This plot was then used to obtain the effective concentration of subsequent solutions of copolymer. All measurements of the electro-optical properties of the solutions were undertaken on the day they were prepared.

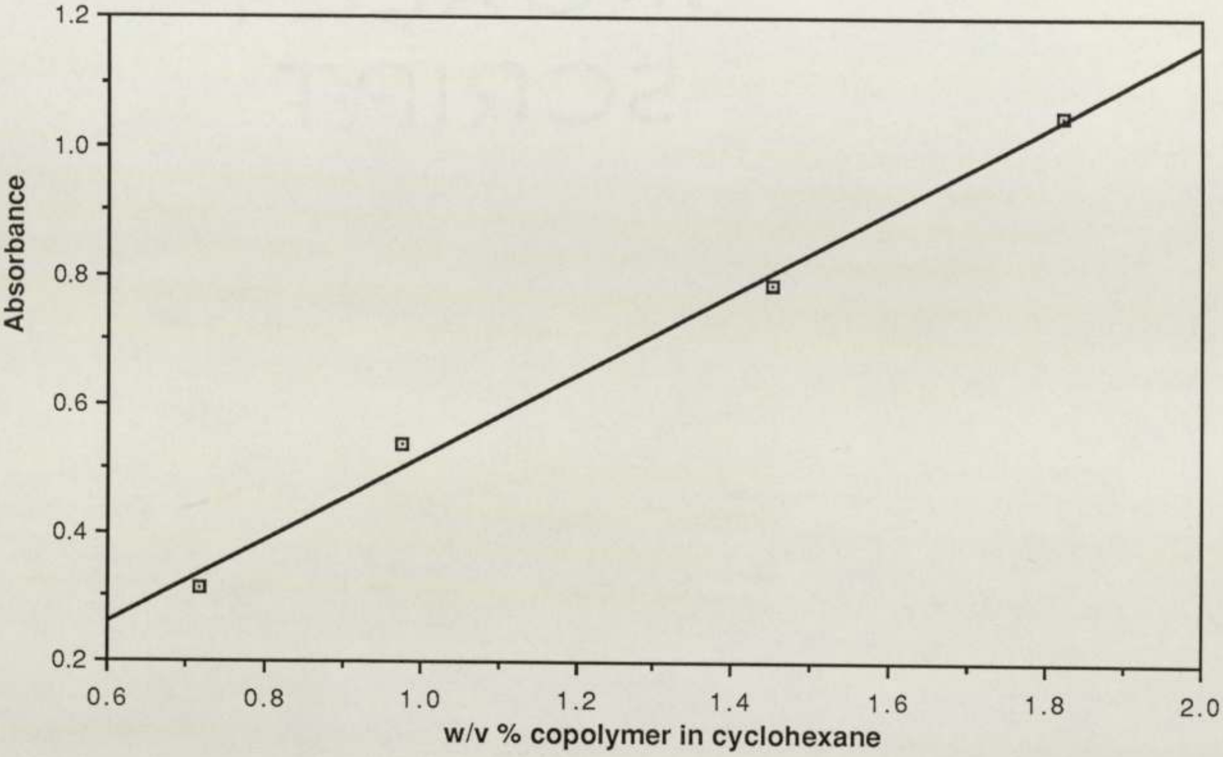

Figure 7.1 Absorbance of various solutions of polypentenylene-block-co-acetylene in cyclohexane at 298K as a function of concentration

7.2 APPARATUS

In this section, a description is given of the components of the apparatus used to measure the electro-optical properties of the copolymeric materials. All the optical components were mounted on a 2m optical bench enclosed in a light-proof cabinet.

7.2.1 Source of light

A beam of plane-polarised light of wavelength 632.8nm was generated by a Spectra Physics helium/neon laser. In these experiments, two laser sources were used, a 0.95mW class two (model 155) and a 10mW (model 132). The latter was used to examine the more optically absorbent samples. The laser was mounted so that the beam of light was directed parallel to the optical bench.

7.2.3 Collimation and reduction in the size of the beam of light

To allow passage of the beam of light (diameter 2mm) between the electrodes in the Kerr cell (electrode separation 1mm), the diameter of the beam was reduced by two lenses separated by the sum of their focal lengths. The first lens had a focal length of 21cm and the second 6cm. This combination resulted in a 60% reduction in the diameter of the beam. The intensity of the beam could be controlled by the introduction of coloured filters into the optical path at a point preceeding the rest of the optical components. The filter assembly consisted of a hollow cylinder into which up to five filters could be introduced allowing the intensity of the beam to be set at the desired level. A single shutter was employed to provide coarse attenuation of the transmitted beam.

7.2.3 Polarisers

The polarisers (P_1 and P_2) were of the Glan-Thompson double refraction type of commercial origin,$^{(160)}$ each being constructed from two calcite prisms glued together and mounted in a hollow brass cylinder. One advantage of using this type of polariser is that the direction of travel of the beam is undeviated by the polarisation process. However for the device to function correctly the light beam must be incident at 90 ± 7^{o} to the polariser face. The brass tubes containing the polarisers were secured into a rotatable graduated circle, which enabled the angle of polarisation, with respect to a fixed point, to be estimated. The angle of polarisation of polariser P_1 could be determined with an accuracy of $\pm 0.25^{o}$ and the angle of polariser (analyser) P_2 to an accuracy of $\pm 0.1^{o}$, using a vernier scale.

7.2.4 Quarter-wave retarding plate

Retarders or wave plates are optical components that convert the polarisation form of light propagating through them. The beam of light that emerges from the Kerr cell is generally elliptically polarised and must be converted to a plane polarised form for analysis by nulled pulse methods (section 6.6.2) This conversion is achieved by employing a quarter wave plate (90° retarder) which consists of a disc of birefringent material. An incident beam is divided into two orthogonally polarised components by the device and one of these is retarded by one quarter of a wave cycle relative to the other. If plane polarised light is incident on the 90° retarder the emergent beam may be represented by the combination of two mutually perpendicular sinusoidally varying waveforms, that are 90° out of phase with one another. The pattern traced by the electric vactor of the light is now an ellipse and the light is said to be elliptically polarised. By the reverse mechanism, elliptically polarised light may be converted to plane polarised light.

As the properties of the quarter-wave plate arise from its macroscopic birefringence, there exist two orthogonal directions of propagation which correspond to maximum and minimum refractive indices within the plate. These two directions correspond to the slow and fast axes, respectively. If these axes are aligned at 45° with respect to the plane of polarisation of incident plane polarised light then circularly polarised light is emitted. If the electric vector of the plane polarised light lies along either the fast or slow axis of the retarder, then there is no effect on the polarisation of the light.

The retardance of the plate depends on the birefringence of the material used for its construction, the plate thickness and the wavelength of incident light used. The quarter-wave plate used in these experiments was cut specifically for use at 632.8nm.

7.2.5 The Kerr Cell(188)

The Kerr cell (Figure 7.2) was constructed from a block of stainless steel which had a channel milled through it. Two stainless steel discs were bolted and sealed into position at each end of the channel, each disc having a 35mm diameter hole drilled at the centre to allow passage of the laser beam in and out of the cell. Two circular quartz plates were used as windows and were held in position by stainless steel discs fitted with rubber `O` rings. To minimise strain birefringence in the windows, care was taken to ensure that the screws holding the window mountings were not over tightened.

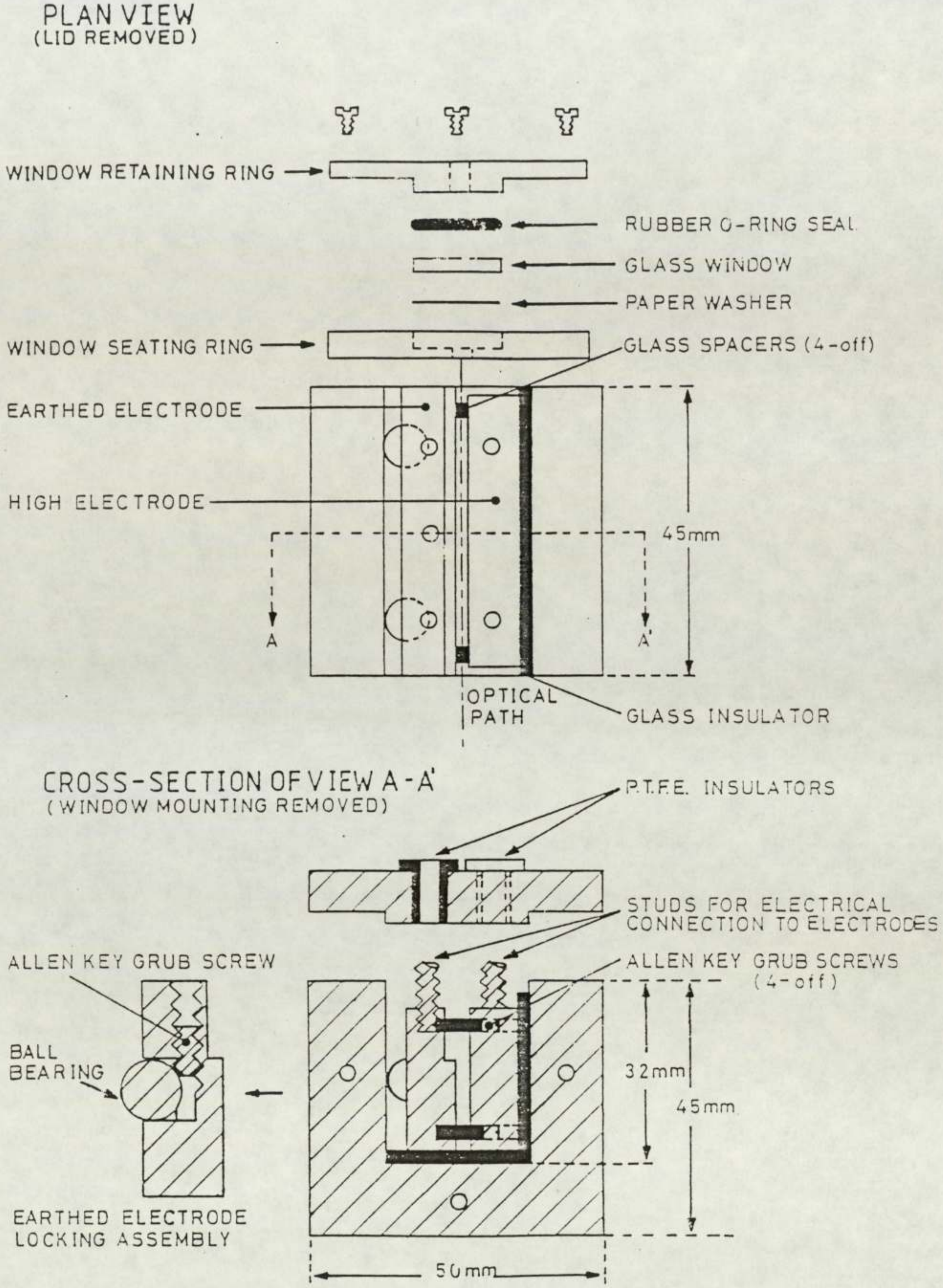

Figure 7.2 The Kerr cell

The electrode assembly consisted of two stainless steel blocks 5cm long which were separated from each other by four glass pegs. A grubscrew allowed the height of each glass peg to be varied thus providing a means of setting the electrode separation. In these experiments a feeler guage was used to set the cell gap to 1.0mm. The electrode assembly could be lowered into the cell and secured in position by the pressure of two ball bearings . The ball bearings were located in recesses in the earth electrode and could be forced into contact with the cell wall by the action of two grub screws. This ensured a good electrical contact between the cell body (connected to the earth lead of the high voltage supply) and the earth electrode. The high-voltage electrode was insulated from the body of the cell by two rectangular pieces of P.T.F.E. Two threaded rods were used to provide electrical connections to the electrodes. A close-fitting stainless steel lid was used to reduce evaporation of solvent. Electrical insulation between the high-voltage connecting rod and the lid was achieved by a PTFE collar.

The Kerr cell was placed between and in intimate contact with two hollow brass blocks. The carrier could be adjusted in three dimensions to allow correct alignment with the laser beam.

7.2.6 Detection of transmitted light

The intensity of the light beam which emerged from the optical system was measured using a photomultiplier (PM). The PM tube was mounted in a brass tube which had a 20mm aperture near the window of the PM A collecting lens positioned just in front of the PM served to minimise interference from stray light Additional collimation of the light was achieved by an aluminium barrel, 80mm long, provided with a 2mm diameter aperture . Amplification of the light was achieved by a series of dynodes within the PM tube which were configured according to the diagram shown in figure 7.3.(188) The HT driving potential was supplied by a Brandenberg model 472B generator and could be varied between 0 and -2kV.

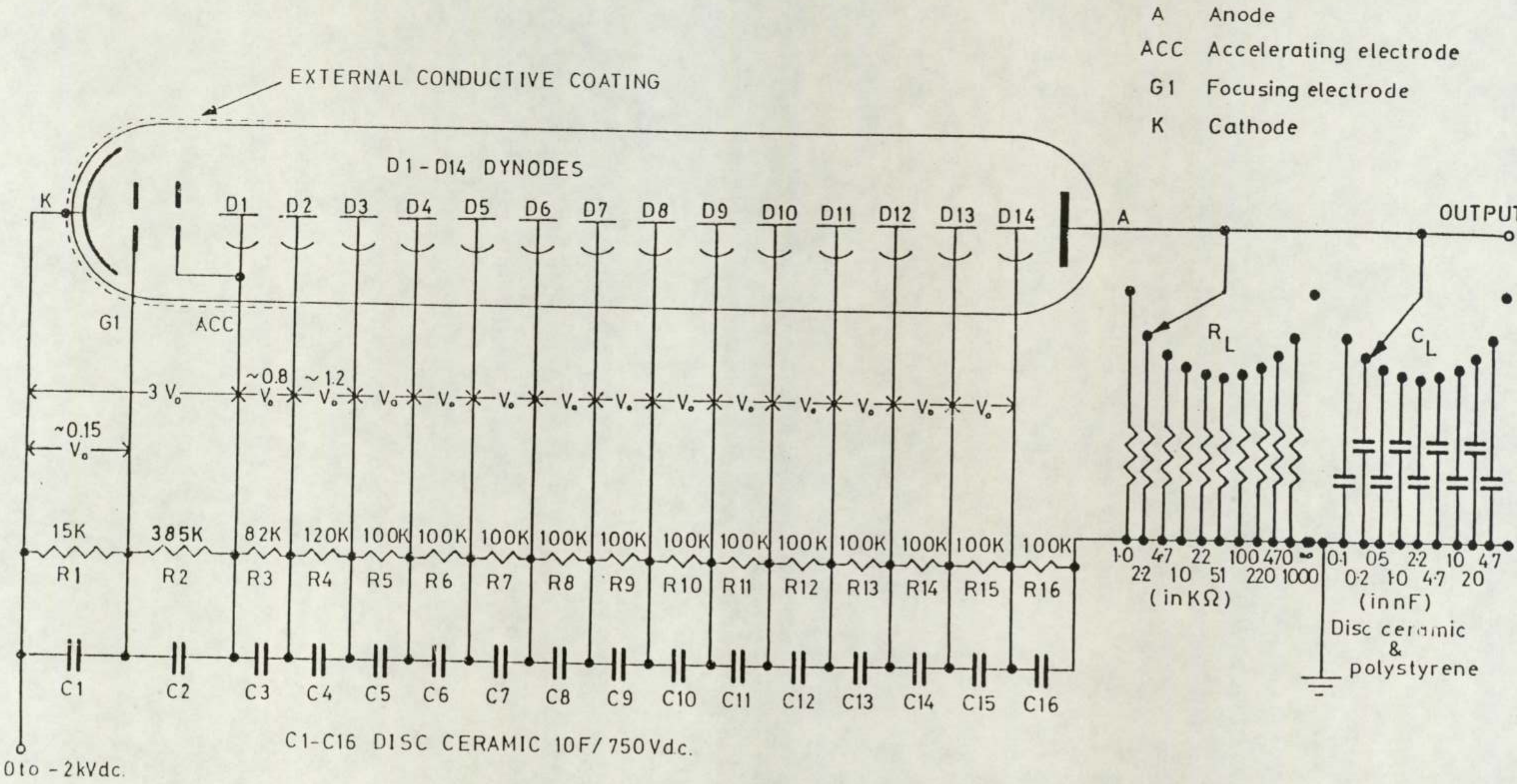

Figure 7.3 Electrical configuration of the photomultiplier

The sensitivity of the signal, output by the PM, could be smoothed by a capacitor/resister network (C_l and R_l in figure 7.3). The sensitivity decreased as the value of R_l was decreased. Increasing the product of the capacitance and resistance smooths out the high frequency components of the optical signal thus permitting the DC light-level of the optical pulses to be estimated more easily. However, to avoid distortion of the optical signals, the detector response time must be short compared with the changes that occur during the optical pulse. In these experiments R_l and C_l were chosen to be 2.2KΩ and 0.2nF, respectively.

7.2.7 Signal display and recording

The optical signal from the photomultiplier was displayed on one channel of a Tektronix 465B double-beam oscilloscope (figure 7.4). Because the PM signal became increasingly negative as the intensity of light increased, the inverting input of the oscilloscope was selected to providing a display that increased upward, in a conventional sense, as the intensity of light increased. The second channel was used to display simultaneously the HT pulse applied across the electrodes of the Kerr cell.

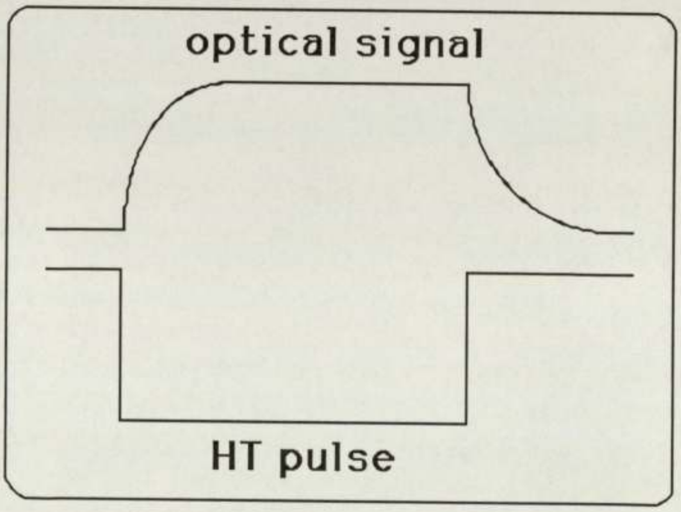

Figure 7.4 Diagram showing the oscilloscope screen during the application of a pulse of voltage to the Kerr cell

Since the maximum permitted voltage at the input terminals of the oscilloscope was 10V, monitoring of the HT voltage was achieved using a Tektronix probe (model P6013A). This reduced the voltage by a factor of 10^3. The oscilloscope was triggered by the 'negative going edge' of a square wave pulse generated within the pulse former circuit. (see Appendix 1). The triggering signal was arranged so that a short delay occurred between the scope triggering and the receipt of the optical signal. This arrangement allowed a portion of the optical baseline (field-off light-level) to be displayed immediately preceeding the transient change in intensity.

Optical transients were recorded using a Datalab model DL905 transient recorder. The captured signal was displayed continuously on the oscilloscope which was set in the X,Y mode, the two channels acting as the X and Y inputs. A permanent copy of the optical transient was obtained, via the plotting facility provided by the instrument, using an Advance X,Y plotter model HR-96. When using the Tektronix scope in the X,Y mode, the HT signal from the Kerr cell was displayed on a second oscilloscope (Telequipment DM64) which could be used to store and display the signal continuously. This enabled a direct comparison to be made between the applied electric pulse and the optical signal.

7.2.8 Generation of pulses of high-voltage

A reversed voltage pulse generator unit was used to supply the pulse of HT-voltage applied across the electrodes of the Kerr cell. A description of the construction and operation of this unit is presented in Appendix 1. The shape of the electric pulse could be selected to be continuously positive and the magnitude and duration of the pulse could be varied. Alternatively, a reversing pulse could be produced for which the polarity could be reversed rapidly during the transient period. The durations of the positive and negative phases could be varied independently from 4 to 86ms. Voltages were adjustable in the range 0 to ±2.5kV. The pulse generator also provided a facility for measuring the magnitude of the HT voltage set to be applied to the Kerr cell. The output was connected, via a 10^3 attenuator, to a Kiethley 616 digital electrometer.

7.2.9 Temperature control

Electro-optical effects often show marked temperature dependences and for this reason the temperature of the Kerr cell was maintained at a constant value using a Churchill circulating unit. The Churchill unit pumped water from a 20 liter glass reservoir through the two hollow brass blocks of the Kerr cell mounting. The temperature of the water could be raised by an internal heater or lowered by means of a cold water supply heat exchanger. Rapid elevation of the temperature was achieved using a 400W boost heater. A 0-60°C mercury-filled thermometer measured the temperature of the water in the reservoir with an accuracy of ±0.1°C.

For most work the temperature of the Kerr cell was maintained at 18°C (below room temperature) to minimise losses of solvent (cyclohexane) by evaporation.

7.3 CALIBRATION OF THE OPTICAL SYSTEM

7.3.1 Determination of the angular position of the plane of polarisation of polariser P_1 and analyser P_2

To permit correct interpretation of the results of the electro-optical experiments, it was necessary to be able to relate the angles measured on the polariser scale to the angle of polarisation of the light beam emerging from the polariser/analyser. The optical system used for this purpose was the same as that employed for the measurement of birefringence (section 6.6.2) and is shown in Figure 7.5. The cell was filled with a 50% v/v solution of nitrobenzene in cyclohexane and a fixed pulse of voltage applied to the cell. The crossed polarisers were rotated until a minimum was detected in the birefringence signal.

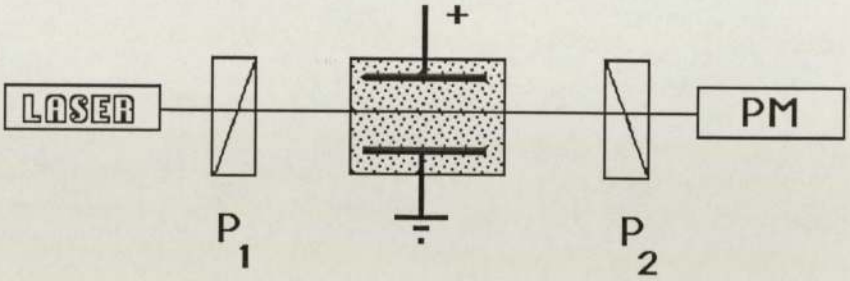

Figure 7.5 Optical arrangement for the evaluation of the angular vaiation of the electrically induced birefringence

Four minima were found at $P_2 = 40^o, 130^o, 220^o, 310^o$. These values corresponded to situations in which the plane of polarisation of the beam was either parallel or perpendicular to the direction of the applied electric field. To distinguish between these possibilities, a separate experiment was performed in which the light from a distant object was arranged to be obliquely incident on a sheet of glass. The reflected image of the object was analysed by one of the polarisers. Under these conditions, when the angle of incidence is equal to the Brewster angle, the reflected beam is totally plane polarised. By rotating the polariser about its optical axis, extinction of the light was achieved and it was concluded that the angles 130^o and 310^o, referred to previously, corresponded to plane polarised light propagating with its plane of polarisation parallel to the direction of the applied electric field.

7.3.2 Identification of the optical axes of the quarter-wave plate

The positions of the slow and fast axes of the quarter-wave plate were determined using the following procedure. The electrically induced birefringence exhibited by a 10%v/v solution of nitrobenzene in cyclohexane was measured using the optical arrangement shown in figure 7.6. The angular position of polariser, P_1, was set so that the plane of polarisation of the beam passing through the cell was at 45^o to the direction of the applied field.

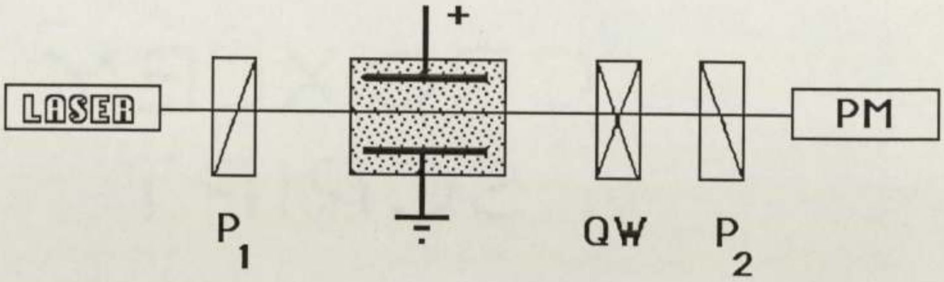

Figure 7.6 Optical arrangement for the measurement of birefringence

Polariser, P_2 was then crossed relative to P_1 in the absence of the quarter-wave plate. When the retarder was introduced, a light-signal was detected by the photomultiplier which was extinguished by a rotation of the quarter-wave plate. At extinction, either the slow or fast axis of the quarter-wave plate must be at 45° to the direction of the electric field (section 7.2.4). When an electric field was applied across the electrodes of the cell, a transient optical signal was observed which, under conditions of equilibrium, could be nulled by rotation of polariser P_2 in a clockwise manner (viewed from the laser along the optical bench) such that the angle subtended by the transmission axis increased. A simulation of this experimental procedure was performed using the computer program "optical simulator" (appendix 2). This enabled a calculation to be made of the normalised intensity of light transmitted by P_2 under these conditions. The results presented in table 7.1 show that with the quarter-wave fast axis at 45° with respect to the applied field, a simulated birefringence signal must be "nulled" by rotating P_2 in an anticlockwise manner such that the angle subtended by the transmission axis decreases. It must therefore be concluded that the slow axis of the quarter-wave on the optical bench plate was set at 45° with respect to the direction of the applied electric field.

Table 7.1 Determination of position of quarter-wave plate slow axis by computer simulation

Polariser P_1 angle of transmission axis / degrees	Quarter-wave plate angle of Fast axis / degrees	Polariser P_2 angle of transmission axis / degrees	Optical phase retardation / degrees	Relative intensity of transmitted light
45	45	135	0	0
45	45	137	+5	6.2×10^{-3}
45	45	135	+5	1.9×10^{-3}
45	45	133	+5	7.6×10^{-5}
45	135	135	0	0
45	135	137	+5	7.6×10^{-5}
45	135	135	+5	1.9×10^{-3}
45	135	133	+5	6.2×10^{-3}

7.4 MEASUREMENT OF ELECTRIC DICHROISM

The method used to determine the electrically-induced dichroism of the copolymer solutions was similar to that described by Fredrique and Housier(164). The arrangement of the optical components is shown in figure 7.7.

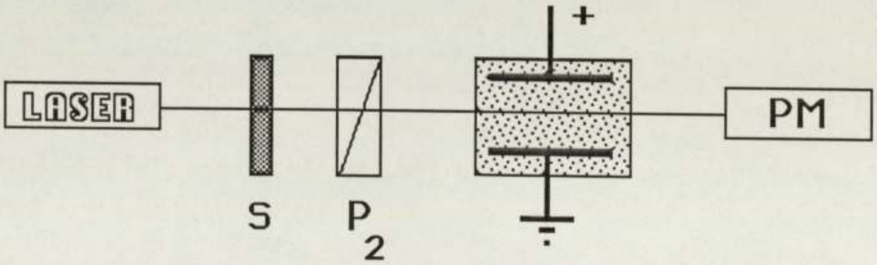

Figure 7.7 Optical arrangement for the measurement of electric dichroism (S = shutter)

The angular position of polariser P_2 was adjusted so that the plane of polarisation of the beam of light passing through the Kerr cell was parallel to the direction of the applied electric field. The solution of copolymer was placed in the Kerr cell and the beam of light was extinguished by placing a shutter (S) in the optical path. The zero light-level was recorded and displayed on the oscilloscope, after setting the lower level of the signal capture window of the transient recorder. A printed copy of the zero-level trace was output to the X,Y plotter. The shutter was then removed and the attenuation of the beam adjusted so that the field-off intensity of light fell within the upper level of the signal capture window of the transient recorder. When a pulse of HT voltage was applied to the cell, a transient reduction in the beam intensity occurred which was recorded by the transient recorder and displayed automatically on the oscilloscope. A printed copy of the optical transient was then drawn on the same sheet of paper as the zero light-level trace. A typical set of readings is shown in figure 7.8.

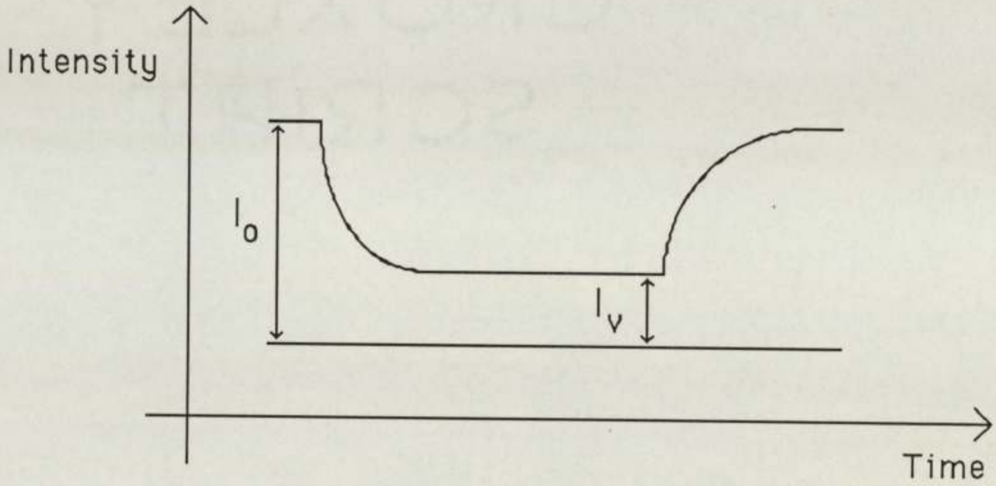

Figure 7.8 A typical dichroism transient

Here, I_o is proportional to the electric field-off intensity of light and I_v the steady state electric field-on intensity of light. A set of optical transients were recorded for various voltages applied to the Kerr cell. Although the measurement of the change in absorbance in the direction parallel to that of the electric field alone can be used to determine the dichroism, measurements of the perpendicular dichroism were also made to test the validity of the assumption that the effect of the the field produced a uniaxial medium (section 6.1). For these measurements, the axis of polarisation of the polariser, P_2, was set perpendicular to the direction of the applied field and the transient increase in the intensity of light, which followed the application of a pulse of voltage, was recorded by the procedure outlined previously.

To facilitate the analysis of the electro-optical traces, the time axes of the optical transients could be expanded so that the non-equilibrium portion under study (rise or decay of dichroism) filled the entire capture window of the transient recorder. When examining the decay transients, the transient recorder was triggered from the trailing edge of the HT pulse via the trigger output of the pulse generator with source "C" selected (see Appendix 1).

7.5 MEASUREMENT OF ELECTRIC BIREFRINGENCE

7.5.1 Corrected light-intensity method

The electrically induced phase difference (δ) of optically absorbing samples has been measured by a few workers(164,169), using the optical arrangement shown in figure 7.6.

When the wavelength of light falls within an absorption band of the sample under test, the transient optical signal detected by the photomultiplier is a composite of both dichroism and birefringence. The birefringence may be obtained by allowing the effects of dichroism and employing an appropriately derived equation (see section 6.6.3). The induced dichroism of samples of polypentenylene-block-co-acetylene in cyclohexane was measured by the method described in section 7.4. A fresh sample was then prepared of an identical concentration to that for which the dichroism had been measured. This solution was then placed in the Kerr cell and the optics re-arranged for the measurement of composite (birefringence plus dichroism) intensities of light (figure 7.6). Thus, the quarter wave plate was orientated with its slow axis parallel to the applied field direction. With the polariser, P_1, set at 45° with respect to the field and polariser, P_2, crossed relative to P_1, the intensity of light incident on the photomultiplier was adjusted using the attenuator so that it fell within the input range of the transient recorder. When a pulse of voltage was applied across the electrodes of the cell, a decrease in the transmitted intensity of light was observed which corresponded to the transient optical signal. The latter was recorded by the method described in section 7.4 and a printed copy obtained for subsequent analysis.

7.5.2 Nulled intensity Method

The limitations of techniques for the determination of electric birefringence, which involve a quantitative measurement of the intensity of light, have been discussed in section 6.6.4.. In this discussion it was suggested that the Kerr cell may be considered equivalent to two separate cells, one exhibiting pure birefringence and the other pure dichroism. A "nulled pulse" method was then described that permitted the simultaneous evaluation of electric birefringence and electric dichroism. The arrangement of the optical components required for these measurements is identical to that used for the measurement of electric birefringence by the nulled pulse technique (figure 7.6).

The slow axis of the quarter-wave plate and the axis of polarisation of polariser, P_1, were set at 45^o with respect to the direction of the applied electric field. Analyser, P_2, was set in the crossed position so that in the field-off state, no light was transmitted by the analyser. When a pulse of voltage was applied to the cell, a transient optical signal was recorded on the oscilloscope. Polariser, P_1, was then rotated to minimise the field-on light-level. It should be noted that although the field-off light-level increased as P_1 was rotated, the position of "null" used in this experiment was the point at which the field-on light-level was a minimum. Polariser P_2 was then rotated to achieve further reduction in the field-on light-level. Initially, the angular positions of the polarisers at the null point were not well defined, but the sensitivity with respect to the angular positions was markedly improved if, after rotation of polariser P_2 to the null point, the entire nulling procedure was repeated. During this process, the sensitivity of the oscilloscope was progressively increased to permit a more accurate measurement of the position of the null point. Figure 7.9 shows the optical signal observed at various stages during the nulling procedure.

The angular positions of polarisers P_1 and P_2 were then recorded. The electric dichroism was calculated from the angle of rotation of P_1 (section 6.6.4) and the electric birefringence from the angle of rotation of P_2 from its initial (field-off) crossed position. A series of measurements was performed on each sample at increasing voltages to test adherence to the Kerr law (section 6.3).

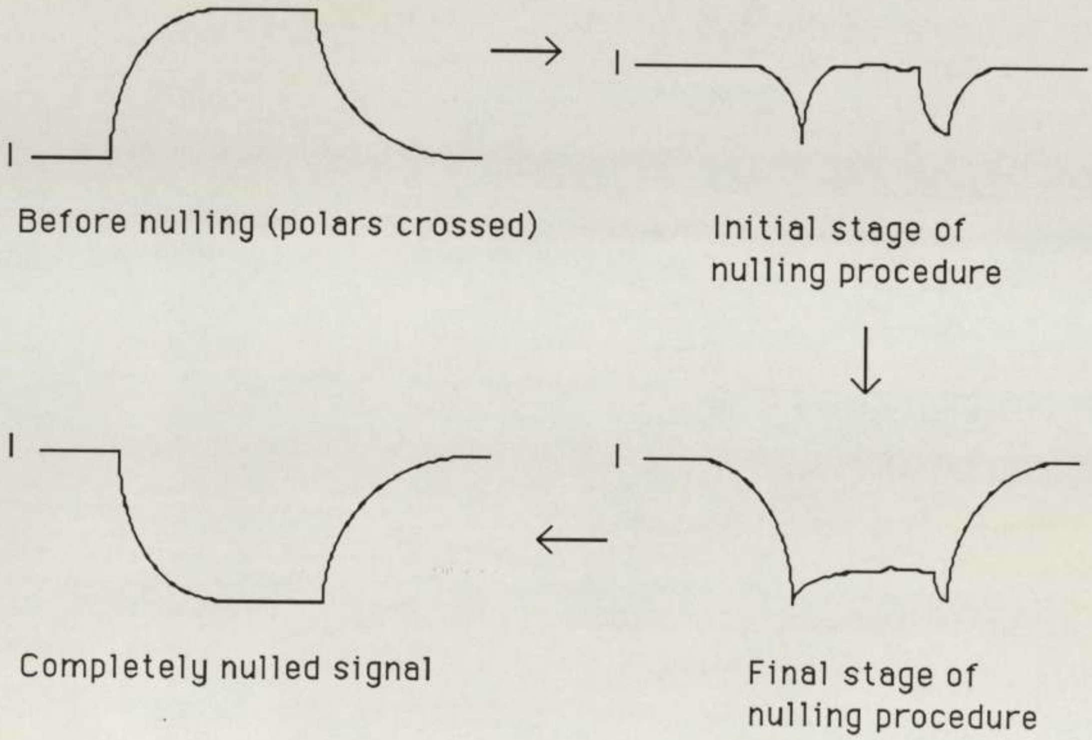

Before nulling (polars crossed)

Initial stage of
nulling procedure

Completely nulled signal

Final stage of
nulling procedure

Figure 7.9 Optical signal observed at various stages during the simultaneous measurement of birefringence and dichroism using the nulled intensity technique.

7.6 DIELECTRIC PROPERTIES OF SOLUTIONS OF POLYPENTENYLENE-BLOCK-CO-ACETYLENE IN CYCLOHEXANE

7.6.1 Apparatus

The dielectric properties of solutions of polypentenylene-block-co-acetylene in cyclohexane were investigated using the two terminal dielectric cell shown in figure 7.10. The electrodes of the cell were constructed from two concentric metal cylinders. The outer cylinder formed the body of the dielectric cell and was hollow to allow the passage of a coolant. Temperature control was achieved by pumping water through the body of the cell using the Churchill temperature control unit. The inner cylinder was constructed of stainless steel and was electrically isolated from the cell body. The electrode separation was approximately 1mm. The parallel capacitance of the cell was determined by a General Radio 1689 precision RLC digibridge. Electrical connections between the cell and the digibridge were by means of a modified General Radio 1657-9600 extender cable connected to BNC sockets mounted on a sheet of Tufnol. The BNC sockets were connected by 16 guage copper wires to the dielectric cell. An automatic, computer controlled zeroing procedure was performed by the digibridge, with the extender cable in place but not connected to the dielectric cell, to compensate for stray capacitances associated with the cable and connections.

7.6.2 Measurement of Capacitance

The dielectric cell (figure 7.10) was thoroughly cleaned and dried prior to use. The volume (12mls) of the solution under test was then admitted and the temperature allowed to equilibrate. Ten measurements of the parallel capacitance were performed with the bridge set in parallel circuit mode and an average value was recorded for each of sixteen spot frequencies in the range 12Hz to 100KHz. Measurements were performed starting from the highest frequency to minimise the effects of degradation of the sample by electro-chemical processes.

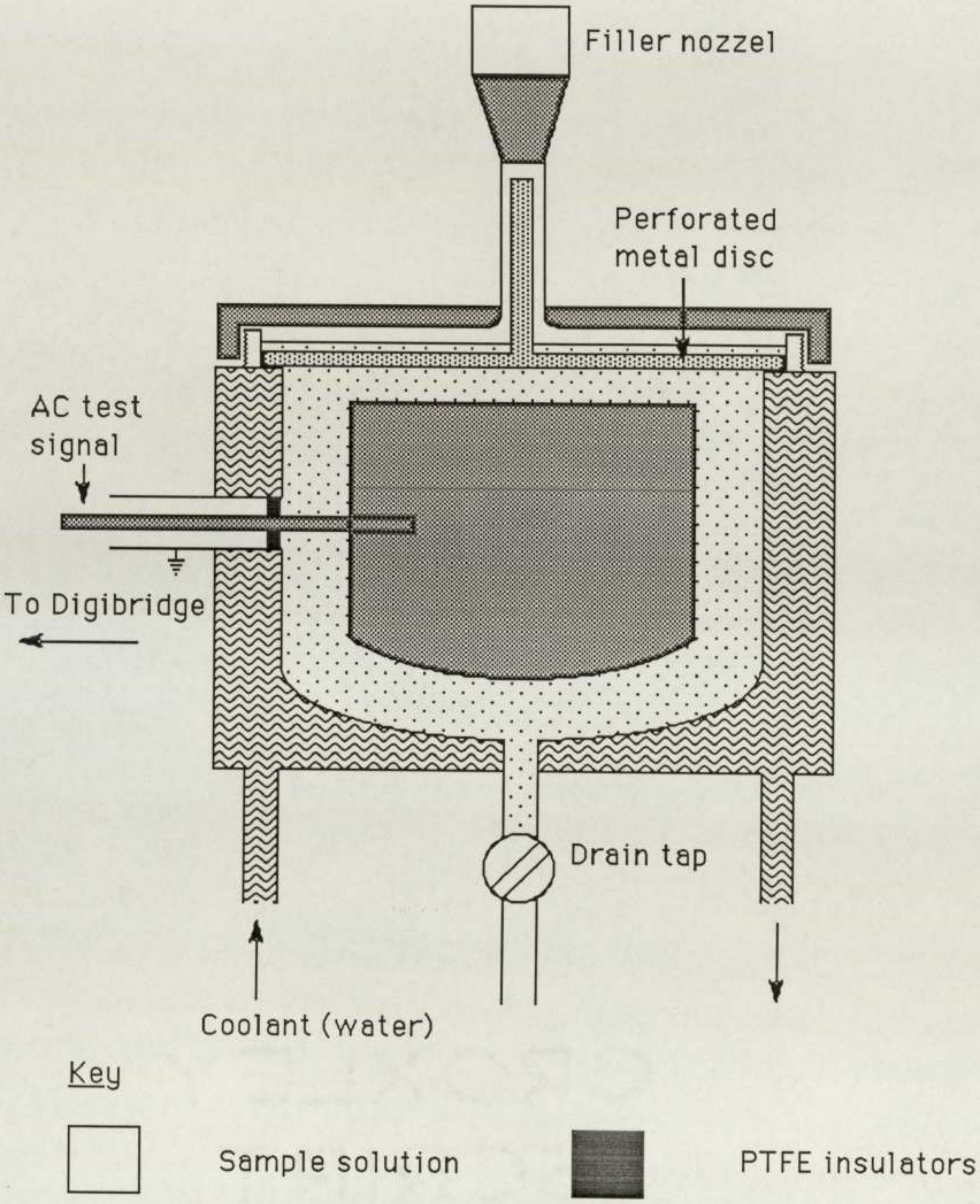

Figure 7.10 The Dielectric Cell

CHAPTER 8

ELECTRO-OPTICAL AND DIELECTRIC RESULTS

8.1 ELECTRIC DICHROISM

The elecrically induced dichroism exhibited by dilute solutions of polypentenylene-block-co-acetylene in cyclohexane was measured using the method described in section 7.4. The intensities of light for the electric field-on (I_V) and the electric field-off (I_o) conditions were measured from the electro-optical traces as shown in figure 7.7. These values are presented in tables 8.1-8.8. An expression relating these measured intensities to the reduced optical dichroism may be derived as follows. If we consider the absorption of a beam of monochromatic plane polarised light, which travels through the Kerr cell such that the plane of polarisation of the light lies parallel to the direction of the applied electric field, then in the absence of the electric field the intensity of the light which is transmitted by the cell (I_2) is given by the Beer-Lambert expression:

$$\log_{10} (I_2/I_1) = -\varepsilon c l = -A \qquad 8.1(a)$$

where I_1 is the intensity of the light incident on the cell which has a length l, and is filled with absorbing material at concentration c. A is the absorbance and ε is the extinction coefficient characteristic of the optical transition. When the plane of polarisation of the incident beam is perpendicular to the direction of the applied electric field, a similar expression characterises the light which is transmitted by the cell, I'_2,

$$\log_{10} (I'_2/I'_1) = -\varepsilon c l = -A \qquad 8.1(b)$$

where I'_1 is the intensity of the incident beam. In the presence of an electric field, when the plane of polarisation of the incident beam is set parallel to the direction of the electric field, the intensity of the light which leaves the cell is $I_{||}$. The absorbance, $A_{||}$, is then given by

$$A_{||} = \log I_1 - \log I_{||} \qquad 8.2$$

Similarly, when the plane of polarisation of the incident beam of light lies perpendicular to the direction of the electric field, the intensity of the light which is transmitted by the Kerr cell is $I_{\perp}$ and the absorbance $A_{\perp}$ is given by

$$A_{\perp} = \log I'_1 - \log I_{\perp} \qquad 8.3$$

From equations 8.1(a) and 8.2,

$$\begin{aligned} A_{||} - A &= \log I_1 - \log I_{||} + \log I_2 - \log I_1 \\ &= \log I_2 - \log I_{||} \qquad 8.4 \end{aligned}$$

similarly from equations 8.1(b) and 8.3,

$$\begin{aligned} A_{\perp} - A &= \log I'_1 - \log I_{\perp} - \log I'_1 + \log I'_2 \\ &= \log I'_2 - \log I_{\perp} \qquad 8.5 \end{aligned}$$

It follows from equations 8.4 and 8.5 that

$$A_{||} = A + \log (I_2 / I_{||}) \qquad 8.6$$

and $$A_{\perp} = A + \log (I'_2 / I_{\perp}) \qquad 8.7$$

If these expressions are used to calculate $A_{||}$ and $A_{\perp}$ from the recorded electro-optical traces then, for measurement in the direction parallel to that of the applied electric field, $I_{||} \equiv I_v$ (the field-on light-level) and $I_2 = I_o$ (the field-off light-level). Similarly for measurement in the perpendicular direction, $I_{\perp} \equiv I_v$ and $I'_2 = I_o$. The dichroism, ΔA, and reduced dichroism, $\Delta A/A$, can now be readily calculated using

$$\Delta A = A_{||} - A_{\perp} \qquad 8.8$$

and

$$\Delta A/A = (A_{||} - A_{\perp}) / A \qquad 8.9$$

The computer program "Calculation of dichroism" (Appendix 2) was used to evaluate $A_{||}$, $A_{\perp}$, ΔA and $\Delta A/A$ using equations 8.6 - 8.9, respectively. The data required by the program were the field-on (I_v) and field off (I_o) intensities of light recorded for both the parallel and the perpendicular orientation of the polariser and the absorbance, A, of the solution.

Since an electric field has axial symmetry (section 6.2), the parallel and perpendicular dichroisms are related to one another by equation 6.9. Therefore, in principle, the electric dichroism of a sample can be calculated directly from the electro-optical traces recorded with the plane of polarisation of the polariser set either parallel or perpendicular to the direction of the applied electric field. It is therefore not necessary to measure both $A_{||}$ and $A_{\perp}$ to obtain ΔA and $\Delta A/A$.

The computer program "Calculation of dichroism" also calculated $A_{\perp}$ using experimentally determined values $A_{||}$ and A (equation 6.10). The resulting value of $A_{\perp}$ could be compared with that obtained using equation 8.7. When only the parallel intensities of light were available, this program could be requested to calculate the dichroism and reduced dichroism using the $A_{\perp}$ value obtained by substituting the experimental values of $A_{||}$ and A into equation 6.10. Tabulated values of the reduced dichroism calculated in this manner are indicated as originating from a single "parallel measurement", whereas those obtained using two pairs of intensities of light, $I_{||}$ and $I_{\perp}$, indicated as "parallel and perpendicular" measurement. In the latter case, only the intensities of light measured in the perpendicular direction are shown in the tables, because the light-levels recorded in the parallel direction are identical to the values shown in the tables of data for the "parallel measurements". Tables 8.1-8.8 show the electric dichroism response of solutions of polypentenylene-block-co-acetylene for the concentration range 0.65-1.80% w/v at 298K, measured using both "parallel" and "parallel and perpendicular" methods. The intensities of light are expressed as light-levels in arbitary units of millimeters corresponding to the values measured from the optical transient curves produced by the transient recorder (see section 7.2.7).

The dependence of the reduced dichroism on the strength of the applied electric field and on the square of the electric field strength for solutions of copolymer at various concentrations at 298K is shown in figures 8.1 to 8.8.

Table 8.1 Electrically-induced dichroism of polypentenylene-block-co-acetylene (0.65 % w/v copolymer in cyclohexane). Parallel measurement

Voltage (V)	Light level Field on (mm)	Light level Field off (mm)	Reduced Dichroism (ΔA /A)
119	35.5	72	0.318
200	49.5	76	0.199
300	44	76	0.254
400	33	62	0.293
1008	14.5	36	0.423

Table 8.2 Electrically-induced dichroism of polypentenylene-block-co-acetylene (0.65 % w/v copolymer in cyclohexane). Parallel and perpendicular measurement

Voltage (V)	Light level Field on (mm)	Light level Field off (mm)	Reduced Dichroism (ΔA /A)
200	38.5	31.5	0.195
400	42	30.5	0.294
1000	42	26.5	0.424

Table 8.3 Electrically-induced dichroism of polypentenylene-block-co-acetylene (1.05% w/v copolymer in cyclohexane). Parallel measurement

Voltage (V)	Light level Field on (mm)	Light level Field off (mm)	Reduced Dichroism (ΔA /A)
50	92	105.5	0.032
100	58	92	0.109
150	45.5	90.5	0.163
201	33.5	84	0.218
250	33.5	93	0.242
300	34	120	0.299
350	30.5	125	0.334
400	27	98.5	0.307
450	27.5	104.5	0.316
500	23.5	100	0.343
600	26	119	0.361
800	22	119	0.400
1000	18	116	0.442

Table 8.4 Electrically-induced dichroism of polypentenylene-block-co-acetylene (1.05% w/v copolymer in cyclohexane). Parallel and perpendicular measurement

Voltage (V)	Light level Field on (mm)	Light level Field off (mm)	Reduced Dichroism (ΔA /A)
200	50.5	33	0.212
400	62	33	0.304
600	79	32	0.384
1000	81	33	0.436

Table 8.5 Electrically-induced dichroism of polypentenylene-block-co-acetylene (1.58% w/v copolymer in cyclohexane). Parallel measurement

Voltage (V)	Light level Field on (mm)	Light level Field off (mm)	Reduced Dichroism ($\Delta A / A$)
150	31	95	0.165
202	23.5	95.5	0.207
250	18	94.5	0.244
300	12.5	79	0.272
350	11.5	83.5	0.292
400	9.5	81	0.316
450	9.5	83.5	0.321
500	7.5	78.5	0.346
600	6.5	94.5	0.395
700	6	94.5	0.407
800	5	86.5	0.421
900	4	81.5	0.445
1002	4	90.5	0.460

Table 8.6 Electrically-induced dichroism of polypentenylene-block-co-acetylene (1.58% w/v copolymer in cyclohexane). Parallel and perpendicular measurement

Voltage (V)	Light level Field on (mm)	Light level Field off (mm)	Reduced Dichroism ($\Delta A / A$)
200	87	42.0	0.209
400	72	22.0	0.327
600	91	22.5	0.368
1000	125.5	24.0	0.470

Table 8.7 Electrically-induced dichroism of polypentenylen-block-co-acetylene (1.80% w/v copolymer in cyclohexane). Parallel measurement

Voltage (V)	Light level Field on (mm)	Light level Field off (mm)	Reduced Dichroism ($\Delta A/A$)
100	12.5	33.5	0.127
150	9.5	36	0.171
200	12	65	0.217
250	8.5	63.5	0.259
300	6.5	58.5	0.283
500	3.5	51	0.345
1000	2	52.5	0.421

Table 8.8 Electrically-induced dichroism of polypentenylene-block-co-acetylene (1.80% w/v copolymer in cyclohexane). Parallel and perpendicular measurement

Voltage (V)	Light level Field on (mm)	Light level Field off (mm)	Reduced Dichroism ($\Delta A/A$)
100	110	64	0.131
150	117	54.5	0.180
200	137	56	0.222
250	108	37	0.265
300	116	35	0.292
500	145	33	0.357
1000	105.5	12.5	0.464

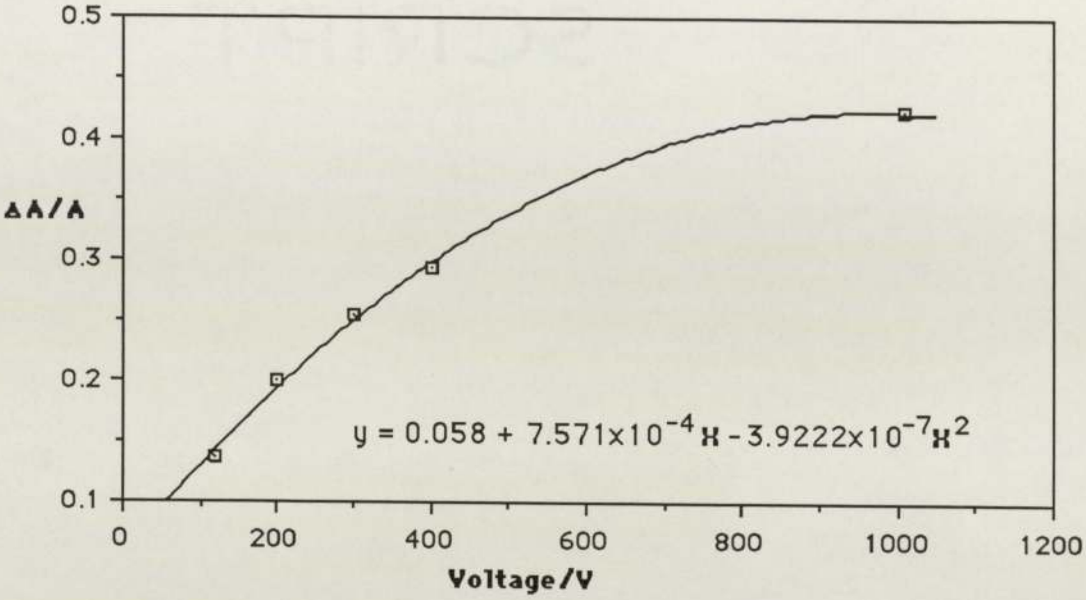

Figure 8.1 Electrically-induced dichroism vs. applied voltage

(0.65% w/v copolymer in cyclohexane)

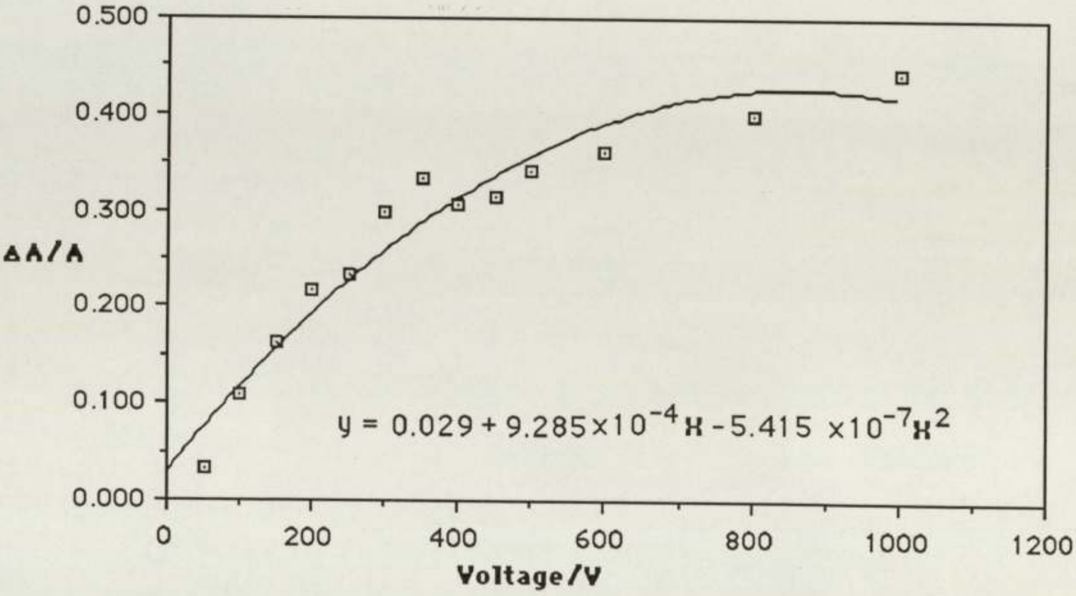

Figure 8.2 Electrically-induced dichroism vs. applied voltage

(1.05% w/v copolymer in cyclohexane)

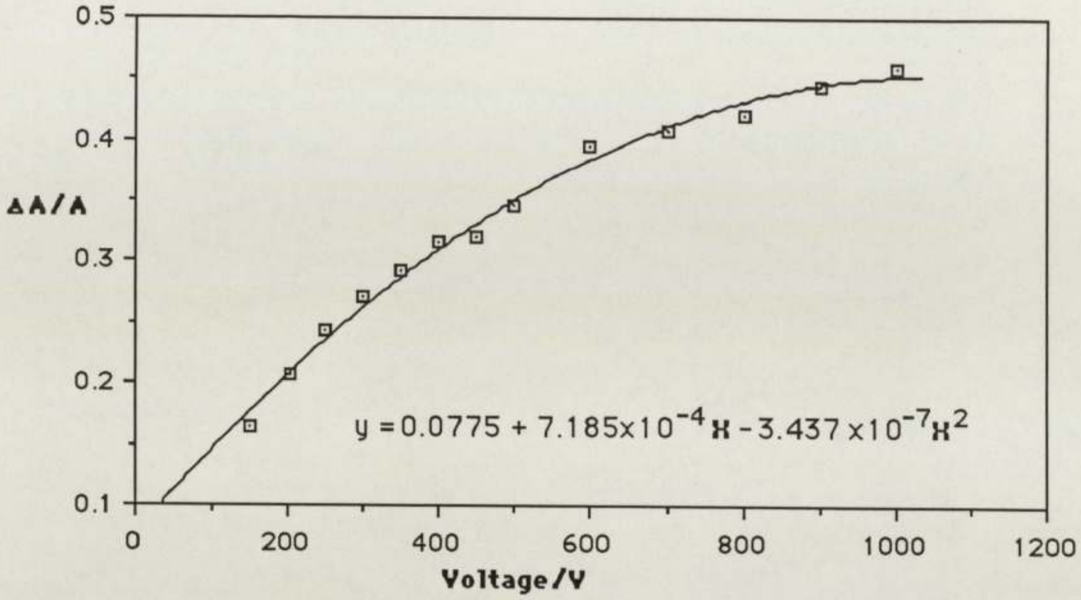

Figure 8.3 Electrically-induced dichroism vs. applied voltage

(1.58% w/v copolymer in cyclohexane)

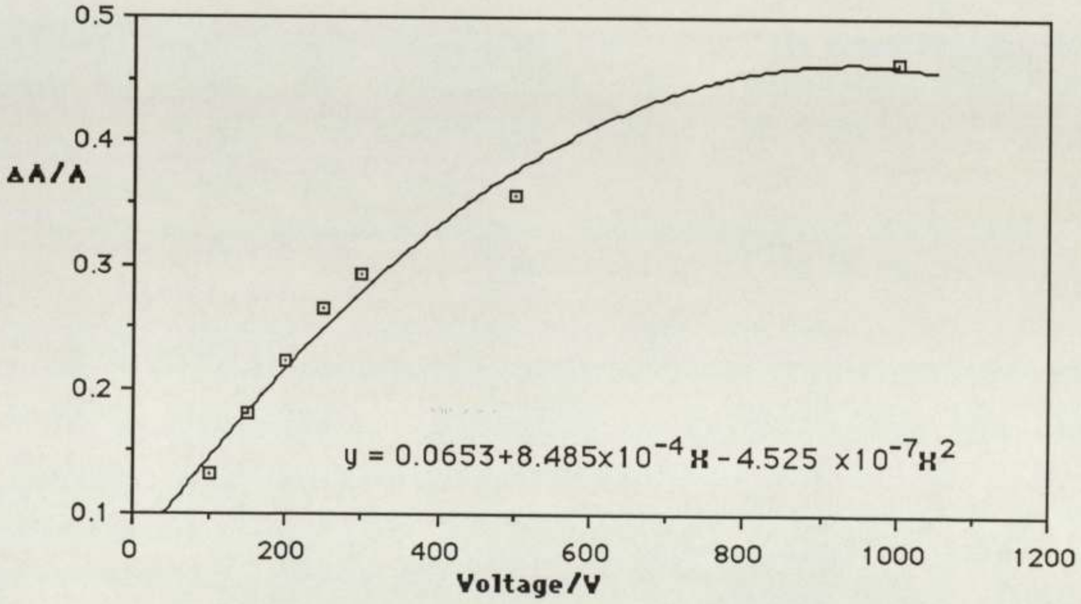

Figure 8.4 Electrically-induced dichroism vs. applied voltage

(1.80% w/v copolymer in cyclohexane)

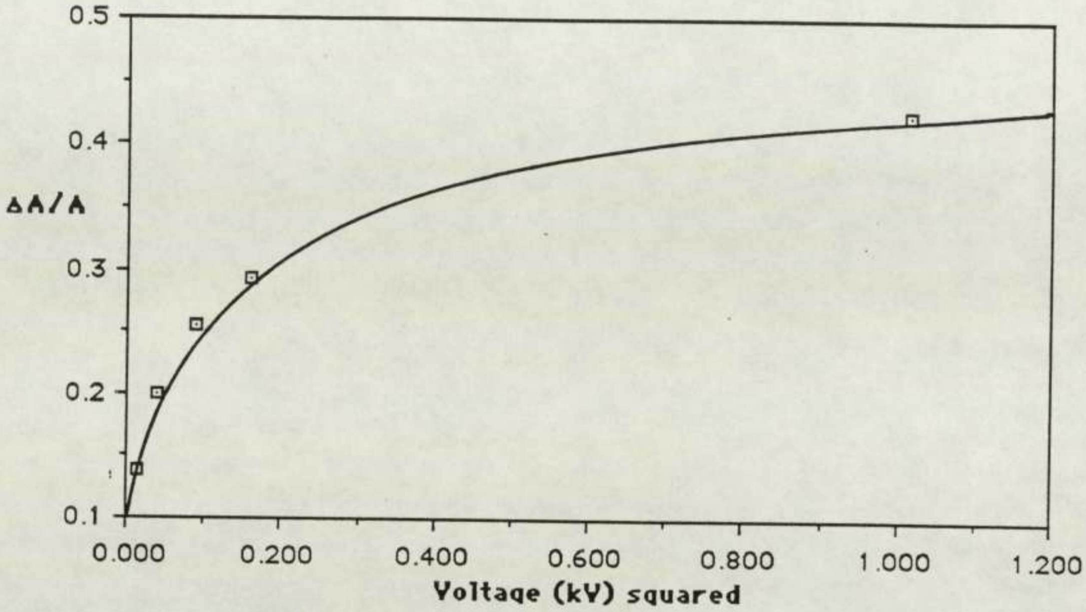

Figure 8.5 Electrically-induced dichroism vs. square of the applied voltage (0.65% w/v copolymer in cyclohexane)

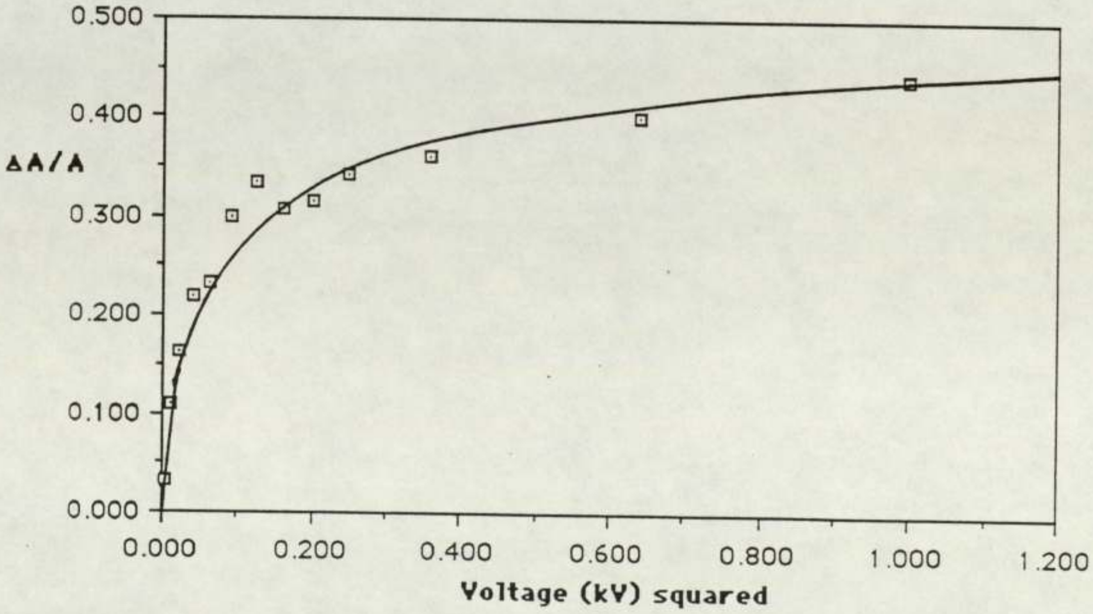

Figure 8.6 Electrically-induced dichroism vs. square of the applied voltage (1.05% w/v copolymer in cyclohexane)

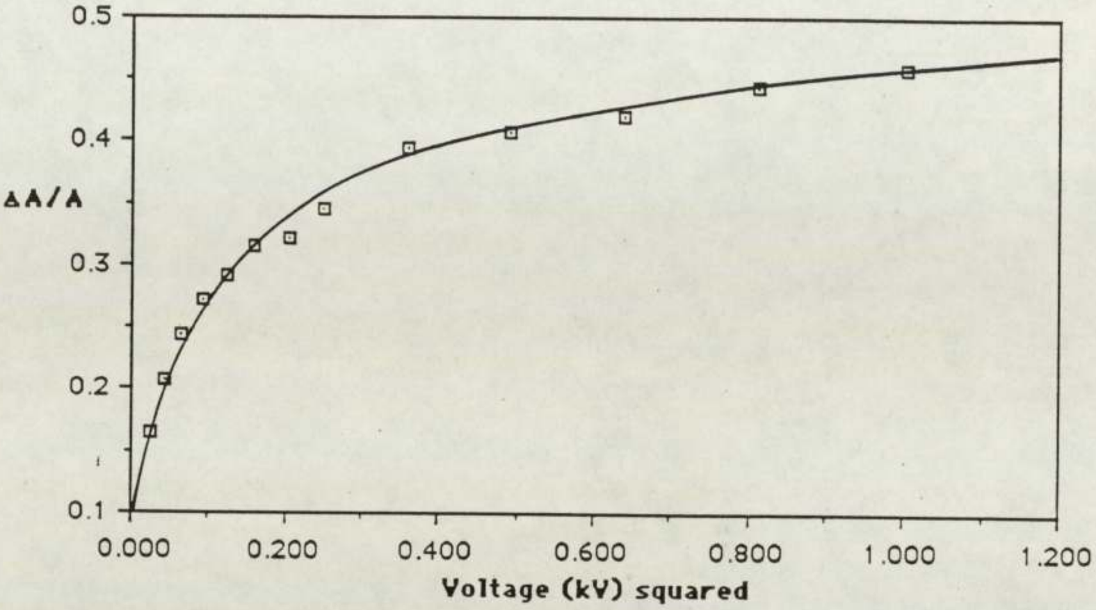

Figure 8.7 Electrically-induced dichroism vs. square of the applied voltage (1.58% w/v copolymer in cyclohexane)

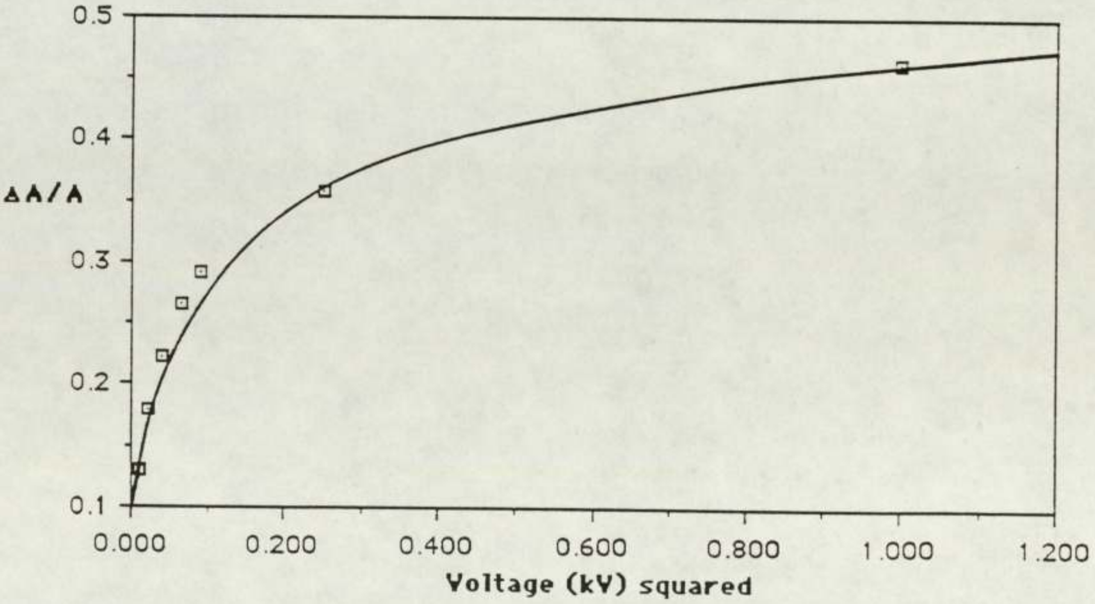

Figure 8.8 Electrically-induced dichroism vs. square of the applied voltage (1.80% w/v copolymer in cyclohexane)

8.2 ELECTRICALLY INDUCED BIREFRINGENCE MEASURED USING THE CORRECTED LIGHT-INTENSITY METHOD

The electrically-induced birefringences of solutions of polypentenylene-block-co-acetylene were evaluated from the transmitted intensities of light recorded using the optical arrangement described in section 7.5.1. The entries in tables 8.9-8.11 are the field-on and field-off intensities of light measured from the chart recorder traces, obtained with the quarter-wave plate oriented with its slow axis parallel to the direction of the applied electric field.

Table 8.9 Electrically-induced birefringence of polypentenylene-block- co-acetylene (0.65% w/v copolymer in cyclohexane)

Voltage (V)	Light level Field on (mm)	Light level Field off (mm)	Phase retardation (δ) Degrees
108	92.5	106.5	5.16
151	93	114	8.29
202	69	91	11.99
250	64.5	89.5	14.65
302	65.5	94	16.59
350	60.5	89	18.17
401	65.5	98	19.47
452	69	104	20.37
501	66.5	101	21.29
600	107.5	164	22.59
700	79	134.5	28.94
800	79.5	141	31.72
905	74	132	32.48
1000	73	133.5	33.72

Figure 8.10 Electrically-induced birefringence of polypentenylene-block-co-acetylene

(1.05% w/v copolymer in cyclohexane)

Voltage (V)	Light level Field on (mm)	Light level Field off (mm)	Phase retardation (δ) Degrees
50	63	72.5	5.05
100	44.5	62.5	15.29
151	43.5	69	22.45
202	41.5	68	26.49
250	43	68.5	28.17
301	44	72	33.54
351	44.5	71	36.56
401	40.5	59.5	36.00
450	45.5	68.5	42.58
501	43.5	64	46.2
601	42	58.5	51.65
700	60.5	76	48.87
800	60.5	72.5	47.92
901	41	47.5	44.46
1000	47.5	53.5	38.37

Figure 8.11 Electrically-induced birefringence of polypentenylene-block-co-acetylene (1.58% w/v copolymer in cyclohexane)

Voltage (V)	Light level Field on (mm)	Light level Field off (mm)	Phase retardation (δ) Degrees
150	16.5	25.5	34.00
197	31.5	45.5	37.88
250	37	48	40.82
302	50.5	57	40.27
350	61.5	60.5	37.25
404	72.5	63	35.45
450	71	57	36.25
504	78	57.5	37.14
602	37.5	23.5	32.37
700	44.5	24.5	26.82
803	55	27	17.72
900	57	25.5	5.14
1002	66	28.5	1.41

Under these conditions, the measured intensities of light may be described as composite intensities since they are comprised of contributions from both dichroism and birefringence. These composite intensities of light are related to the parallel, perpendicular and normal absorbances, $A_{||}$, $A_{\perp}$, and A and to the induced phase retardation δ by equation 6.25. Rearrangement of this equation gives:

$$\sin\delta = 2 \times [(\Delta I/I) + 1] - 10^{(A-A_{||})} - 10^{(A-A_{\perp})} / -2 \times 10^{\{A - (A_{||} + A_{\perp})/2\}} \quad 8.10$$

where $\Delta I = I_v - I_o$ and $I = I_o$.

The values of the phase retardation, δ, shown in tables 8.9 to 8.11 were obtained by solving equation 8.10 using the computer program "Kerr Effect plus

Dichroism" (see appendix 2). Values of the parallel and perpendicular absorbances ($A_{||}$ and $A_{\perp}$), required as input by the program, were obtained from a separate measurement of the electrically-induced dichroism using the technique described in section 7.4. In principle, the changes in the intensity of light (due to dichroism) measured for voltages corresponding to those employed in the composite (birefringence and dichroism) measurements, could be used in conjunction with equations 8.6 and 8.7 to calculate $A_{||}$ and $A_{\perp}$. However errors associated with the intensities of light, voltage settings and absorbances may result in large errors in the calculated values of δ. To minimise the effects of these errors, the following procedure was adopted. The reduced dichroism (tables 8.1 to 8.8) was plotted as a function of the applied voltage, V (figures 8.1 to 8.4) and an Apple Macintosh computer curve fitting routine was used to obtain the "curve of best fit" for a second order polynomial of the form

$$\Delta A/A = a.V + b.V^2 + c \qquad 8.11$$

A subroutine of the program "Kerr Effect plus dichroism" evaluated equation 8.11 using the values of the constants a, b and c obtained from the curve fitting procedure described above. By this method, a value of the reduced dichroism could be generated for the exact voltage at which the composite (birefringence + dichroism) light-levels were recorded. Values of the parallel ($A_{||}$) and perpendicular ($A_{\perp}$) dichroisms were then calculated from the reduced dichroism ($\Delta A/A$) in the following manner: Substitution of the expressions obtained earlier for $A_{||}$ and $A_{\perp}$ (equations 6.10 and 6.11) into equation 8.9 give,

$$\Delta A/A = [(3A-2A_{\perp}) - A_{\perp}]/A \qquad 8.12$$

and $$\Delta A/A = [A_{||} -(3A - A_{||})/2]/A \qquad 8.13$$

which, after rearranging yield

$$A_{\perp} = A - (\Delta A/A)\,A/3 \qquad 8.14$$

$$\text{and } A_{||} = A + 2(\Delta A/A)\,A/3 \qquad 8.15$$

Values of $A_{||}$ and $A_{\perp}$ obtained from this curve fitting procedure were then substituted into equation 8.10 along with the measured composite intensities of light, to obtain the electrically induced phase retardation, δ.

The dependence of δ upon the square of the applied voltage for three concentrations of copolymer is shown in figures 8.9 to 8.11.

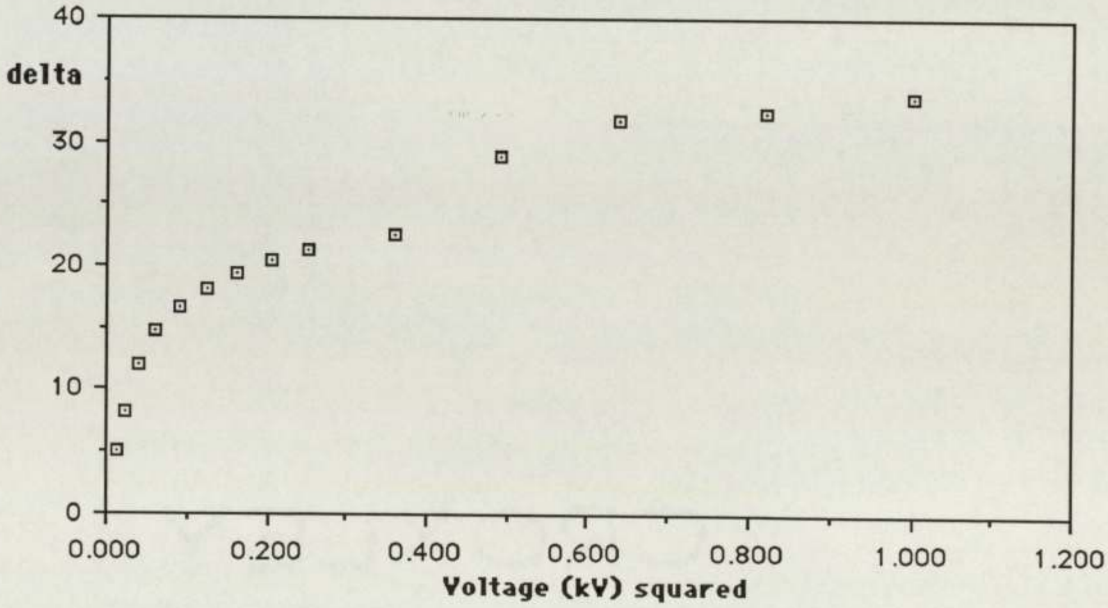

Figure 8.9 Electrically-induced phase retardation vs the square of the applied voltage (0.65% w/v solution of copolymer in cyclohexane).

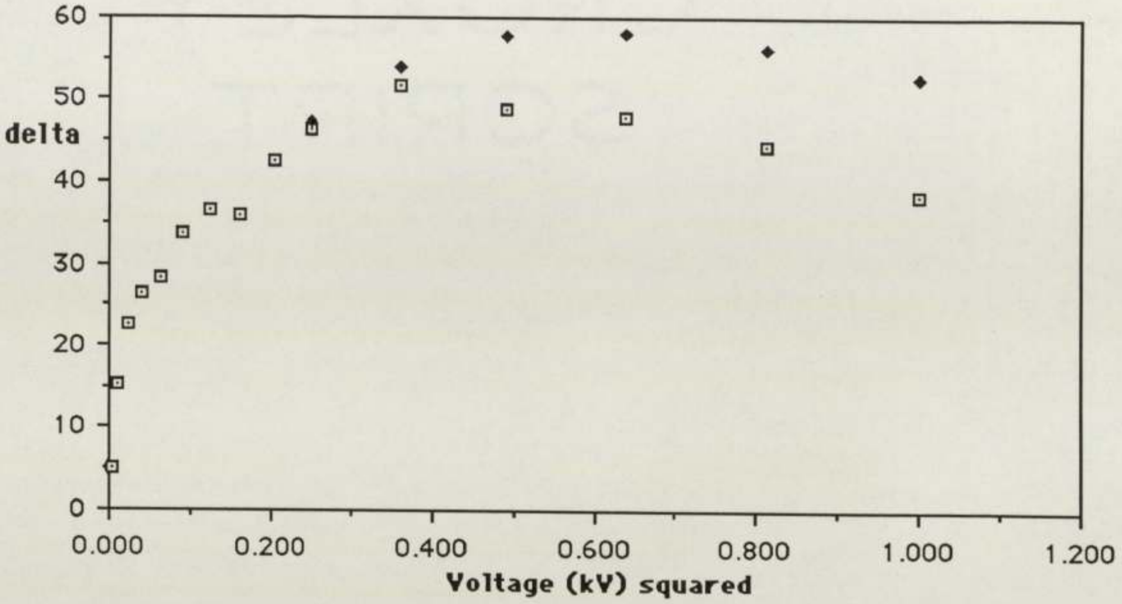

Figure 8.10 Electrically-induced phase retardation vs the square of the applied voltage

(1.05% w/v solution of copolymer in cyclohexane)

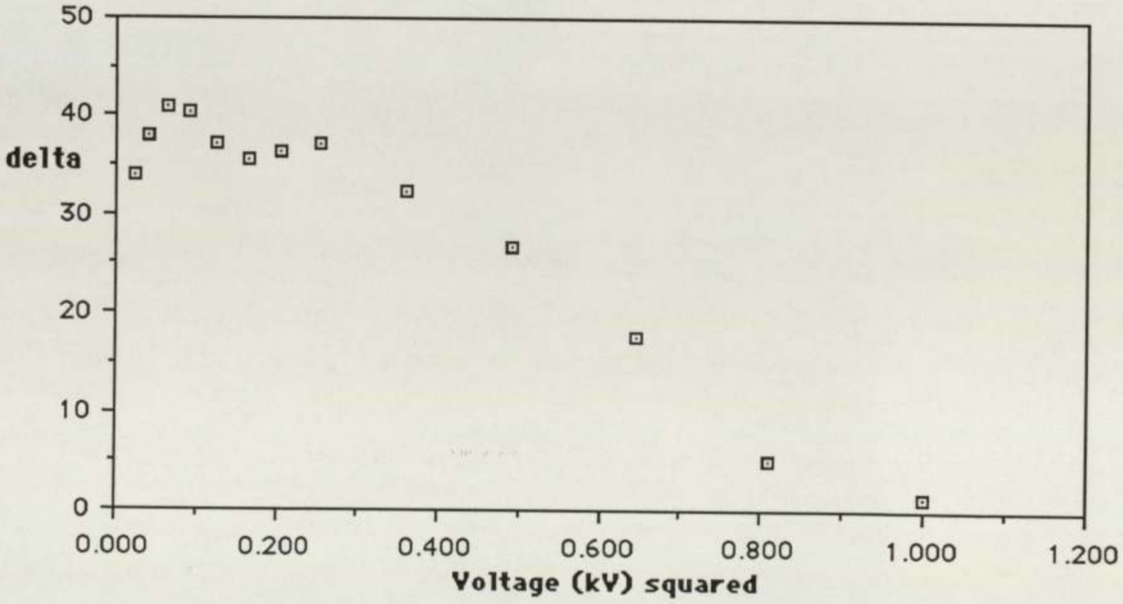

Figure 8.11 Electrically-induced phase retardation vs the square of the applied voltage

(1.58% w/v solution of copolymer in cyclohexane)

Figure 8.9 (low concentration of copolymer) shows significant departure from the quadratic Kerr law similar in magnitude to that observed for the reduced dichroism (figures 8.1 to 8.8). Figure 8.10 shows an apparent decrease in the magnitude of delta with increasing field strengths at high-voltages. When the transients corresponding to these measurements were examined it was noticed that the 'equilibrium' light level as judged by the output voltage of the photomultiplier, did not remain constant throughout the duration of the electric pulse. The shape of the transients suggested that some anomalous process was occurring, perhaps an overloading of the photomultiplier, which was affecting the linearity of the signal produced by the device. This effect could be minimised in the case of the 1.05% w/v sample by taking the equilibrium light-level to be that attained in the initial region of the optical pulse. These light-levels are shown in table 8.12, which when plotted against the square of the applied voltage (points marked with the symbol ♦ in figure 8.10) show non-quadratic behaviour similar to that observed in the plots of the reduced dichroism (Figures 8.1 to 8.4).

Table 8.12 Revised birefringence calculated from observed transients

Voltage (V)	Light level Field on (mm)	Light level Field off (mm)	Phase retardation (δ) Degrees
501	43	64	47.15
601	41	58.5	54.10
700	56	76	57.64
800	55.5	72.5	58.22
901	37	47.5	56.34
1000	41.5	53.5	52.62

Figure 8.11 shows very large departures from Kerr law behaviour and the variation of δ with the square of the applied voltage does not resemble that obtained for

the dichroism. Even at low voltages, a consideration of the shape of the transients indicated that correction of the light signals to calculate the phase retardation, was not possible. It seems reasonable to concluded that some distortion of the signal generated by the photomultiplier is occurring as a result of the high intensities of light generated by the combined effects of birefringence and dichroism. The measurement of birefringence using the corrected light intensity method, does not appear feasible for the range of solutions of polypentenylene-block-co-acetylene considered in the present study.

8.3 ELECTRIC BIREFRINGENCE MEASURED USING THE NULLED INTENSITY METHOD

The nulled intensity method described in section 7.5.2 was used to determine simultaneously the reduced dichroism and the electrically-induced phase retardation (birefringence) of solutions of copolymer. For a series of increasing voltages, the polarisers P_1 and P_2 were rotated to positions where the intensity of light emitted by P_2 was minimised. At this "null point", the angular positions of the polarisers P_1 and P_2, relative to their crossed positions in the absence of the electric field, were recorded. The results of measurements obtained for four concentrations of copolymer are shown in tables 8.13 to 8.16

Table 8.13 Simultaneous measurement of birefringence and dichroism using the nulled intensity method (0.65% w/v copolymer in cyclohexane)

Voltage (V)	P(1) angle degrees	P(2) angle degrees	α angle degrees	β angle degrees	δ degrees	$\Delta A/A$
0	43.5	174.7				
152	55	165.7	9	11.5	18	0.226
200	56.5	164	10.7	13	21.4	0.258
252	58	163	11.7	14.5	23.4	0.290
305	58.5	162.8	11.9	15	23.8	0.301
350	59	162.1	12.6	15.5	25.2	0.313
400	59.75	161.4	13.3	16.25	26.6	0.330
500	63	160	14.7	19.5	29.4	0.406

Table 8.14 Simultaneous measurement of birefringence and dichroism using the nulled intensity method (1.05% w/v copolymer in cyclohexane)

Voltage (V)	P(1) angle degrees	P(2) angle degrees	α angle degrees	β angle degrees	δ degrees	$\Delta A/A$
0	43	174.4				
97	51	167.4	7	8	14	0.091
151	57	163	11.4	14	22.8	0.163
201	60	160.5	13.9	17	27.8	0.203
251	62	158.7	15.7	19	31.4	0.230
303	64	156.7	17.7	21	35.4	0.260
360	66.5	153	21.4	23.5	42.8	0.299
400	68	152.7	21.7	25	43.4	0.325
450	70	149.9	24.5	27	49	0.361
500	70.5	148.5	25.5	27.5	51	0.371
600	71.5	147.2	27.2	28.5	54.4	0.391
800	74	144.1	30.3	31	60.6	0.446

Table 8.15 Simultaneous measurement of birefringence and dichroism using the nulled intensity method (1.28% w/v copolymer in cyclohexane)

Voltage (V)	P(1) angle degrees	P(2) angle degrees	α angle degrees	β angle degrees	δ degrees	ΔA/A
0	222.5	175				
100	235	167.5	7.5	12.5	15	0.112
200	243.5	159	16	21	32	0.202
300	249	153.5	21.5	26.5	43	0.274
400	251.5	148.5	26.5	29	53	0.312
500	253	147	28	30.5	56	0.338
600	254.5	146.5	28.5	32	57	0.366
700	255.5	142	33	33	66	0.387

Table 8.16 Simultaneous measurement of birefringence and dichroism using the nulled intensity method (1.43% w/v copolymer in cyclohexane)

Voltage (V)	P(1) angle degrees	P(2) angle degrees	α angle degrees	β angle degrees	δ degrees	ΔA/A
0	43	174.5				
203	69	151.3	23.2	26	46.4	0.235
250	72	147.3	27.2	29	54.4	0.276
300	75	143.4	31.2	32	62.2	0.323
350	76	142.1	32.4	33	64.8	0.342
400	77	140	34.5	34	69	0.362
500	78.5	137.1	37.4	35.5	78.4	0.395

At the "null point" the effects of dichroism are compensated by polariser P_1 (section 6.6.4). The angle of rotation of the polariser P_2, relative to the crossed position (V=0) is represented by the angle α which is related to the induced phase retardation, δ, by equation 6.24.

An expression relating the angle of displacement, β, of polariser P_1 from the crossed position, to the reduced dichroism ($\Delta A/A$) was derived as follows. Initially, in the absence of the electric field, the plane of polarisation of the beam of light which propagates through the Kerr cell is at 45^o ($\beta = 0^o$) to the direction of the applied electric field (figure 8.12).

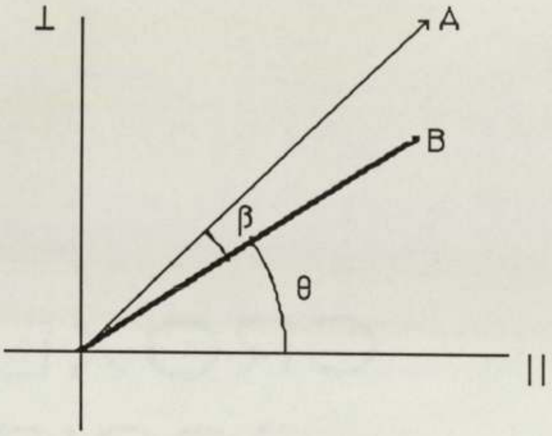

Figure 8.12 View showing the plane of polarisation of polariser P_1, looking down the optical axis. Position A corresponds to orientation of the plane of polarisation of the light which is transmitted at the crossed position, in the absence of the electric field. Position B shows the direction of the plane of polarisation at the null point in the presence of the electric field.

Initially, the wave forms of the components of the beam of light, that propagate in directions parallel and perpendicular to the direction of the electric field, are

$$W_{||} = a_o \sin \omega t \cos 45^o$$

and $$W_{\perp} = a_o \sin \omega t \sin 45^o$$

where a_o is the amplitude of the waveforms. The intensities are given by

$$I_{||} = \int_0^{2\pi/\omega} (W_{||})^2 \, dt = a_o^2 \cos^2 45^o$$

and $$I_{\perp} = \int_0^{2\pi/\omega} (W_{\perp})^2 \, dt = a_o^2 \sin^2 45^o$$

For optical absorption in the presence of the electric field,

$$I_{||} = 10^{-A_{||}} \; a_o^2 \cos^2 45^o$$

and $$I_{\perp} = 10^{-A_{\perp}} \; a_o^2 \sin^2 45^o$$

To compensate for the electrically induced dichroism, the polariser is rotated by an angle β until $I_{||} = I_{\perp}$. For this "null" condition,

$$10^{-A_{||}} \; a_o^2 \cos^2 (45 - \beta)^o = 10^{-A_{\perp}} \; a_o^2 \sin^2 (45 - \beta)^o$$

which simplifies to

$$\tan^2 (45 - \beta) = 10^{-A_{||}} / 10^{-A_{\perp}} = 10^{-\Delta A}$$

$$\Delta A = -2 \log_{10} [\tan \{45^o - \beta\}] \qquad 8.16$$

$$\text{reduced dichroism } (\Delta A/A) = -2 \log_{10} [\tan \{45^o - \beta\}] / A \qquad 8.17$$

The computer program "Calculation of electric dichroism by the nulled intensity method" (appendix 2) was used to calculate the reduced dichroism ($\Delta A/A$) from the measured values of β using equation 8.17.

Values of α, β, δ and $\Delta A/A$ were calculated from the measured polariser angles using the procedures described above and the values obtained for the various solutions of copolymer are listed in tables 8.13 -8.16.

Figures 8.13-8.20 show the dependence of the electro-optical parameters on the square of the applied voltage. The values of reduced dichroism compare well with those presented in figures 8.5 -8.8 which were obtained using the single polariser method (section 8.1). The phase retardation data produces steady curvature in the plots unlike the behaviour observed for the optical response obtained using the corrected light intensity method (section 8.2)

A nulled pulse technique was also used to evaluate the electro-optical properties of toluene, cyclohexane and solutions of polypentenamer in cyclohexane. As none of these materials were found to exhibit dichroic behaviour at the wavelengths of light used in these experiments, the electrically-induced birefringence was readily determined using the nulled pulse method (section 6.6.2). In this method, attainment of the null-point condition is achieved by the rotation of polariser P_2 alone, the plane of polarisation of polariser P_1 remaining at 45° throughout the nulling procedure. The position of the null point is defined as the angular position for which the field-on intensity of light is the same as the intensity of light in the absence of the electric field. Although both polypentenamer and cyclohexane undoubtedly show electrically induced birefringence, the Kerr constants for these materials are small. Consequently, measurable optical signals for these materials could not be obtained even at the highest field strengths (2.5×10^6 V/m). However, the electro-optical Kerr effect for toluene was easily observed and the values of the induced phase retardation were found to obey the Kerr law (figure 8.21).

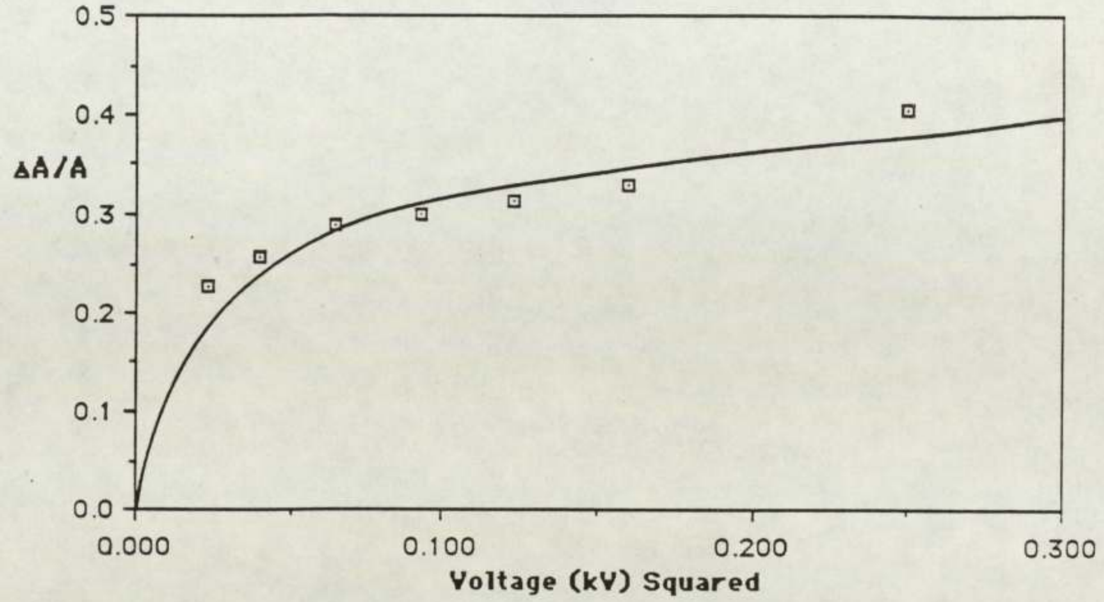

Figure 8.13 Electrically induced reduced dichroism vs square of the applied voltage

(0.68% w/v solution of copolymer in cyclohexane)

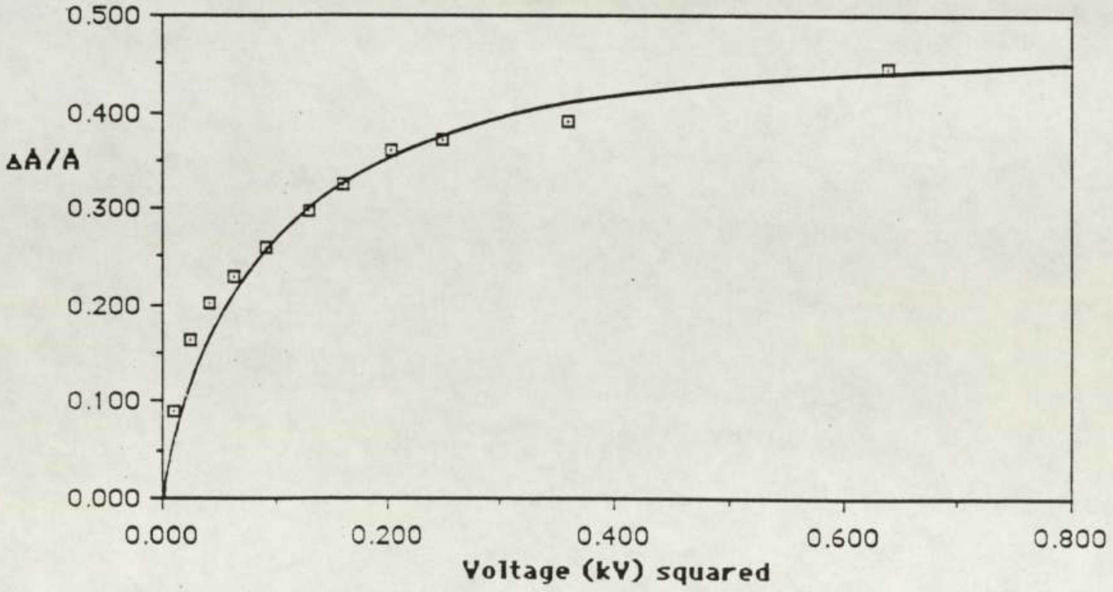

Figure 8.14 Electrically induced reduced dichroism vs square of the applied voltage

(1.05% w/v solution of copolymer in cyclohexane)

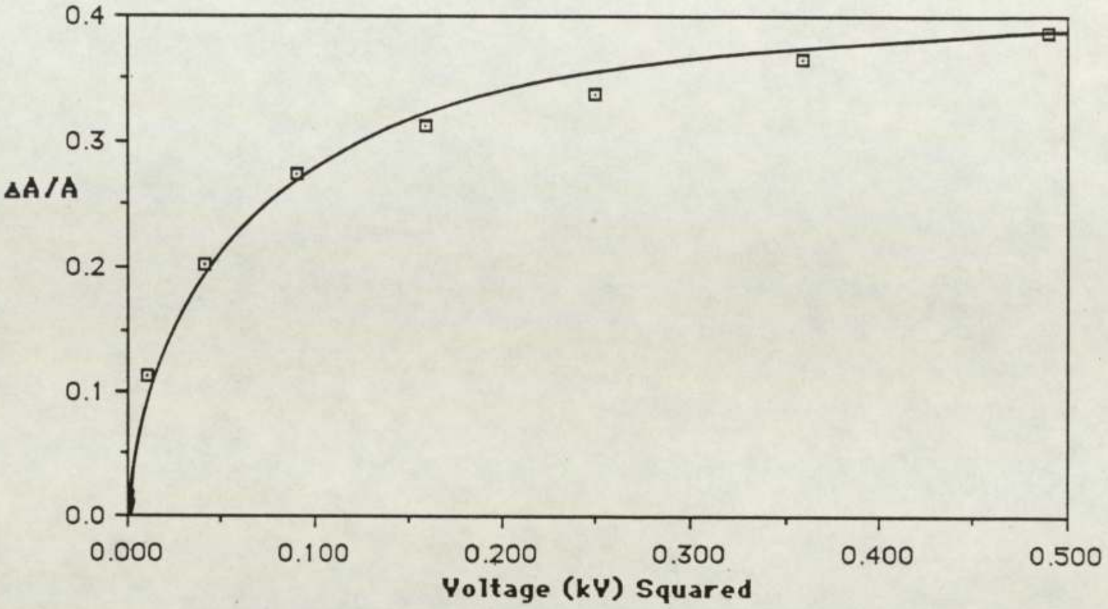

Figure 8.15 Electrically induced reduced dichroism vs square of the applied voltage

(1.28% w/v solution of copolymer in cyclohexane)

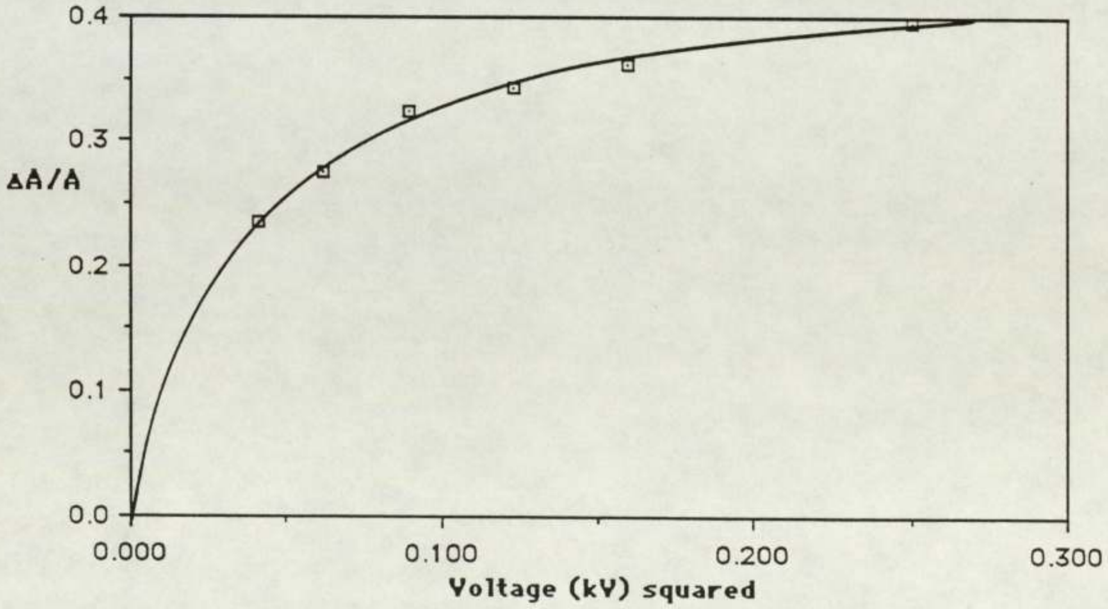

Figure 8.16 Electrically induced reduced dichroism vs square of the applied voltage

(1.43% w/v solution of copolymer in cyclohexane)

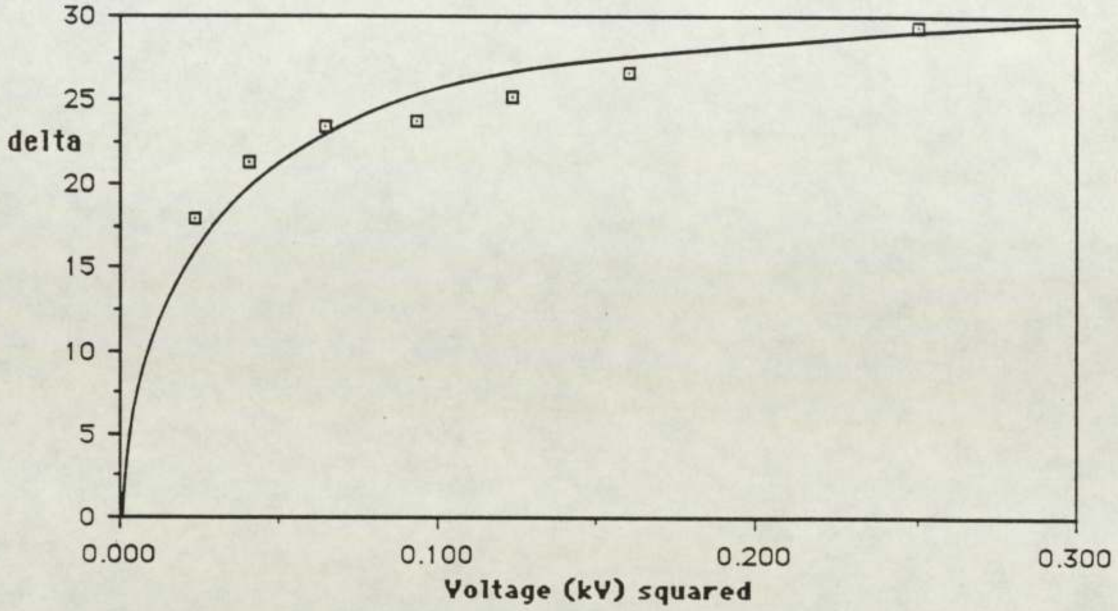

Figure 8.17 Electrically-induced phase retardation (δ) vs square of the applied voltage (0.68% w/v solution of copolymer in cyclohexane)

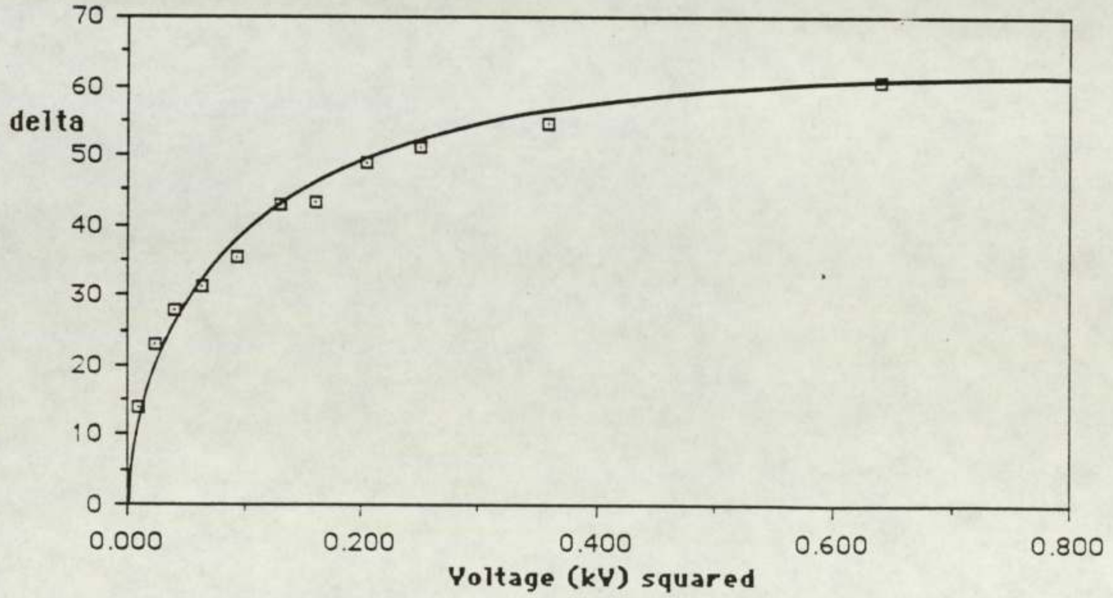

Figure 8.18 Electrically-induced phase retardation (δ) vs square of the applied voltage (1.05% w/v solution of copolymer in cyclohexane)

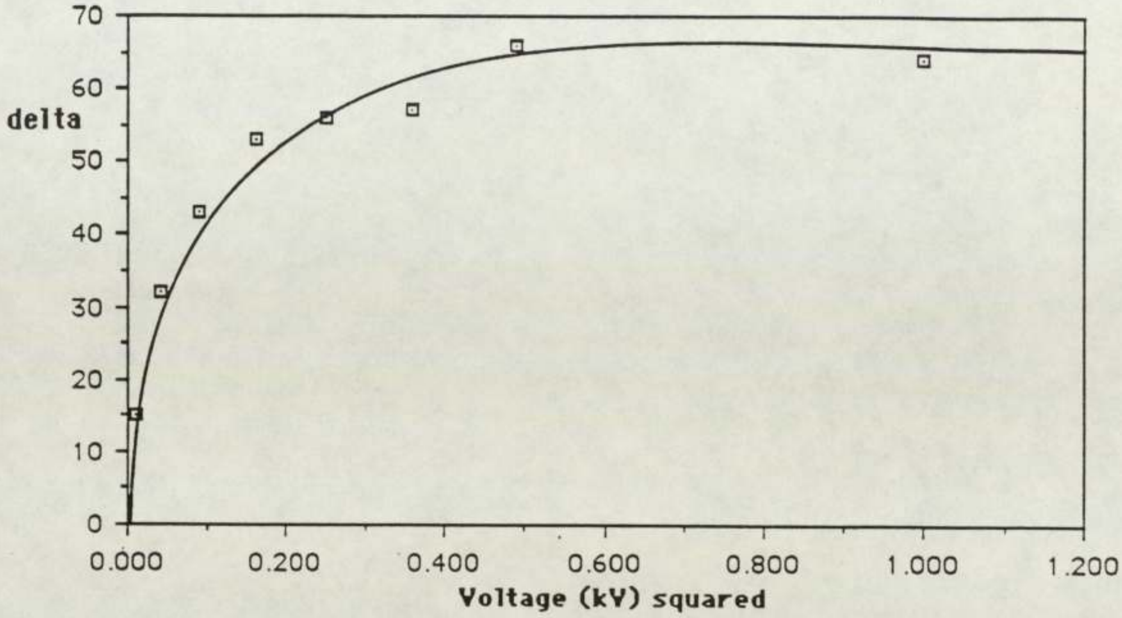

Figure 8.19 Electrically-induced phase retardation (δ) vs square of the applied voltage

(1.28% w/v solution of copolymer in cyclohexane)

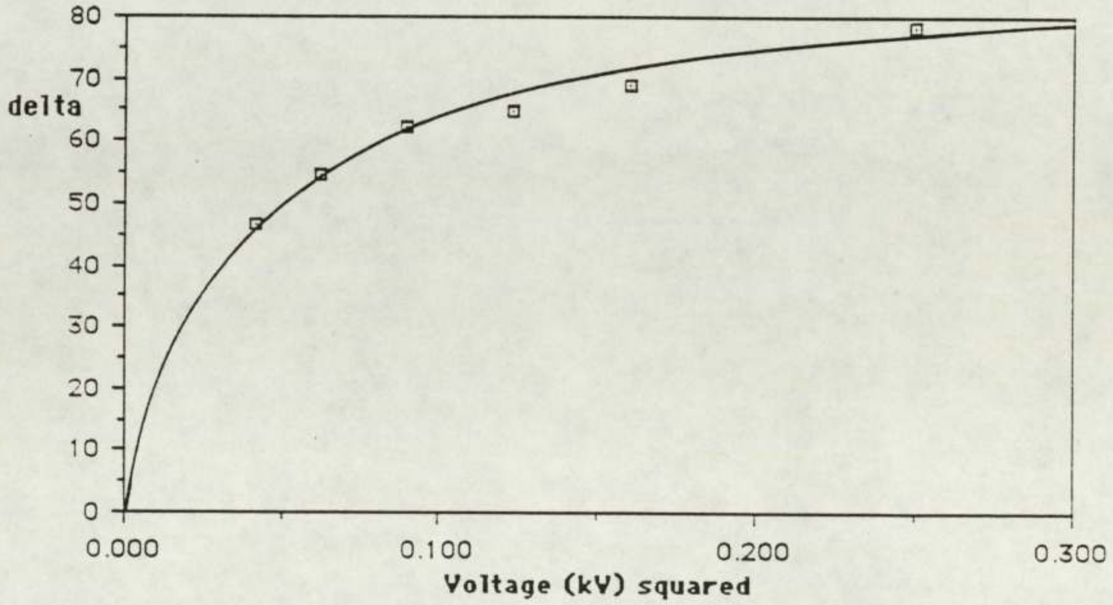

Figure 8.20 Electrically-induced phase retardation (δ) vs square of the applied voltage

(1.43% w/v solution of copolymer in cyclohexane)

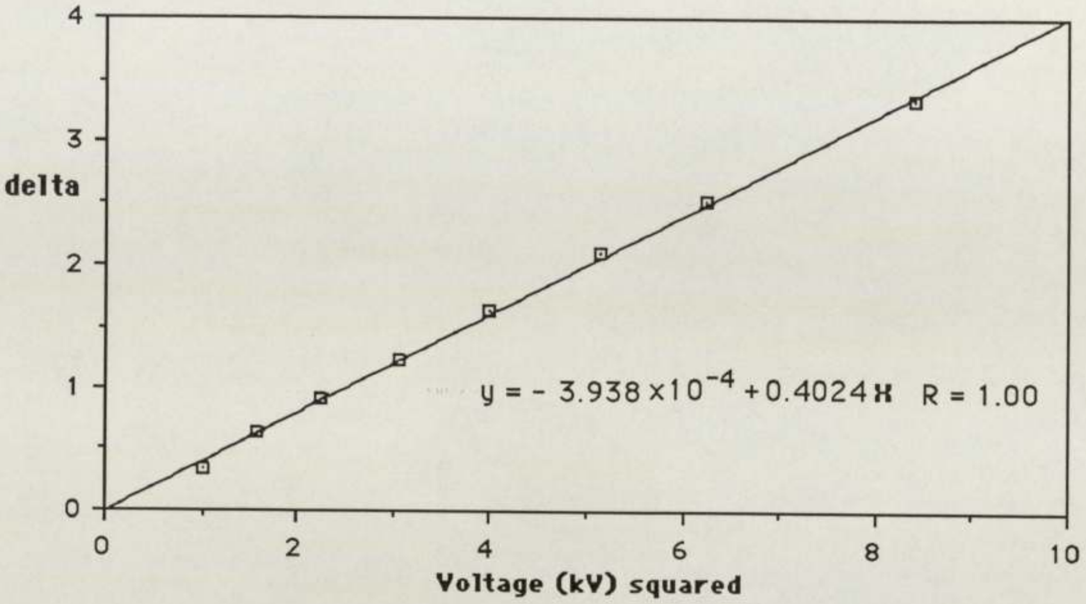

Figure 8.21 Electrically-induced birefringence of toluene vs the square of the applied voltage.

The theory of molecular orientation in an electric field (section 6.2) predicts that at low field strengths, all materials should show a linear dependence of δ on the square of the strength of the applied electric field. The experimental Kerr constant (B_x) of a sample, that obeys the Kerr law, may be determined by comparison of the gradient (M_x) of a plot of δ against the square of the voltage with the gradient (M_s) of a similar plot obtained for a calibrant material of known Kerr constant (B_s). Hence

$$B_x/B_s = M_x/M_s \qquad 8.18$$

The experimental solution Kerr constants (B_{12}) of solutions of copolymer were calculated using values of δ obtained for an applied voltage of 200V and toluene as calibrant ($B_s = 8.57 \times 10^{-15}\ V^{-2}m$). The experimental values (B_{12}) are recorded in table 8.17.

Table 8.17 Experimental Kerr constants, calculated relative to toluene using the initial gradients of plots of delta vs the square of the applied voltage.

w/v% of copolymer in solution in cyclohexane at 298K	Experimental Kerr Constant $B_{12} \times 10^{12} V^{-2} m$ (V = 200V)
0.68	1.8
1.05	2.4
1.28	2.7
1.43	4.0

8.4 DYNAMIC BEHAVIOUR

8.4.1 Analysis of Time Dependent Optical Dichroism

The rise and decay of electrically induced birefringence has been extensively used to probe the shape, size and rotational dynamics of polymer molecules.(170,174,186,187) When the optical arrangement shown in figure 7.6 is used to determine the electric birefringence of a system which exhibits dichroism, the intensity of the light incident on the photomultiplier is comprised of components due to birefringence and dichroism. It is therefore impossible to measure the transient electric birefringence of the system alone by this method. The theory of rotational diffusion shows that the optical transient behaviour of dichroism and birefringence depend on the same time dependent orientational distribution function. The analysis of optical transient dichroism curves may therefore be used to derive parameters related to molecular dimensions and rates of molecular re-orientation (section 6.5).

Dichroism transients were obtained for solutions of copolymer using the method described in section 7.4. The optical transient curves were recorded for variations in the intensity of plane polarised light travelling with its electric vector parallel to the direction of the applied electric field since this arrangement gave the optimum ratio of signal to noise. A labelled schematic dichroism transient is shown in figure 8.22. Since the dichroism is positive the intensity of the light which is transmitted by the optical cell decreases in response to the applied electric field. Thus, the rise transient corresponds to a decrease in the intensity of light transmitted and the decay curve is characterised by a return to the field-off light-level. The optical transient curves were analysed using the following procedure. The zero time points (t=0) were marked on the rise and decay curves. These corresponded to the times when the electric field was applied and removed. The height (h(t) in arbitary units) of the curve from the zero intensity baseline (I=0) was measured at different times (t) along the time axis. Also measured were the minimum (h_{min}) and maximum (h_{max}) light-levels corresponding to field-off and equilibrium field-on conditions respectively (figure 8.22).

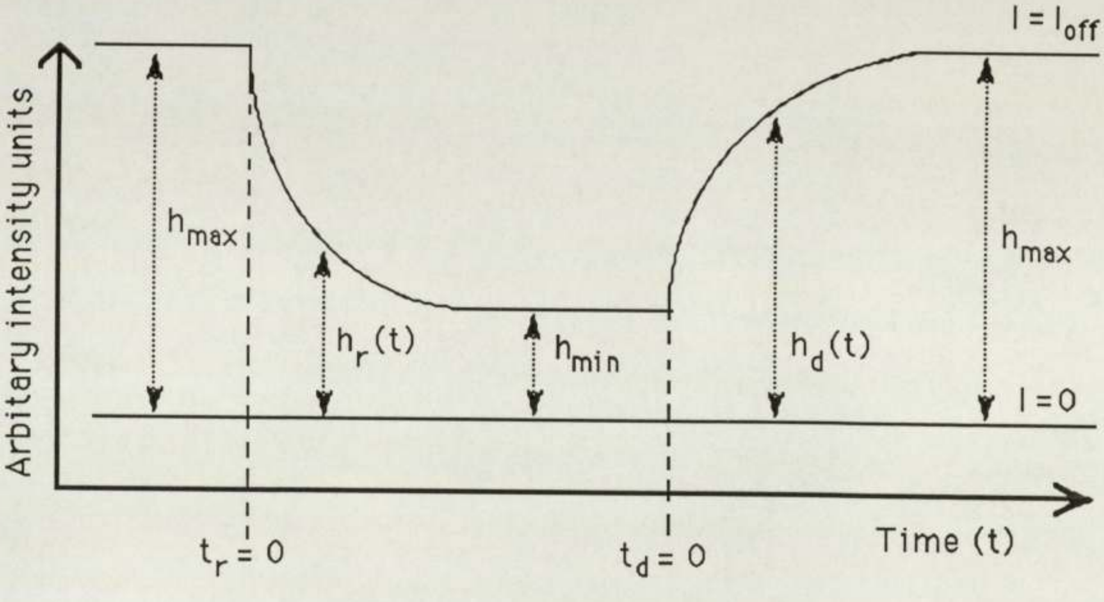

Figure 8.22 Analysis of time dependent optical dichroism

In principle, the measured heights, h_{max}, h_{min}, and h(t) have to be converted into the corresponding intensities of light I_{max}, I_{min}, and I(t) using the simple relationship

$$I = c\,h \qquad 8.19$$

where c is a constant the value of which depends on the properties of the detection system. Recalling that the intensity of light incident on the Kerr cell is I_1 (section 8.1) then the optical transient curve can be characterised in terms of the following absorbances, For the field-off condition,

$$A_{max} = \log_{10} (I_1/c\, h_{max}) \qquad 8.20$$

For the equilibrium field-on condition,

$$A_{min} = \log_{10} (I_1/c\, h_{min}) \qquad 8.21$$

and

$$A_{r,d}(t) = \log_{10} (I_1/c\, h_{r,d}) \qquad 8.22$$

To make the shape of the optical transient curves independent of the absolute intensities of light, the curves were normalised. For the rise curve, the normalised time-dependent absorbance $\mathbf{A}_r(t)$ is defined by

$$\mathbf{A}_r(t)= [(A_r(t)-A_{min})/(A_{max}-A_{min})] \qquad 8.23$$

and for the decay curve the normalised time dependent absorbance $\mathbf{A}_d(t)$ is defined by

$$\mathbf{A}_d(t) = 1 - [(A_d(t)-A_{min})/(A_{max}-A_{min})] \qquad 8.24$$

The values of t, which were associated with each of the heights $h_{r,d}(t)$, were measured in millimeters from the $t_{r,d}=0$ points (figure 8.22). These values were converted to units of time in seconds by applying a scaling factor. The latter was calculated by measuring the distance in millimeters between two calibration marks generated by the transient recorder before and after the output of each captured electro-optical transient.

8.4.2 Calculation of the relaxation parameters

For a monodisperse system of molecules or particles whose rotational motion is characterised by a single rotational relaxation time, τ, then the normalised time dependent optical response $\phi(t)$ (birefringence or dichroism) may be described by a single exponential function (section 6.5),

$$\phi(t) = \exp -(t / \tau) \qquad 8.25$$

Although the description of the rise curve is more complicated than that of the decay, for the case where molecular orientation occurs by a purely induced dipolar mechanism, or where the contribution from permenant dipoles is small, the shape of the rise curve may also be approximated by equation 8.25. For a system of particles of different sizes, the optical decay curves will be a superposition of a set of weighted exponential curves and it has been found that this behaviour can be described using the empirical relationship of Williams and Watts(175,176),

$$\phi(t) = \exp -(t / \tau)^{\beta} \qquad 8.26$$

where β is a constant indicative of the degree of polydispersity and has a value that normally lies between 0 and 1.

A double logarithmic plot of $\phi(t)$ vs time allows the constants τ and β to be obtained. On equating $\phi(t)$ to $A_d(t)$ equation 8.26 becomes

$$\ln[\, -\ln\, (A_d(t))\,] \;=\; \beta\, \ln t\, - \beta\, \ln \tau \qquad 8.27$$

For ease of graphical presentation, it is convenient to rearrange equation 8.27 to obtain

$$\ln[\, -\ln\, (A_d(t))\,] \;=\; -\beta\, (-\ln\, t\,) - \beta\, \ln \tau \qquad 8.28$$

and to construct graphs of $\ln[\, -\ln\, (A_d(t))\,]$ vs $-\ln t$. To facilitate the analysis of the large number of optical transients, the computer program "Analysis of optical transients" (Appendix 2) was used to convert the ordinates and abscissa values taken from the rise and decay curves into values of t, $-\ln t$, $A_d(t)$ and $\ln[\, -\ln\, (A_d(t))\,]$ following the methods set out in the preceding paragraphs. The relaxation data obtained from sets of transients recorded at various voltages and different concentrations of copolymer are presented in appendix 3. As a representative example, values of t and the normalised, time dependent absorbance $A_d(t)$ derived from the transient decay curve of dichroism of a 1%w/v solution of copolymer in cyclohexane obtained using an applied voltage of 1000V are shown in table 8.18. The calculated values of $\ln[\, -\ln\, (A_d(t))\,]$ and $-\ln t$ were used to construct a double logarithmic plot (figure 8.23). An Apple Macintosh computer curve-fitting routine was then used to perform a linear regression analysis on the data and values of τ and β calculated from the slope and intercept are shown in tables 8.19 to 8.22, along with those calculated from the rise and decay data presented in appendix 3. The standard error of estimation in the gradient of the double logarithmic plots (and hence the error in the values of β) was calculated by the "least mean squares" method. Thus the error in the values of β shown in tables 8.19 and 8.20 (decay of electric dichroism) did not exceed 0.075. The error in the values of β shown in tables 8.21 and 8.22 (rise of electric dichroism) was not greater than 0.16.

Table 8.18 Dichroism decay transient for a 1.05%w/v solution of copolymer in cyclohexane at 1000V

time, t /s	$h_d(t)$/mm	$A_d(t)$	$\ln[-\ln(A_d(t))]$	$-\ln(t/s)$
0.008	35.5	0.660	-0.88	4.83
0.018	48.5	0.483	-0.32	4.01
0.028	58.5	0.376	-0.02	3.57
0.038	66.5	0.304	0.18	3.26
0.049	73.0	0.251	0.33	3.03
0.059	78.0	0.213	0.44	2.84
0.069	82.0	0.185	0.53	2.68
0.079	86.0	0.158	0.61	2.54
0.089	89.0	0.138	0.68	2.42
0.099	92.0	0.119	0.76	2.31
0.109	94.5	0.104	0.82	2.21
0.119	97.0	0.091	0.88	2.13
0.129	98.5	0.080	0.93	2.04
0.140	100.0	0.072	0.97	1.97
0.150	101.0	0.066	1.00	1.90
0.160	102.5	0.059	1.04	1.83
0.170	103.0	0.055	1.06	1.77
0.180	104.0	0.050	1.10	1.71
0.200	105.5	0.041	1.16	1.61
0.221	106.5	0.036	1.20	1.51
0.241	108.0	0.028	1.27	1.42
0.261	109.5	0.020	1.36	1.34
0.281	110.0	0.018	1.40	1.27
0.294	110.5	0.015	1.43	1.23
0.302	110.5	0.015	1.43	1.20
0.322	111.5	0.010	1.53	1.13
0.342	111.5	0.010	1.53	1.07
0.362	112.0	0.008	1.59	1.02
0.383	112.5	0.005	1.67	0.96
0.403	112.5	0.005	1.67	0.91
0.423	113.0	0.003	1.79	0.86

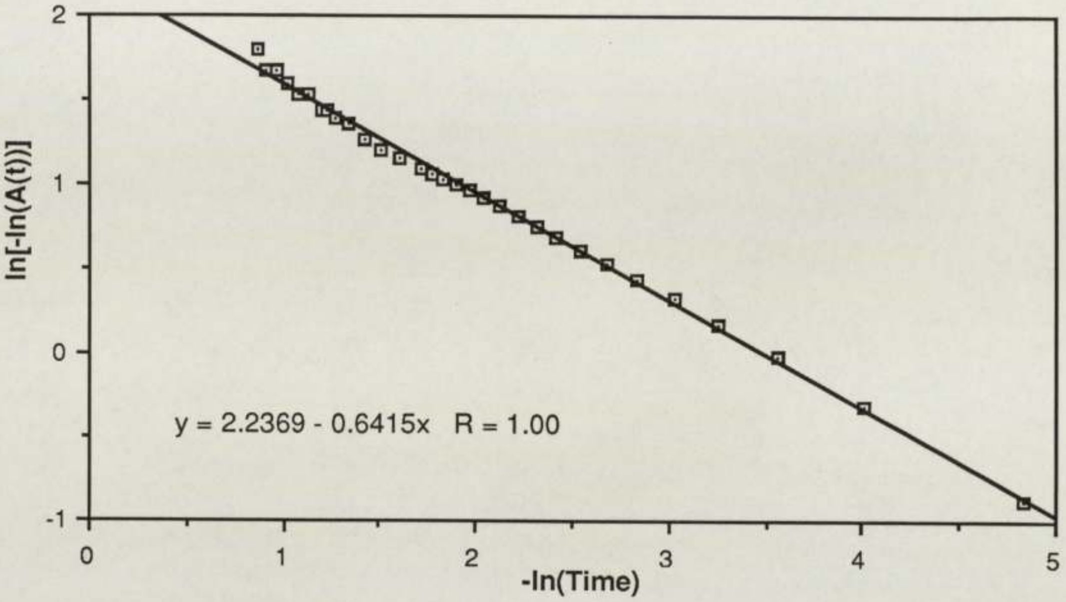

Figure 8.23 Double Logarithmic Plot of Dichroism decay data for a 1.05%w/v solution of copolymer in cyclohexane at 1000V

Table 8.19 Relaxation parameters for dichroism decay at 1000V

w/v % copolymer in cyclohexane at 298K	β	τ/ms
0.65	0.87	17.7
1.05	0.64	30.6
1.58	0.53	35.7
1.80	0.61	21.4

Table 8.20 Relaxation parameters for dichroism decay at 250V

w/v % copolymer in cyclohexane at 298K	β	τ/ms
0.65	-	-
1.05	1.03	94.3
1.58	0.72	77.3
1.80	0.79	59.2

Table 8.21 Relaxation parameters for dichroism rise at 1000V

w/v % copolymer in cyclohexane at 298K	β	τ/ms
0.65	1.09	1.3
1.05	1.02	2.7
1.58	1.25	2.9
1.80	1.37	1.2

Table 8.22 Relaxation parameters for dichroism rise at 250V

w/v % copolymer in cyclohexane at 298K	β	τ/ms
0.65	-	-
1.05	1.06	15.0
1.58	1.13	20.7
1.80	1.07	14.0

8.4.3 Analysis of transients obtained using reversed pulses of voltage

The pulse generator described in appendix 1 was designed so that the polarity of the voltage applied across the electrodes of the Kerr cell could be reversed rapidly during the application of the pulse. The shape of the dichroism transients obtained for solutions of polypentenylene-block-co-acetylene using the method described in section 7.4 were not affected when reversed pulses of voltage were used. However the optical transients produced using the optical arrangement shown in figure 7.6 exhibited a small depression (Figure 8.24). Although the latter result suggests that the solution of copolymer contained species that possessed permanent dipolar groups, it should be noted that the intensities of light that are produced using this optical arrangement are a composite of birefringence and dichroism and therefore this interpretation may be invalid. Indeed the fact that no phase reversal transients were observed in the traces of electric dichroism offers strong evidence that the orientation of the particles in solution occurred predominantly by an induced dipolar mechanism.

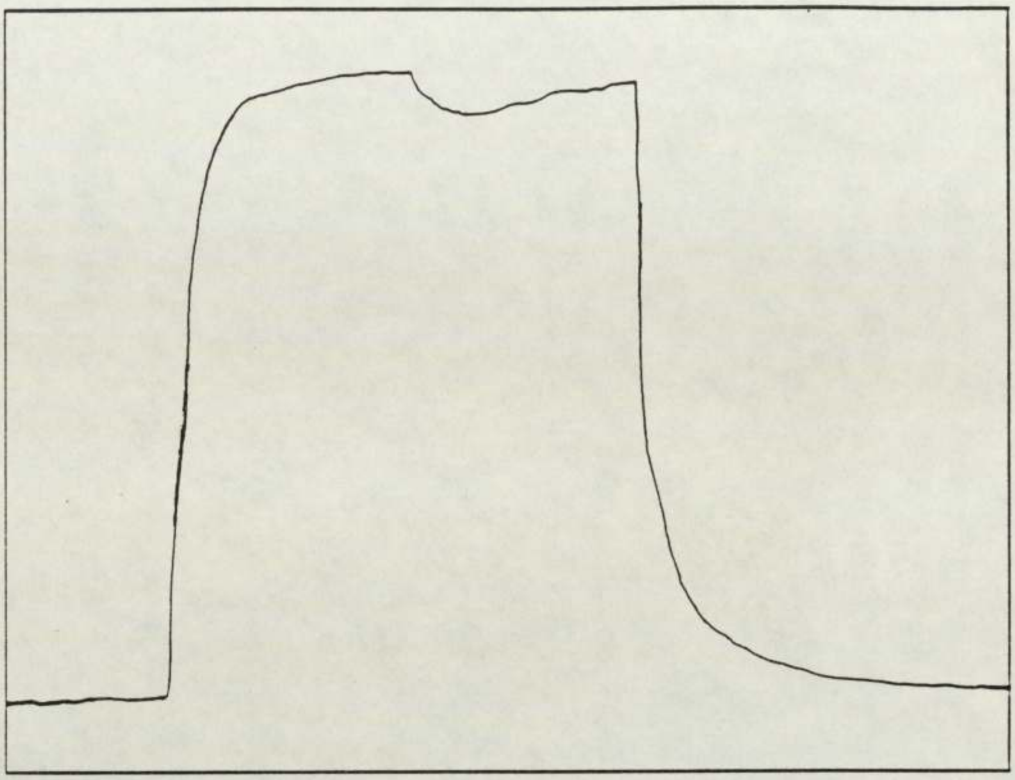

Figure 8.24 Electro-optical transient produced using the apparatus shown in figure 7.6

8.5 DIELECTRIC MEASUREMENTS

Although electro-optical measurements provide a sensitive method for probing the dynamic behaviour of molecules in solution, the range of sample concentrations which may be investigated is severely limited for samples that absorb light strongly. With the optical system shown in figure 7.6, signals from solutions of polypentenylene-block-co-acetylene in excess of 2% w/v could not be recorded. Dielectric relaxation studies also provide information concerning dipolar dynamics and offer the advantage of not being affected by the optical characteristics of the material under test.

Measurement of the parallel capacitance (C_p) of an 18.8% w/v solution of polypentenylene-block-co-acetylene was made by the method described in section 7.6.2. The parallel capacitances for air, cyclohexane, toluene and the solution of copolymer over the frequency range 12Hz-100kHz are shown in figure 8.25. The dispersion curve for the copolymer solution is featureless and is insensitive to temperature suggesting that either no permanent dipolar groups are present or that the relaxation is occurring outside the frequency range over which the capacitance was measured.

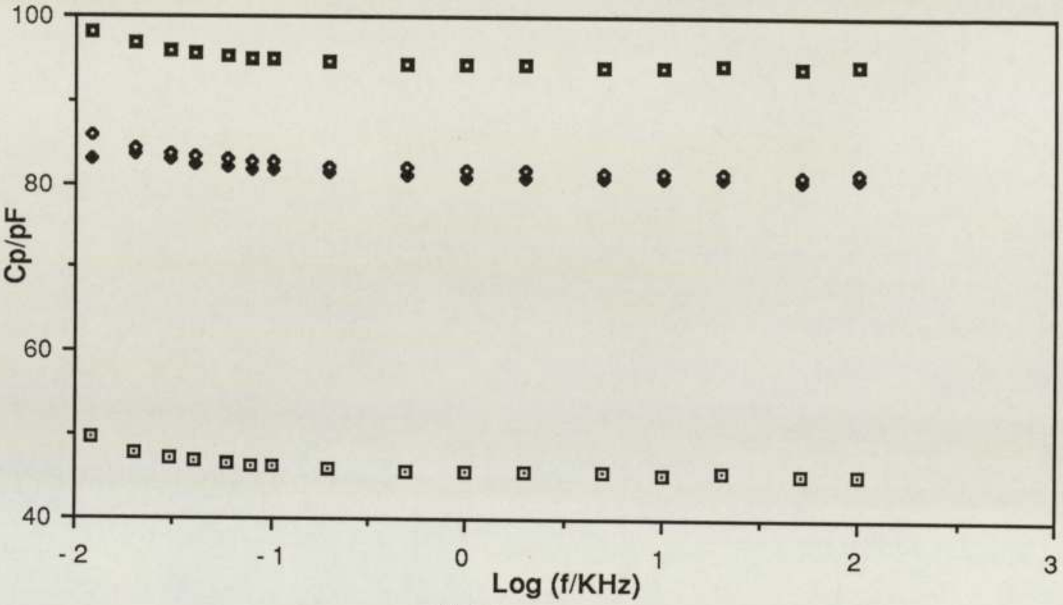

Figure 8.25 Dependence of the parallel capacitance (Cp) on frequency (f) at 20.5°C ■ = toluene, ◇ =14.8% w/v solution of copolymer in cyclohexane, ◆ = cyclohexane, ▣ = air.

CHAPTER 9

DISCUSSION AND CONCLUSIONS

9.1 MECHANISM OF THE POLYMERISATION OF ACETYLENE USING METATHESIS CATALYSTS

The results presented in chapter 3 have shown that WCl_6/n-BuLi, $WCl_6/AlEtCl_2$ and $WCl_6/AlEt_3$ will catalyse the polymerisation of acetylene. As these systems are also known to be catalysts with varying degrees of effectiveness for the ring opening polymerisation of cyclic alkenes, the question arises as to whether polymerisation of the two types of monomer proceeds by a common mechanism involving an identical metallocarbene intermediate. There is considerable evidence to suggest that the metathesis polymerisation of cyclic alkenes proceeds by a mechanism involving a metal carbene intermediate and recent evidence, in which metallocyclobutanes have been detected by NMR during such polymerisations, strongly supports this view(127). The mechanism of the polymerisation of phenylacetylene catalysed by tungsten hexachloride has been investigated by Masuda(131,132). The main conclusions from this study were:

(i) The polymerisation proceeded by a co-ordination mechanism; the propagating centre was not cationic, as is the case for the polymerisation of styrene with this catalyst (when it is assumed that water was added as a cocatalyst).

(ii) The use of tetraphenyltin as a cocatalyst enhanced the rate of polymerisation of phenylacetylene whereas the addition of oxygen acted as a retarder. Measurements suggested that the state of the tungsten atom during propagation was in an oxidation state lower than IV and in view of the fact that $WCl_6/SnPh_4$ was known to catalyse the ring opening polymerisation of cyclic alkenes, it was suggested that a metal carbene or a metallocyclobutane may be the active species responsible for the polymerisation of phenylacetylene. Katz(177,178) has also published evidence for the polymerisation of phenylacetylene propagating by a metathesis mechanism. When phenylacetylene was mixed with WCl_6, the resulting species was found to initiate the polymerisation of cyclopentene(154). Gel permeation chromatography of the polymer produced by this reaction showed that blocks of polyphenylacetylene had become attached to the polypentenylene chains. If the reaction was carried out in the presence of diphenylacetylene, the amount of polyphenylacetylene present in the copolymer did not vary, but the growth of the polypentenylene chain could be suppressed by diphenylacetylene. This indicated that the polyphenylacetylene was present as a block prior to the initiation of the polymerisation of cyclopentene and that the diphenlyacetylene initiated only the metathesis reaction. The implication was that the metathesis polymerisation of cyclopentene was initiated by the living polyphenylacetylene complex. This was claimed as strong evidence that the polymerisation of phenylacetylene was propagated by metal carbenes and similar in nature to the conventional metathesis reaction.

Based on the conclusions advanced by Masuda and Katz, Schue(142) suggested that the polymerisation of acetylene using the WCl_6/n-BuLi catalyst proceeded by a carbene mechanism (figure 9.1). If this mechanism occurred during the polymerisation, then the stereochemistry of the resulting polymer would be determined by the direction of rotation of the C2-C3 bond in intermediate III. The high trans contents of the polymers prepared in these experiments were attributed to the preferred rotation of this bond in a direction such that the steric repulsion caused between the propyl group (Pr) and the tungsten atom was minimised.

Studies concerning the linear polymerisation of acetylene using Ziegler/Natta catalysts have been accompanied by investigation of the cyclotrimerisation reaction. The production of cyclic trimers, particularly benzene, during acetylene polymerisations was claimed to show that cis opening of the triple bond occurs in a mechanism similar to that of the co-ordinated anionic polymerisation of linear alkenes.(38)

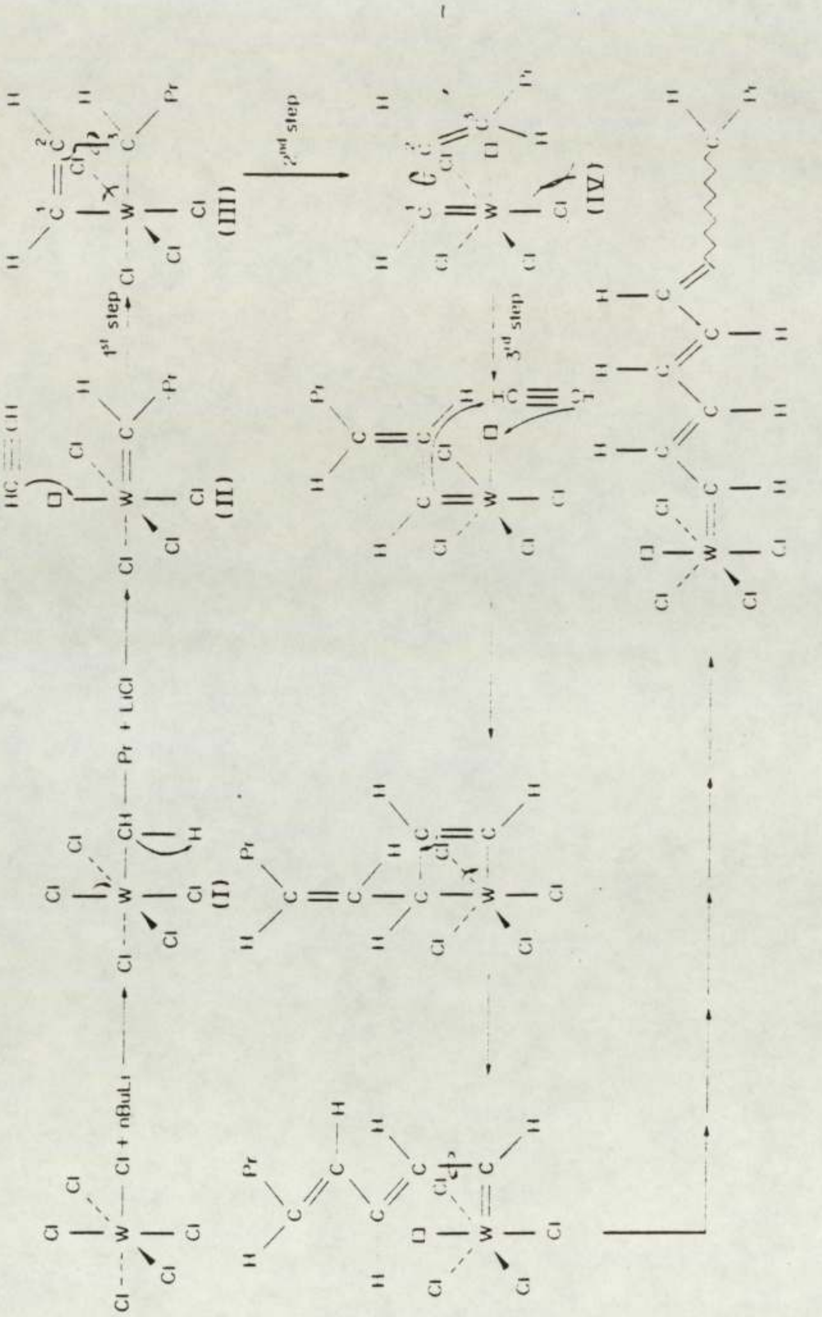

Figure 9.1 Carbene mechanism for the polymerisation of acetylene

Ikeda and Tamaki(179) studied the effect of varying the components of the catalyst on the yield of the cyclotrimerisation reaction. The results suggested that the active species for both linear polymerisation and cyclotrimerisation were very similar, but the selectivity was determined by the chlorine content of the active species. Thus catalysts that possessed no chlorine atoms gave linear polyacetylenes (eg. $AlEt_3/Ti(OBu)_4$, $AlEt_2(OC_2H_5)/Ti(OBu)_4$) whereas all catalysts which comprised a chlorine containing compound gave predominantly cyclisation products. These authors verified that the cyclisation process proceeded by a similar mechanism to that of the linear polymerisation of acetylene by considering the nature of the end groups in the polymer. Phenyl end groups were detected indicating that termination of acetylene polymerisation had occurred by a cyclisation mechanism. It was suggested that the polymerisation of acetylene occurred by a co-ordinated anionic route that involved a cis insertion of the acetylene molecule into the metal-carbon bond of the propagating centre (figure 2).

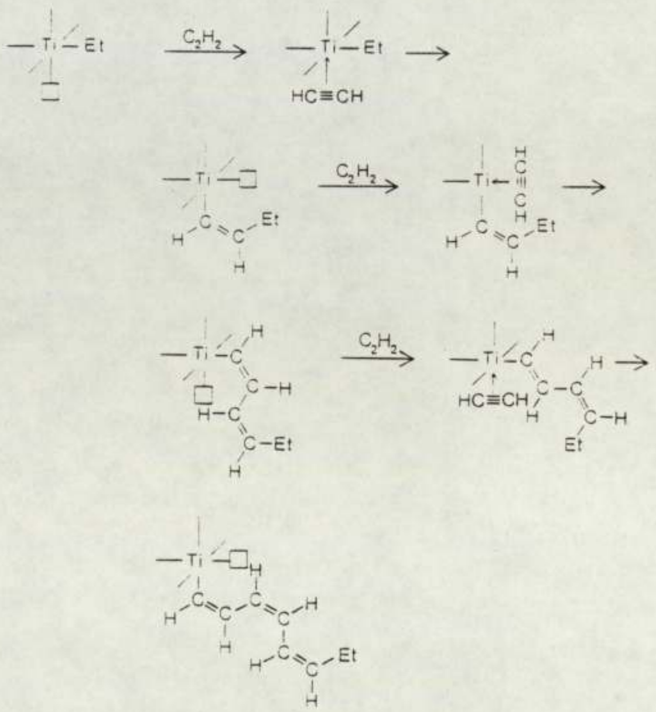

Figure 2 The "cis-insertion" mechanism for the propagation step during the polymerisation of acetylene.

The high trans contents of certain polyacetylenes prepared using Ziegler/Natta catalysts may be explained by the temperature dependent cis/trans isomerisation which is known to occur after polymerisation.(180)

The results presented in chapters 3 and 4 demonstrated that $WCl_6/AlEtCl_2$ is an effective catalyst for the ring opening polymerisation of cyclopentene but only exhibits modest activity towards acetylene in homopolymerisation and in the copolymerisation of acetylene and cyclopentene. Conversely, $WCl_6/AlEt_3$ is a more efficient catalyst for the polymerisation of acetylene but gives only modest yields of polypentenylene, which invariably lead to the production of insoluble products during the copolymerisation reaction. These observations, coupled with the fact that premixing the components of the catalyst, which retards the ring opening polymerisation of cyclopentene and enhances the production of polyacetylene, show that the active species responsible for the polymerisation of acetylene and cyclopentene cannot be identical. It is known that the ring opening metathesis polymerisation of cyclic alkenes propagates by a mechanism that involves a metal carbene, but it may be concluded, from the evidence cited above, that the mechanism operating during the polymerisation of acetylene using the metathesis catalysts described in chapter 3 is not similar to that shown in figure 9.1. Rather it is more likely that the mechanism of propagation is of the co-ordinated anionic type described for the Ziegler/Natta catalysts. It is interesting to note that the least efficient of the catalyst systems which comprise aluminium alkyl cocatalysts towards the polymerisation of acetylene is that which contains cocatalyst chlorine atoms. When Ziegler/Natta catalysts systems were used, it was observed that those systems which had a high chlorine content gave low yields of high molecular weight polyacetylene and large amounts of cyclotrimerisation products. If the mechanism of the polymerisation of acetylene using the WCl_6/aluminium alkyl catalysts proceeds by a Ziegler/Natta type mechanism, then it would be expected that the yield of benzene when $AlEtCl_2$ is used as cocatalyst may be greater than that observed when $AlEt_3$ is used. Recent studies have shown that benzene is not produced when $AlEt_3$ is used as cocatalyst.(181)

Although WCl_6/LiBu has been used successfully to catalyse the ring opening polymerisation of cyclic alkenes, it showed only modest activity towards the polymerisation of acetylene. Studies concerned with eludicating the mechanism of the initiation step in metathesis polymerisations have indicated that the LiBu cocatalyst behaves as an alkylating agent.(182) When this cocatalyst is complexed with a titanium species, the activity of the resulting complex in Ziegler/Natta polymerisations is poor. In these systems it has been shown that a strong reducing agent with some degree of Lewis acidity is essential if highly active catalysts are to be formed. The aluminium containing cocatalysts which were used in the acetylene polymerisations are much stronger reducing agents and are Lewis acids. This supports the view that the polymerisation of acetylene proceeds by a Ziegler/Natta co-ordinated anionic mechanism and not via the metal carbene.

9.2 MECHANISM OF THE COPOLYMERISATION OF ACETYLENE AND CYCLOPENTENE USING METATHESIS CATALYSTS.

The results of GPC presented in chapter 4 showed that a block copolymer was generated by sequential addition of cyclopentene and acetylene to an active metathesis catalyst. The formation of a block copolymer by this method indicated that the ring opening metathesis polymerisation of cyclopentene produced a "living polymer" in which the average lifetime of the propagating centres was exceptionally long. During the ring opening polymerisation of cyclopentene it is likely that the polypentenylene chains were attached to the tungsten atom by a metal carbene bond, which formed the locus of subsequent additions of monomer. If termination reactions of these active centres were absent, then it would be expected that propagation would have occurred until the concentration of monomer reached its equilibrium value, then the sites of polymerisation would have remained active indefinitely. The ring opening metathesis polymerisation of norbornene using carbene catalysts provides an example of this type of living system (section 1.5.4.4). Initiation is very rapid and intermolecular reactions of the propagating polymeric carbene are suppressed by the steric effects of the polynorbornene chain which results in a polymer with a very narrow distribution of molecular weight. In the case of the ring opening metathesis polymerisation of cyclopentene using $WCl_6/AlEtCl_2$, bimolecular termination reactions have been found to occur.(151) The double bonds present in the polypentenylene chains may also compete with monomeric double bonds for the active sites of the catalyst via a ring chain equilibrium. This process yields highly polydisperse polymer. For these reasons, it seems unlikely that the living system, present during the synthesis of polypentenylene-block-co-acetylene, is identical to that described for the polymerisation of norbornene.

The formation of a block copolymer by sequential addition of the two monomers to a solution of catalyst normally requires that both monomers polymerise by a common mechanism. On this basis, it is tempting to suggest that during the preparation of polypentenylene-block-co-acetylene, both the ring opening polymerisation of cyclopentene and the polymerisation of acetylene proceeded through a common mechanism involving a tungsten carbene. The results of GPC and uv/visible spectroscopy (section 4.3) however indicate that the yield of copolymer produced using the sequential addition method was low and that the product of the copolymerisation contained an excess of unreacted homopolypentenylene. When WCl_6 /$AlEt_3$ was used to catalyse the copolymerisation of acetylene and cyclopentene, the product was an insoluble powder similar in nature to polyacetylene. These observations cannot easily be explained if a carbene type mechanism is assumed for the polymerisation of both cyclopentene and acetylene since $WCl_6/AlEtCl_2$ is known to be a much more effective catalyst for ring opening metathesis polymerisations than is $WCl_6/AlEt_3$. It would seem more likely in view of the conclusions drawn from the studies of acetylene homopolymerisation (section 9.1) that acetylene polymerises by a co-ordinated anionic mechanism the active centre being a metal-carbon single bond. On this basis, it may be concluded that, during the ring opening metathesis polymerisation of cyclopentene using $WCl_6/AlEtCl_2$, two types of active centre are present namely the tungsten carbene, which promotes metathesis polymerisation and the tungsten alkyl, which does not catalyse metathesis polymerisation but may be active in the Ziegler/Natta polymerisation of acetylene. Further since the product of the copolymerisation reaction was a block copolymer and not merely a mixture of the two parent homopolymers, it seems likely that for solutions of quasi-living polypentenylene the two active species (carbene and alkyl) may be in equilibrium. The interconversion of these two species may occur by an α hydrogen shift as depicted in figure 9.3. In the generation of metathesis centres it has been shown that alkylation is an important step.(182)

$$W\text{-}CH_2\text{-}P_n \quad \longleftrightarrow \quad H\text{-}W{=}CH\text{-}P_n$$

Figure 9.3 Interconversion of the two active centres present during the ROMP of cyclopentene

The low yields of copolymer obtained when $WCl_6/AlEtCl_2$ was used as catalyst for the copolymerisation reaction suggests that in this case the equilibrium lay in favor of the tungsten carbene, whereas when $AlEt_3$ was used as cocatalyst, the tungsten alkyl became the principal species present in solution.

The conversion of a tungsten carbene to a tungsten alkyl during the ring opening polymerisation of cyclopentene may be regarded as a termination reaction as, in this scheme, the alkyl does not participate in metathesis polymerisations. The polymer chain therefore ceases to propagate but remains dormant until it is either converted to the metal carbene form or until acetylene is added and a block copolymer is formed. "Temporary" termination reactions of the type described above for the metathesis polymerisation are a feature of certain cationic polymerisations(183) and the living systems which are generated in these cases are termed "quasi-living".

An approach that is often used for the synthesis of a block copolymer, where the constituent monomers polymerise by different mechanisms, involves a transformation reaction of the active centre (section 1.6.2.1). The results presented in chapter 5 showed that an increase in both the yield of copolymer and the average length of the polyene sequences could be achieved if $AlEt_3$ was added to the quasi living polypentenylene prior to the introduction of acetylene. This supports the view that two types of active centre are present during the ring opening polymerisation of cyclopentene and suggests that the addition of $AlEt_3$ causes a displacement in the position of the equilibrium shown in figure 9.3 in favour of the tungsten alkyl. This may be considered as a metathesis to Ziegler/Natta transformation reaction. Although the exact nature of these chemical processes is uncertain, it was observed that a gas was evolved and a colour change occurred. Patat and Sinn (184) have shown that ethene and ethane are produced when aluminium alkyls react with transition metal halides.

It is notable that samples of polypentenylene-block-co-acetylene prepared by the transformation technique show anomalously high adhesive properties whereas those prepared using the single catalyst method did not. This suggests that the structure of the two types of copolymer were different. Since polypentenylene showed no anomalous adhesion, the origin of this effect must have been the polyene sequences of the copolymer. In copolymers prepared by the single catalyst method, the excluded volume and protecting effects of the polypentenylene chains presumably stabilised the polyacetylene segments of the copolymer against reaction with surfaces. Since the average length of the polyene sequences and the yield of copolymer were greater in the samples prepared by the transformation technique, it seems plausible that the protecting and excluded volume effects of the polypentenylene chains in these materials were insufficient to stabilise the polyacetylene segments against reaction with surfaces.

9.3 STRUCTURE OF POLYPENTENYLENE-BLOCK-CO-ACETYLENE IN SOLUTION IN CYCLOHEXANE

Polypentenylene-block-co-acetylene may be prepared, using the methods described in chapters three and four, as a black elastomeric material that can be dissolved in a range of common organic solvents to produce highly coloured solutions even at low concentration (<1%w/v). The uv/visible spectrum of the copolymer dissolved in cyclohexane exhibited a broad absorption in the visible region which was attributed to the presence of a series of short chain polyenes, attached to blocks of polypentenylene. The average length of the polyene segments was estimated to be 10 acetylenic units. Examination of the solution by GPC indicated the presence of material which had an effective hydrodynamic radius far in excess of that expected for an isolated copolymer molecule. It was concluded that the polyene chains of the copolymer aggregate when in solution to form large micellar type structures. It was also observed that the overall concentration of polyene segments in the copolymeric material was very low and that there was an excess of unreacted polypentenylene.

The results of the electro-optical experiments described in chapter 8 showed that solutions of polypentenylene-block-co-acetylene in cyclohexane became highly optically anisotropic when subjected to an electric field. Indeed the magnitude of the Kerr constant measured at 200V was almost three orders of magnitude greater than that of pure toluene. Large values of electro-optical anisotropy may have arisen because: (i) the particles within the solution were intrinsically anisotropic and/or (ii) the materials possessed dipoles that coupled strongly with the applied electric field and produced a high degree of orientation. The latter effect is opposed by intermolecular collisions and in order to maintain a high degree of alignment and a large electro-optical anisotropy, the particles must either possess very large dipoles or have effective hydrodynamic radii that are very much larger than those of the solvent molecules. The non-linearity observed in the plots of birefringence and dichroism against the square of the strength of the applied field show that when the field is applied, strong coupling between the particles and the field occurs which results in the production of a highly ordered state and not just a minor perturbation as is the case for materials which obey the quadratic Kerr law (see chapter 6). As both polypentenylene and cyclohexane show no observable electro-optical anisotropy at the field strengths used in these experiments, it may be concluded that the origin of the electro-optical signal resides in the conjugated polyene segments of the copolymer.

The application of reversed pulses of voltage to solutions of the copolymer produced no effect on the shape of the dichroism transients and indicates that the particles orientate in the electric field by a predominantly induced dipolar mechanism. It would seem unlikely that a large dipole could be induced in a short polyene chain and if the copolymer existed in solution as discrete molecules, a high degree of dipolar coupling would not be expected. The high couplings which are evident from the electro-optical plots must have resulted from aggregation of the polyene sequences of the copolymer into micellar type structures. Since the concentration of copolymer in solution is very low and the average length of the polyene sequences is short, the effective hydrodynamic radii of the aggregates of polyene segments will be small. In the absence of attached polypentenylene chains, such small aggregates even if they were of a highly anisotropic structure, would not be expected to give rise to a large value of birefringence and would exhibit a relaxation time that was relatively short. The relaxation times which characterise the decay of dichroism shown by solutions of polypentenylene-block-co-acetylene are long, typically 30ms (at 1000V). This provides very strong evidence that long blocks of polypentenylene are attached to the polyene chains.

Since the concentration of copolymer in the solution is so low, the viscosity of the medium cannot explain the long observed relaxation times. Clearly the long relaxation times arise from the rotational motion of large particles. If the copolymer exists in solution as particles with small aggregated cores of polyene segments and a large shell of polypentenylene chains, then, provided that the polypentenylene chains are sufficiently long, these chains will adopt a random coil arrangement and will cause the overall shape of the aggregate to be approximately spherical. If the polyene sequences were arranged in a random manner then this would result in a spherical "core" to the micelle (Figure 9.4(a)).

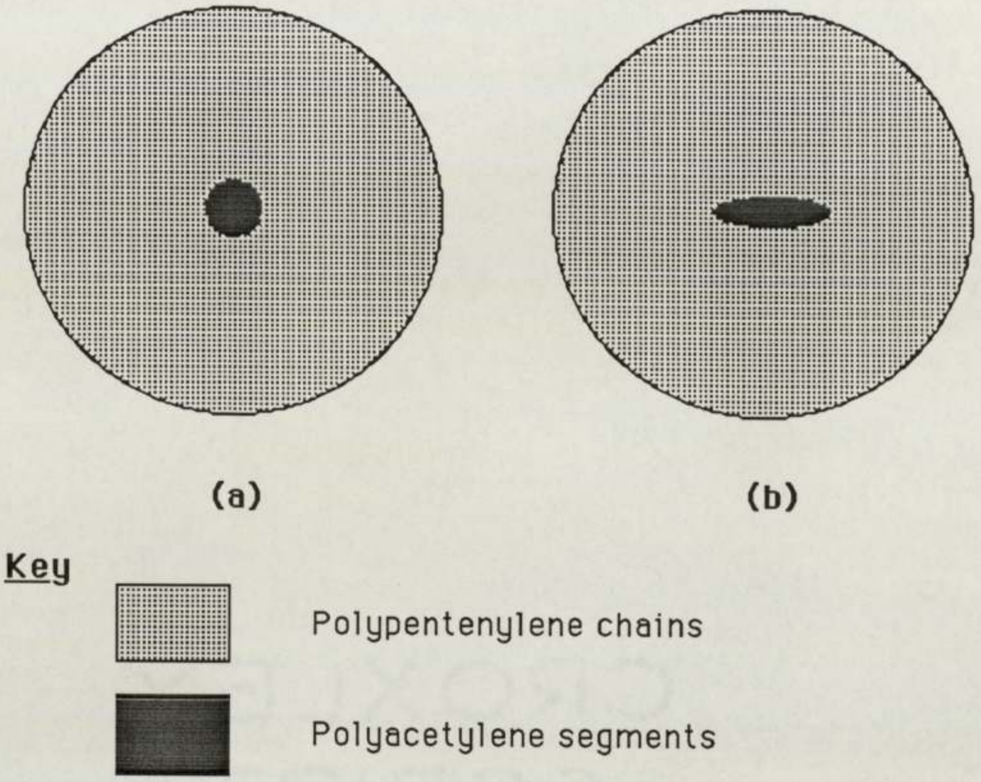

Figure 9.4 Possible structures of polypentenylene-block-co-acetylene in solution in cyclohexane.

When an electric field is applied to a solution that contains aggregated particles of the type shown in figure 9.4(a), then it would be expected that a small net dipole moment would be induced in the polyene sequences which would give rise to a small induced optical anisotropy. However, no net rotation of the particles would result and therefore very short relaxation times would be expected. Since the relaxation times observed for solutions of polypentenylene-block-co-acetylene are long and the electro-optical anisotropy large, it may be concluded that this copolymer does not adopt a structure in solution in which the core is randomly packed and spherical.

If the polyene segments of the core are packed in an anisotropic manner, then a structure similar to that shown in figure 9.4(b) would result. If an electric field is applied to a micelle of this type, then it may be expected that a large net dipole moment would be induced in the particle and the core would begin to rotate to a position of minimum free energy with respect to the direction of the electric field. Since the polyene chains which comprise the core are attached to the chains of polypentenylene of the "shell", rotation of the core would necessitate that the whole particle rotated. The rotation of the entire micelle would be expected to be a slow process and would restrict the motion of the core, producing a slow rise of birefringence (long τ_r). As large particles are less susceptible to the effects of collisions with molecules of solvent in diffusion and Brownian motion processes, a high degree of alignment of the induced dipoles with the field would eventually occur resulting in a large value of the induced optical anisotropy of the solution and departures from Kerr law behaviour. When the field is removed, it would also be expected that many collisions between the particles and the molecules of solvent would be required to completely destroy the induced optical anisotropy, therefore long relaxation times are predicted for this model. The predicted behaviour of a structure in which the core of the micelle was anisotropic is very similar to that observed in solutions of polypentenylene-block-co-acetylene, however the results presented in tables 8.19-8.22 show that, for solutions of polypentenylene-block-co-acetylene in cyclohexane, $\tau_r << \tau_d$. A situation in which τ_r is short may be explained if it is assumed that it is the small cores of polyacetylene of the micelle that give rise to the electro-optical anisotropy. In this case, the observed τ_r will result from the rotation of these species alone. Since the linkages between the core and the "shell" of polypentenylene are flexible, the core may rotate rapidly and independently of the shell, to a position of orientational equilibrium with respect to an applied electric field. This process would be characterised by a short τ_r. Although the optical properties of the system would appear to have achieved equilibrium, a torque would still remain on the micellar core and this would relax, by a slow rotation of the surrounding shell of polypentenylene, to a new position of minimum free energy.

9.4 CONCLUSIONS AND FURTHER WORK

The results presented in this thesis show that it is possible to polymerise acetylene using the metathesis catalysts WCl_6/LiBu, $WCl_6/AlEtCl_2$ and $WCl_6/AlEt_3$. Although only modest yields of polyacetylene were obtained, low efficiencies are not untypical of polymerisations catalysed by transition metal compounds. In the polymerisation of acetylene using Ziegler/Natta catalysts, the yield of polyacetylene may be improved by increasing the concentration of catalyst. In the metathesis systems examined in the present study, the concentration of catalyst that may be used is limited by the low solubility of WCl_6 in cyclohexane. Therefore, to obtain high yields of polyacetylene using metathesis catalysis, either a solvent would have to be used in which the solubility of WCl_6 was considerably greater or else a catalyst system that was completely soluble even at high concentration would be required. One advantage of using cyclohexane as solvent for the polymerisation of acetylene over aromatic solvents is that the products of cyclotrimerisation (eg. benzene) may be studied quantitatively. In view of the differing activities of the metathesis catalysts described in this thesis towards the polymerisation of acetylene, it may prove interesting to correlate the yield of benzene with the activity of the catalyst in the polymerisation reaction. Investigation of this type may provide useful mechanistic information.

Block copolymers were prepared by sequential addition of cyclopentene and acetylene to a solution of an active metathesis catalyst. The copolymers obtained when $WCl_6/AlEtCl_2$ was used as catalyst were black elastomeric materials that dissolved in a range of organic solvents to produce highly coloured solutions even at low concentration.

The efficiency of the catalyst in the copolymerisation reaction was improved by employing a reaction scheme that involved an active site transformation reaction. This route to polypentenylene-block-co-acetylene also enabled the lengths of the constituent blocks of polypentenylene and polyacetylene to be controlled. The length of the polyene segments was controlled by varying the ratio of the concentrations of the two co-catalysts ($AlEtCl_2$ and $AlEt_3$) used during the synthesis. The length of the polypentenylene segments could be reduced by the incorporation of 1-octene during the ring opening polymerisation of cyclopentene. Although the addition of 1-octene reduced the molecular weight of the polypentenylene sequences of the copolymer, it is likely that the presence of this additive may have had a deleterious effect on the subsequent polymerisation of acetylene. An improved method of controlling the length of the polypentenylene sequences may be considered in which the block copolymer is prepared, in the absence of 1-octene, to yield a copolymer that contains high molecular weight chains of polypentenylene. If a metathesis catalyst was then mixed with a solution of the copolymer and 1-octene added, then the double bonds present in the polypentenylene segments would undergo degradative metathesis thus reducing the length of the polymeric chains.

The observation that the activities of the catalyst systems $WCl_6/AlEtCl_2$ and $WCl_6/AlEt_3$ towards the polymerisation of acetylene were different from those of the same catalysts towards the ring opening metathesis polymerisation of cyclopentene indicated that the catalytic species that polymerises cyclopentene is not identical to that responsible for the polymerisation of acetylene. On the basis of this observation, it was suggested that the polymerisation of acetylene using the metathesis catalysts $WCl_6/AlEtCl_2$ and $WCl_6/AlEt_3$ proceeded by a Ziegler/Natta type mechanism, involving a cis insertion of the monomer into a metal-carbon bond. A detailed study of the mechanism of this copolymerisation would be aided by using "well characterised" carbene or metallocyclobutane catalysts of the type synthesised by Schrock.(185)

Investigations concerning the use of electro-optical methods to study solutions of polypentenylene-block-co-acetylene in cyclohexane have resulted in the development of a convenient optical technique for determining electrically induced dichroism and electrically induced birefringence simultaneously. This method may prove useful in the study of the structure an hydrodynamics of materials that absorb light strongly (eg. dye molecules that are attached to polymer chains).

Electro-optical studies have indicated that polypentenylene-block-co-acetylene exists as a polydisperse distribution of optically anisotropic particles. The structure that best fits the experimental data is one in which the polyene chains of the copolymer aggregate into small rod shaped cores that are surrounded by large "shells" of polypentenylene. The effective hydrodynamic shape of the shell is most likely spherical. If this is indeed the structure that is present in solution, then it may prove interesting to reduce the size of the shell while keeping the dimensions of the core constant. The effect of this on the electro-optical and hydrodynamic properties of the solution may indicate that there is a critical size of the shell that must be exceeded if the copolymer is to be prevented from agglomerating and forming a precipitate.

REFERENCES

1. Davidson,T. (Ed.), Polymers in electronics, ACS symposium series no. 242, Washington D.C. 1984.
2. Wilson, G.C., Bowden, M.J., Resist materials for electronics, Chemtech, 102-111, 19, (2), Feb. 1989.
3. Carter, F.L. (Ed.), Molecular electroinics devices, Marcel Dekker, New York, 1982.
4. Mort, J., Pfister, G. (Ed.), Electronic properties of polymers, Wiley Interscience, New York, 1982.
5. Blythe, A.R., Electrical properties of polymers, Cambridge University Press, 1979.
6. Seymour, R.B., Conductive polymers, Plenum press, New York, 1981.
7. Duke, C.B., Frontiers in the development of polymers as electronic materials, Synthetic metals, 21, 5-12, 1987.
8. Roth, S., Conductive polymers (Electronic properties of polymers and related compounds), Springer series solid state science, 63, 2-7, 1985.
9. Roth, S, Polyene chains in molecular electronics, Synthetic metals, 21, 52-55, 1987.
10. Inganas, O., Lundstrom, I, Some potential applications of conductive polymers, Synthetic metals, 21, 13-19, 1987.
11. Potember, R.S., Hoffman, R.C., Hu,, H.S., Cocchiaro, J.E., Viands, C.A., Murphy, R.A., Poheler, T.O., Conducting organics and polymers for electronic and optical devices, Polymer, 28, 574-580, 1987.
12. MacDiarmid, A.G., Conducting polymers: what does the future hold?, Synthetic metals, 21, 79-83, 1987.
13. Munn, R.W., Molecular electronics, Chem. Brit., 20, (6), 518-524, 1984.
14. Bloor, D., Plastics that conduct electricity, New scientist, 93, 577-580, 1982.
15. Bryce, M.R., Organic conductors, Chem. Brit., 24(8), 781-785, 1988.
16. Naarman, H., New aspects of intrinsically conducting organic systems and their synthesis, Makromol. Chem. Macromol. Symp., 8, 1-15, 1987.
17. Skotheim, T.A., Handbook of conducting polymers, volumes 1 and 2, Marcel Dekker, New York, 1986.
18. Ivin, K.J., Olefin Metathesis, Academic press, London, 1983.
19. Dragutan, A.T., Balaban, A.T., Dimonie, M., Olefin metathesis and ring-opening polymerisation of cyclo-alkenes, Wiley, New York, 1985.
20. Amass, A.J., Metathesis polymerisation chemistry, 109-134, Comprehensive polymer science, Pergamon press, 4, (6), 1988.
21. Proceedings of the seventh international symposium on olefin metathesis, Journal of molecular catalysis, 46, (1-3), 1988
22 Banks, R.L., Discovery and development of olefin disproportionation, Chem

Tech, 16, (2), 112-117, Feb. 1968.

23. Mol, J.C., Metathesis of functionalised olefins, Chem Tech, 250-255, 1983.

24. Basset, J.M., Leconte, M., Progress in olefin metathesis, Chem Tech, 10, 762-766, 1980.

25. Banks, R.L., Bailey, G.C., Olefin disproportionation, Ind. Eng. Chem. Prod. Res. Dev., 3, 170-173, 1964.

26. Calderon, N., Metathesis polymerisation, Chem. Eng. News, 45 (18), 51-53, 1967

27. Natta, G., Dall'Asta, G., Mazzanti, G., Stereospecific homopolymerisation of cyclopentene, Angew. Chem. (Int. Ed.), 3, 723-729 ,1964.

28. Calderon, N., Ofstead, E.A., Ward, J.P., Judy, W.A., Scott, K.W., Olefin metathesis: Acyclic vinylenic hydrocarbons, J.A.C.S., 90, 4133-4140, 1968.

29. Dall'Asta, G., Motroni, G., The site of ring cleavage in the ring opening polymerisation of low strain cyclic olefins, European polymer J., 7, 707-716, 1971.

30. Eleuterio, H.S., Polymerisation of cyclic olefins, Ger. Offen, 1,072,811, January 7th 1960.

31. Patton, P., McCarthy, T.J., Running the impossible reaction-metathesis of cyclohexene, Chem. Tech., 17, (7), 442-446, July 1987.

32. Korshak, Y.V., Korshak, V., Hocker, H., A new route to polyacetylene: ring opening polymerisation of 1,3,5,7-cyclo-octatetrene with metathesis catalysts, Makromol. Chem. Rapid Commun, 6, 685-692, 1985.

33. Klavetter, F.L., Grubbs, R.H., Poly-cyclo-octatetrene (alias polyacetylene) synthesis and properties, Proc. A.C.S. Div. Polymeric materials (L.A. Calafornia), 58, 586-590, 1988.

34. Ivin, K.J., Laverty, D.T., Rooney, J.J., The ^{13}C nmr spectra of poly(1-pentenylene) and poly(1,3-cyclopentylene vinylene) Makromol. Chem., 178, 1545-1560, 1977.

35. Katz, T.J., The olefin metathesis reaction, Advances in organometallic chemistry, 16, 283-317, 1977.

36. Chien, J.C.W., Polyacetylene, Academic press, Florida, 1984.

37. Wegner, G., Polymers with metal like conductivity: a review of their synthesis structure and properties, Angew. Chem. Int. Eng. Ed., 20, 361-381, 1981.

38. Simonescu, C.I., Percec, V., Progress in polyacetylene chemistry, Prog. Polym. Sci., 8, 133-207, 1982.

39. Aldissi, M., Review of the synthesis of polyacetylene and its stabilisation to ambient atmosphere, Synthetic metals, 9, 131-141 1984.

40. MacDiarmid, A.G., Heeger, A.J., The chemistry of polyacetylene and its derivatives, Synthetic metals, 1, 101-118, 1979/80.

41. Saxman, A.M., Liepins, R., Aldissi, M., Polyacetylene, its synthesis, doping

and structure, Prog. Polym. Sci., 11, 57-89, 1985.

42. Natta, G., Mazzanti, G., Pino, P., Hoch-polymere von Acetylen-Kohlenwasserstoffen erhalten mittels organometal Komplexen von Zwischenschalenelementen als Katalysaboren, Angew. Chem., 69 (21), 685-686, 1957.

43. Ito, T., Shirakawa, H., Ikeda, S., Simultaneous polymerisation and formation of polyacetylene film on the surface of a concentrated soluble Ziegler-type catalyst solution, J. Polymer Science Polym. Chem. Ed., 12, 11-20, 1974.

44. Seeger, K., Gill, W.G., Electrical and optical properties of polyacetylene, Colloid and Polymer science, 258, 252-260, 1980.

45. Haberkorn, H., Naarman, H., Penzien, K., Schulag, J. and Simak, P., Structure and conductivity of polyacetylene, Synthetic metals, 5, 51-71, 1982

46. Chien, J.C.W., Structure and properties of conducting polymers, 27th International Symposium on Macromolecules (Benoit Ed.), Pergammon, Oxford, 233-249, 1982.

47. Baughman, R.H., Shacklette, L.W., The dependence of electronic conductivity upon conjugation length in conducting polymers, Synthetic metals, 17, 173-181, 1987.

48. Aldissi, M., Schue, F., Polyacetylene fibril growth in soluble Ziegler/Natta catalysts, Macromolecules, 17, 1633-1634, 1984.

49. Epstein, A.J., Rommelmann, H., Fernquist, R., Gibson, H.W., Druy, M.A., Woener, T., Morphology of polyacetylene and doped polyacetylene, Polymer, 23, 1211-1221, 1982.

50. Shirakawa, H., Ikeda, S., Preparation and morphology of as prepared and highly stretch aligned polyacetylene, Synthetic metals, 1, 175-184, 1979/80.

51. Montaner, A., Rolland, M., Sauvajol, J., Galtier, M., Almairac, R. and Ribet, J.L., Physical properties of highly ordered polyacetylene films, Polymer, 29, 1101-1104, 1988.

52. Akagi, K., Shirakawa, H., Araya, K., Mukoh, A., Narahara, T., Highly conductive polyacetylene film prepared in a liquid crystal solvent, Polymer J., 19(1), 185-189, 1987.

53. Akagi, K., Katenyana, S. Shirakawa, H., Araya, K., Mukoh, A., Narahara, T., Highly conductive polyacetylene film prepared by the liquid crystal polymerisation method under magnetic field, Synthetic metals, 17, 241-246, 1987.

54. Chiang, C.K., Fincher, C.R., Park, Y.W., Heeger, A.J., Shirakawa, H., Lois, E.J., Gau, S.C., MacDiarmid, A.G., Synthesis of electrically conducting polymers, Phys. Rev. Lett., 39, 1098-1101, 1977.

55. Baughman, R.H., Bredas, J.L., Chance, R.R., Elsenbaumer, R.L., Shacklette, L.W., Structural basis for semiconducting metallic polymer/dopant systems, Chem. Rev., 82, 209-222, 1982.

56. Mihaly, G., Vancso, G., Pekker, S., Janossy, A., Electric properties of Iodine doped polyacetylene, Synthetic metals, 1, 357-362, 1979-80.

57. Diets, W., Cukor, P., Rubner, M., The effect of structural variables on the conductivity of iodine doped polyacetylene, A.C.S. Org. Coat. Plast. Chem., 43, 867-871, 1980.

58. Chen, S., Huang, C., Conductivity variations of Iodine and tungsten hexachloride doped polyacetylene under applied voltages, Die. Angew. Makromoleculare Chemie, 150, 171-178, 1987.

59. Chiang, C.K., Heeger, A.J., MacDiarmid, A.G., Synthesis structure and electrical properties of doped polyacetylene, Ber. Bunsenges. Phys. Chem. 83, 404-417.

60. Naarman, H., Synthesis of new conducting polymers, Synthetic metals, 17, 223-228, 1987.

61. Naarman, H., Theophilou, N., New process for the production of metal like, stable polyacetylene, Synthetic metals, 22, 1-8, 1987.

62. Zurer, P., Organic polymer exhibiting copper like conductivity developed, Chemical and Engineering News, 20-21, June 1987.

63. Basescue, N., Liu, Z., Moses, D., Heeger, A.J., Naarman, H., Theophilou, N., High electrical conductivity in doped polyacetylene, Nature, 327, 403-405, June 1987.

64. Schimell, T., Rieb, W., Greiner, J., Denninger, G., Schwoerer, M., DC-conductivity of a new type of highly conducting polyacetylene, Solid State Commn., 65(11), 1311-1315, 1988.

65. Muller, H.K., Hocker, J., Menke, K., Ehinger, K., Roth, S., Long term conductivity decrease in polyacetylene samples, Synthetic metals, 10, 273-280, 1985.

66. Druy, M.A., Rubner, M.F., Walsh, S.P., An experimental approach towards the synthesis and characterisation of environmentally stable conducing polymers, Synthetic metals, 13, 207-217, 1986.

67. Galvin, M.E., Wnek, G.E., Electrically conductive polymer composites: polymerisation of acetylene in polyethylene, Polymer, 23, 795-797, 1982.

68. Schoch, K.F., Sadhir, R.K., Conductive polyacetylene blends, Ind. Eng. Chem. Res., 26, 678-680, 1987.

69. Chiang, J.C., Smith, P., Heeger, A.J., Wundl, F., Electrically conductive polyacetylene fibres through polymerisation in carrier gels, Polymer communications, 29, 161-162, 1988.

70. Edwards, J.H., Feast, J.W., Bott, D.C., New routes to conjugated polymers : A two step route to polyacetylene, Polymer, 25, 395-398, 1984.

71. Bott, D.C., Brown, C.S., Edwards, J.H., Feast, W.J., Parker, D., Winter, J.N., Some aspects of the two step Durham route to polyacetylene, Mol. Cryst. Liq. Cryst., 117, 9-14, 1985.

72. Kahlert, H., Leising, G., Properties of $(CH)_x$ fibres and films prepared from

BTFM -TCDT, Mol. Cryst. Liq. Cryst., 117, 1-8, 1985.

73. Feast, W.J., Winter, J.N., An improved synthesis of polyacetylene, J. Chem. Soc. Chem. Commn., 202-203, 1985.

74. Swager, T.M., Dougherty, D.A., Grubbs, R.H., Strained rings as a source of unsatturation : polybenzvalene, a new soluble polyacetylene precursor, J.Am.Chem.Soc., 110, 2973-2974, 1988.

75. Enkelmann, V., Muller, W., Wegner, G., Structure, morphology and techniques of chemical modification of polyacetylene, Synthetic metals, 1, 185-192, 1979/80.

76. Diets, W., Cukor, P., Rubner, M., Jopson, H., Stability and stabilisation of polyacetylene, polyphenylacetylene and acetylene/phenylacetylene copolymers, Synthetic metals, 4, 199-210, 1982.

77. Wegner, G., Polymers with metal-like conductivity, Angew. Chem. Int. Eng. Ed., 20, 361-381, 1981.

78. Chien, J.C.W., Wnek, G.E., Karasz, F.E., Hirsch, J.A., Electrically conducting acetylene-methylacetylene copolymers. Synthesis and properties, Macromolecules, 14, 479-485, 1981.

79. Rutledge, T.F., Acetylenes and allenes, Reinhold book, New York, 1969.

80. Chien, J.C.W., Polymerisation of acetylene, J.Polym.Sci. Polym.Lett.Ed., 18, 45-50, 1980.

81. Galvin, M.E., Wnek, G.E., Towards the synthesis of block copolymers via anionic to Ziegler/Natta transformation reactions., Polymer bulletin, 13, 109-114, 1985.

82. Galvin, M.E., Wnek, G.E., Towards the synthesis of block copolymers via anionic to Ziegler/Natta transformation reactions, Polymer preprints, 24 (2), 14-15, 1983.

83. Dandreaux, G.F., Galvin, M.E., Wnek, G.E., Synthesis of graft and block copolymers containing $(CH)_x$ segments, J. Physique colloque, C3, 135-138, 1983.

84. Galvin, M.E., Wnek, G.E., Blends and block copolymers containing polyacetylene, Polymer preprints, 25 (2), 299-230, 1984.

85. Aldissi, M., Soluble conducting polyacetylene block copolymers, J.Chem. Soc. Chem. Commn., 1347-1348, 1984.

86. Aldissi, M., Bishop, A.R., Synthesis of highly conducting polystyrene/ polyacetylene copolymers, Polymer, 26, 622-644, 1985.

87. Aldissi, M., Bishop, A.R., Electrochemistry of polyacetylene block copolymers, Synthetic Metals, 14, 13-18, 1986.

88. Aldissi, M., Physical characteristics of diblock polyacetylene copolymers : processability-conductivity correlation, Synthetic metals, 17, 229-234, 1987.

89. Aldissi, M., Polyacetylene block copolymers, Synthetic metals, 13, 87-100, 1986.

90. Aldissi, M., Physical properties, electrochemistry and environmental

stability of polyacetylene copolymers and composites, Synthetic metals, 15, 141-153, 1986.

91. Galvin, M.E., Wnek, G.E., Block copolymers containing polyacetylene units, Mol. Cryst. Liq. Cryst, 117, 33-37, 1985.

92. Galvin, M.E., Wnek, G.E., Characterisation of polyacetylene/low density polyethylene composites prepared by in-situ polymerisation, J. Polym. Sci. Polym. Chem. Ed., 21, 2727-2737,1983.

93. Ambegaokar, V., Halperin, B.I., Langer, J.S., Hopping conductivity in disordered systems, Physical Review B, 4, 2612-2620, 1971.

94. Nigrey, P.J., MacInnes, D., Nairns, D.P.,MacDiarmid, A.G., Lightweight rechargable storage batteries using polyacetylene as a cathode active material, J. Electrochemical Soc, 128, 1651-1654, 1981.

95. Armes, S.P., Vincent, B., White, J.W., A novel route for producing soluble polyacetylene-polyisoprene block copolymers. J. Chem. Soc. Chem. Commn., 1525-1527, 1986.

96. Luttinger, L.B., Hydridic reducing agent- Group VIII metal compound : A new catalyst system for the polymerisation of acetylene, J. Org. Chem., 27, 1591-1596,1962.

97. Dias, A.J., McCarthy, T.J., Poly(acetylene-co-ethylene) via isomerisation of poly(1,3-butadiene), Macromol.,18, 869-871, 1985.

98. Dias, A.J., McCarthy, T.J., Poly(acetylene-co-ethylene) via isomerisation of poly(1,3-butadiene), Polymer preprints, 26 (1), 162-163, 1985.

99. Baker, G.L., Bates, F.S., Soluble polyacetylene graft copolymers, Macromolecules, 16, 704-707, 1983.

100. Baker, G.L., Bates, F.S, Polyacetylene single crystals, Macromolecules, 16, 1013-1015, 1983.

101. Baker, G.L., Bates, F.S, Synthesis of polyacetylene block/graft copolymers, Macromolecules, 17, 2619-2626, 1984.

102. Baker, G.L., Bates, F.S, Soluble polyacetylene, J.Phys.Colloq., C3, 11-16, 1983.

103. VanNice, F.L., Bates,F.S., Baker, G.L., Carroll, P.J., Patterson, G.D., Light scattering from solubilised polyacetylene, Macromolecules, 17, 2626-2629, 1984.

104. Maricq, M.M., Waugh, J.S., MacDiarmid, A.G., Shirakawa, H., Heeger, A.J., ^{13}C nmr resonances of cis and trans polyacetylene, J.Am.Chem.Soc., 100, 7729-7730, 1978.

105. Marvel, C.S., Sample, J.H., Rov, M.F., The structure of vinyl polymers 1-Polyvinyl halides, J.Am.Chem.Soc., 61, 3241-3244 , 1939.

106. Kise, H., Dehydrochlorination of poly(vinylchloride), J.Polym.Sci. Polym.Chem.Ed., 20, 3189-3197, 1982.

107. He, F., Kise, H., Dehydrochlorination of vinylidene chloride/ vinyl chloride copolymer, J.Polym.Sci.Polym.Chem.Ed., 21, 1729-1740, 1983.

108. Kise, H., Ogata, H., Phase transfer catalysis in dehydroflourination of poly(vinylidene flouride) by aqueous sodium hydroxide solution, J.Polym.Sci.Polym.Chem.Ed., 21, 3443-3451, 1983.

109. Destri, S., Catellani, M., Bolognesi, A., Soluble graft polyacetylene: a new synthetic route, Makromol.Chem, Rapid Commn., 5, 353-358, 1984.

110. Tubino, R., Dorsinville, R., Lann, W., Alfano, R., Birman, J., Destri, S., Catellani, M., Bolognesi, Porzio, W., Optical properties and photoexcitation of a novel form of soluble polyacetylene, Physical Review B., 30 (11), 6601-6605, 1984.

111. Porzio, W., Destri, S., Catellani, M., Bolognesi, Meille, S., Pedemonte, E., The morphology and structure of polyacetylene-polyisoprene graft copolymer films, Mol.Cryst.Liq.Cryst., 117, 71-74, 1985.

112. Piaggio, P., An infra-red spectroscopic study of a grafted polyacetylene copolymer, Mol.Cryst.Liq.Cryst., 117, 311-314, 1985.

113. Bolognesi, A., Destri, S., Catellani, M., Synthesis of graft polyacetylene copolymers, Mol.Cryst.Liq.Cryst., 117, 29-32, 1985.

114. Bolognesi, A., Catellani, M., Destri, S., Porzio, W., Synthesis and characterisation of a comblike polyacetylene copolymer, Polymer, 27, 1128-1130, 1986.

115. Cuniberti, C., Piaggio, P., Dellepiane, G., Catellani, M., Piseri, L., Porzio, W., Tubino, R., Soluble polyacetylene: evidence for aggregation in solution, Makromol. Chem. Rapid Commn., 7, 471-476, 1986.

116. Cuniberti, C., Fuso, S., Piaggio, P., Dellepiane, G., W., Tubino, R., Orientational order in particles of solubilised polyacetylene, Synthetic Metals, 21, 313-318, 1987.

117. Siove, A., Fontanille, M., Activite de complexes macromoleculaires a base de titane et de lithium en polymerisation Ziegler/Natta de l'ethylene, European Polymer Journal, 17, 1175-1183, 1981

118. Kminek, I., Trekoval, J., A soluble graft copolymer of polyacetylene, Makromol. Chem. Rapid Commn., 5 (1), 53-55, 1984.

119. Pfleger, J., Kminek, I., Trekoval, J., Electrical properties of a soluble copolymer of polyacetylene, Materials Science, X (1-2), 213-216, 1984.

120. Szwark, M., J.Polym.Sci, Polymerisation of methylmethacrylate initiated by an electron transfer to the monomer, 22, 189-191, 1956

121. British Patent, GB 2 107 331 A, The preparation of acetylene copolymers.

122. Han, C.C., Katz, T.J., A procedure identifying a polyacetylene initiator of olefin metathesis, The reactivities of metal carbenes towards alkenes and alkynes, Organometallics, 4, 2186-2195, 1985.

123. Ramakrishnan, S., Chien, J.C.W., Acetylene-cyclopentene copolymers, Polymer Bulletin, 18, 425-432, 1987.

124. Schrock, R.R., Feldman, J., Cannizzo, L.F., Grubbs, R.H., Ring opening polymerisation of norbornene by a living tungsten alkylidene complex, Macromolecules, 20, 1172-1174, 1988.

125. Cannizzo, L.F., Grubbs, R.H., Block copolymers containing monodisperse segments produced by ring opening metathesis polymerisation of cyclic olefins, Macromolecules, 21, 1961-1967, 1988.

126. Murdzek, J.S., Schrock, R.R., Low polydispersity homopolymers and block copolymers by ring opening of 5,6-dicarbomethoxynorbornene, Macromolecules, 20, 2640-2642, 1987.

127. Kress, J., Osborn, J.A., Amir-Ebrahaim, V., Ivin, K.J., Rooney, J.J., Metathesis polymerisation of norbornene and derivatives. Relative stability of tungstcyclobutane intermediates and kinetics of their ring opening to form tungsten carbene complexes, J.Chem.Soc.Chem.Commn., 1164-1166, 1988.

128. Krouse, S.A., Schrock, R.R., Preparation of polyacetylene chains in low polydispersity diblock and triblock copolymers, Macromolecules, 21, 1885-1888, 1988.

129. Masuda, T., Hasegawa, K., Higashimura, K., Polymerisation of phenylacetylenes catalysed by WCl_6 and $MoCl_5$, Macromolecules, 7 (6), 728-731, 1974.

130. Hasegawa, K., Masuda, T., Higashimura, K., Polymerisation of phenylacetylenes: Copolymerisation catalysed by WCl_6, Macromolecules, 8 (3), 255-259, 1975.

131. Masuda, T., Sasaski, N., Higashimura, K., Polymerisation of phenylacetylenes: Structure and properties of polyphenylacetylenes obtained from WCl_6 and $MoCl_5$, Macromolecules, 8 (6), 717-721, 1975.

132. Masuda, T., Thie, K., Sasaski, N., Higashimura, K., Polymerisation of phenylacetylenes: Effect of $SnPh_4$ and initiation mechanism in the WCl_6 catalysed polymerisation of phenylacetylene, Macromolecules, 9 (4), 661-664, 1976.

133. Sasaski, N., Masuda, T., Higashimura, K., Polymerisation of phenylpropyne catalysed by $WCl_6/SnPh_4$, Macromolecules, 9 (4), 664-667, 1976.

134.. Higashimura, K., Deng, Y., Masuda, T., Polymerisation of 2-hexyne and higher 2-alkynes catalysed by $MoCl_5.SnPh_4$, Macromolecules, 15, 234-238, 1982.

135. Kunzler, J., Percec, V., Living non-conjugated polyacetylenes, Polym. Preprints (A.C.S. Div. Poly. Chem.), 28 (2), 252-253, 1987.

136. Katz, T.J., Polymerisation of acetylenes and cyclic olefins induced by metal carbynes, J.Am.Chem.Soc., 106, 2659-2665 , 1984.

137. Woon, P.S., Farona, M.F., Polymerisation of acetylenes catalysed by arene group six B tricarbonyls, J.Polym.Sci.Polym.Chem.Ed., 12, 1749-1757, 1974.

138. Voronkov, M.G., Pukhernarevich, V.B., Sushchinskaya, S., Annekova, V., Andreeva, N.J., Polymerisation of acetylene and monosubstitutes in the presence of halides and oxo-halides of molybdenum and tungsten,

J.Polym.Sci.Polym.Chem. Ed. ,18, 53-57, 1980.

139. Deits, W., Cukor, P., Rubner, M., Jopson, H., Physical chemical and electrical properties of various preparations of polyacetylene, Journal of electronic materials, 10 (4), 683-701, 1981.

140. Aldissi, M., Linaya, C., Sledz, J., Schue, F., Giral, L., Fabre, J.M., Rolland, M., New catalyst systems for the polymerisation of acetylene, Polymer, 23, 243-245, 1982.

141. Schue, F., Aldissi, M., Dubois, J.C., Giral, L., Rolland, M., Sledz, J., Polymerisation of acetylene with new catalysts and doping agents, morphology and electrical conductivity of the doped polyacetylene films, IUPAC. Macromolecular micro-symposia, 28th, 417.

142. Thiophilou, N., Munardi, A., Aznar, R., Sledz, J., Schue, F., Naarman, H., Polymerisation of acetylene in the presence of a tungsten based catalyst and geometric structure and electrical properties and morphology of the polymer, European Polymer Journal, 23 (1), 15-20, 1987.

143. Schue, F., Aldissi, M., Polymerisation of acetylene with new catalysts, J.Physique Colloque, C3 (6), 17-19, 1983.

144. Rolland, M., Aldissi, M., Schue, F., Physical properties of polyacetylene films doped with $MoCl_5$ and WCl_6, Polymer, 23, 834-838, 1982.

145. Amass, A.J., Tuck, C.N., The kinetics of the polymerisation of cyclopentene with $WCl_6/AliBu_3$, European Polymer Journal, 14, 812-823, 1978.

146. Amass, A.J., Zurimendi, J.A., Kinetics of metathesis polymerisation, J.Molecular Catalysis, 8, 243-248, 1980.

147. Ito, T., Shirakawa, H., Ikeda, S., Simultaneous polymerisation and formation of polyacetylene film on the surface of a concentrated soluble Ziegler type catalyst solution, J.Polym.Sci.Polym.Chem.Ed., 12, 11-20, 1974.

148. J.C. McGrath (Ed.), Anionic Polymerisation, Kinetics mechanisms and synthesis, ACS symposium series, 166, 1981.

149. Amass, A.J., Gregory, D., British polymer journal, Anionic to metathesis transformation polymerisation, 19, 263-268, 1987.

150. Stowell, J.A., Amass, A.J., Beevers, M.S., Farren, T.R., Studies in electro-active polymers 2: Makromol.Chem, 188, 1635-1639, 1987.

151. Amass A.J., Zurimendi, J.A., Termination reactions in metathesis polymerisation, European polymer journal, 17, 1-6, 1981.

152. Imaizumi, F., Matsumoto, S., Kotani, T., Enyo, K., Ring opening block copolymerisation of norbornene derivatives with cycloalkenes, Japan Kokai, 77 51500 (Cl. C08G6/08), 25th April, 1977.

153. Ofstead, E.A., Calderon, N., Equilibrium ring opening polymerisation of mono and multicyclic unsatturated monomers, Makromol Chem, 154, 21-34, 1972.

154. Han, C.C., Katz, T.J., A procedure identifying a polyacetylene initiator of olefin metathesis. The reactivities of metal carbenes towards alkenes and alkynes, Organometallics, 4, 2186-2195, 1985.

155. Hein, P.R., J.Polym.Sci.Polym.Chem.Ed., Ring opening polymerisation of cyclo-olefins, 11, 163-173, 1973.

156. Sondheimer, F., BenEfraim, D., Wolovsky, R., Unsatturated macrocyclic compounds 17: The prototropic rearrangements of linear 1,5-enynes to conjugated polyenes. Synthesis of vinylogs of butadiene, J.Am.Chem.Soc., 83, 1675-1685, (1961).

157. Amass, A.J., Zurimendi, J.A., Non-equilibrium molecular weight studies in the polymerisation of cyclopentene, Polymer, 23, 211-214, 1982.

158. Tosi, C., Ciampelli, F., Dall'Asta, G., Spectroscopic methods for the analysis of polyalkenamers, J.Polym.Sci.Polym.Phys.Ed., 11, 529-538, 1973.

159. Pampus, G., Witte, J., Hoffman, M., Transposition cis-trans et polymerisation greffee des polyenes a l'aide de catalyseurs au tungstene, Rev.Gen. Caoutchouc Plast., 47 (11), 1343-1347, 1970.

160. Shurncliff, W.A., Ballard, S.S., Polarized Light, Van Nostrand Momentum books, New York, 1964.

161. Kerr, J., Phil. Mag, A new relation between electricity and light-dielectrified media birefringence, 50, 337-348,1875.

162. LeFevre, C.G., LeFevre, R.J.W., Molecular polarisibility: the measurement of molecular Kerr constants in solution, J.Chem.Soc., 4041-4050, 1953.

163. LeFevre, C.G., LeFevre, R.J.W., p339-452 in Physical methods in chemistry part IIIC: polarimetry, Wiley Interscience, 1972.

164. Fredericq, E., Houssier, C., Electric dichroism and Electric birefringence, Clarendon Press, Oxford, 1973.

165. Foweraker, A.R., Jennings, B.R., Electro-optic decay analysis for polydisperse systems III: experimental data for rods, Advances in molecular relaxation processes, 8, 103-110, 1976.

166. Tricot, M., Houssier, C., Electro-optical properties of synthetic polyelectrolytes, p43-90 in Polyelectrolytes (Frisch Ed.), Technomic publishers, West Port, 1976.

167. Matsumoto, M., Watanabe, H., Yoshioka, K., Transient electric birefringence of rigid molecules in solution under the action of a rectangular pulse and a reversing pulse, J.Physical Chemistry., 74, 2182-2188, 1970.

168. O'Konski, C.T., Zimm, B.H., New method for studying electrical orientation and relaxation in aqeuous colloids, Science, 111,, 113-116, Feb. 1950.

169. Houssier, C., Kuball, H.G., Electro-optcal properties of nucleic acids and nucleoproteins III. Kramer-Kronig relationships in linear birefringence and dichroism, Biopolymers, 10, 2421-2433, 1971.

170. Trimm, H.H., Parslow, K., Jennings, B.R., Electric birefringence, Journal of Chemical education, 61 (12), 1114-1118, 1984.

171. M.S. Beevers, Khanarian, G., Measurement of Kerr constants of conducting liquids, Austrailian journal of chemistry, 32, 263-269, 1979.

172 Beevers, M.S., Elliot, D.A., Williams, G., Static and dynamic Kerr effect

studies of glycerol in its highly viscous state, J.Chem.Soc. Faraday II, 76, 112-121, 1980.

173 Ravey, J.C., Houssier, C., Simultaneous measurement of dichroism and birefringence on suspensions of absorbing particles, p.67-76 in Electro-optics and dielectrics of macromolecules and colloids (Ed. Jennings, B.R.), Plenum press, New York, 1979.

174. Jennings, B.R., Brown, B.L., Aggregation of poly-L-proline, Biopolymers II, 9, 1119-1124, 1970.

175. Williams, G., Watts, D.C., Non-symmetrical dielectric behaviour arising from a simple decay function, Trans. Faraday Soc., 66, 80-85 , 1970.

176. Williams, G., Watts, D.C., Dev, S.B., North, A.M., Further considerations of non-symmetrical dielectric relaxation behaviour arising from a simple empirical decay function, Trans. Faraday Soc., 67, 1323-1335, 1971.

177. Katz, T.J., Lee, S.J., Initiation of acetylene polymerisation by metal carbenes, J.Am.Chem.Soc., 102 (1), 422-424, 1980.

178. Clarke, T.C., Yannoni, C.S., Katz, T.J., Mechanism of the Ziegler/Natta polymerisation of acetylene, Gov. Report Announce Index, 84, (8), 1984.

179. Ikeda, S., Tamaki, A., IUPAC International symposium on macromolecular chemistry, Tokyo-Kyoto, preprint 1-244, 1966.

180. Ito, T., Shirakawa, H., Ikeda, S., Thermal cis-trans isomerisation and decomposition of polyacetylene, J.Polym.Sci.Polym.Chem.Ed., 13, 1943-1950, 1975.

181. Hothi, H.S., Final Year Project, Department of applied chemistry and chemical engineering, University of Aston in Birmingham, Investigation of benzene formation during the polymerisation of acetylene, 1989.

182. Gregory, D., Ph.D. Thesis, University of Aston in Birmingham, "Block copolymer formation by transformation reactions", 1984.

183. Percec, V., Recent developments in cationic polymerisation p.96-130 in Applied polymer science, American chemical society, 1985.

184. Patat, F., Sinn, H., Zum ablauf der niederdruck polymerisation der α-olefine, Angewante Chemie, 70 (16), 496-500, 1958.

185. Controlled ring opening metathesis polymerisation by tungsten and molybdnum complexes, J.Molecular catalysis, 46, 243-253, 1988.

186. Beevers, M.S., Elliot, D.A., Williams, G., Molecular motion in samples of poly(propylene glycol) studied using dielectric and Kerr effect relaxation, Polymer, 21, 13-20, 1980.

187. Beevers, M.S., Garrington, D.C., Williams, G., Dielectric and dynamic Kerr effect studies of poly(n-butyl isocyanate) and poly(n-octyl isocyanate) in solution, Polymer, 18, 540-546, 1977.

188. Mumby, S.J., Experimental and theoretical investigations of the dielectric and electro-optical properties of polycarbazoles and polysiloxanes, PhD. Thesis, Aston University, 1983.

APPENDIX 1

DESIGN AND CONSTRUCTION OF THE REVERSED VOLTAGE PULSE GENERATOR

A1.1 Introduction

An essential requirement for the measurement of electro-optical anisotropy using a nulled pulse technique is that a short duration pulse of HT voltage must be applied to the electrodes of the Kerr cell. It is also essential that the rise and decay times of the pulse are much shorter than the relaxation times which characterise the optical response of the material under test, if meaningful information is to be derived from the optical transients. As no apparatus was readily available that satisfied these requirements, a reversed voltage pulse generator was designed and built in the laboratory.

A1.2 The high tension circuit

A Teltron H.T. generator unit, driven by a transistor oscillator circuit was used as the source of H.T voltage. This unit provided two equal magnitude outputs of opposite polarity which could be varied in the range 0 to ± 2.5kV. The profile of the electrical pulse which was applied to the Kerr cell was controlled by the pulse former unit shown in figure A1.1. The outputs of the H.T. generator (+HT, -HT and earth) were used to charge two capacitors C_1 and C_2 (figure A1.2) which could be connected to the "high electrode" of the Kerr cell by the action of two reed switches RS1 and RS2. The +HT voltage was supplied through RS1 and the -HT voltage through RS2. A third reed switch, RS3, which closed after a suitable time delay, connected the high electrode to earth and allowed rapid termination of the electrical signal. The magnitude of the output voltage of the pulse former could be monitored by connecting a digital voltmeter to the HT/1000 output of the pulse former unit.

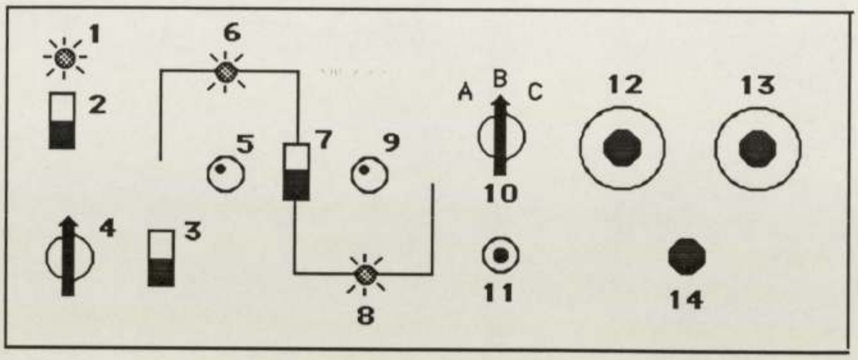

FRONT VIEW

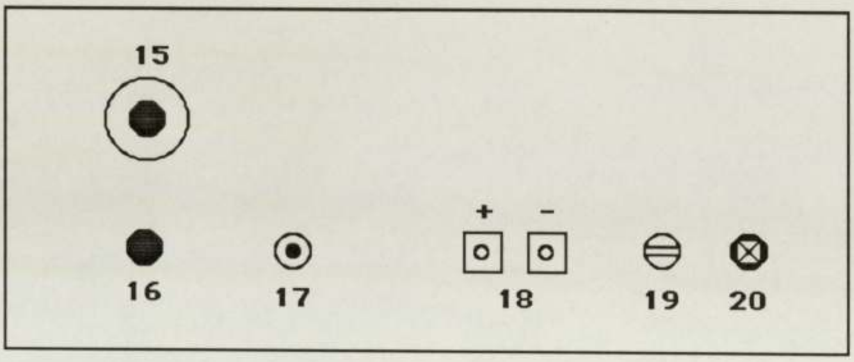

REAR VIEW

Figure A1.1 Controls and connections for the reversed voltage pulse generator

Key

1 Power-on LED (D1 fig.A1.7)

2 Mains on/off

3 Select single pulse or repeated pulse (S2)

4 Set frequency of repeated pulse (SS1)

5 Set duration of positive voltage (VR1)

6 Positive HT on indicator LED (D1 fig A1.3)

7 "Single shot" switch (S1)

8 Negative HT on indicator LED (D2 fig A1.3)

9 Set duration of negative voltage (VR3)

10 Select trigger source (SS2)

11 Trigger output for oscilloscope

12 Positive HT input

13 Negative HT input

14 Earth

15 HT output to Kerr cell

16 Earth electrode of Kerr cell

17 HT voltage/1000 output to digital voltmeter

18 24V output to Teltron HT unit

19 Fuse (2A)

20 ~240V AC mains

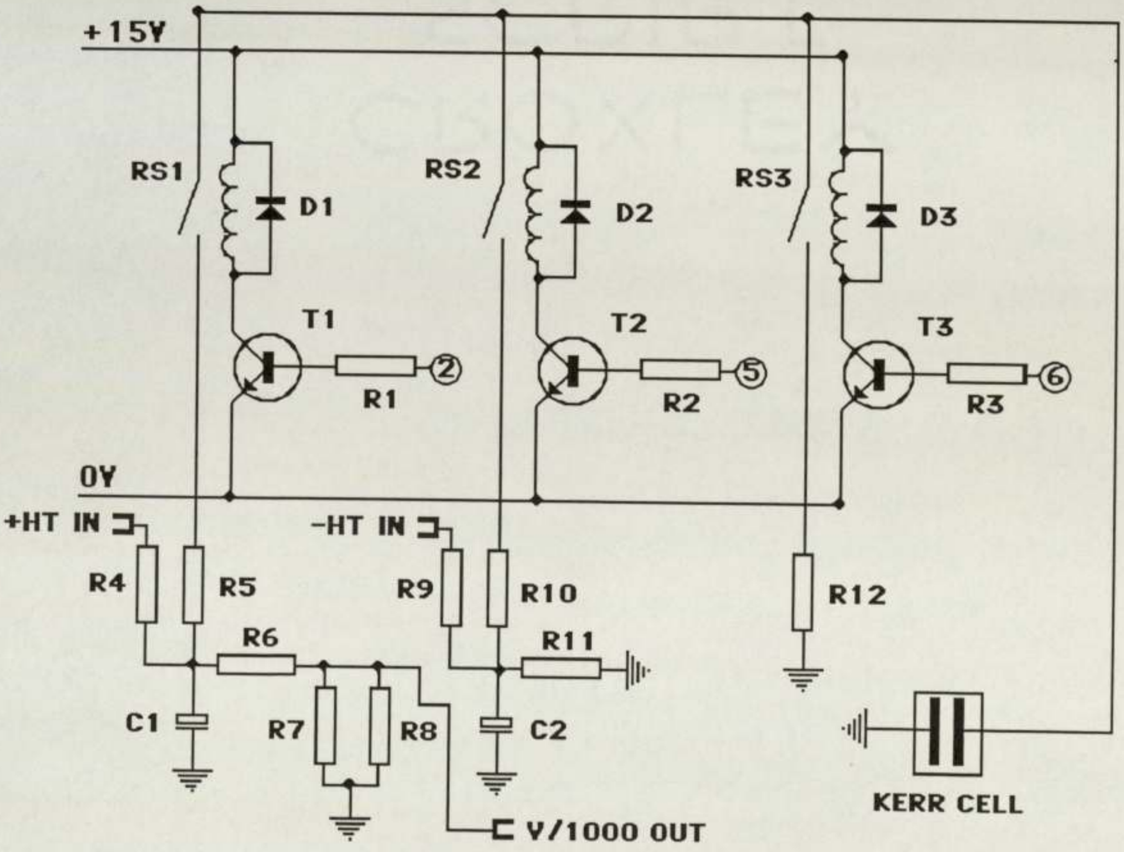

Figure A1.2 The High Tension Circuit

A1.3 The timer circuit

To produce an electrical signal with a reversed pulse profile similar to that shown in figure 6.4, the reed switches RS1, RS2 and RS3 had to be operated at precise times. To avoid excessive currents, it was essential that at any given time during the pulse sequence only one HT reed switch at a time was closed. It was also desirable that the time of application of the positive and negative portions of the pulse could be varied independently of one another. These requirements were met by the construction of a timer circuit (figure A1.3) based on a series of interconnected 74LS123 monostable integrated circuits, T, A-G (figure A1.4). The action of the timer circuit may be demonstrated by considering the blocked schematic of the timer circuit (A1.4) together with the timing diagram shown in figure A1.5.

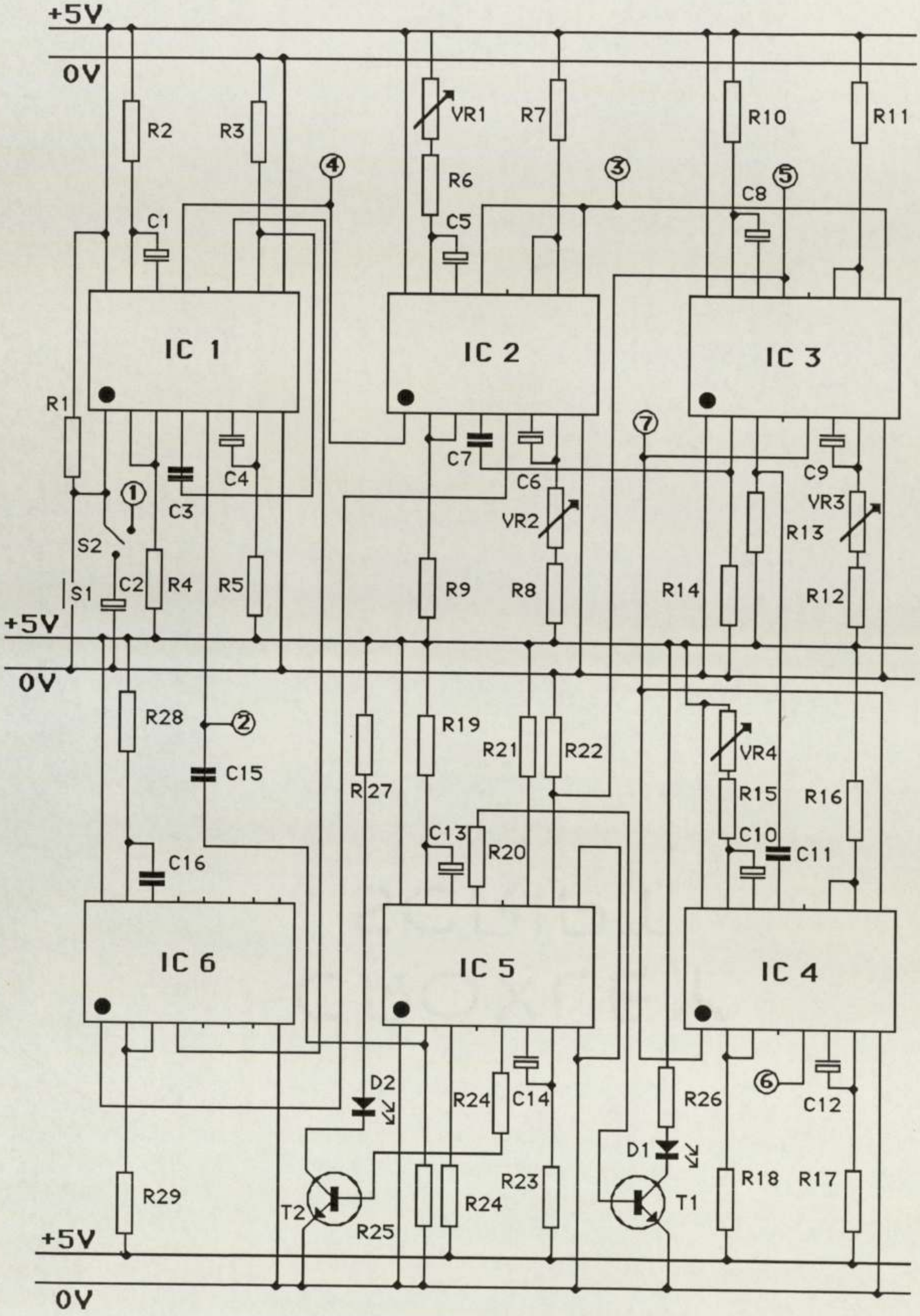

Figure A1.3 The timer circuit

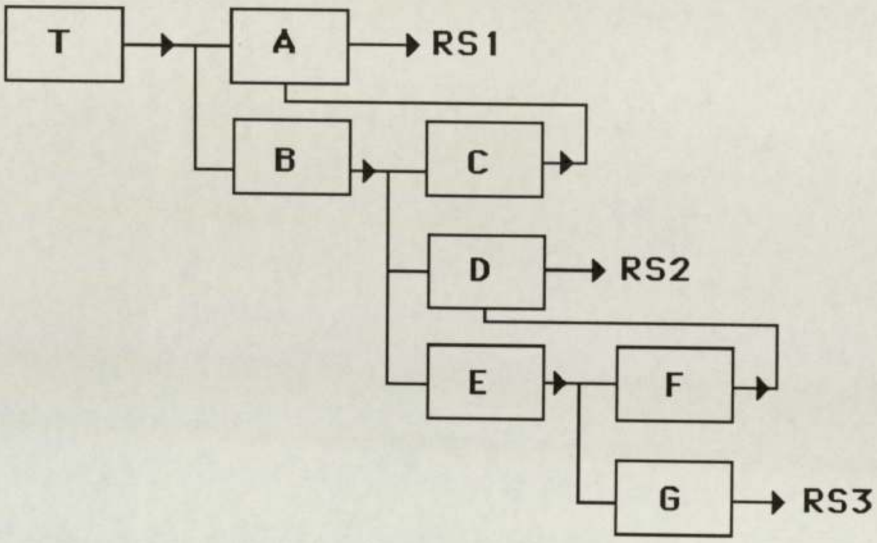

Figure A1.4 Simplified diagram showing the action of the timer circuit

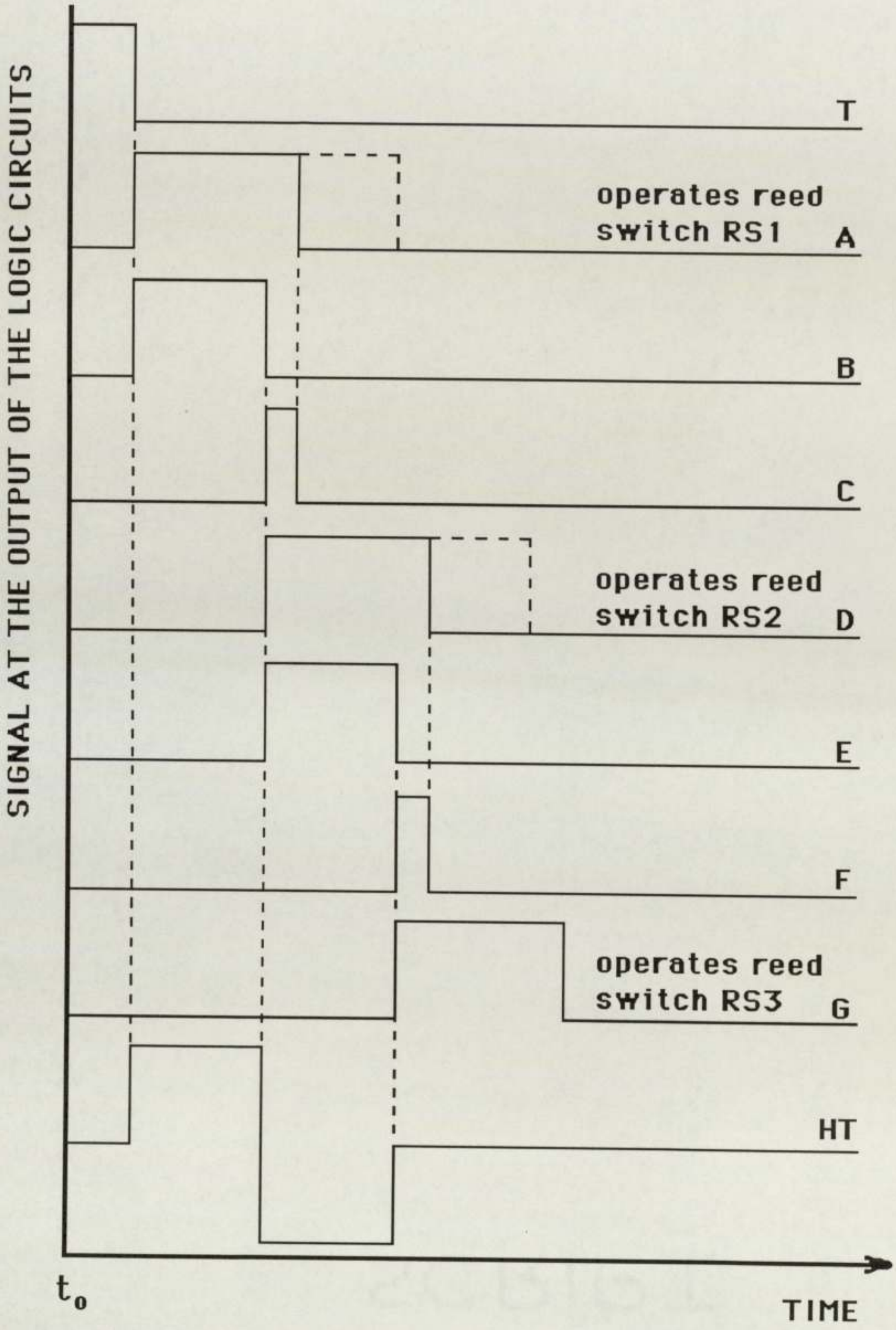

Figure A1.5 Timing diagram showing the status of the outputs of the monostables (**T**, **A**-**G**) and the high voltage pulse (**HT**) after triggering monostable **T** at time t_o.

When the trigger monostable **T** is activated, a square wave pulse of voltage is produced at the output. The trailing edge of this pulse simultaneously triggers monostables **A** and **B**. The output of monostable **A**, after amplification by T1, closes reed switch RS1, thus applying the positive HT potential to the active electrode of the Kerr cell. The duration of the pulse of voltage at the output of monostable **A** is set at an arbitary long value (186ms) corresponding to the maximum value attainable using this component. The duration of the positive HT voltage applied to the Kerr cell corresponds to the duration of the square wave pulse at the output of **B** and this can be varied by VR1 (Figure A1.3). The output of monostable **B** is connected to the trigger inputs of monostables **C**, **D** and **E**. The trailing edge of the pulse output from **B**, simultaneously triggers units **C**, **D** and **E**. The output of **D** is amplified by T2 and closes RS2 to apply the negative HT potential to the Kerr cell. To prevent direct connection between the output terminals of RS1 and RS2, a short time delay (monstable **C**) was introduced which retards the disconnection of RS1 so that the operation of RS2 occurs at the same time as RS1 is disconnected. The duration of the square wave pulse produced by unit **C** is preset by adjusting VR2 (located on the top of the logic circuit board). The output of monostable **C** is connected to the reset input of monostable **A** so that, when the output of monostable **C** terminates, the pulse at the output of unit **A** is also terminated, thereby opening RS1 and disconnecting the positive HT supply from the cell. The time of application of the positive supply to the Kerr cell is therefore governed by the action of monostable **B** and may be adjusted using VR1. In a similar manner the duration of the negative voltage pulse is controlled by monostable **E** and may be varied using VR3. When the pulse at the output of **E** terminates, monostable **G** is activated which closes RS3, rapidly grounding the high-voltage electrode of the Kerr cell. Monostable **F** provides a time delay for the opening of relay RS2. The duration of the pulse at the output of **F** is preset by VR4 (located on the top of the logic circuit board).

The monostables **H** and **I** are triggered from the outputs of **A** and **D** respectively and control the indicator lights 6 and 8 in figure A1.1. Monostable **J** does not contribute to the timing circuit but is included to provide the reset conditions required by the 74LS123 devices.

The rotary switch SS2 selects the signal used to trigger the oscilloscope. By selecting one of the signals marked A,E or G in the timing diagram (figure A1.5) the sweep of the beam along the horizontal axis of the oscilloscope can be initiated at times which correspond to the application of the positive voltage, the negative voltage or the point at which the cell is grounded, respectively.

A1.4 The Clock Circuit

When switch S2 (No. 3 in figure A1.1) is in the "single pulse" position, the input of the monostable **T** is connected to a 10μF capacitor which may be discharged through switch S1 (No. 7 in figure A1.1) thereby triggering monostable **T**. When S2 is in the "repeated pulse" position, the input of monostable **T** is connected, at point (1), to the clock circuit (figure A1.6).

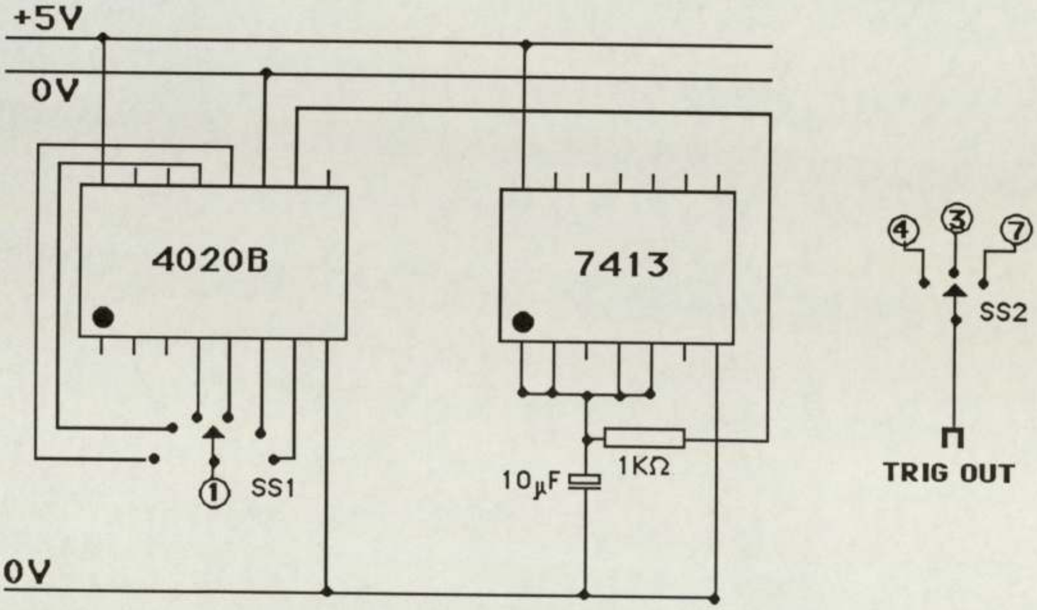

Figure A1.6 The clock circuit

The clock circuit comprises a Schmitt trigger oscillator (7413) and a 14 bit binary counter (4020B). A repeating square wave pulse, approximately 17ms in duration, is generated at the output of the oscillator. This signal drives the counter which provides 12 "divided-by two" outputs. Selector switch, SS1 (switch 4 in figure A1.1), connects monostable **T** to one of six of these outputs thereby allowing the timer circuit to be triggered repeatedly at rates between 1 pulse/250ms and 1 pulse/9s.

A1.5 Power Supplies

Three separate DC power supplies are required to power the pulse generator (figure A1.7). The mains supply (240V AC) is passed through a 2A fuse and a mains switch to the primary windings of three transformers connected in parallel. The outputs of the transformers (6V AC, 15V AC and 30V AC) are connected to three separate rectifier circuits (figure A1.7). The +5V DC output is used to power the clock and timer circuits. The +15V output of the 7815 rectifier is used to power the reed switches and the "mains on" indicator LED. The third rectifier circuit is based on a RS738 variable output device and its output voltage (24V) is determined by the resistances R2, R3 and R5. This is used to power the Teltron HT unit.

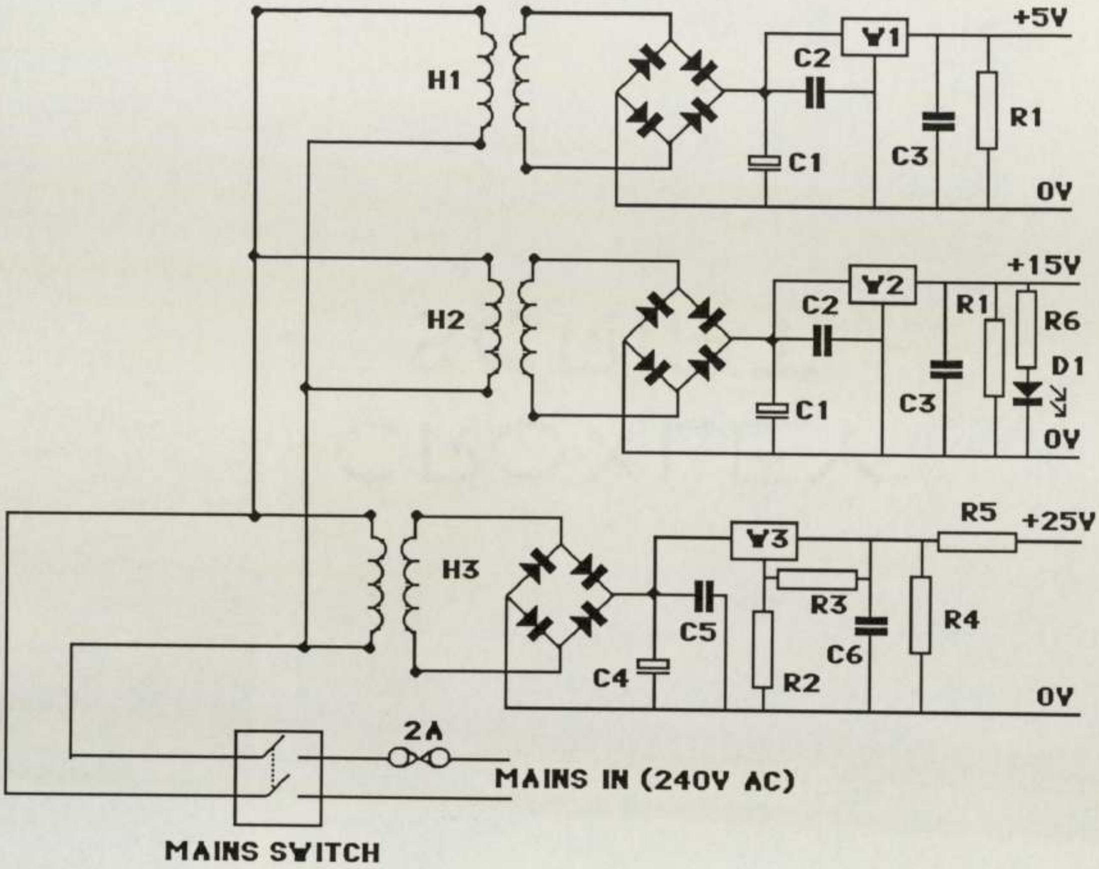

Figure A1.7 Power supplies

A1.6 List of components

A1.6.1 HT circuit (figure A1.2)

Semiconductors

T1,T2,T3 2N3053

D1,D2,D3 signal diodes 1N4148

Resistors

1KΩ	0.125W metal film	R1,R2,R3
12KΩ	2W carbon	R5,R10
1MΩ	1W (composite) carbon	R4,R9
16.8MΩ	1W (composite) carbon	R6,R11

Capacitors

C1	0.01μF 8KV polyester (LCR Components Ltd.)
C2	0.04μF 8KV polyester (LCR Components Ltd.)

Switches

RS1,RS2,RS3	Reed switches DTA 812 (FR Electronics Ltd.)
Coils SD12	(Osmor Electronics Ltd.)

A1.6.2 Timer and Clock circuits

Semiconductors

IC1	74LS123 dual monostable (**T** and **A**)
IC2	74LS123 dual monostable (**B** and **C**)
IC3	74LS123 dual monostable (**D** and **E**)
IC4	74LS123 dual monostable (**F** and **G**)
IC5	74LS123 dual monostable (**H** and **I**)
IC6	74LS123 dual monostable (**J** and **K**)
T1,T2	BC108L
D1	standard 0.2" 10mA LED (red)
D2	standard 0.2" 10mA LED (green)

Resistors (0.125W metal film)

39Ω	R8
560Ω	R15,R26,R27
1KΩ	R3,R4,R6,R7,R9,R11,R12,R14,R16,R18,R21,R22, R25,R28,R29
2.2KΩ	R13
10KΩ	R2,R17,R20,R24
22KΩ	R1,R19,R23
44KΩ	R5,R10

Capacitors

0.1μF polyester	C3,C7,C11,C15,C16
4.7μF tantalum	C6,C10,C12
10μF tantalum	C1,C2,C4,C5,C8,C9,C13,C14

Switches

S1	SPST off/(on) minature
S2	SPST on/on minature
SS1	single-pole rotary switch (6-way)
SS2	single-pole rotary switch (3-way)

A1.6.3 Power supplies

Transformers

H1	2 x 6V/1.6A
H2	2 x 15V/0.2A
H3	2 x 15V/0.2A in series

Semiconductors

W1	RS7805 1A regulator
W2	RS7815 1A regulator
W3	RS783 adjustable regulator
D1	standard 0.2" 10mA LED (red)

Resistors

1KΩ 0.125W metal film	R6
3.2KΩ 0.125W metal film	R3
4.7KΩ 0.125W metal film	R1,R4
57KΩ 0.125W metal film	R2
22KΩ 1W carbon	R5

Capacitors

4700μF electrolytic (12V)	C1
2200μF electrolytic (50V)	C4
0.47μF polyester	C2,C3,C5,C6

APPENDIX 2

COMPUTER PROGRAMS

The computer programs used to analyse the experimental data presented in chapter 8 are listed in this appendix. Each program is accompanied by a brief outline of its function and a list of the parameters required as input. The programs were written in "Applesoft basic" and run on an Apple II computer.

PROGRAM 1

OPTICAL SIMULATOR

This program calculates the normalised intensity of light which emerges from polariser P_2 for the optical arrangement shown in figure 7.7. the program requires the following input:

(i) The angle of the transmission axis of polariser P_1.

(ii) Whether or not a quarter-wave plate is used and if present, the angular position of the fast axis.

(iii) The angle of the transmission axis of the analyser, P_2.

(iv) The optical absorbance, $A_{||}$, for plane polarised light parallel to the direction of the electric field.

(v) The perpendicular absorbance, $A_{\perp}$, for plane polarised light parallel to the direction of the electric field.

(vi) The electrically-induced optical phase retardation, δ.

The program calculates the effect of the optical components on the plane polarised components of a beam of light by employing trigonometric expressions similar to those described in appendix 4. A numerical integration converts the calculated amplitudes of the waveforms into intensities.

```
5       REM
10      REM  KERR EFFECT + DICHROISM SYNTHESIS
20      REM

30      LET N = 200
35      LET DX = 1 / (N)
38      REM  N=NO. OF INTEGRATION STEPS

40      LET PA = 45 :
        LET QW = 45 :
        LET AN = 135
42      REM  INITIAL POSNS OF POLARISER,
44      REM  QUARTER WAVE & ANALYSER
50      REM  AM(1) PARALLEL AMPLITUDE
52      REM  AM(2) PERPENDICULAR AMPLITUDE

60      LET RAD = .0174533
62      REM  CONVERTS DEGREES TO RADIANS

70      LET QW = QW * RAD :
        LET AN = AN * RAD :
        LET R2 =  SQR (2)
80      LET PR = 0
82      REM  PHASE RETARDATION

90      LET AM(1) = 1 / R2 :
        LET AM(2) = AM(1) :
        LET B = AM(1) :
        LET C = AM(2)
100     HOME  :
        VTAB 6 :
        HTAB 2 :
        INVERSE  :
        PRINT " SYNTHESIS OF THE KERR EFFECT AND " :
        PRINT  :
        PRINT  :
        HTAB 9 :
        PRINT " ELECTRIC DICHROISM " :
        NORMAL
110     VTAB 21 :
        FLASH  :
        HTAB 9 :
        PRINT " ANY KEY "; :
        NORMAL  :
        PRINT "TO CONTINUE "; :
```

```
        HTAB 10
120     GET K$ :
        PRINT
121     HOME  :
        VTAB 1 :
        PRINT "POSN OF POLARISER       <            "; :
        HTAB 25 :
        PRINT PA;"> "; :
        INPUT PA$ :
        IF PA$ = "" THEN
            123
122     PA =  VAL (PA$) :
        GOTO 121
123     LET AM(1) =  COS (PA * RAD) :
        LET AM(2) =  SIN (PA * RAD) :
        LET B = AM(1) :
        LET C = AM(2)
124     VTAB 3 :
        LET QF = 0 :
        PRINT "DO YOU WANT QUARTER-WAVE PLATE ? (Y/N)"; :
        GET K$ :
        PRINT  :
        IF K$ = "Y" THEN
            QF = 1 :
            GOTO 130
125     IF K$ <  > "N" THEN
            124
126     VTAB 3 :
        INVERSE  :
        PRINT " NO QUARTER WAVE RETARDER              " :
        NORMAL  :
        GOTO 150
130     VTAB 3 :
        PRINT "POSN.OF QW FAST AXIS   <                 "; :
        VTAB 3 :
        HTAB 25 :
        PRINT  INT (100 * QW / RAD + .1) /
            100;"> "; :
        INPUT QW$ :
        IF QW$ = "" THEN
            150
140     QW =  VAL (QW$) * RAD :
        GOTO 130
150     VTAB 5 :
        PRINT "ANALYSER TRANS.AXIS     <            "; :
        HTAB 25 :
```

```
          PRINT  INT (100 * AN / RAD + .1) /
              100;"> "; :
          INPUT AN$ :
          IF AN$ = "" THEN
              170
160       AN =  VAL (AN$) * RAD :
          GOTO 150
170       VTAB 7 :
          PRINT "PARALLEL ABSORBANCE    <              "; :
          HTAB 25 :
          PRINT A1;"> "; :
          INPUT A1$ :
          IF A1$ = "" THEN
              190
180       A1 =  VAL (A1$) :
          GOTO 170
190       VTAB 9 :
          PRINT "PERPENDICULAR ABS.     <              "; :
          HTAB 25 :
          PRINT A2;"> "; :
          INPUT A2$ :
          IF A2$ = "" THEN
              208
200       A2 =  VAL (A2$) :
          GOTO 190
208       LET B = AM(1) * (10 ^ ( - A1 / 2)) :
          LET C = AM(2) * (10 ^ ( - A2 / 2))
210       VTAB 11 :
          PRINT "PHASE RETARDATION/DEG  <              "; :
          HTAB 25 :
          PRINT PR / RAD;"> "; :
          INPUT PR$ :
          IF PR$ = "" THEN
              230
220       PR =  VAL (PR$) * RAD :
          GOTO 210
230       REM
240       REM
250       REM
270       REM
300       REM  EVALUATE SINES AND COSINES
302       REM  OF ANGLES ASSOCIATED WITH
304       REM  QUARTER WAVE AND ANALYSER

310       LET SA =  SIN (AN) :
          LET CA =  COS (AN) :
```

```
        LET SQ =  SIN (QW) :
        LET CQ =  COS (QW)
315     IF QF = 0 THEN
            C1 = C * SA :
            LET C2 = B * CA :
            GOTO 435
320     LET C1 =  + C * SA * CQ * CQ
330     LET C2 =  - B * SA * SQ * CQ
340     LET C3 =  + C * SA * SQ * SQ
350     LET C4 =  + B * SA * SQ * CQ
360     LET C5 =  + B * CA * CQ * CQ
370     LET C6 =  + C * CA * SQ * CQ
380     LET C7 =  + B * CA * SQ * SQ
390     LET C8 =  - C * CA * SQ * CQ
400     LET D1 = (C1 + C8)
410     LET D2 = (C2 + C7)
420     LET D3 = (C3 + C6)
430     LET D4 = (C4 + C5)
433     REM
435     REM  DO NUMERICAL INTEGRATION
437     REM  OVER ONE WAVE CYCLE

438     LET IN = 0
439     REM  SET INTENSITY TO ZERO

440     FOR I = 0 TO N :
            LET X = (I / N) * 360 * RAD
450         LET SX =  SIN (X) :
            LET CX =  COS (X)
460         LET SD =  SIN (X - PR) :
            LET CD =  COS (X - PR)
465         IF QF = 0 THEN
                WA = C1 * SX + C2 * SD :
                GOTO 480
470         LET WA = D1 * CX + D2 * CD + D3 *
            SX + D4 * SD
480         LET AS = WA * WA
490         LET IN = IN + AS * DX
500     NEXT
510     LET IN = IN + IN
520     REM
600     REM  OUTPUT THE RESULTS
605     REM

610     PRINT  :
        PRINT  :
```

```
        INVERSE  :
        PRINT " INTENSITY OF LIGHT TRANSMITTED BY THE "
620     PRINT "ANALYSER IS :-" :
        NORMAL  :
        PRINT  :
        PRINT  :
        HTAB 5 :
        PRINT  INT (10000000000 * IN) / 10000000000;
625     PRINT " (";IN * 100;" % TRANS)"
630     VTAB 21 :
        HTAB 5 :
        INVERSE  :
        PRINT " ANOTHER CALCULATION ? (Y/N) "; :
        NORMAL  :
        HTAB 26
640     GET K$ :
        PRINT
650     IF K$ = "Y" THEN
           121
660     IF K$ <  > "N" THEN
           630
670     HOME  :
        END
```

PROGRAM 2

CALCULATION OF DICHROISM

This program evaluates equations 8.6-8.9 and calculates $A_{||}$, $A_{\perp}$, ΔA and $\Delta A/A$. In addition the optical absorbance, $A_{\perp}$ is calculated using equation 6.10. The program requires the following data:

(i) Field-on light-level measured parallel to the direction of the applied electric field.

(ii) Field-off light-level measured parallel to the direction of the applied electric field.

(iii) Field-on light-level measured perpendicular to the direction of the applied electric field.

(iv) Field-off light-level measured perpendicular to the direction of the applied electric field.

(v) Normal absorbance of the solution in the Kerr cell.

```
10      REM  DICHROISM CALC'S FROM
20      REM  EXPL. LIGHT-LEVELS
30      REM
40      REM  EQUATIONS USED ARE :
45      REM
50      REM  A'PARA' = A + LOG(I/I'PARA')
55      REM
60      REM  A'PERP' = A + LOG(I/I'PERP')
65      REM
70      REM  NOTE.MUST USE MATCHED
75      REM  PAIRS OF I/I'PARA' AND
80      REM  I/I'PERP' BECAUSE I
85      REM  IS NOT USUALLY THE SAME
90      REM  IN EACH MEASUREMENT.
95      REM

100     HOME
110     VTAB 5 :
        INVERSE  :
        PRINT " DICHROISM CALCULATIONS " :
        NORMAL
120     PRINT  :
        PRINT
130     VTAB 21 :
        INVERSE  :
        PRINT " ANY KEY TO CONTINUE "; :
        NORMAL
140     GET K$ :
        PRINT
150     HOME
155     GOSUB 500
157     HOME
160     PRINT "LIGHT LEVELS IN ARBITRARY UNITS :-" :
        PRINT  :
        PRINT
170     PRINT "MEASUREMENT PARALLEL TO ELECTRIC FIELD" :
        PRINT
180     INPUT "  FIELD-ON LIGHT LEVEL  ";P1
190     INPUT "  FIELD-OFF LIGHT LEVEL ";P0
195     IF I = 1 THEN
            GOTO 240
200     PRINT
210     PRINT "MEASUREMENT PERPENDICULAR TO FIELD" :
        PRINT
220     INPUT "  FIELD-ON LIGHT-LEVEL  ";N1
```

```
230       INPUT "  FIELD-OFF LIGHT LEVEL ";NO
240       PRINT
250       PRINT "NORMAL ABSORBANCE OF SOLN IN KERR CELL"
260       INPUT "IS EQUAL TO ";A
270       PRINT
280       LET AP = A + 0.4343 *  LOG (PO / P1)
285       IF I = 1 THEN
               GOTO 295
290       LET AN = A + 0.4343 *  LOG (NO / N1)
295       LET CN = (3 * A - AP) / 2
297       REM  CALCD PERP. ABSORBANCE
298       REM  FROM PARALLEL ABSORBANCE

300       PRINT "PARALLEL ABSORBANCE IS        "; INT (1000 * AP) /
               1000 :
          PRINT
305       IF I = 1 THEN
               315
310       PRINT "PERPENDICULAR ABSORBANCE IS "; INT (1000 * AN) /
               1000
312       PRINT
315       PRINT "CALCULATED PERPENDICULAR VALUE IS  "; INT (1000 *

               CN) / 1000
316       IF I = 1 THEN
               GOTO 318
317       LET DL = AP - AN :
          GOTO 319
318       LET DL = AP - CN
319       PRINT  :
          PRINT "DICHROISM IS  "; INT (1000 * DL) / 1000
320       LET DR = DL / A
322       PRINT  :
          PRINT "REDUCED DICHROISM IS  "; INT (1000 * DR) /
               1000
325       VTAB 24 :
          INVERSE  :
          PRINT "DUMP SCREEN TO PRINTER? (Y OR N)"; :
          NORMAL
330       GET K$ :
          PRINT
340       IF K$ = "Y" THEN
               VTAB 24 :
               PRINT  SPC( 40) :
               PR£ 1 :
               PRINT  CHR$ (9);"S" :
               PR£ 0 :
```

```
348     GOTO 360
350     IF K$ <  > "N" THEN
            330
360     HOME  :
        VTAB 2
370     INVERSE  :
        PRINT " ANOTHER CALCULATION ? (Y/N) "; :
        NORMAL
380     GET K$ :
        PRINT
390     IF K$ = "Y" THEN
            150
400     IF K$ <  > "N" THEN
            380
410     HOME  :
        END
500     VTAB 5 :
        INVERSE  :
        PRINT "OPTIONS" :
        NORMAL
510     VTAB 10 :
        PRINT "CALCULATION BASED ON PARALLEL AND"; :
        PRINT "PERPENDICULAR VALUES (A) OR PARALLEL ONLY (B)"
515     GET ANS$
520     IF ANS$ = "A" THEN
            I = 0 :
            RETURN
525     IF ANS$ = "B" THEN
            I = 1 :
            RETURN
530     GOTO 510
```

PROGRAM 3

KERR EFFECT PLUS DICHROISM

Equation 8.10 is used to calculate the phase retardation, δ, from measurements made using the optical arrangement described in section 8.2. The following data is required:

(i) The voltage applied to the Kerr cell.

(ii) The field-on light-level.

(iii) The field-off light level.

(iv) The normal absorbance of the solution in the Kerr cell.

(v) The parallel ($A_{||}$) and perpendicular ($A_{\perp}$) absorbances or values of the constants a, b, and c obtained from the curve fitting procedure (equation 8.11).

```
10        REM   KERR+DICHROISM (CROSSED)
15        REM
20        REM  POLARS $ QUARTER WAVE
30        REM  RETARDER SET WITH ITS
40        REM  SLOW AXIS PARALLEL TO
50        REM  THE APPLIED ELECTRIC
60        REM  FIELD IN KERR CELL.
70        REM
80        REM

100       HOME
110       VTAB 5 :
          INVERSE  :
          PRINT " KERR EFFECT + DICHROISM " :
          NORMAL  :
          PRINT  :
          PRINT
120       PRINT "WITH CROSSED POLARS AND"
130       PRINT "QUARTER-WAVE RETARDER PLATE"
140       PRINT "(SLOW AXIS SET PARALLEL TO"
150       PRINT "THE APPLIED ELECTRIC FIELD)"
155       VTAB 21 :
          INVERSE  :
          PRINT " ANY KEY TO CONTINUE "; :
          NORMAL
160       GET K$ :
          PRINT
162       LET XX = 0
165       GOSUB 1000
167       IF XX = 1 THEN
              GOTO 195
170       HOME  :
          VTAB 2 :
          INVERSE  :
          PRINT "INPUT FOLLOWING DATA FOR EACH VOLTAGE " :
          NORMAL
180       PRINT  :
          PRINT
190       INPUT "APPLIED VOLTAGE (IN VOLTS)";V :
          PRINT
195       PRINT "LIGHT LEVELS IN ARBITRARY UNITS" :
          PRINT
200       INPUT "  FOR ELECTRIC FIELD ON  ";L1
210       INPUT "  FOR ELECTRIC FIELD OFF ";L2 :
          PRINT
```

```
215     IF XX = 1 THEN
            GOTO 250
220     INPUT "PARALLEL ABSORPTION        ";A1
225     PRINT
230     INPUT "PERPENDICULAR ABSORPTION ";A2
235     PRINT
240     INPUT "NORMAL ABSORPTION          ";A
245     PRINT
250     REM
260     REM  EQUATION FROM FREDERIQUE
270     REM   AND HOUSSIER
280     REM
290     REM  DELTA-I/I=-1 + 0.5 * (10^( )
292     REM  + 10^( ) - 10^( ) *
294     REM  SIN(PHASE RETARDATION)
300     REM
310     REM  REWRITE EQUATION AS :
320     REM
330     REM   DI/I = -1 + 0.5*(C1 + C2
332     REM  - C3 * SIN(D))
340     REM
350     REM   SOLVING FOR THE PHASE
352     REM  RETARDATION GIVES :
360     REM
370     REM    SIN (D) = (2 * ( DEL(I) / I
372     REM  + 1) - C1 -C2)/(-C3)
375     REM
380     REM   I.E., SIN (D) = C4 THEREFORE
382     REM  D = ARCSIN (C4)
390     REM

400     LET DI = L1 - L2 :
        LET I = L2
410     LET C1 = 10 ^ (A - A1)
412     REM  A1 = PARALLEL ABSORPTION

420     LET C2 = 10 ^ (A - A2)
422     REM  A2 = PARPENDICULAR ABSORPTION

430     LET C3 = 2 * 10 ^ (A - (A1 + A2) /
            2)
435     LET C3 =  - C3
440     LET C4 = (2 * (DI / I + 1) - C1 -
            C2) / C3
450     LET D =  ATN (C4 /  SQR ( - C4 * C4 +
            1))
```

```
452     REM  D = ARCSIN (C4)
460     REM

470     PRINT
480     PRINT "PHASE RETARDATION IS "; INT (1000 * D *
            57.29578) / 1000;" DEG"
490     VTAB 20 :
        INVERSE  :
        PRINT "DUMP SCREEN TO PRINTER ? (Y/N) "; :
        NORMAL
500     GET K$ :
        PRINT
502     VTAB 2 :
        PRINT  SPC( 40)
505     IF K$ = "Y" THEN
            VTAB 20 :
            PRINT  SPC( 40) :
            PR£ 1 :
            PRINT  CHR$ (9);"S" :
            PR£ 0 :
            GOTO 510
507     IF K$ <  > "N" THEN
            500
510     HOME  :
        VTAB 5 :
        HTAB 5
520     PRINT "ANOTHER CALCULATION ? (Y/N) ";
530     GET K$ :
        PRINT
540     IF K$ = "N" THEN
            570
550     IF K$ <  > "Y" THEN
            530
560     GOTO 162
570     HOME  :
        END
1000    REM ****CURFIT****

1010    HOME  :
        VTAB 4 :
        INVERSE  :
        PRINT "OPTIONS" :
        NORMAL
1020    PRINT
1030    PRINT "USE MEASURED VALUES OF AP ";
1032    PRINT "AND AN TO CALCULATE DATA (A) ";
```

```
1034     PRINT "OR CALCULATED VALUES FROM CURFIT (B)"
1040     GET ANS$
1050     IF ANS$ = "A" THEN
              RETURN
1060     IF ANS$ = "B" THEN
              GOTO 1070ELSE GOTO 1040
1070     HOME  :
         VTAB (1) :
         INVERSE  :
         PRINT "ENTER VALUES FROM DICHROISM CURFIT" :
         NORMAL
1075     PRINT
1080     PRINT "CALCULATION BASED ON "; :
         PRINT "RY = NV^2 + MV + C"
1090     VTAB (5) :
         PRINT "CONSTANT M = ";M; :
         INPUT " ";M$ :
         IF M$ = "" THEN
              1100
1095     M =  VAL (M$) :
         GOTO 1090
1100     VTAB 7 :
         PRINT "CONSTANT N = ";N; :
         INPUT " ";N$ :
         IF N$ = "" THEN
              1110
1102     REM

1105     LET N =  VAL (N$) :
         GOTO 1100
1110     VTAB (9) :
         PRINT "CONSTANT C = ";C; :
         INPUT " ";C$ :
         IF C$ = "" THEN
              1120
1115     C =  VAL (C$) :
         GOTO 1110
1120     PRINT
1130     VTAB (11) :
         PRINT "ABSORPTION IN KERR CELL = ";A; :
         INPUT " ";A$ :
         IF A$ = "" THEN
              1150
1135     A =  VAL (A$) :
         GOTO 1130
```

```
1140    PRINT
1150    PRINT  :
        INPUT "VOLTAGE IN VOLTS = ";V
1160    PRINT
1170    LET RY = (N * V * V) + (M * V) + C
1180    LET AP = A + (2 * A * RY / 3)
1190    LET AN = A - (RY * A / 3)
1200    PRINT " PARALLEL ABSORPTION = "; :
        PRINT  INT (1000 * AP) / 1000
1210    PRINT
1220    PRINT "PERPENDICULAR ABSORPTION = "; INT (1000 * AN) /
            1000
1225    PRINT
1230    PRINT "REDUCED DICHROISM = "; INT (1000 * RY) /
            1000
1235    LET A1 = AP :
        LET A2 = AN
1237    REM  MATCHED VARIABLES FOR USE IN
1238    REM  FREDERIQUE & HOUSSIER EQN.

1240    LET XX = 1
1250    PRINT
1260    PRINT
1270    VTAB (21) :
        INVERSE  :
        PRINT "DUMP SCREEN TO PRINTER? (Y/N)" :
        NORMAL
1280    GET R$
1290    IF R$ = "Y" THEN
            GOTO 1310
1300    HOME  :
        RETURN
1310    VTAB (1) :
        PRINT  SPC( 40)
1315    VTAB (3) :
        PRINT  SPC( 40)
1320    VTAB (21) :
        PRINT  SPC( 40)
1325    PR£ 1 :
        PRINT  CHR$ (9);"S" :
        PR£ 0
1330    HOME  :
        RETURN
```

PROGRAM 4

CALCULATION OF ELECTRIC DICHROISM USING THE NULLED INTENSITY METHOD

This short program calculates the reduced dichroism from the measured angles of polariser P_1 obtained using the nulled intensity method for the simultaneous determination of birefringence and dichroism (equation 8.17). The only input that is required is a value of the angle "β" of polariser P_1 determined by the null point condition described in section 8.3.

```
2000     REM **CALCULATES DICHROISM**

2005     LET PI = 3.1415
2010     REM **FROM ANGLE P(1)**
2015     REM    DEL(A)    = -2 * LOG[TAN(ALPHA)]
2016     REM  ALPHA = 45 - BETA

2020     HOME
2030     DEF  FN DTR(Q) = Q * (PI / 180)
2050     VTAB (4) :
         INVERSE  :
         PRINT "POLARISER ANGLE TO DICHROISM" :
         NORMAL
2060     PRINT
2070     INPUT "ABSORPTION IN CELL = ";A
2080     PRINT
2090     INPUT "ANGLE BETA = ";B
2100     LET Q = (45 - B)
2120     LET T =  TAN ( FN DTR(Q))
2140     LET D = 0.4343 *  LOG (T)
2150     LET RD =  - 2 * D / A
2155     PRINT
2160     PRINT "REDUCED DICHROISM = "; INT (1000 * RD) /
             1000
2170     PRINT
2180     PRINT "ANOTHER CALCULATION? "
2190     GET ANS$
2200     IF ANS$ = "Y" THEN
             GOTO 2000
2210     END
```

PROGRAM 5

ANALYSIS OF OPTICAL TRANSIENTS

This program calculates the values of t, -ln (t), $A_{r,d}(t)$ and ln [-ln $A_{r,d}(t)$] using the equations described in section 8.4. The following input is required:

(i) The distance measured in millimeters, between the two calibration marks on the time axis of the transient electro-optical trace.

(ii) The time measured in seconds, between the calibration marks in (i).

(iii) The maximum light-level, $I_{(max)}$, expressed in mm.

(iv) The minimum light-level, $I_{(min)}$, expressed in mm.

(v) Pairs of ordinate, $t_{r,d}$ (mm) and abscissa $h_{r,d}(t)$ (mm) values of a series of points on the electro-optical trace for the rise and decay transients.

```
10       REM  TRANSIENT CALCULATION
20       REM

30       HOME  :
         CLEAR
35       DIM D(50,2) :
         LET CO = 1
40       VTAB 4 :
         INVERSE  :
         PRINT "TRANSIENT CALCULATION" :
         NORMAL
50       VTAB (10) :
         PRINT "ANALYSE RISE (R)"; :
         PRINT " OR DECAY (D) CURVE ? "
60       GET K$ :
         IF K$ = "" THEN
             60
62       IF K$ = "R" THEN
             Z = 1
64       IF K$ = "D" THEN
             Z = 2
66       IF Z = 0 THEN
             GOTO 60
70       HOME
80       VTAB 4 :
         INPUT "ENTER WINDOW WIDTH IN MM ";W
90       PRINT  :
         INPUT "ENTER WINDOW TIME IN SECS ";TW
100      PRINT  :
         INPUT "ENTER I(MIN) IN MM ";IL
105      LET PA = 0.4343 *  LOG (IL)
110      PRINT  :
         INPUT "ENTER I(MAX) IN MM ";IH
115      LET PB = 0.4343 *  LOG (IH)
120      REM

130      GOSUB 500
132      PR£ 1
135      PRINT  TAB( 1);"TIME"; TAB( 8);"HEIGHT"; TAB( 16); :
         PRINT "AP"; TAB( 24);"LN(A)"; TAB( 32);"LN(LN)"
137      PRINT
140      FOR K = 1 TO CO
145          LET TX = D(K,1) :
             LET HY = D(K,2)
150          REM
```

```
160         LET PC = 0.4343 *  LOG (HY)
165         LET NA = PC - PA
170         LET NB = NA / (PB - PA)
172         IF Z = 2 THEN
                AP = 1 - NB
173         IF Z = 1 THEN
                AP = NB
175         LET LP =  LOG (AP)
176         LET LP = LP * ( - 1)
177         LET LL =  LOG (LP)
178         LET LP =  INT (10000 * LP) / 10000
179         LET LL =  INT (10000 * LL) / 10000
180         LET T = (TW / W) * TX
185         LET T =  INT (10000 * T) / 10000
190         LET AP =  INT (AP * 10000) / 10000
220         PRINT  TAB( 1);T; TAB( 8);HY; TAB( 16);AP; TAB(
            24);LP; TAB( 32);LL
225     NEXT K
227     PR£ 0
260     HOME  :
        VTAB 7
270     PRINT "NEW TRANSIENT (Y O N) ?"
275     GET RE$
280     IF RE$ = "Y" THEN
            GOTO 30
290     IF RE$ = "N" THEN
            GOTO 310
300     GOTO 275
310     END
500     FOR J = 1 TO 50
505         PRINT
510         INPUT "ENTER TIME ON DECAY CURVE IN MM ";TX
520         INPUT "ENTER HEIGHT ON DECAY CURVE IN MM ";HY
530         PRINT "ACCEPT VALUES (Y OR N)?"
540         GET ANS$
550         IF ANS$ = "" THEN
                540 :
                IF ANS$ = "N" THEN
                    GOTO 510
560         LET D(J,1) = TX :
            LET D(J,2) = HY
570         PRINT "ANOTHER VALUE ? "
580         GET RE$
590         IF RE$ = "N" THEN
                GOTO 610
592         IF RE$ = "Y" THEN
```

```
594     GOTO 600 : REM  BELONGS TO 'IF'

595     GOTO 580
600     LET CO = CO + 1 :
    NEXT J
610 RETURN
```

APPENDIX 3

DATA OBTAINED FROM PLOTS OF TRANSIENT ELECTRIC DICHROISM

A3.1 Introduction

Curves of optical transients depicting the electrically-induced optical dichroism of solutions of polypentenylene-block-co-acetylene were obtained by the techniques described in section 7.4. Tables A3.1-A3.14 summarise the relaxation data derived from the electro-optical plots obtained by the methods outlined in section 8.4.1. The time dependent absorbances for rise (r) and decay (d) transients, $\mathbf{A}_{r,d}(t)$, were used to construct double-logarithmic plots required for the empirical analysis of Williams and Watts (section 8.4.2). These are shown in figures A3.1-A3.14.

A3.2 Electro-optical Data

Table A3.1 Decay of electrically-induced dichroism at 1000V (0.65% w/v solution of copolymer in cyclohexane)

time, t /s	$h_d(t)$ /mm	$\mathbf{A}_d(t)$	$\ln[-\ln(\mathbf{A}_d(t))]$	$-\ln(t/s)$
0.006	35.5	0.668	-0.91	5.19
0.010	39.5	0.538	-0.48	4.64
0.014	43.5	0.421	-0.14	4.29
0.018	46.5	0.340	0.08	4.03
0.022	49.5	0.264	0.29	3.83
0.026	52.5	0.192	0.50	3.65
0.030	53.5	0.169	0.58	3.51
0.034	55.0	0.136	0.69	3.38
0.038	55.5	0.125	0.73	3.27
0.042	56.0	0.114	0.78	3.17
0.050	56.5	0.103	0.82	2.99
0.058	58.0	0.071	0.97	2.84
0.066	59.5	0.040	1.17	2.71
0.074	59.5	0.040	1.17	2.60
0.083	60.0	0.030	1.26	2.50
0.091	60.0	0.030	1.26	2.40
0.099	60.5	0.020	1.37	2.32
0.107	61.0	0.010	1.53	2.24

Table A3.2 Decay of electrically-induced dichroism at 1000V (1.05% w/v solution of copolymer in cyclohexane)

time, t /s	$h_d(t)$ /mm	$\mathbf{A}_d(t)$	$\ln[-\ln(\mathbf{A}_d(t))]$	$-\ln(t/s)$
0.008	35.5	0.660	-0.88	4.83
0.018	48.5	0.483	-0.32	4.01
0.028	58.5	0.376	-0.02	3.57
0.038	66.5	0.304	0.18	3.26
0.049	73.0	0.251	0.33	3.03
0.059	78.0	0.213	0.44	2.84
0.069	82.0	0.185	0.53	2.68
0.079	86.0	0.158	0.61	2.54
0.089	89.0	0.138	0.68	2.42
0.099	92.0	0.119	0.76	2.31
0.109	94.5	0.104	0.82	2.21
0.119	97.0	0.091	0.88	2.13
0.129	98.5	0.080	0.93	2.04
0.140	100.0	0.072	0.97	1.97
0.150	101.0	0.066	1.00	1.90
0.160	102.5	0.059	1.04	1.83
0.170	103.0	0.055	1.06	1.77
0.180	104.0	0.050	1.10	1.71
0.200	105.5	0.041	1.16	1.61
0.221	106.5	0.036	1.20	1.51
0.241	108.0	0.028	1.27	1.42
0.261	109.5	0.020	1.36	1.34
0.281	110.0	0.018	1.40	1.27
0.294	110.5	0.015	1.43	1.23
0.302	110.5	0.015	1.43	1.20
0.322	111.5	0.010	1.53	1.13
0.342	111.5	0.010	1.53	1.07
0.362	112.0	0.008	1.59	1.02
0.383	112.5	0.005	1.67	0.96
0.403	112.5	0.005	1.67	0.91
0.423	113.0	0.003	1.79	0.86

Table A3.3 Decay of electrically-induced dichroism at 1000V (1.58% w/v solution of copolymer in cyclohexane)

time, t /s	$h_d(t)$ /mm	$\mathbf{A}_d(t)$	$\ln[-\ln(\mathbf{A}_d(t))]$	$-\ln(t/s)$
0.020	19.0	0.509	-0.39	3.91
0.040	29.0	0.371	-0.01	3.21
0.060	42.0	0.252	0.32	2.81
0.081	49.5	0.196	0.49	2.52
0.101	55.0	0.163	0.60	2.30
0.121	59.5	0.136	0.69	2.11
0.141	64.0	0.112	0.79	1.96
0.161	67.0	0.097	0.85	1.83
0.181	69.5	0.085	0.90	1.71
0.202	72.5	0.071	0.97	1.60
0.222	74.0	0.065	1.01	1.51
0.242	76.0	0.056	1.06	1.42
0.262	77.0	0.052	1.08	1.34
0.282	78.0	0.047	1.12	1.27
0.302	78.5	0.045	1.13	1.20
0.323	79.0	0.043	1.15	1.13
0.343	80.0	0.039	1.18	1.07
0.363	80.5	0.037	1.20	1.01
0.383	81.0	0.036	1.21	0.96
0.423	81.5	0.032	1.23	0.86
0.464	83.5	0.025	1.31	0.77
0.504	84.0	0.023	1.33	0.69
0.544	86.0	0.016	1.42	0.61
0.585	86.5	0.013	1.47	0.54
0.625	87.5	0.009	1.54	0.47
0.665	88.0	0.007	1.59	0.41
0.706	88.0	0.007	1.59	0.35
0.746	88.5	0.006	1.62	0.29
0.786	89.0	0.004	1.73	0.24

Table A3.4 Decay of electrically-induced dichroism at 1000V (1.80% w/v solution of copolymer in cyclohexane)

time, t /s	$h_d(t)$ /mm	$\mathbf{A}_d(t)$	$\ln[-\ln(\mathbf{A}_d(t))]$	$-\ln(t/s)$
0.014	7.5	0.446	-0.21	4.25
0.025	11.0	0.341	0.07	3.71
0.035	14.0	0.275	0.26	3.36
0.045	16.5	0.229	0.39	3.10
0.055	19.5	0.183	0.53	2.90
0.066	21.5	0.157	0.62	2.73
0.076	23.0	0.138	0.68	2.58
0.086	25.5	0.110	0.79	2.45
0.096	27.0	0.094	0.86	2.34
0.107	28.5	0.079	0.93	2.24
0.117	29.5	0.070	0.98	2.15
0.127	30.5	0.060	1.03	2.06
0.148	32.5	0.043	1.15	1.91
0.168	34.5	0.027	1.29	1.78
0.189	35.0	0.023	1.33	1.67
0.209	35.5	0.019	1.38	1.57
0.230	36.0	0.015	1.44	1.47
0.250	36.5	0.011	1.51	1.39
0.270	37.0	0.007	1.59	1.31
0.291	37.0	0.007	1.59	1.24
0.311	37.5	0.004	1.73	1.17

Table A3.5 Decay of electrically-induced dichroism at 250V (1.05% w/v solution of copolymer in cyclohexane)

time, t /s	$h_d(t)$ /mm	$A_d(t)$	$\ln[-\ln(A_d(t))]$	$-\ln(t/s)$
0.024	48.5	0.656	-0.86	3.73
0.044	57.5	0.482	-0.32	3.12
0.065	64.5	0.366	0.01	2.74
0.085	69.0	0.297	0.19	2.47
0.105	72.5	0.247	0.34	2.26
0.125	75.5	0.206	0.46	2.08
0.145	78.5	0.166	0.58	1.93
0.165	80.5	0.141	0.67	1.80
0.185	82.0	0.122	0.74	1.69
0.206	83.5	0.104	0.81	1.58
0.226	85.0	0.089	0.88	1.49
0.246	85.5	0.080	0.93	1.40
0.266	86.0	0.074	0.96	1.32
0.286	87.0	0.062	1.02	1.25
0.306	87.5	0.056	1.06	1.18
0.327	89.0	0.042	1.15	1.12
0.347	89.0	0.039	1.18	1.06
0.367	89.5	0.033	1.22	1.00
0.387	90.0	0.028	1.28	0.95
0.407	90.5	0.022	1.34	0.90
0.448	91.0	0.017	1.41	0.80
0.488	92.0	0.003	1.76	0.72

Table A3.6 Decay of electrically-induced dichroism at 250V (1.58% w/v solution of copolymer in cyclohexane)

time, t /s	$h_d(t)$ /mm	$\mathbf{A}_d(t)$	$\ln[-\ln(\mathbf{A}_d(t))]$	$-\ln(t/s)$
0.012	28.0	0.776	-1.37	4.42
0.032	38.5	0.571	-0.58	3.44
0.052	47.5	0.436	-0.19	2.95
0.072	52.0	0.380	-0.03	2.63
0.092	58.0	0.307	0.17	2.38
0.112	62.0	0.264	0.29	2.19
0.133	65.5	0.229	0.39	2.02
0.153	68.5	0.198	0.48	1.88
0.173	72.0	0.170	0.57	1.76
0.193	73.0	0.159	0.61	1.65
0.213	75.0	0.140	0.68	1.55
0.233	76.5	0.129	0.72	1.46
0.253	80.0	0.102	0.82	1.37
0.273	81.0	0.094	0.86	1.30
0.293	83.0	0.079	0.93	1.23
0.313	83.5	0.073	0.96	1.61
0.333	84.5	0.065	1.01	1.10
0.353	85.5	0.058	1.05	1.04
0.373	87.0	0.048	1.11	0.99
0.394	87.0	0.044	1.14	0.93
0.414	88.0	0.039	1.18	0.88
0.434	89.0	0.032	1.24	0.84
0.454	90.0	0.025	1.31	0.79
0.474	90.0	0.025	1.31	0.75
0.494	91.0	0.017	1.40	0.71
0.534	91.5	0.012	1.48	0.63
0.574	91.0	0.017	1.40	0.56
0.614	92.5	0.007	1.60	0.49
0.655	92.5	0.007	1.60	0.42
0.695	93.0	0.003	1.74	0.36

Table A3.7 Decay of electrically-induced dichroism at 250V (1.80% w/v solution of copolymer in cyclohexane)

time, t /s	$h_d(t)$ /mm	$\mathbf{A}_d(t)$	$\ln[-\ln(\mathbf{A}_d(t))]$	$-\ln(t/s)$
0.006	11.5	0.861	-1.90	5.07
0.017	16.0	0.674	-0.93	4.09
0.027	19.5	0.562	-0.55	3.60
0.038	23.0	0.468	-0.27	3.28
0.048	]26.0	0.398	-0.08	3.03
0.059	28.0	0.356	0.03	2.83
0.069	30.5	0.308	0.16	2.67
0.080	32.5	0.272	0.26	2.53
0.090	34.5	0.238	0.36	2.41
0.101	36.0	0.214	0.43	2.30
0.111	37.0	0.198	0.48	2.20
0.121	38.5	0.176	0.55	2.11
0.132	39.5	0.161	0.60	2.02
0.143	40.5	0.147	0.65	1.95
0.153	41.5	0.133	0.70	1.88
0.174	43.5	0.107	0.81	1.75
0.195	44.5	0.094	0.86	1.63
0.216	46.0	0.075	0.95	1.53
0.237	47.0	0.063	1.02	1.44
0.258	48.0	0.051	1.09	1.35
0.279	48.5	0.045	1.13	1.28
0.300	49.5	0.033	1.22	1.20
0.321	50.5	0.022	1.34	1.14
0.342	51.0	0.016	1.41	1.07
0.363	51.5	0.011	1.51	1.01
0.384	52.0	0.005	1.65	0.96

Table A3.8 Rise of electrically-induced dichroism at 1000V (0.65% w/v solution of copolymer in cyclohexane)

time, t / ms	$h_r(t)$ / mm	$A_r(t)$	$\ln[-\ln(A_r(t))]$	$-\ln(t/s)$
0.2	58.5	0.869	-1.97	8.51
0.4	54.0	0.770	-1.34	7.82
0.6	49.0	0.650	-0.84	7.42
0.8	45.5	0.558	-0.54	7.13
1.0	42.5	0.474	-0.29	6.91
1.2	39.5	0.383	-0.04	6.73
1.4	37.0	0.302	0.18	6.57
1.6	36.5	0.285	0.23	6.44
1.8	35.0	0.233	0.38	6.32
2.0	34.5	0.215	0.43	6.22
2.3	33.5	0.179	0.54	6.08
2.5	32.5	0.141	0.67	5.99
2.7	31.5	0.102	0.82	5.92
3.1	30.0	0.042	1.15	5.78
3.5	30.0	0.042	1.15	5.66
3.9	30.0	0.042	1.15	5.55
4.3	29.5	0.021	1.35	5.45

Table A3.9 Rise of electrically-induced dichroism at 1000V (1.05% w/v solution of copolymer in cyclohexane)

time, t / ms	$h_r(t)$ / mm	$A_r(t)$	ln[-ln($A_r(t)$)]	- ln(t / s)
0.4	96.0	0.888	-2.13	7.82
0.8	77.0	0.763	-1.31	7.13
1.2	62.0	0.636	-0.79	6.73
1.7	52.0	0.535	-0.47	6.38
2.1	44.0	0.439	-0.20	6.17
2.5	38.5	0.362	0.02	5.99
2.9	34.5	0.299	0.19	5.84
3.3	32.5	0.265	0.28	5.71
3.7	30.0	0.224	0.40	5.60
4.1	29.0	0.199	0.48	5.50
4.5	27.5	0.169	0.58	5.40
4.9	26.5	0.148	0.65	5.32
5.3	26.0	0.141	0.67	5.24
5.7	25.0	0.114	0.78	5.17
6.1	25.0	0.108	0.80	5.10
6.5	25.0	0.097	0.85	5.04
7.3	23.0	0.066	1.00	4.92
8.1	22.0	0.047	1.12	4.82
8.9	22.0	0.041	1.17	4.72
9.7	21.5	0.027	1.28	4.64
10.6	21.5	0.027	1.28	4.51
11.4	21.0	0.014	1.46	4.47

Table A3.10 Rise of electrically-induced dichroism at 1000V (1.58% w/v solution of copolymer in cyclohexane)

time, t / ms	$h_r(t)$ / mm	$A_r(t)$	$\ln[-\ln(A_r(t))]$	$-\ln(t/s)$
0.4	82.0	0.939	-2.77	7.82
0.8	60.5	0.833	-1.70	7.13
1.2	43.0	0.711	-1.07	6.73
1.6	30.5	0.589	-0.64	6.44
2.0	22.5	0.482	-0.32	6.22
2.4	18.0	0.408	-0.11	6.03
2.8	15.0	0.339	0.08	5.88
3.2	13.5	0.302	0.18	5.75
3.6	11.5	0.252	0.32	5.63
4.0	10.5	0.213	0.44	5.52
4.4	9.5	0.177	0.55	5.43
4.8	8.5	0.148	0.65	5.34
5.2	8.0	0.117	0.77	5.26
5.6	7.5	0.094	0.86	5.19
6.4	7.0	0.069	0.98	5.05
7.2	7.0	0.069	0.98	4.93
8.0	6.5	0.043	1.14	4.82

Table A3.11 Rise of electrically-induced dichroism at 1000V (1.80% w/v solution of copolymer in cyclohexane)

time, t / ms	$h_r(t)$ / mm	$\mathbf{A}_r(t)$	$\ln[-\ln(\mathbf{A}_r(t))]$	$-\ln(t/s)$
0.167	40.0	0.951	-3.00	8.70
0.271	35.0	0.896	-2.21	8.21
0.375	30.5	0.839	-1.74	7.89
0.479	25.5	0.765	-1.32	7.64
0.583	21.5	0.695	-1.01	7.45
0.688	18.0	0.921	-0.74	7.28
0.792	16.5	0.585	-0.63	7.14
0.896	14.5	0.532	-0.46	7.02
1.000	12.5	0.471	-0.28	6.91
1.104	11.0	0.418	-0.14	6.81
1.313	8.5	0.311	0.15	6.64
1.521	7.0	0.231	0.38	6.49
1.729	6.0	0.168	0.58	6.36
1.938	5.0	0.092	0.87	6.25

Table A3.12 Rise of electrically-induced dichroism at 250V (1.05% w/v solution of copolymer in cyclohexane)

time, t /s	$h_r(t)$ /mm	$\mathbf{A}_r(t)$	$\ln[-\ln(\mathbf{A}_r(t))]$	$-\ln(t/s)$
0.001	94.5	0.956	-3.10	7.13
0.002	85.0	0.845	-1.78	6.08
0.005	78.0	0.755	-1.27	5.34
0.007	71.5	0.664	-0.89	4.99
0.009	66.5	0.591	-0.64	4.73
0.011	63.0	0.531	-0.46	4.53
0.013	59.0	0.462	-0.26	4.36
0.015	56.5	0.416	-0.13	4.21
0.017	54.0	0.369	0.00	4.09
0.019	51.5	0.324	0.12	3.97
0.021	49.5	0.278	0.25	3.87
0.023	48.0	0.245	0.34	3.78
0.025	46.5	0.212	0.44	3.70
0.027	45.0	0.178	0.55	3.62
0.029	44.0	0.154	0.63	3.54
0.031	43.0	0.130	0.71	3.48
0.033	42.0	0.105	0.81	3.41
0.035	41.5	0.093	0.89	3.36
0.037	40.5	0.073	0.96	3.30
0.039	40.0	0.054	1.07	3.25
0.041	40.0	0.047	1.12	3.20
0.045	39.0	0.027	1.28	3.10
0.049	38.5	0.014	1.46	3.02

Table A3.13 Rise of electrically-induced dichroism at 250V (1.58% w/v solution of copolymer in cyclohexane)

time, t /s	$h_r(t)$ /mm	$\mathbf{A}_r(t)$	$\ln[-\ln(\mathbf{A}_r(t))]$	$-\ln(t/s)$
0.002	89.5	0.950	-2.98	6.44
0.004	78.0	0.865	-1.93	5.63
0.006	70.0	0.798	-1.49	5.19
0.008	60.5	0.708	-1.06	4.88
0.010	54.5	0.644	-0.82	4.65
0.012	48.5	0.571	-0.58	4.42
0.014	45.5	0.532	-0.46	4.27
0.016	40.5	0.464	-0.26	4.14
0.018	39.0	0.437	-0.19	4.02
0.019	36.5	0.396	-0.08	3.96
0.022	34.0	0.356	0.03	3.82
0.024	32.0	0.319	0.13	3.73
0.026	29.5	0.264	0.29	3.65
0.028	28.5	0.243	0.35	3.58
0.030	28.0	0.232	0.38	3.51
0.032	27.0	0.209	0.45	3.44
0.034	26.0	0.186	0.52	3.38
0.036	25.5	0.174	0.56	3.32
0.038	24.5	0.149	0.64	3.27
0.040	23.5	0.129	0.71	3.22
0.044	23.5	0.123	0.74	3.12
0.048	21.5	0.076	0.95	3.04
0.052	21.5	0.068	0.99	2.96
0.056	21.0	0.053	1.07	2.88
0.060	20.0	0.031	1.24	2.81
0.064	20.0	0.031	1.24	2.75
0.068	20.0	0.024	1.32	2.69
0.071	19.5	0.008	1.58	2.65

Table A3.14 Rise of electrically-induced dichroism at 250V (1.80% w/v solution of copolymer in cyclohexane)

time, t /s	$h_r(t)$ /mm	$\mathbf{A}_r(t)$	$\ln[-\ln(\mathbf{A}_r(t))]$	$-\ln(t/s)$
0.003	37.5	0.848	-1.80	5.88
0.005	33.0	0.766	-1.32	5.32
0.007	29.5	0.694	-1.01	4.98
0.009	25.5	0.601	-0.67	4.71
0.011	23.5	0.548	-0.51	4.50
0.013	21.0	0.476	-0.30	4.34
0.015	19.0	0.412	-0.12	4.19
0.017	17.5	0.359	0.02	4.06
0.019	16.0	0.302	0.18	3.95
0.021	14.5	0.238	0.36	3.85
0.023	12.5	0.143	0.67	3.76
0.026	12.0	0.117	0.76	3.67
0.030	11.0	0.061	1.03	3.52
0.034	10.5	0.031	1.24	3.39

A3.3 Analysis of decay of electrically-induced dichroism using the Williams-Watts relationship

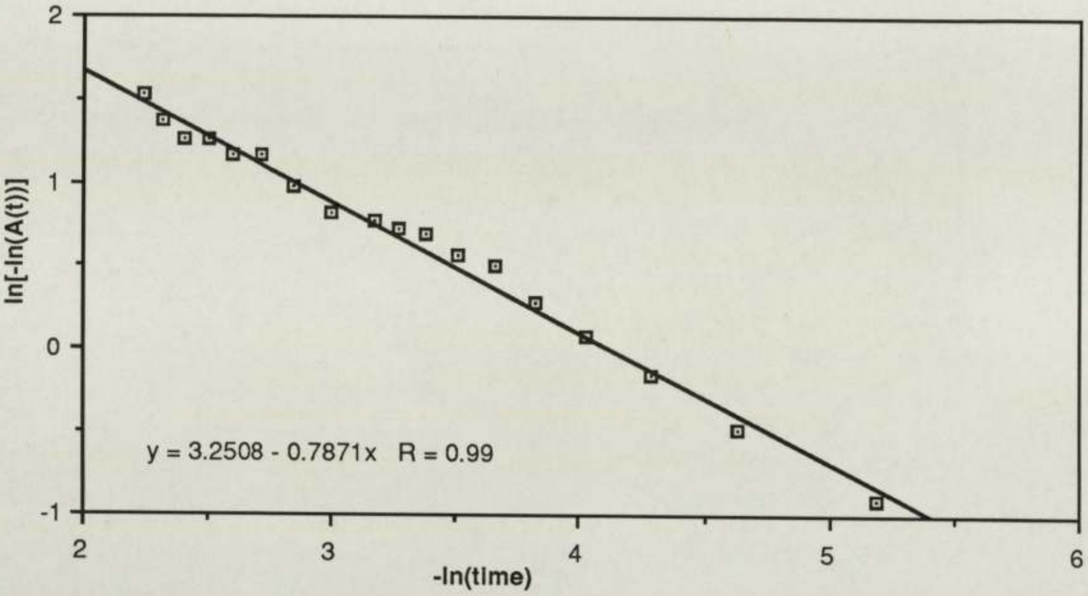

Figure A3.1 Double-logarithmic plot of electro-optical dichroism decay at 1000V (0.65% w/v solution of copolymer in cyclohexane)

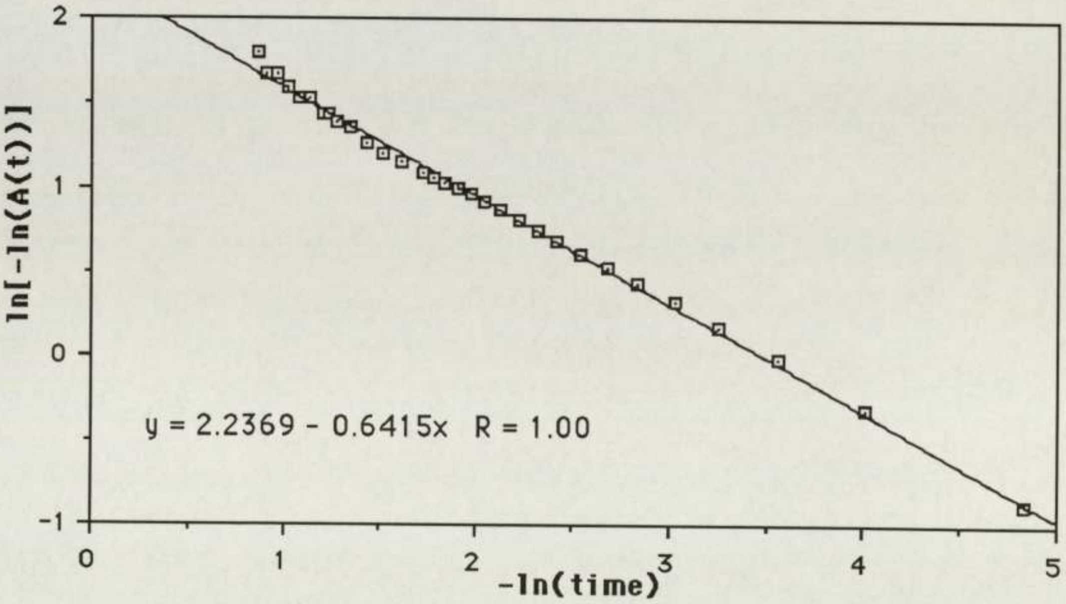

Figure A3.2 Double-logarithmic plot of electro-optical dichroism decay at 1000V (1.05% w/v solution of copolymer in cyclohexane)

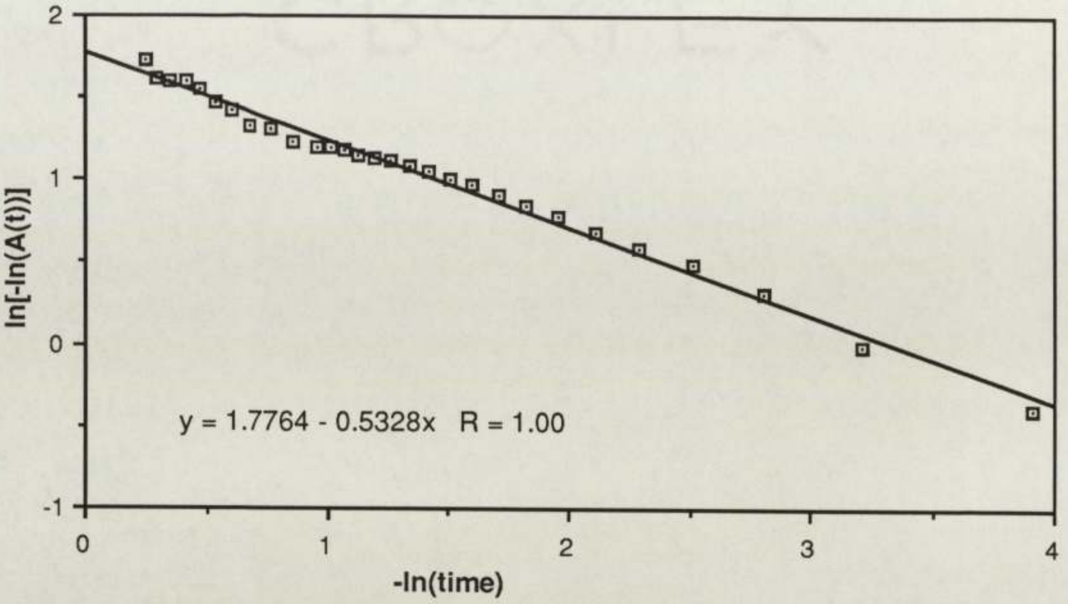

Figure A3.3 Double-logarithmic plot of electro-optical dichroism decay at 1000V (1.58% w/v solution of copolymer in cyclohexane)

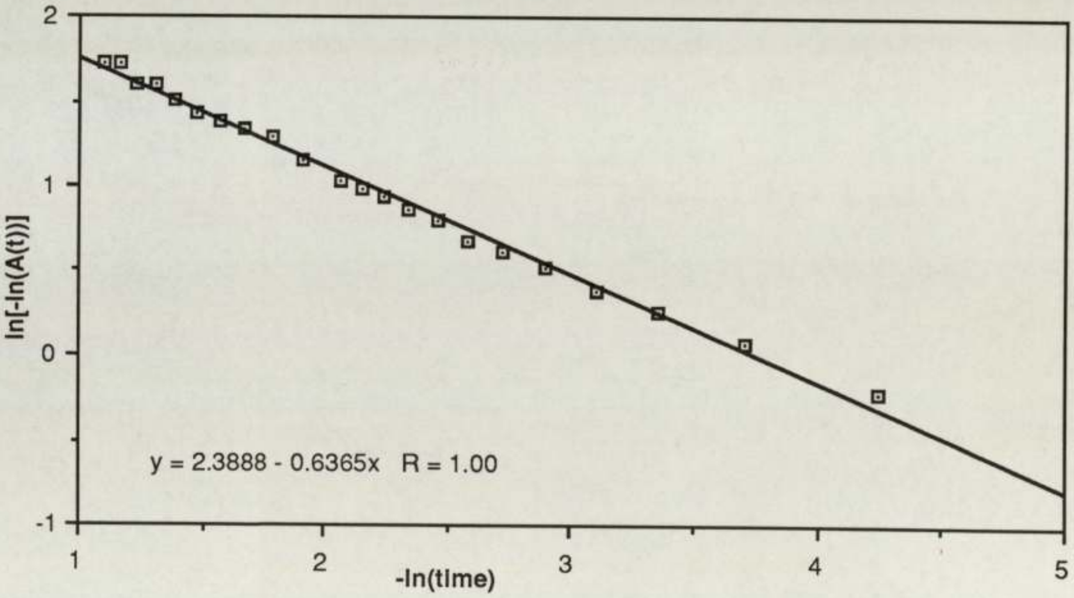

Figure A3.4 Double-logarithmic plot of electro-optical dichroism decay at 1000V (1.80% w/v solution of copolymer in cyclohexane)

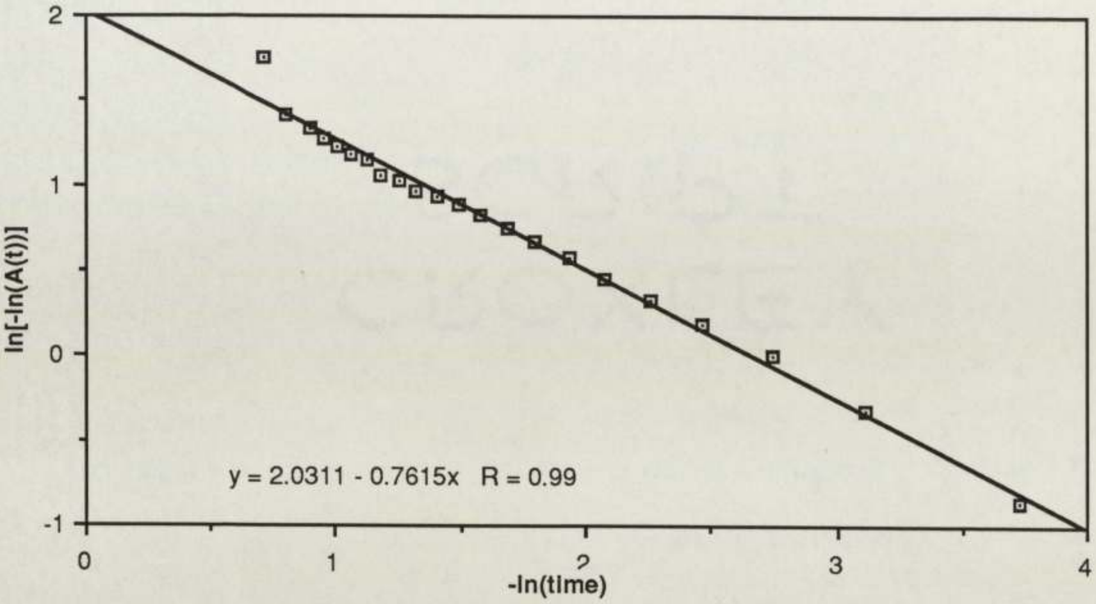

Figure A3.5 Double-logarithmic plot of electro-optical dichroism decay at 250V

(1.05% w/v solution of copolymer in cyclohexane)

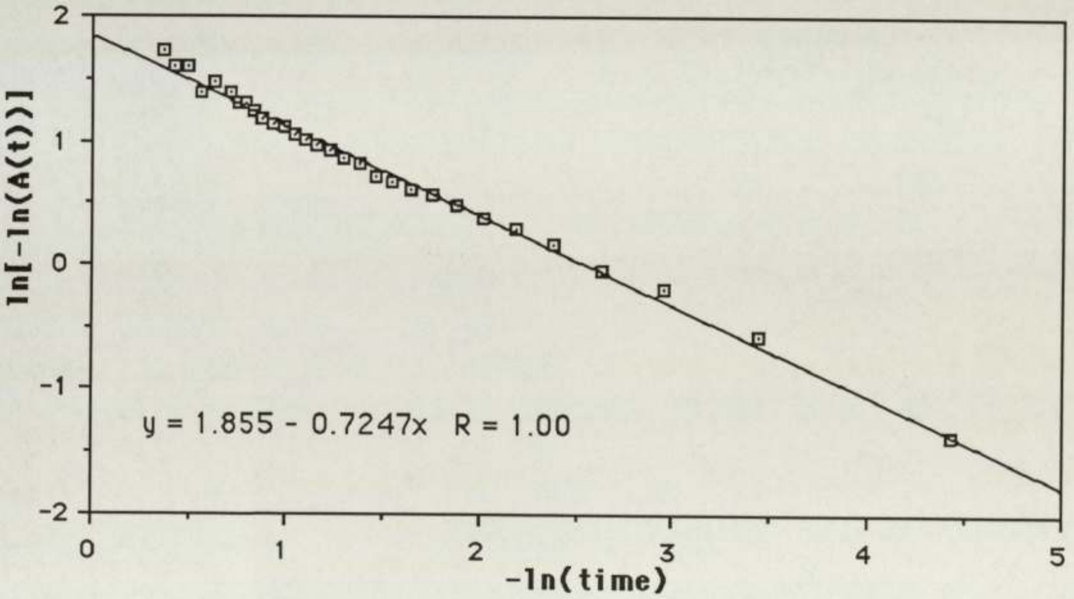

Figure A3.6 Double-logarithmic plot of electro-optical dichroism decay at 250V

(1.58% w/v solution of copolymer in cyclohexane)

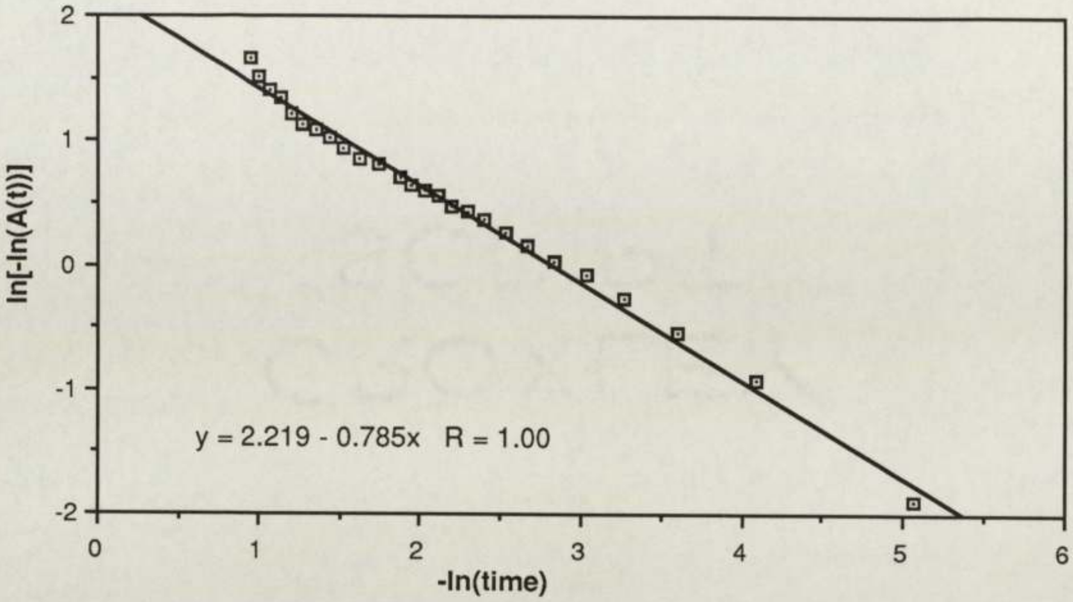

Figure A3.7 Double-logarithmic plot of electro-optical dichroism decay at 250V

(1.80% w/v solution of copolymer in cyclohexane)

A3.4 Analysis of rise of electro-optical dichroism using the Williams-Watts relationship

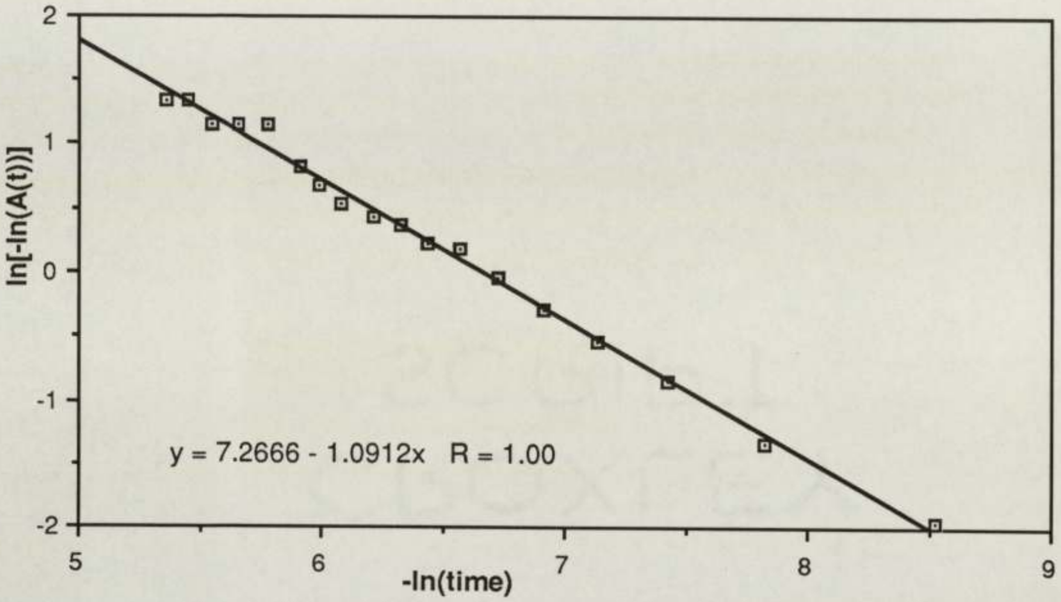

Figure A3.8 Double-logarithmic plot of electro-optical dichroism rise at 1000V (0.65% w/v solution of copolymer in cyclohexane)

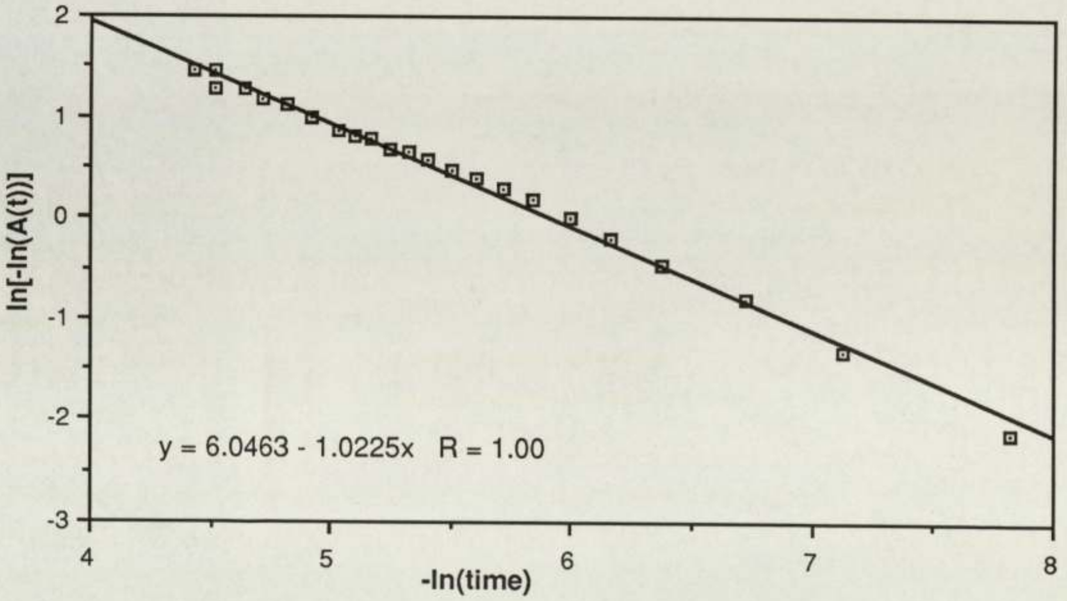

Figure A3.9 Double-logarithmic plot of electro-optical dichroism rise at 1000V (1.05% w/v solution of copolymer in cyclohexane)

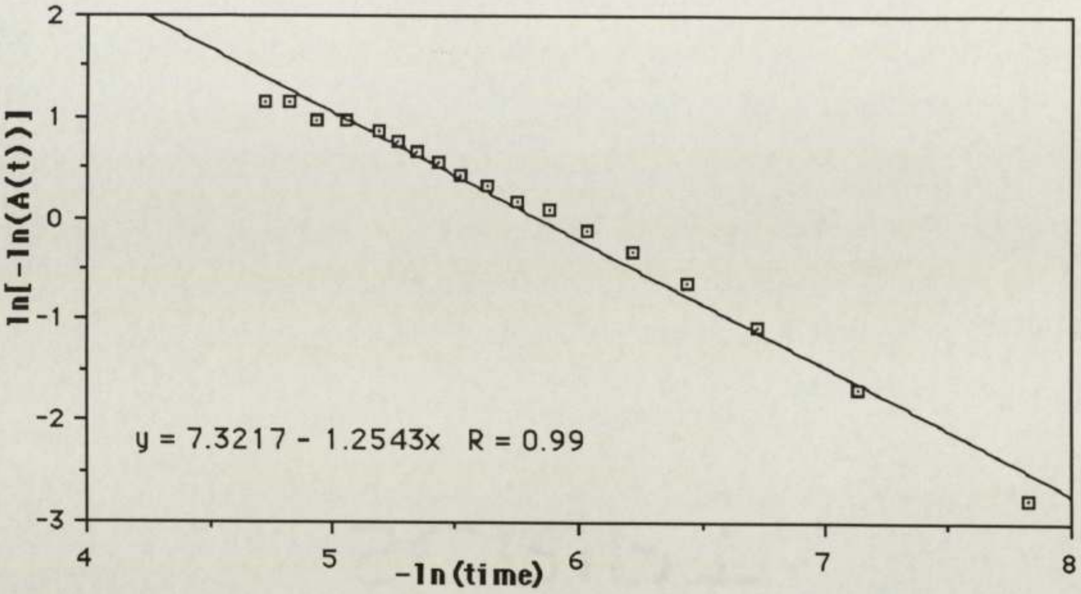

Figure A3.10 Double-logarithmic plot of electro-optical dichroism rise at 1000V (1.58% w/v solution of copolymer in cyclohexane)

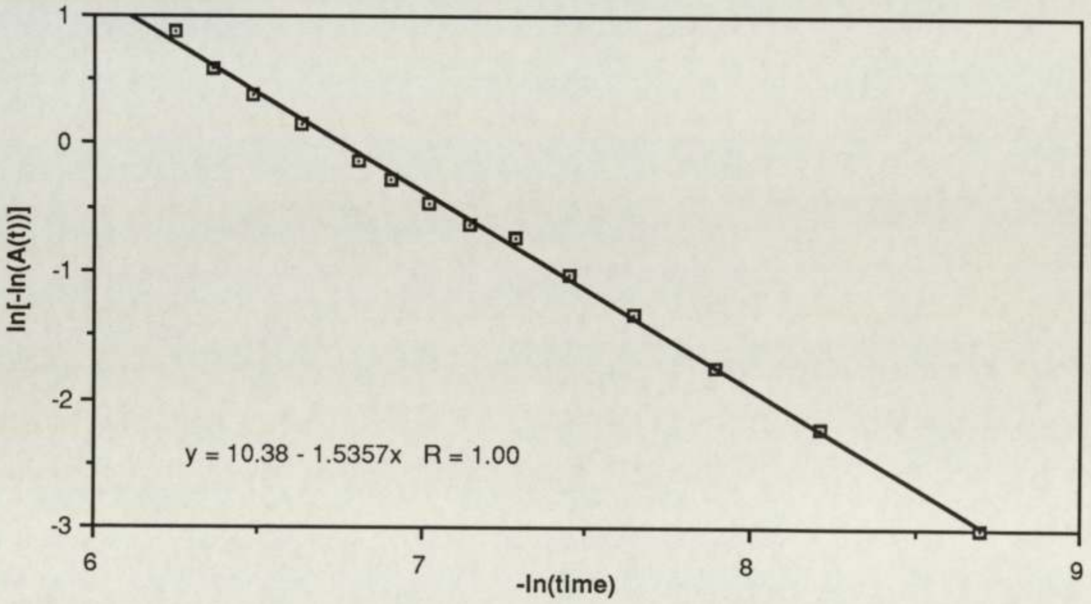

Figure A3.11 Double-logarithmic plot of electro-optical dichroism rise at 1000V (1.80% w/v solution of copolymer in cyclohexane)

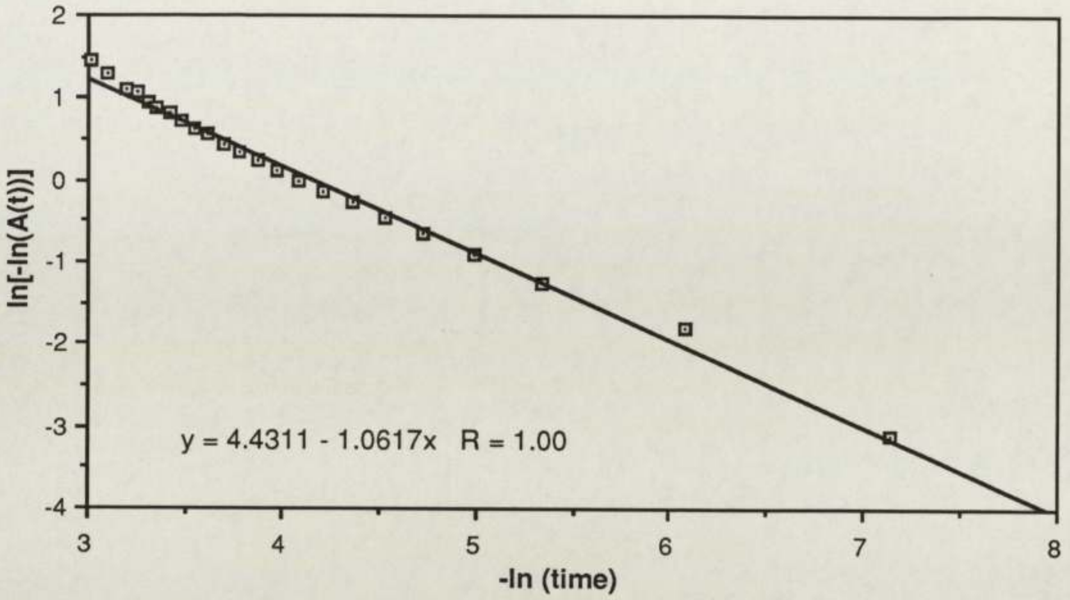

Figure A3.12 Double-logarithmic plot of electro-optical dichroism rise at 250V (1.05% w/v solution of copolymer in cyclohexane)

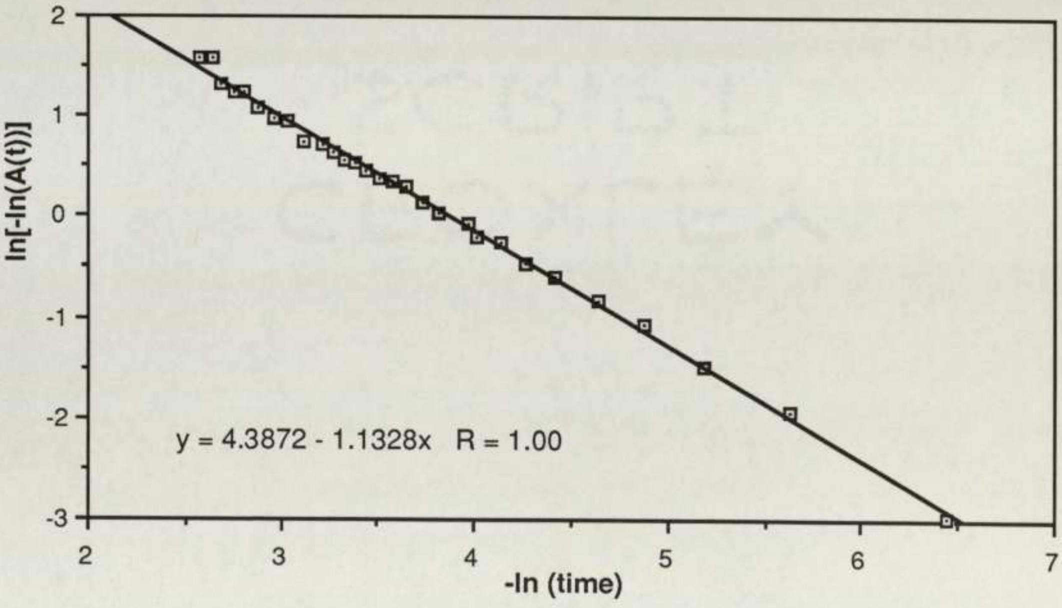

Figure A3.13 Double-logarithmic plot of electro-optical dichroism rise at 250V (1.58% w/v solution of copolymer in cyclohexane)

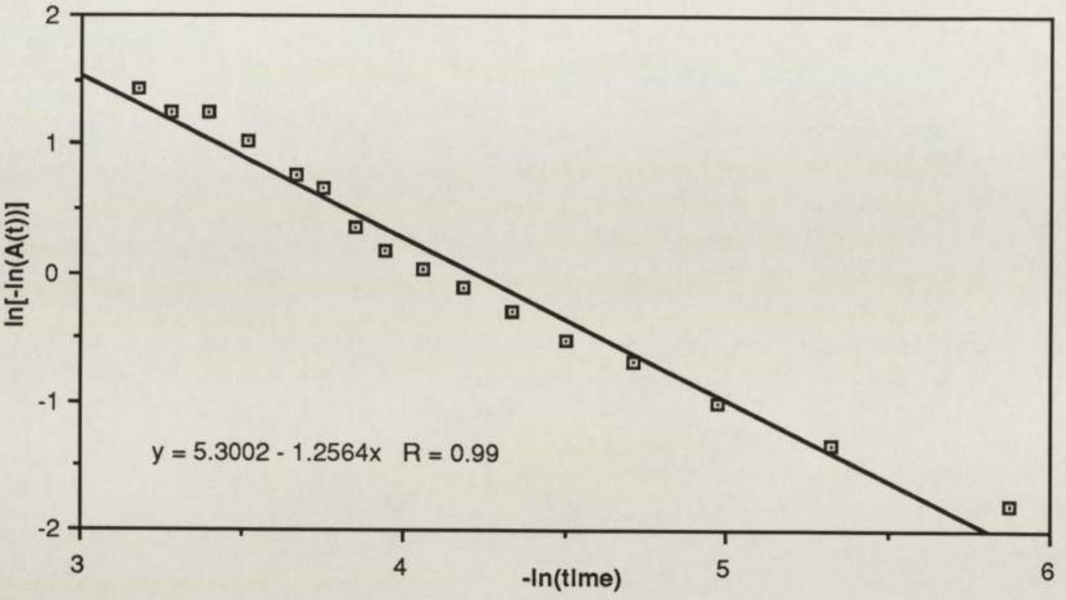

Figure A3.14 Double-logarithmic plot of electro-optical dichroism rise at 250V (1.80% w/v solution of copolymer in cyclohexane)

APPENDIX 4

MEASUREMENT OF THE BIREFRINGENCE OF AN OPTICALLY ABSORBING SAMPLE USING THE COMPENSATED LIGHT- INTENSITY METHOD.

The optical arrangement shown in figure 7.6, with the quarter-wave plate oriented with its slow axis parallel to the direction of the applied electric field, may be used to measure the electric birefringence of an optically absorbing sample. An equation (6.25) which describes the change in the intensity of light which is transmitted by the analyser in response to the application of a pulse of voltage to the Kerr cell may be derived as follows:

In the absence of the electric field, the waveform W of the plane polarised light incident on the Kerr cell is given by,

$$W = A_o \sin \omega t$$

where A_o is the amplitude of the wave, ω the angular frequency and t has units of time. This waveform may be resolved into two orthogonal components W_x and W_y which lie respectively at $+45^o$ and -45^o to the plane of polarisation of the incident beam of light,

$$W_x = A_o \cos 45^o \ \sin \omega t$$
$$W_y = A_o \sin 45^o \ \sin \omega t$$

On passage through the Kerr cell, these wave forms suffer optical absorption and their corrseponding intensities become

$$I_x = I_1 \ 10^{-A_x}$$

and $$I_y = I'_1 \ 10^{-A_y}$$

respectively, where A_x and A_y are the absorbances for the propagation of light in the x and y directions and I_1 is the intensity of the incident light, before passage through the cell. The corresponding amplitudes a_x and b_y of the waveforms which propagate along the x and y axes respectively are given by the square root of the intensities and may be defined as

$$a_x = a_o \ 10^{-A_x/2} \qquad \text{A 4.1}$$

$$b_y = b_o \ 10^{-A_y/2} \qquad \text{A 4.2}$$

Where a_o and b_o are the amplitudes of the component waveforms incident on the cell. In the absence of the electric field, there is no dichroism therefore $A_x = A_y = A$ (the mean absorbance), $a_o = b_o$ and $a = b = a_o \ 10^{-A/2}$. The waveforms which leave the Kerr cell may now be expressed as,

$$Wx = a_o \ 10^{-A/2} \cos 45^o \ \sin \omega t \qquad \text{A4.3}$$

$$Wy = a_o \ 10^{-A/2} \sin 45^o \ \sin \omega t \qquad \text{A4.4}$$

When the quarter-wave plate (positioned immediately after the Kerr cell) is orientated with its slow axis coincident with the x-direction, the phase of W_x is retarded by 90^o and W_x becomes

$$Wx = a_o \ 10^{-A/2} \cos 45^o \ \cos \omega t \qquad \text{A 4.5}$$

The plane of polarisation of the analyser may be defined as an axis p (Figure A 4.1) which lies at 45^o to the x-direction.

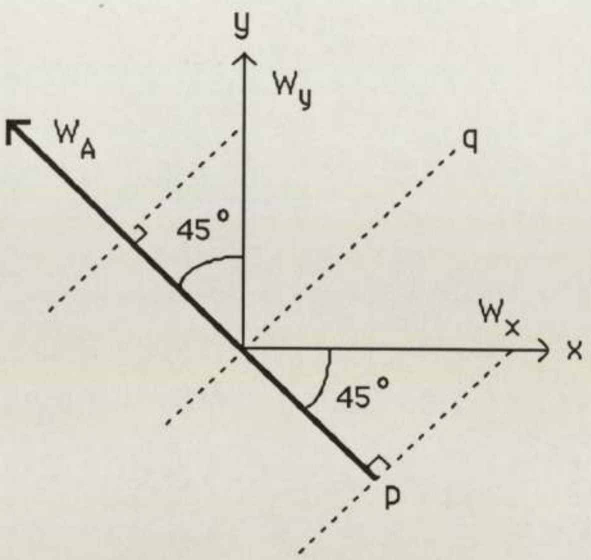

Figure A4.1 Propagation of light through the analyser.

The waveform (W_A) that emerges from the analyser is given by

$$W_A = W_y \cos 45^o - W_x \cos 45^o \qquad \text{A 4.6}$$

By substituting A4.4 and A 4.5 and recognising that $\cos 45^o = \sin 45^o = \sqrt{2}/2$,

$$W_A = a_o\ 10^{-A/2}\ 0.5\ (\sin \omega t - \cos \omega t)$$

The intensity of the light, transmitted by the analyser, I_A, is given by

$$I_A = \int_0^{2\pi/\omega} (W_A)^2\, dt \qquad 4.7$$

where

$$W_A{}^2 = [\sin^2 \omega t - 2 \sin \omega t \cos \omega t + \cos^2 \omega t]\ (a_o{}^2\ 10^{-A})/4$$

Integration leads to,

$$I_A = [\ 1 - 0 + 1\ ]\ (a_o{}^2\ 10^{-A})\ /4 \ = \ (a_o{}^2\ 10^{-A})\ /2 \qquad 4.8$$

When an electric field is applied along the x-direction, the component W_x which leaves the Kerr cell will have undergone a retardation δ relative to W_y for a material possessing a positive Kerr constant. The components of the light beam which leave the Kerr cell are then given by,

$$W_x = a_x \cos 45^o \sin (\omega t - \delta)$$
$$W_y = b_y \sin 45^o \sin \omega t$$

In the field-on condition, where dichroism is present, $A_{||} \neq A_{\perp}$ therefore $a_x \neq b_y$. The components of the beam, after passage through the quater-wave plate oriented with its slow axis coincident with the x-direction, are

$$W_x = a \cos 45^o \cos (\omega t - \delta)$$
$$W_y = b \sin 45^o \sin \omega t$$

The waveform that emerges form the analyser may then be obtained using equation 4.6, where

$$W_A = [b \sin 45^o \sin \omega t \cos 45^o] - [a \cos 45^o \cos (\omega t - \delta) \cos 45^o]$$

recognising that $\sin 45^o = \cos 45^o = \sqrt{2}/2$.

$$W_A = 0.5\ [\ b\ \sin \omega t\ - a\ \cos (\omega t - \delta)\ ]$$

Expanding cos ($\omega t-\delta$) using the standard trignometrical expansion

$\cos(x-y) = \cos x \cos y + \sin x \sin y$,

$$W_A = 0.5\,[\, b \sin \omega t \; - a \cos \omega t \cos\delta - a \sin \omega t \sin\delta \,]$$

The intensity of light, $I_A{}'$, which is transmitted by the analyser may be obtained using equation 4.7 where

$$\begin{aligned} W_A{}^2 = 0.25\ [\, & b^2 \sin^2 \omega t + a^2 \cos^2 \omega t \cos^2 \delta + a^2 \sin^2 \omega t \sin^2 \delta \\ & -2b \sin^2 \omega t \, a \sin \delta + 2a^2 \cos \omega t \cos \delta \sin \omega t \sin \delta \\ & \qquad -2\, b \sin \omega t \, a \cos \omega t \cos \delta \,] \end{aligned}$$

By integration

$$I_A{}' = 0.25\,[\, b^2 + a^2 \cos^2 \delta + a^2 \sin^2 \delta - 2ab \sin \delta]$$

and using the identity $\cos^2 x + \sin^2 x = 1$,

$$I_A{}' = 0.25\,[a^2 + b^2 - 2ab \sin \delta] \qquad \text{A4.9}$$

Now the normalised change in the intensity of light which is transmitted by the analyser in response to the application of a voltage pulse is given by

$$\Delta I / I = (I_A{}' - I_A) / I_A$$

therefore by substituting equations A4.8 and A4.9,

$$\Delta I / I = 0.25\ [(\, a^2 + b^2 - 2ab \sin \delta) - (a_o{}^2\ 10^{-A})/2] \,/\, (a_o{}^2\ 10^{-A})/2$$

$$\Delta I/I = [(a^2 + b^2 - 2ab \sin \delta) / 2 (a_o^2\ 10^{-A})] - 1$$

multiplying out and substituting for a and b (equations A4.1 and A4.2)

$$\Delta I/I = [(a_o^2\ 10^{-A_x} + b_o^2\ 10^{-A_y} - 2a_o b_o\ 10^{-(A_x+A_y)/2} \sin \delta)/ 2 (a_o^2\ 10^{-A})] - 1$$

If the angle of polarisation of polariser P_1 lies at an angle of 45° to the direction of the applied field then $a_o = b_o$ and $A_x = A_{||}$ and $A_y = A_{\perp}$

$$\Delta I/I = -1 + (a_o^2 / 2\ a_o^2 10^{-A})\ [10^{-A_{||}} + 10^{-A_{\perp}} - 2 \times 10^{-(A_{||} + A_{\perp})/2} \sin \delta]$$

rearranging,

$$\Delta I/I = -1 + 0.5[\ 10^{(A-A_{||})} + 10^{(A-A_{\perp})} - 2 \times 10^{\{A - (A_{||} + A_{\perp})/2\}} \sin \delta]$$

APPENDIX 5

LIST OF SUPPORTING PUBLICATIONS

1. Amass, A.J., Beevers, M.S., Farren, T.R., Stowell, J.A., *Studies in electro-active polymers 1 : Metathesis polymerisation of acetylene,* Makromol. Chem. Rapid Commn., **8**, 119-122, 1987.
2. Stowell, J.A., Amass, A.J., Beevers, M.S., Farren, T.R., *Studies in electro-active polymers 2 : Soluble Polyacetylene, A new synthetic route.,* Makromol. Chem. , **188**, 1635-1639, 1987.
3. Farren, T.R., Amass, A.J., Beevers, M.S., Stowell, J.A., *Studies in electro-active polymers 3 : Synthesis of cyclopentene/acetylene copolymers using metathesis catalysts*, Makromol. Chem. , **188**, 2535-2541, 1987.

4 Stowell, J.A., Amass, A.J., Beevers, M.S., Farren, T.R., *The synthesis of block and graft copolymers containing polyacetylene units : A review*, Polymer, **30**, 195-201, 1989.

5. Farren, T.R., Amass, A.J., Beevers, M.S., Stowell, J.A., *The synthesis, characterisation and electro-optical properties of polypentenylene-block-co-acetylene*, Polymer, **30** (6), 1008-1011.